조선대학교
CHOSUN UNIVERSITY

February 2021

Ph.D. Thesis

Study on thermal comfort based on bio-signals of driver according to seat condition under heating and cooling environment

The Graduate School of Chosun University

Department of Mechanical Engineering

Yunchan Shin

Study on thermal comfort based on bio-signals of driver according to seat condition under heating and cooling environment

자동차 실내환경에서 냉난방시 시트조건에 따른 생체신호 기반 열쾌적성 연구

February 25, 2021

The Graduate School of Chosun University

Department of Mechanical Engineering

Yunchan Shin

Study on thermal comfort based on bio-signals of driver according to seat condition under heating and cooling environment

Supervising Professor: Honghyun Cho

A Dissertation Submitted in Partial Fulfillment of Requirements for the Degree of Doctor of Philosophy.

October 2020

The Graduate School of Chosun University

Department of Mechanical Engineering

Yunchan Shin

I hereby recommend that the thesis prepared by
Yunchan Shin
is accepted in partial fulfillment for the
Degree of Doctor of Philosophy
in the Department of Mechanical Engineering

■ **Chair of committee:**

Dongwook Oh, Ph.D.
Chosun University

■ **Member of committee:**

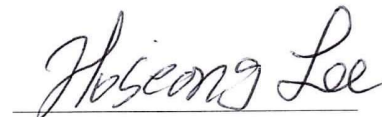Jungsoo Park, Ph.D.
Chosun University

Honghyun Cho, Ph.D.
Chosun University

Chasik Park, Ph.D.
Hoseo University

Hoseong Lee, Ph.D.
Korea University

December 2020

Graduate School of Chosun University

Contents

List of Figures

List of Tables

Nomenclature

A_D : Body area [m^2]

CSV   : Comfort sensation vote

ECG   : Electrocardiogram

EEG   : Electroencephalogram

FFT   : Fast Fourier transform

GSR   : Galvanic skin response

HF   : High frequency [Hz]

HRV   : Heart rate variability

I   : Thermal resistance in clo units [1 clo=0.155$m^2 \cdot$ K/W]

IAQ   : Indoor air quality

$I_{clo,i}$: Garment insulation values [clo]

LF   : Low frequency [Hz]

LF/HF   : The ratio of low frequency and high frequency

NREM   : Non rapid eye movement

MET   : Metabolic rate [1 met=58.1 W/m^2]

MST   : Mean skin(surface) temperature [°C]

PMV   : Predicted mean vote

PPD   : Predicted percent dissatisfied

PPG   : Photoplethysmography

Q   : Cooling or heating capacity [W]

RMSSD   : Root mean square standard deviation [ms]

SDNN   : Standard deviation N-N interval [ms]

SMR   : Sensory motor rhythm [12~15 Hz]

TSV   : Thermal sensation vote

Greek symbols

α : Alpha wave [8~12.99 Hz]

β : Beta wave [13~30 Hz]

δ : Delta wave [0.5~3.99 Hz]

θ   : Theta wave [4～7.99 Hz]

γ   : Gamma wave [30～50 Hz]

Subscripts

clo   : Clothed body or clothing

clu,i   : Effectiveness insulation of clothes i

D   : DuBios value

ABSTRACT

Study on thermal comfort based on bio-signals of driver according to seat condition under heating and cooling environment

Shin, Yunchan

Advisor : Prof. Cho, Honghyun, Ph.D.

Department of Mechanical Engineering,

Graduate School of Chosun University

In this study, EEG, PPG, and surface temperature of subjects were measured while performing a driving simulation as the automobile cabin temperature and vent discharge temperature in summer and winter were changed from discomfortable conditions to comfortable conditions. Besides, subjective questionnaires (TSV, CSV, CLV) were used to analyze the subject's thermal comfort under the various driving environment. Besides, the subject's bio-signals such as brain waves, pulse waves, and skin temperature were measured according to using various seats under the thermal environment of the vehicle interior in summer and winter condition. At the same time, the subject's thermal comfort was analyzed through subjective questionnaires (TSV, CSV, CLV). In addition, thermal comfort was analyzed at the different location of local heating in winter by measuring the subject's bio-signals and performing a subjective questionnaire. Through this, the following conclusions were obtained.

As the simulation results for the thermal comfort of the automobile indoor, when using the basic seat in summer condition, the temperature of the back and hips which are in contact with the seat is high. In case of using the cold water seat, the temperature of the back and hips is greatly decreased, therefore the PPD is also

significantly reduced. In addition, when the basic seat is used in winter condition, a slight dissatisfaction on the PPD (10.1%) is presented, and it is 7.8% in the initial 5 minutes when the hot water seat is used, which confirming that a pleasant thermal environment is achieved.

As the average surface temperature measurement result for the thermal comfort of a driver in the automobile indoor during cooling in summer condition, it was confirmed that the surface temperature of the subject during driving could be reduced by operating the vent of 12.5°C at the cabin temperature of 35°C. As comprehensively analyzing the subjective survey results, PPG analysis results, and EEG analysis results, at cabin and vent temperatures of 27.5°C and 18.5°C, it was confirmed that a pleasant driving environment could be provided to the driver and concentration on driving could be increased. In case of the average surface temperature measurement result for the thermal comfort of a driver in the automobile indoor during heating in winter condition, it was confirmed that the surface temperature of the subject while driving could be increased by operating the vent temperature of 40°C under the cabin temperature of 15°C. As the subjective survey results, PPG analysis results, and EEG analysis results, at cabin and vent temperatures of 17.5°C and 37.5°C and cabin and vent temperatures of 20°C and 35°C, it was confirmed that a pleasant driving environment could be provided to the driver and concentration on driving could be increased.

As experimental results on the use of various seats based on bio-signals and subjective surveys, the use of the ventilation seat in summer condition provided an unpleasant environment to the driver by blowing the surrounding hot air. While, it was confirmed that the use of the cold water seat was lower the driver's stress index and provided the proper environment with high concentration on driving. In addition, as the results of thermal comfort based on bio-signals and subjective surveys under winter condition, the use of the heating seat provided an unpleasant environment to the driver due to the high temperature of the heating wire. The use of the hot water seat decreased the concentration on driving, however, it was confirmed that the stress

index and relative β/α in the occipital lobe were reduced, which was provided a thermally comfortable environment to the driver.

As the results of local heating position in winter, the temperature of the parts where was applied local heating increased significantly regardless of the use of HVAC, but there was no effect of increasing the temperature in other parts. In the analysis results of PPG and EEG, when a local heating to the thighs was applied, the stress index was the lowest, and SDNN and RMSSD were relatively high when the local heating to the chest and thighs was used. In addition, it was confirmed that the relative β/α in the occipital lobe was low, thus it could provide a comfortable thermal environment to the driver.

Therefore, it was confirmed that thermally comfortable environment can be provided to the driver in the automobile indoor environment by using the cold water seat in the summer. In addition, a hot water seat and local heating to the thighs and chest in winter are also increased thermal comfort to the drive during driving.

I. Introduction

A. Background

As industry has developed, transportation technologies have also developed. Car ownership has reached more than one car per household in some developed countries. The automobile has become indispensable, and it is recognized as another living space beyond being a means of transportation. Consequently, many parts of the vehicle are rapidly changing from simple mechanical systems to electric, electronic, and control systems for the safety and comfortable of the passengers. Many companies have been developing autonomous vehicles, and they intend to commercialize them within 10 years. In addition, many technologies have been developing rapidly because of increasing investments in key technologies related to autonomous vehicles [1, 2]. In the case of self-driving cars, the safety issue is the most important; however, it is also important to provide a comfortable environment to drivers and passengers while managing and optimizing the energy of the car simultaneously. Because the heating, ventilating, and air-conditioning (HVAC) system in an electric vehicle uses electricity, the air flow and temperature distribution in the car cabin are important for saving energy and providing effective cooling or heating. Therefore, the development of a smart control method for an efficient automobile air-conditioning system are required [3]. Besides, the heat pump is an attractive option to use as the HVAC system of electric vehicles because this system consumes less energy in electric vehicles. The improved control and optimal operation in electric vehicles are other important technology to improve the performance of heat pump as the HVAC system. Moreover, when integrated thermal management can be realized in EVs, energy saving and thermal comfort can be improved at the same time, and this technology is indispensable for the practical use of smart EV. In addition, as fuel economy requirements are strengthened and the market of EVs increases, the thermal comfort

of passengers becomes more and more important in part of energy management [4]. Like an electric vehicle, autonomous vehicles are becoming an issue worldwide. It is classified into five levels and Table 1 shows five levels of technology for self-driving vehicle according to the SAE standards [1]. By 2030, Level 3 and Level 4 functions of autonomous driving are expected to account for about 0.8% and 2.3% of vehicle in the world, respectively [1]. Accordingly, the driver becomes more free in the car, and the importance of thermal comfort in the car interior increases rapidly.

In particular, the cabin temperature of a vehicle can rise to a maximum of 85°C in summer, and the surface temperature of dashboard exposed to direct sunlight reaches a maximum of 100°C [5]. Accordingly, solar energy passing through the window of a car during the summer increases the temperature inside a car significantly and transmits radiant energy directly to the driver, providing great discomfort to the driver. In addition, the incidence of traffic accidents resulting from driver discomfort or drowsiness when a car is driven for a long time in the summer is increasing. Moreover, excessive use of air conditioners in a car can cause health problems for passengers [6, 7]. Besides, passengers feel the chill in the seat when sitting in a car in winter, thus they use the heater excessively. Excessive use of a heater in a car during winter can decrease the concentration of driving and cause drowsiness due to reduction of oxygen in a car. Also, direct blowing the heater air on driver's face can dry the skin of driver and cause skin aging problems such as wrinkles and blemishes [8, 9]. Therefore, much information is needed to optimize the control of the HVAC system to provide a comfortable environment and improve the concentration of drivers and passengers.

However, because the flow direction of the cold air, the temperature and outlet speed of the discharged air, and the amount of external solar radiation change continuously, the indoor environment of the car is more complex and unpredictable than that of buildings or offices. It is important to provide an appropriate thermal comfort environment to the driver by using an HVAC system, even though the thermal environment of the vehicle changes every moment; however, it is difficult to

create an optimal environment with an effective control method through experimentation with a real system. Therefore, the current research on the thermal comfort of the human body conducted continuously according to environmental changes in the interior of the building, but research on the thermal comfort of the passengers inside the vehicle is insufficient. Besides, the research on the thermal comfort of automobiles is being analyzed based on research data in the field of architecture. The thermal environment of an interior building has a uniform temperature distribution, but the thermal environment inside a vehicle has a significant non-uniform temperature distribution and it has a characteristic that changes according to the external environment occur quickly. Moreover, due to the narrow indoor space, the airflow disturbances by complex internal structure, and the variability due to the external environments such as solar radiation, humidity, the cooling capacity per unit volume is required more than 20 times in summer although the volume ratio of building and car is about 10:1 [10]. Therefore, research is really needed to save energy and provide high level the thermal comfort of passengers.

The previous study on the evaluation for thermal comfort of the human body was carried out whether there was a comfortable environment by predicting the predicted percentage of dissatisfied (PPD) using a subjective questionnaire after the finish of the experiment under specific experimental conditions. However, generally it is difficult to secure the reliability of the data and to present objective and quantitative data because the number of subjects is small. Thus, it has low reliability for directly utilizing the research results in the real system. Recently, it has become possible to accurately measure bioelectric signals such as brain waves and electrocardiograms with the development of measurement technology for various bio-signals. Interface technology to measure various bio-signals is also being continuously developed. Interface technology based bio-signals is being used as an increasingly human-friendly and portable interface such as wearables and mobile devices, and is applied to future-oriented technologies for next-generation user interfaces after text, voice, gesture, and facial expression recognition. This bio-signal processing technology has been

developed as a monitoring technology using bio-signals as well as a user's interface, and can be applied to medical fields such as various rehabilitation and health examination, etc. Therefore, it has unlimited the potential for its utility and compatibility [11]. The human sensibility can be indexed through quantitative and objective measurement for human comfort and the degree of body response in a specific environment using high efficiency bio-signal measurement technology.

Existing researches on the thermal comfort of the human body using bio-signals have been conducted mostly in the indoor environment of the occupant or the work environment of the workplace, and studies on the thermal comfort of the passengers in the interior of vehicles is very insufficient. Therefore, as a method of predicting the thermal comfort of the human body in the vehicle interior, a quantitative study on the thermal comfort of the human body through a subjective survey technique is needed as a existing method, and a psychological model using bio-signals such as brain waves, pulse waves, and skin temperature is also needed simultaneously. Hot and cold environments such as summer and winter provide a very unpleasant environment for passengers at the beginning. Under these situation, the excessive use of air conditioner and heater can bring bad effects on the health of passengers adversely. Nowadays, the ventilation and heating seats are commonly installed in automobiles to increase the thermal comfort of passengers. However, the ventilation seat installed in existing automobiles blows the wind to the back of passenger. There is no temperature decrease because it only blows the surrounding air to the passenger. Accordingly, it is difficult to provide instantly a comfortable environment to drivers. The heating seat of automobiles makes the heat by using the heat wires in winter, however, electromagnetic waves were generated at this time, which may have a harmful effect on the human body [12]. In addition, the excessive use of heating seats may cause fire and burns [13]. Therefore, it is necessary to develop a seat with more safety and improve thermal comfort effectively more than the ventilation seat and heating seat in the automobile.

Table 1.1 Summary table of the SAE's levels of vehicle automation

Level	Name	Narrative definition
0	No Automation	the full-time performance by the human driver of all aspects of the dynamic driving task, even when enhanced by warning or intervention systems
1	Driver Assistance	the driving mode-specific execution by a driver assistance system of either steering or acceleration/deceleration using information about the driving environment and with the expectation that the human driver perform all remaining aspects of the dynamic driving task
2	Partial Automation	the driving mode-specific execution by one or more driver assistance systems of both steering and acceleration/deceleration using information about the driving environment and with the expectation that the human driver perform all remaining aspects of the dynamic driving task
3	Conditional Automation	the driving mode-specific performance by an automated driving system of all aspects of the dynamic driving task with the expectation that the human driver will respond appropriately to a request to intervene
4	High Automation	the driving mode-specific performance by an automated driving system of all aspects of the dynamic driving task, even if a human driver does not respond appropriately to a request to intervene
5	Full Automation	the full-time performance by an automated driving system of all aspects of the dynamic driving task under all roadway and environmental conditions that can be managed by a human driver

B. Previous studies

1. Research trends on the thermal comfort in building

In previous studies on thermal comfort, Yao et al. [14] investigated three physiological parameters—skin temperature (local and average), electrocardiogram (ECG), and electroencephalogram (EEG) to determine the relationship between ambient temperature and thermal comfort. They reported that the average skin temperature increased, while the maximum difference between local skin temperature decreased when the ambient temperature increased from 21°C to 29°C. In addition, the average skin temperature for a neutral heat sensation was approximately 32.1°C, and the maximum difference of the local skin temperature showed 5.3°C. Ciuha et al. [15-17] investigated the difference in skin sensitivity by the change of temperature stimulation in the recognition of thermal comfort. They reported that regional differences in the boundaries and size of the thermal comfort zone in a comfortable environment (33°C) between male and female subjects were not present. Lai et al. [18] studied the dynamic thermal comfort in an outdoor environment, and they showed that the local skin temperature of the human body' torso in a cold environment did not decrease (34°C) because of strong heat insulation and a large heat capacity. Moreover, it was confirmed that the temperature of the face was relatively low (19°C). They developed a human body heat transfer model according to the outdoor thermal environment. Zhang et al. [19] conducted a climate chamber experiment on buildings equipped with a centralized air conditioning (CAC) system and a split-type air conditioner (SAC) under the same experimental conditions. No significant differences of skin temperature and wetting were found between the two groups of subjects under neutral conditions by checking the physiological signs (mean skin temperature, skin wetness, and heart rate) and psychological responses (thermal sensation, thermal acceptability, thermal comfort, and dissatisfaction percentage). In a non-neutral condition, the skin temperatures of subjects were significantly higher in the CAC building, while the skin

wetness showed no significant difference. In addition, the ability to control the temperature of the subject in the CAC building was lower than that in the SAC building. Luo et al. [20] studied the dynamic process of thermal adaptation in heated and unheated building environments. They reported that the northern group took three years to adapt the cold room temperatures, whereas the southern group adapted to neutral and warm room temperatures within one year. Chang et al. [21] investigated the effects on the EEG of subjects of warm and cold stimulation. They confirmed that specific EEG activation occurred during warm and cold stimulation. Roelofsen [22], Lorsch et al. [23], Woods [24] reported that indoor air quality (IAQ) has a greater effect on the work efficiency of a human. In addition, the major factors used to evaluate the quality of an indoor environment are the thermal environment, IAQ, light, and noise, etc. The effects of the thermal environment to the workers were investigated by many researchers because human thermal comfort is very sensitive to the surrounding thermal environment. Cui et al. [25] reported that hot environments have a negative effect on work efficiency and motivation. Pepler and Warner [26] analyzed and investigated the effect of air temperature on test subjects to determine the finish times for work completed under different air temperatures. They reported that a decrease in efficiency was shown at an indoor air temperature of 26.7°C. Seppänen et al. [27] measured the work efficiency of subjects under exposure to air temperature ranges of 23–32°C and concluded that the work efficiency decreased by 2% when the indoor air temperature was increased by 1°C. Lee et al. [28, 29] investigated the concentration of occupants under indoor air temperature changes by studying brain waves, and presented the effect on the body relaxation under varied floor temperatures. Kum et al. [30, 31] carried out studies to measure the brain wave signals and ECG (electrocardiogram) of the occupants at different indoor temperatures, and to evaluate thermal comfort of humans at various levels of the difference between outdoor and indoor temperatures in summer. Kim et al. [32] evaluated thermal comfort during sleep in summer using physiological signals and average skin temperature. Besides, Kim et al. [33] also studied the method of evaluation of

comfort using brain wave signals at the frontal lobe and parietal lobe. Further, Kang et al. [34] evaluated the amenity and physical characteristics of an air-conditioning system that applies fluctuation characteristics similar to those of natural wind, by measuring skin temperature. Lan et al. [35] reported thermal comfort levels during sleep for different air temperatures using mean skin temperature (MST) and the responses to subjective thermal comfort questionnaires. Further, Liu et al. [36] investigated the variations in the average temperature of the human skin and surface in stable and unstable thermal environments. Nguyen et al. [37] developed a correlation for an adaptive thermal comfort model for a hot and humid climate like the one in South East Asia using the responses to a subjective thermal comfort questionnaire. Sarhadi et al. [38] evaluated thermal comfort using personal perceptions in open urban spaces. According to their results, air temperature, wind speed, relative humidity, and radiant temperature had the greatest influence on outdoor thermal comfort, and emissivity of materials, placement in open spaces, and surface transparency. They reported that transparency and material texture had the least influence on thermal comfort in open urban spaces. Chan et al. [39] studied the influence of the composition of the park and surrounding buildings to the thermal comfort of the park. It was confirmed that the thermal comfort of the park in summer can be greatly improved by increasing the area of the park, and the thermal comfort of the park in winter can be improved when the space between neighboring buildings is narrowed or in a narrow rectangular shape. Tsang et al. [40] investigated the thermal environment, thermal sensation, satisfaction, and sleep quality of college students living in university dormitories in Hong Kong. They reported that the quality of sleep was greatly influenced by the thermal comfort and satisfaction, and the subjects who satisfied the thermal sensation and the people with a neutral thermal sensation showed much better sleep quality. In addition, it was confirmed that the quality of sleep was higher in the cold environment than in the hot environment. Wang et al. [41] investigated the effect of local wearable heating devices on the thermal comfort of workers while doing manual work in cold environments.

Experiments were conducted using local radiant heating, ankle heating, wrist heating, torso heating, and combined heating, and compared with the environment without heating. As their results, it was confirmed that wrist heating did not significantly improve the heat sensation, but effectively improved work efficiency. Wang et al. [42] investigated the effect of emotional state on people's thermal perception and comfort. It was confirmed that systolic blood pressure and heart rate in light activity were increased in the bored state than in the neutral and pleasant state. Rosaria et al. [43] conducted experimentally on a comfortable seat design to improve the thermal sensitivity for the back and buttock of human. As a result of statistical analysis, it was confirmed that the effect of temperature was recognized most in the upper body and less in the lower body. In addition, it was reported that the shoulders, sides of the back, back and hips were most sensitive to temperature changes at the interface.

Because the most previous studies on thermal comfort have been conducted in the building or indoor, the experiments on thermal comfort were carried out in conditions in which the range of temperature change in the space was not large. In addition, experimental studies on temperature control methods were mostly conducted to provide a comfortable thermal environment according to the type of air conditioner. Martinho et al. [44] measured the temperature and airflow velocity around the human body experimentally and through modeling. They evaluated thermal comfort using the EHT (Equivalent homogeneous temperature) method. A significant difference was found in the calculated equivalent temperature based on the maximum and minimum air velocities of the approximate planes at each body part. They also reported that this corresponded to a body part located in a place directly affected by jets from the air intake, which generated a high local air velocity gradient. Cheong et al. [45] presented a simulation-based approach to improve the lighting and thermal condition inside building. In a real case study of an office building in Singapore, they demonstrated the methodology to significantly improve lighting and thermal condition through the passive daylighting equipment and reconfiguration of climate-controlled air supply vents in office space. They reported that lighting and cooling costs had

achieved significant energy consumption reductions exceeding 7%. Chen et al. [46] conducted a CFD simulation combined with experimental correction to analyze air quality and thermal comfort in a kitchen environment. It was confirmed that kitchen fume could be easily discharged to the outside when the exhaust volume was about 14 m^3/min, and the fume concentration in the mouth and nose could be reduced to a satisfactory level. In addition, they reported that it had good thermal comfort when the exhaust volume was about 11 to 14 m^3/min. Alizadeh et al. [47] performed a CFD simulation to improve the indoor thermal comfort level using a ceiling fan. They confirmed that the thermal comfort level was highest at a blade pitch of 5.75°, a fan speed of 99 rpm, an inlet air temperature of 36°C, and an inlet air humidity of 73.3%, respectively.

2. Research trends on the thermal comfort in automobile

Unlike in buildings, the indoor thermal environment of automobiles is affected by various factors, such as solar radiation, external air temperature, low-temperature air temperature from the HVAC system, and complicated air flow. Thus, further studies that consider these factors are required. In a previous analytical study on thermal comfort in an automotive thermal environment, Hodder et al. [48] performed an analysis of heat flow in the interior of a vehicle in consideration of solar radiation to determine the effects of the spectral type of the sunlight and the physical properties (absorption rate, transmittance, etc.) of the glass on thermal comfort. When the body was exposed to a simulated solar radiation of 400 W/m^2, the spectral content of the radiation did not affect the thermal sensation. Furthermore, the thermal comfort vote increased by 1 scale at an increase of 200 W/m^2 of solar radiation. Chien et al. [49] studied the validity of analysis results based on experimental results and analyzed thermal comfort using the predicted mean vote (PMV) evaluation method to investigate the thermal environment inside the vehicle. It was confirmed that, after the air conditioner was turned on, the average temperature in the car interior rapidly decreased, and the PMV value at 1200 seconds resulted in discomfort for only the feet. Lin et al. [50] analyzed the thermal environment in an automobile interior according to the flow rate and location of the air conditioner outlet, and it was confirmed that the location of the air conditioner vent and the airflow of the total system are the most important parameters directly affecting thermal comfort. In addition, the solar heat load, which is the main heat source of the passenger compartment, could be reduced by the characteristics of the glass material. Kobayashi et al. [51] measured local thermal sensation for four cases of air flow to the head, head and foot, chest, and chest and foot and compared them with Zhang's model. It was confirmed that the evaluation of local thermal sensation by Zhang's model had a high accuracy. However, the estimation of overall sensation and local/overall comfort was still inaccurate and needed significant improvement. Zhang et al. [52, 53]

performed an analysis of the thermal environment inside an automobile and compared experimental and numerical analysis results. They reported that the predicted temperature matched the experimental value well, and the temperature distribution of the simulation model was also similar to that of the experimental value. Barone et al. [54] performed energy design of HVAC system using TRNSYS to improve train performance. All considered hourly weather variables such as air temperature and humidity, incident solar radiation, system-wind relative velocity were implemented as the actual rail track and train speed. They confirmed that thermal comfort was greatly improved through train envelope enhancement, and an additional comfort time of up to 132 hours per year was achieved in relation to a standard railway coach without changing the indoor air temperature setting value.

In previous experimental research on thermal comfort in an automotive thermal environment, Zhou et al. [55] and Qi et al. [56] investigated the thermal comfort of automobile passengers under indoor parking, outdoor parking, and outdoor driving conditions during summer. They reported that the internal air and surface temperatures of a vehicle were temporarily nonuniform, and the surface temperature in outdoor driving conditions changed more quickly than that in indoor and outdoor parking because of the rapid change of solar radiation. Jung et al. [57] investigated the effects of individual responses on individual thermal comfort sensitivity and collective control according to temperature change. They confirmed that thermal comfort sensitivity had a statistically important role in group conditioning. Among the evaluated scenarios, in 86% of the cases (134 out of 152), statistically significant differences in temperature set points were observed in consideration of thermal comfort sensitivity, but the probability of having a comfortable state increased overall. Kristanto et al. [58] performed a simulation study on the sensitivity of energy conversion to air quality, thermal comfort, and energy consumption in automobile interiors. They reported that the use of a cover for parking could reduce the windshield transmittance by 5% and decreased the PMV by 0.9%. In addition, the thermal comfort and the energy consumption could be increased by controlling the volume and temperature of air

supply. Alahmer et al. [59-61] evaluated temporal and non-uniform changes of vehicle interior temperature and relative humidity, as well as changes in the skin temperatures of the driver in the forehead, hands, and feet. They confirmed that the control of the relative humidity during the heating and cooling process by the air-conditioning system could produce a comfortable environment more quickly than when the relative humidity was not controlled.

In addition, in the experimental studies of bio-signal measurement for thermal comfort in an automotive environment, Ting et al. [62] and Tsutsumi et al. [63] quantified the fatigue progress of the driver using multipurpose and subjective measurements. Principal component analysis was used to measure the temporal decrease of driver performance from alert to fatigue using various measurements of driving performance throughout the experiment. They reported that 80 min was the limitation of safety in monotonous highway driving. Shin et al. [64, 65] measured the bio-signals of the driver during heating and cooling condition by the HVAC system, and they reported that the cabin and vent outlet air temperatures should be set to 27.5°C and 18.5°C, respectively, to improve driver comfort and concentration in cooling mode without solar radiation. In heating mode, the cabin and vent outlet temperatures of 25°C and 30°C were ideal. Ikenishi et al. [66] investigated the driver's EEG parallel factors while driving a car, and they reported that the driver preferentially recognized the shape and color more than the distance and motion of a vehicle during driving. Yang et al. [67] predicted driving behaviors based on EEG results under various traffic conditions by a simulation method. They found that the average classification accuracy of prediction was 69.5% and the highest accuracy was 83.5%. In addition, there was a significant correlation between EEG pattern and car-following behavior. Jones [68] compared the performance and limitations of vehicle thermal simulation models in winter using the various thermal sensation models and measured data. His results presented a big difference on the thermal comfort in the warm-up condition of vehicle. Chakroun et al. [69] analyzed thermal comfort in a parked car during the daytime in the summer in Kuwait. Chowdhury

[70] analyzed the driving type of drivers by classifying a total of three vehicle cabin temperature (high: 21–26.67°C, low: 10–15.5°C, and medium: 16–21.1°C) using a car simulator and reported that the road departure and temperature were not closely related, but the speed variation had a meaningful effect on drivers according to the cabin temperature. Pilcher et al. [71] analyzed driver concentration under various ambient temperatures and they presented that it decreased by 14.88% for more than temperature of 32.3°C and decreased by 13.91% for less than temperature of 10°C. Zhou et al. [72] conducted an experimental study on a thermal sensation model for drivers of a car with varying solar radiation and they confirmed that the driver was more sensitive to changes in solar radiation when the outdoor temperature was high. The new model could predict a root-mean-square error (RMSE) of less than 1 unit for all three outdoor driving conditions (summer, winter, and shoulder season) with an accuracy of 87.1%. Ravindra et al. [73] carried out a study on the evaluation of thermal comfort parameters of various vehicle models and strategies to mitigate extreme thermal health risks in tropical climates. The SUV's PMV ranged from 8.36 to 11.81 for the front of the vehicle and from 11.57 to 16.75 for the rear in the ASHRAE 55-2017 [74] standard. According to the EN15251 [75] standard, it was reported that the PMV at the front of the SUV ranged from 9.58 to 13.16, and that the rear was in the range of 13.25 to 18.5. In the case of the hatchback model, the PMV at the front was 8.54 to 11.74 based on ASHRAE 55-2017, and the range was 9.25 to 12.84 in EN15251. PMV for the rear of the hatchback model was found to be 12.24 to 17.38 based on ASHRAE 55-2017, and it was confirmed that the range of 13.15 to 18.87 was shown in EN15251.

3. Research trends on bio-signals

In recent years, U-Health using bio-signals has been expanding more and more as interest for pursuing the quality of life has increased with the global well-being craze [76]. In particular, as the development of autonomous driving systems, monitoring of the driver's condition through the recognition of bio-signals is becoming more important in the automobile industry. As new technologies and the automobile industry are developed, automobiles are being recognized as living spaces breaking away from just concept of transportation. Accordingly, concerns and requirements for safety and convenience in automobiles are continuously increasing [77]. In the existing research on biological signals, Runkle et al. [78] applied a wearable sensor based approach to investigate occupational, environmental, and behavioral factors contributing to individual level changes in thermal deformation of ground maintenance workers. Outdoor workers from three climatic regions in the southeastern of United States (High temperature, high temperature and high humidity, medium temperature environments) participated in personal heat exposure monitoring during a five-day summer working period. As a result, there was a discrepancy between the worker's perception of thermal deformation and the actual thermal deformation spread between the exposure groups. In addition, it was reported that the association between temperature rising and thermal deformation was nonlinear and showed a U-shaped relationship. Lee et al. [79] investigated the reliability and usefulness of the wearable sensor to monitor working and off-duty activities of roofing workers. As a result, the data collection period of three days was recommended to demonstrate the usefulness of these sensors and to obtain an intraclass correlation coefficient of 0.75 or less for heart rate, energy expenditure, metabolic equivalents and sleep efficiency. In addition, they reported that participants were significant differences in physical responses, health statuses, and safety behaviors.

In addition, Kalaivaani et al. [80] designed an ASIC (Application-specific integrated circuit) of WBSN (Wireless body sensor networks) for application in medical

applications. As a their simulation result, it was confirmed that the noise tolerance was changed and the power utilization decreased in contrast to the existing wireless body sensor design due to a similar delay. Accordingly, they reported that the ASIC of prototype WBSN could work effectively. Hashem et al. [81] conducted a study to design and develop a wireless wearable GBTS (Graphite bio-tooth sensor) to diagnose coughing, drinking, chewing, fracture, infection, and biofluid. They reported that GBTS could be monitored and analyzed with 97% accuracy by analyzing the tooth surface and transmitting it to a nearby device with possible reconstruction of the tooth surface through wireless readout of the surface information.

Zhang et al. [82] conducted a study to detect and analyze MEG (Magnetoencephalography) signals in the occipital region using a dual-channel OPM (Optically-pumped magnetometer) sensor. As a their result, the developed wearable OPM-MEG system could mount the sensor close to the scalp of less than 1 cm in general, so it was greatly improved detection efficiency. Therefore, it was confirmed that the subject's alpha rhythm around the occipital region was successfully detected. Liu et al. [83] developed a personal thermal comfort model using lab grade wearables in daily activities and they reported that the predictive performance of a personal convenience model with a wearable sensor could reach 21%/71% and 0.7 (Cohen's kappa/accuracy/AUC (Area under a curve)) after about 200 votes. Kartsch et al. [84] developed a driver's drowsiness detection system in automobiles based on sensor fusion technology implemented in a low-power embedded processor and they reported that the developed wearable device detected five levels of drowsiness with an average accuracy of 95.2% and a battery life of 6 hours using a 200 mAh battery.

Sinnapolu et al. [85] measured and compared the heart rate and cardiac variability data for a cardiac disorder and stroke or emergency conditions that occurred using ECG (electrocardiogram) and PPG (photoplethysmography) sensors in automobiles. They used 4 cascading filters and they reported LMS (Least mean square) and Kalman filter technologies during driving showed tremendous results. Besides, these filters played an important role when they applied to sensors such as PPG in the ear

area and ECG in the chest. Paschalidis et al. [86] conducted a study to integrate the stress effect into vehicle tracking behavior by combining driving simulator and physiological sensor data into a latent variable model. It was confirmed that the existing car following models mainly influenced the driver's acceleration or deceleration decision by the surrounding traffic conditions. However, driving decisions were greatly influenced by personal characteristics and emotional states such as stress and fatigue according to research on human factors and safety.

Existing studies on bio-signals have been generally conducted in the medical field, and studies on bio-signals in automobiles have mainly been conducted to prevent drowsiness and to confirm only the health status of drivers. However, the bio-signals of the human body constantly change while driving in a car space, and there are still insufficient studies on the effects of not only driving conditions but also thermal comfort through cooling and heating on the human body of passengers. Therefore, there is a really need for research that can provide thermal comfort to a driver while driving and improve concentration on driving.

C. Objectives

Most of the previous studies on the thermal comfort in automobiles were analytical studies, and the most experimental studies on the thermal comfort of drivers were conducted by measuring only one of the bio-signals of the driver or passenger. However, it is difficult to investigate driver thermal comfort accurately by using only a single bio-signal, and the uncertainty of the experiment is high. In addition, because the condition of the driver can be comprehensively analyzed by simultaneously measuring various biological signals, such as brain waves, pulse waves, and skin temperature, the thermal comfort can be objectively and effectively investigated. Therefore, further studies based on comprehensive data on the bio-signals of drivers under various conditions are urgently needed. Although the effect of solar radiation on the indoor environment of automobiles has a significant effect on drivers, experimental research is still insufficient.

In addition, energy is excessively used because a general HVAC system is applied to the entire indoor space. Local cooling and heating can keep passengers comfortable and save energy by making a local comfortable environment around passengers. There are technologies such as a electric heater in the seat and steering wheel, thermoelectric cooling, and air blowing through the seat and back cushion, and are already spreaded in commercial market. However, many studies are just conducted to verify the effectiveness and quantify the effectiveness of local HVAC technology in terms of thermal comfort and energy saving. In particular, the technology of intensively heating using an electric or radiant heater on cold-sensitive area such as hands and feet is very effective in reducing the time to reach thermal comfort during the initial preheating period. In addition, the initial heating in EVs takes some time and the heating energy consumption is very large, thus it can be applied as the main HVAC technology of EV in combination with the convection heating method [4]. Besides, as the development of the autonomous vehicle has progressed, the driver

becomes more and more free in the car. Therefore, thermal comfort in the vehicle indoor is becoming important.

In this study, the analysis of thermal comfort of the driver according to the operation of the air conditioner and heater in the car interior during summer and winter condition was performed. In addition, in order to make the interior environment of the car in the summer and winter, the temperature and humidity were controlled in the thermal environment chamber, and solar lighting was used to simulate the solar radiation in summer and winter. In this environment, as measuring the bio-signals of the subjects in virtual driving and performing a subjective questionnaire, the thermal comfort of the driving subjects was determined according to the discharge air temperature of vents in summer and winter condition with solar irradiation. When the driver gets in a car during summer and winter season, the driver initially has thermal discomfort. To solve this problem, the ventilation seat and a cold water seat are applied in summer, and a heating seat and hot water seat are applied in winter conditions. The analysis of driver's thermal comfort was performed by measuring the driver's bio-signals and conducting a subjective questionnaire survey. In last, the driver's thermal comfort when local heating was applied to each part (chest, hand, thigh, and foot) of the subject was investigated according to the use and non-use of the HVAC system in winter.

The results of this study can be expected to provide basic data that can be applied to future vehicles such as electric and autonomous vehicles.

II. Thermal comfort and emotional signal (bio-signal) theory

A. Theory of thermal comfort

1. Relationship between humans and the thermal comfort environment

Humans have continuously developed technology to make a pleasant environment by attempting to improve the surrounding environment in order to maintain their own comfort. In modern society, unlike the old generation which realized a comfortable environment while acclimatizing to the external environment, it became possible to maintain comfort very easily by constructing an artificial environment by oneself. In addition, the interest in improving indoor comfort is increasing continuously due to pollution of the external environment with technological development. Accordingly, as the concern and awareness about energy consumption are increasing, it is important to create an environment with indoor comfort as well as energy simultaneously.

In order to investigate the relation between the indoor environment or the cabin environment of a vehicle and the thermal comfort response of human body, all sensory factors of humans must be considered, but it is a very complex and inefficient method. In order to complement this method, it is necessary to select the measurable thermal factors and the individual factors. Fig. 2.1 shows the factors to determine the thermal comfort of a car [87]. Measurable thermal factors are the physical factors for the human body's sense of temperature including the temperature, humidity, airflow, and average radiant temperature. Moreover, the individual factors mean to the metabolism and thermal resistance of clothing worn by human, and this is defined as 6 elements of the thermal environment. Besides, the persistence of the

external thermal stimulation and the exposure time for the subject's stimulation of the thermal environment are considered in more detail. Since psychological and physiological reaction factors which felt by human subjectively under the environment created by physical factors have a very large influence on the evaluation of comfort, it is very important to investigate the relation between two factors.
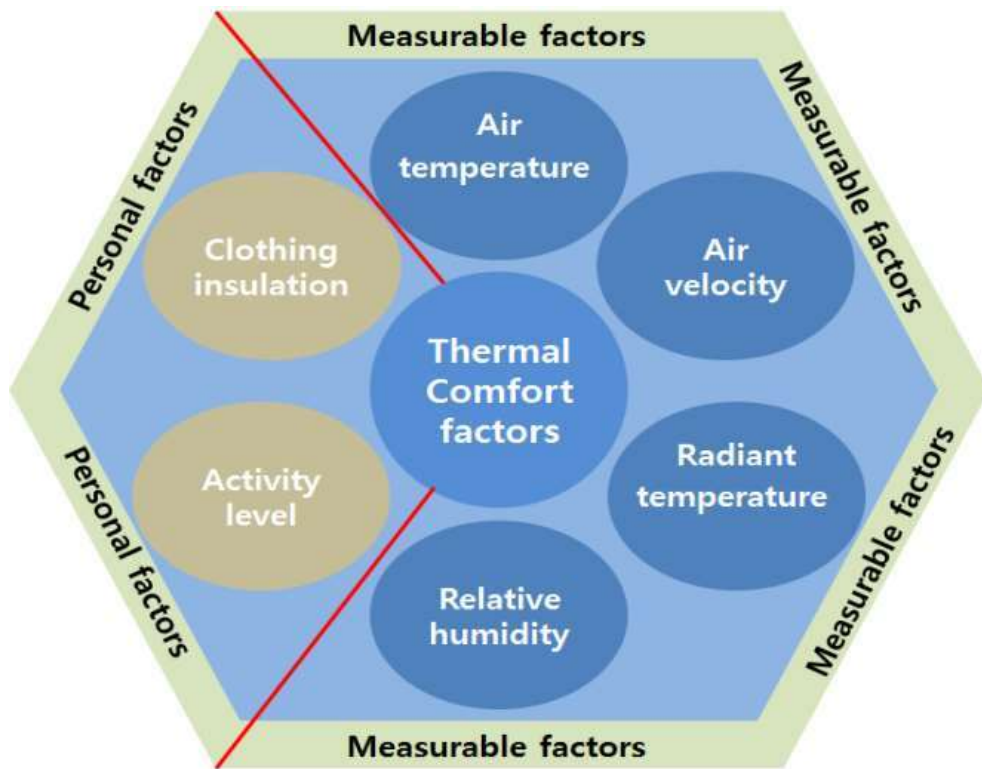
Fig. 2.1 Measurable and personal factor to determine the thermal comfort in vehicle

2. Physical factors of thermal comfort environment

(1) Air temperature

Air temperature refers to the dry bulb temperature of the air and is one of the most important physical factors, which has the significant influence on human thermal comfort [88].

(2) Humidity

Humidity directly affects by the skin and respiratory system of the human body. In low or high humidity condition, it causes discomfort because of affecting the sensation of cold and warmth to the human body. For example, the sensory temperature index decreases when the wind blows hard at low humidity. Also, it causes respiratory disease due to skin irritation and infection of mucous membranes such as the neck and bronchi because the skin and respiratory system become dry. Sweats on the skin surface do not evaporate well due to high moisture in the air under high humidity condition, so it feels hotter, the discomfort index rises. In addition, the proliferation of bacteria and fungi becomes active and these can cause various diseases of human. Therefore, in order to maintain comfort indoor condition, a comfortable environment can be maintained the indoor humidity with the range of about 30%~60% in the form of lowering the humidity when the temperature is high and increasing the humidity when the temperature is low according to the temperature condition.

(3) Air movement

Air movement is the flow of air, and air movement in the thermal environment factors means the natural wind flows into the inside from the outside or artificial air flow created by the HVAC equipment. In particular, when indoor airflow is generated by an artificial airflow fan such as an HVAC system, heat loss of the human body occurs through convective heat exchange in the human body, which affects the heat

balance of the human body. In general, the speed of comfortable air movement in a building is about 0.25~0.5 m/s, and it also requires more than 1 m/s in the summer and winter. However, the vehicle requires a higher airflow velocity than the building due to highly variable and irregular by external environmental factors [88].

(4) Mean radiant temperature

Mean radiation temperature refers to a uniform ambient temperature at which the human body in an indoor space performs the same amount of radiant heat exchange with the surrounding wall or environment. For example, when the roof and window are heated during a day with a lot of solar radiation in spite of the same environmental temperature, the human feels hot and the average radiation temperature rises. Conversely, the average radiation temperature decreases due to cold radiation near the cooled window. Since the average radiation temperature includes the shape factor of the surrounding environment and the human body, the average radiation temperature is different separately depending on where they are located. For convenience, the weighted value of the average radiant temperature of the up, down, left, right side wall is sometimes used as the average radiant temperature [88].

3. Personal factors of thermal comfort environment

(1) Activity

The activity of human refers to the amount of energy consumed in the body when the human body performs any activity, and is expressed as met (Metabolic rate). 1 met (=58.2 W/m^2) represents the amount of activity when a general adult (AD=1.8 m^2) sits in a chair under a comfortable environment to be stable. In general, the metabolism of 1.1 to 1.4 met is shown when performing a moderate task while sitting in the office. Besides, playing a basketball and wrestling, which are vigorous leisure activities, show a metabolism of 5.0 to 8.7 met. The metabolic rate for each activity are shown in Table 2.1 [88].

Table 2.1 Typical metabolic heat generation for various activities

Item		W/m^2	met[*]
Resting	Sleeping	40	0.7
	Reclining	45	0.8
	Standing, quiet	60	1.0
	Standing, relaxed	70	1.2
Walking(on level surface)	3.2 km/h (0.9 m/s)	115	2.0
	4.3 km/h (1.2 m/s)	150	2.6
	6.4 km/h (1.8 m/s)	220	3.8
Office activities	Reading, seated	55	1.0
	Writing	60	1.0
	Typing	65	1.1
	Filing, seated	70	1.2
	Filing, standing	80	1.4
	Walking about	100	1.7
	Lifting/packing	120	2.1
Driving/Flying	Car	60~115	1.0~2.0
	Aircraft, routine	70	1.2
	Aircraft, instrument landing	105	1.8
	Aircraft, combat	140	2.4
	Heavy vehicle	185	3.2
Miscellaneous occupational activities	Cooking	90~115	1.6~2.0
	Housecleaning	115~200	2.0~3.4
	Seated, heavy limb movement	130	2.2
	Maching work — Sawing (Table saw)	105	1.8
	Maching work — Light (Electric industry)	115~140	2.0~2.4
	Maching work — Heavy	235	4.0
	Handling 50kg bags	235	4.0
	Pick and shovel work	235~280	4.0~4.8
Miscellaneous leisure activities	Dancing, social	140~255	2.4~4.4
	Calisthenics/exercise	175~235	3.0~4.0
	Tennis, singles	210~270	3.6~4.0
	Basketball	290~440	5.0~7.6
	Wrestling, competitive	410~505	7.0~8.7

Sources: Compiled from various sources. For additional information, see Buskirk (1960), Passmore and Durnin (1967), and Webb (1964).
[*]1 met=58.1 W/m^2

(2) Clothing

Clothing is defined as the amount of clothing wearing by the human body or insulation. By adjusting the clothing, the heat loss on the surface of the human body exposed to the external environment can be controlled. The unit of clothing is clo, and the thermal resistance value from the wearing state to the skin surface in equilibrium with the metabolism of 1 met is 1 clo under the indoor conditions; temperature of 21°C, relative humidity of 50%, and air flow velocity of 0.5 m/s. It is marked as 1 clo=0.155 $m^2 \cdot °C/W$. As the most common method to measure the insulation of clothing, the value of clothing is defined after measuring using thermal manikin, and then it is possible to calculate an exact value of the amount of clothing by comparing and correcting the value through an actual human experiment. Table 2.2 shows the amount of clothing for various clothes [88].

Table 2.2 Garment insulation values

Item		Value	Item		Value
Garment description[a]		$I_{clo,i}$, clo[b]	Garment description[a]		$I_{clo,i}$, clo[b]
Under-wear	Briefs	0.04	Trousers and coveralls	Short Shorts	0.06
	Panties	0.03		Walking shorts	0.08
	Bra	0.01		Straight trousers (thin)	0.15
	T-shirt	0.08		Straight trousers (thick)	0.24
	Full slip	0.16		Sweatpants	0.28
	Half slip	0.14		Overalls	0.30
	Long top	0.20		Coveralls	0.49
	Long bottoms	0.15			
Footwear	Ankle socks	0.02	Suit jackets and vests	Single-breasted (thin)	0.36
	Calf socks	0.03		Single-breasted (thick)	0.44
	Knee socks (thick)	0.06		Double-breasted (thin)	0.42
	Panty hose	0.02		Double-breasted (thick)	0.48
	Sandals/throngs	0.03		Sleeveless vest (thin)	0.10
	slippers	0.03		Sleeveless vest (thick)	0.17
	boots	0.10			
Shirts and blouses	Sleeveless, scoop-neck blouse	0.12	Sweaters	Sleeveless vest (thin)	0.13
	Short-sleeve, dress	0.19		Sleeveless vest (thick)	0.22
	Long-sleeve, dress	0.25			
	Long-sleeve, flannel	0.34		Long-sleeve (thin)	0.25
	Short-sleeve, knit sport	0.17		Long-sleeve (thick)	0.36
	Long-sleeve, sweat	0.34			

Dresses and skirts	Skirt (thin)	0.14	Sleepwear and Robes	Sleeveless, short gown	0.18
	Skirt (thick)	0.23		Sleeveless, Long gown	0.20
	Long-sleeve, shirtdress (thin)	0.14		Short-sleeve hospital gown	0.31
	Long-sleeve, shirtdress (thick)	0.23		Long-sleeve, long gown	0.46
				Long-sleeve, pajamas (thick)	0.57
	Short-sleeve, shirtdress (thin)	0.29		short-sleeve, pajamas (thin)	0.42
	Sleeveless, scoop neck(thin)	0.23		Long-sleeve, long wrap robe (thick)	0.69
	Sleeveless, scoop neck (thick)	0.27		Long-sleeve, short wrap robe (thick)	0.48
				Short-sleeve, short robe (thin)	0.34

a : "Thin" garments are summer weight, "thick" garment are winter weight.

b : 1 clo=0.155 $(m^2 \cdot K)/W$

c : Knee-length

(3) Age

In general, the amount of activity decreases with age and it is easily susceptible to the cold and warm feeling. Moreover, it is greatly affected by changes in the surrounding environment [88].

(4) Sex

Women generally has a lower skin temperature than men and heat loss due to evaporation on the skin surface is smaller than that of men. In case of woman, there is a slight difference from men in the perception of the cold and warm feeling and the range of comfortable thermal environments because woman wear thin clothes and the body composition is slightly different [88].

4. PMV (Predicted mean vote)

PMV is defined in ISO 7730 [89] as an index that predicts the voting average of a large group on a 7-point thermal sensation scale based on the heat balance of the human body. PMV is calculated by various combinations such as metabolism, amount of clothing, air temperature, average radiant temperature, air velocity and humidity, and is expressed by Eq. (2-1). PMV is expressed as -3 (cold), +3 (hot), and 0 is thermally neutral based on a 7 steps scale. In general, the predicted mean vote that occupants feel comfortable is the range of -0.5 to +0.5.

$$PMV = [0.303 \cdot \exp(-0.036 \cdot M) + 0.028] \cdot$$
$$\left\{ \begin{array}{l} (M-W) - 3.05 \cdot 10^{-3} \cdot [5733 - 6.99 \cdot (M-W) - p_a] - 0.42 \cdot [M-W) - 58.15] \\ -1.7 \cdot 10^{-5} \cdot M \cdot (5867 - p_a) - 0.0014 \cdot M \cdot (34 - t_a) \\ -3.96 \cdot 10^{-8} \cdot f_{clo} \cdot [(t_{clo} + 273)^4 - (\overline{t_r} + 273)^4] - f_{clo} \cdot h_c \cdot (t_{cl} - t_a) \end{array} \right\}$$

(2-1)

Where,

$$t_{clo} = 35.7 - 0.028 \cdot (M-W)$$
$$- I_{clo} \cdot \left\{ 3.96 \cdot 10^{-8} \cdot f_{clo} \cdot [(t_{clo} + 273)^4 - (\overline{t_r} + 273)^4] + f_{clo} \cdot h_c \cdot (t_{clo} - t_a) \right\}$$

(2-2)

$$h_c = \left\{ \begin{array}{ll} 2.38 \cdot |t_{clo} - t_a|^{0.25} & \text{f or } 2.38 \cdot |t_{clo} - t_a|^{0.25} > 12.1 \cdot \sqrt{v_{ar}} \\ 12.1 \cdot \sqrt{v_{ar}} & \text{f or } 2.38 \cdot |t_{clo} - t_a|^{0.25} < 12.1 \cdot \sqrt{v_{ar}} \end{array} \right.$$

(2-3)

$$f_{clo} = \left\{ \begin{array}{ll} 1.00 + 1.290 I_{clo} & \text{f or } I_{clo} \leq 0.078 m^2 \cdot K/W \\ 1.05 + 0.645 I_{clo} & \text{f or } I_{clo} > 0.078 m^2 \cdot K/W \end{array} \right.$$

(2-4)

Where, M is metabolic rate, W is effective mechanical power, I_{clo} is clothing insulation, f_{clo} is clothing surface area factor, t_a is air temperature, $\overline{t_r}$ is mean radiant temperature, v_{ar} is relative air velocity, p_a is partial water vapour pressure.

5. PPD (Predicted Percentage of Dissatisfied)

PPD is an index that quantitatively predicts the proportion of thermally dissatisfied people who feel too cool or too hot [89]. For the purposes of these international standard, those who are thermally dissatisfied are those who voted hot, warm, cool and cold on the 7-point thermal sensation scale. Generally, occupants feel comfortable when the PPD value is under 10%. When the PMV value is determined, PPD is calculated using Eq. (2-5), and the relationship between PMV and PPD is shown in Fig. 2.2.

$$PPD = 100 - 95 \cdot \exp(-0.03353 \cdot PMV^4 - 0.2179 \cdot PMV^2) \hspace{2cm} \text{(2-5)}$$
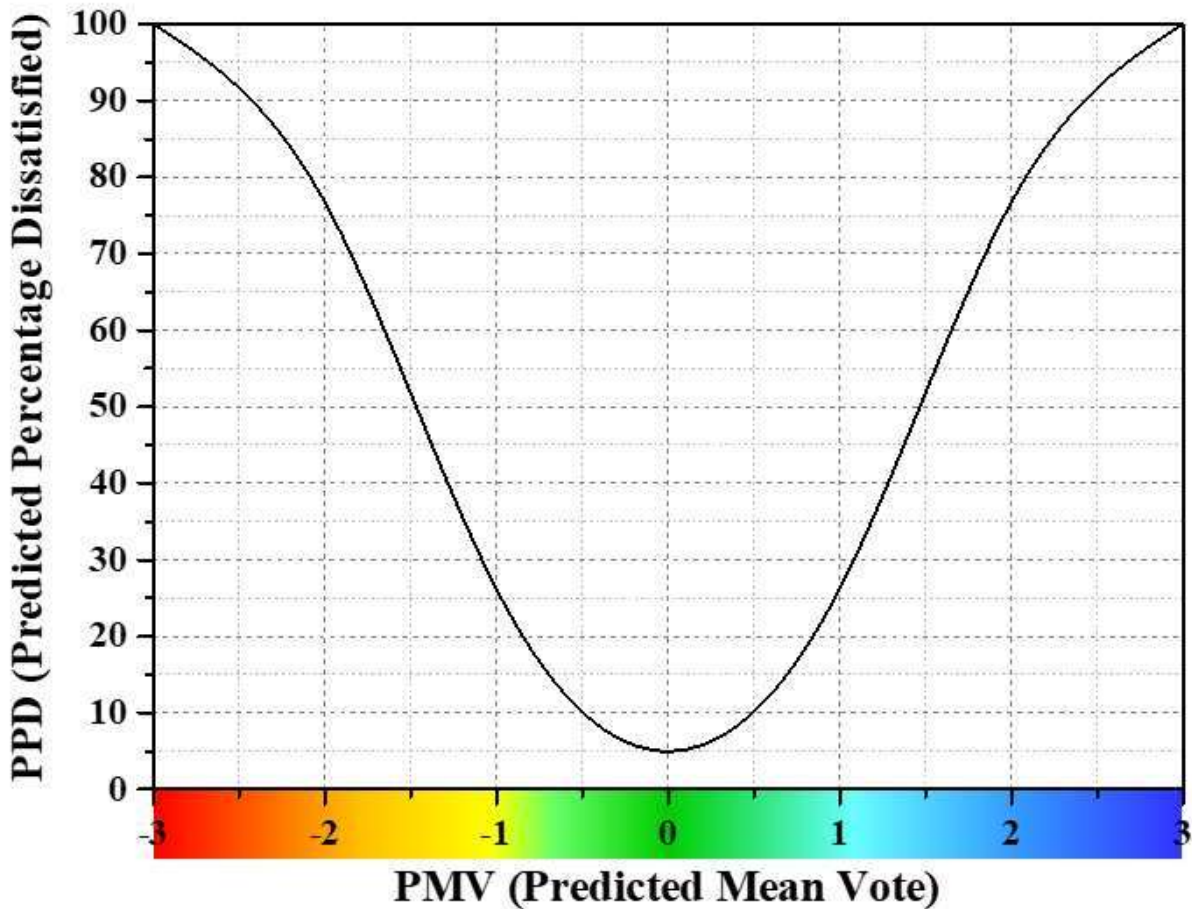
Fig. 2.2 PPD as function of PMV

B. Emotional signals of the human body

1. Overview of emotional signals (bio-signals)

Emotional signals are signals that scientifically analyze the complex emotions, which occur inside human due to sensation and perception. Besides, that respond to physical stimuli obtained through user experience. By using these signals, a lot of researches have been actively conducted both domestically and internationally for improving product quality and designing a comfortable environment system. In particular, a signal, that quantitatively measures and evaluates human emotions among the emotional signals, is called a bio-signal and generally refers to an internal and external reaction of the human body that occurs when a person takes any stimulus action internally or externally. Bio-signals refer to physical and chemical signals obtained from human body organs such as muscles, blood and organs including the brain and heart. As a example for practical applications, there is a method of analyzing the internal structure of the human body by simple palpation of a doctor, hormone test through blood sampling, and advanced medical equipment such as CT (Computed Tomography). In order to measure various bio-signals, the accurate data must be obtained through the signal processing process because the signal is very weak and contains a large number of noises. The example for signal processing process is shown in Fig. 2.3.
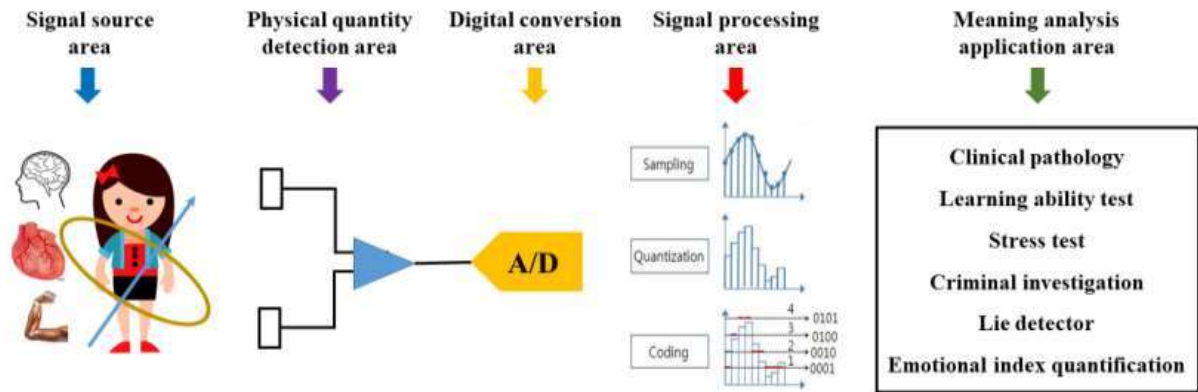
Fig. 2.3 Bio-signal processing

The signal source area means an area to generate signals, and signal outputs are in various forms and sources of occurrence include the brain, heart, and muscle. The physical quantity detection area is an area in which a desired signal is extracted after converting the generated signal into an electrical signal. As a first step, a sensor is required. In general, an electrode is used to measure a current in the skin surface or muscle. However, the obtained signal is very weak and contains some noise. Thus, after amplifying the signal and filtering out unnecessary noise, the necessary signal is extracted. The digital conversion area converts this to a digital signal because the signal extracted from the sensor part of the physical quantity detection area is an analog signal.

Signal-processing area includes complex from simple functions that display waveform in real time, save or load files to functions that perform frequency analysis, correlation coefficient, and spectrum analysis using mathematical processing. The semantic analysis application area is to apply and utilize the signal-processed data.

2. EEG (Electroencephalogram)

The nervous system is divided into the central and the peripheral nervous system. The nervous system transmits command from the central nervous system composed of the brain and spinal cord to the peripheral nervous system or transmits external stimuli felt in the peripheral nervous system to the brain. Among them, the brain is an organ with a weight of about 1.6 kg located inside the skull and can perform high-dimensional mental functions such as recognition, memory, learning, association, and language. In addition, it plays a role of a reflex center. The brain consists of gray matter, white matter, ventricle, and cerebrovascular system. Among them, gray matter consists of cerebral cortex, cerebellar cortex, nucleus, and it contains most of the neurons. The ventricle fills with spinal fluid and plays a role in protecting from external shock.

The cerebral hemisphere is located at the top part of the brain and accounts for about 83% of the total weight of the brain, and it is the most important part of the central nervous system. The surface of the cerebrum is wrinkled, and the wrinkles are composed of cerebral sulci and cerebral gyri, and are composed of several cerebral lobes by the sulci of cerebral.

The frontal lobe is the primary motor cortex, which controls muscle movement, is in charge of speech and thought activities, and is known as an indicator of arousal and attention. The temporal lobe is known to receive auditory information as the primary auditory area and recognize olfactory stimuli. The parietal lobe is known to play a role in sensory recognition such as tactile, pain, and position. In addition, it charges for perception, integration of cognitive information, and memory control as the primary sensory area. The occipital lobe is known to recognize visual stimuli and control visual information as the primary visual area. Fig 2.4 shows the location of each cerebral lobe.
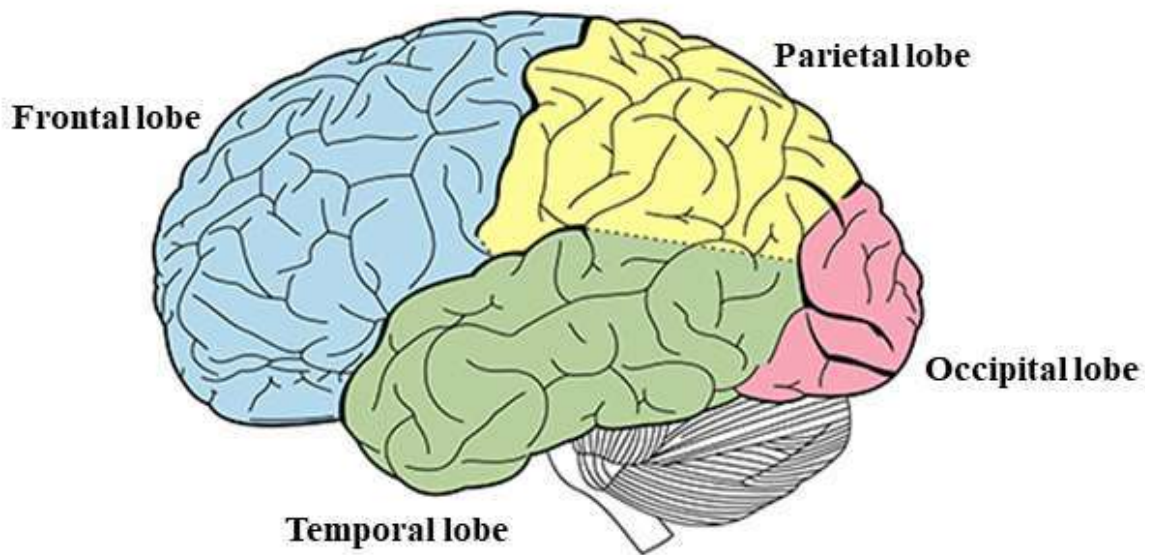
Fig. 2.4 Location of each lobe of the cerebral hemispheres

Electroencephalography (EEG) is a kind of bioelectrical signal that has been continuously studied since Caton who first recorded the brain waves of animals in 1875, and Berger first measured brain waves by attaching electrodes to the human scalp in 1929. EEG is defined as recorded on the intact scalp with the potential as the vertical axis and the time as the horizontal axis by amplifying and filtering this signal which deriving the summation of brain electrical activity generated by neurons in the cerebral cortex to the outside of the body. Depending on the installation method or electrode, EEG measurement methods include scalp EEG which is attached to the scalp to measure and analyze brain wave non-invasively, and intracranial EEG which directly attaches a sensor to the brain after opening the skull. In general, EEG measurement means scalp EEG. It is because it is objective, continuous, and non-invasive, so there is no sequela after measurement. The scalp EEG shows the form of potential fluctuation with a frequency of 1–60 Hz and 5–300 μV.

EEG is a signal measured by the numerous activities of neurons in the brain, and it vibrates rapidly in short period of time. There is a potential deviation between individuals. When observing EEG, it can be classified according to frequency and amplitude. It is divided as δ wave (0.5～3.99 Hz), θ wave (4～7.99 Hz), α wave (8

~12.99 Hz), β wave (13~30 Hz), and γ wave(30~50 Hz). Fig. 2.5 shows the types of the basic EEG waveform [90].

The δ wave is a waveform that shows a large amplitude of an average of 100~200 μV in the frequency range of 0.5~3.99 Hz. It is generally occurred in deep sleep state in normal people, and also in coma with brain neurological diseases such as epilepsy and dementia. Fig. 2.5(a) shows the basic waveform of the δ wave.

The θ wave is a slow wave with an amplitude of 20~100 μV in the frequency band of 4~7.99 Hz. It is an EEG wave that is mainly expressed in the light sleep situation and in the mental stability through meditation. EEG rhythm during human sleep shows δ wave and θ wave with a constant period. When the θ wave appears dominantly, it is referred to as REM sleep. When the δ wave is predominant, it is defined as NREM sleep. Fig. 2.5(b) shows the basic waveform of the θ wave.

The α wave is the most basic and representative waveform of human brain waves, and shows a regular and continuous waveform with an average of 50 μV potential fluctuations at a frequency of 8~13 Hz. In general, it is mainly observed in the parietal and occipital lobes, and tends to be suppressed in the frontal lobe. The α wave appears constant in a stable state with eyes closed. When the brain changes an arousal state through an open eye, looking at an object, performing learning, or performing mathematical operations, α wave is suppressed and β wave tends to be activated. This is called α-wave deactivation or blocking phenomena. The α wave is related to the development of the brain. The α wave in infancy represents the frequency band of 4~6 Hz, and when someone becomes an adult, it represents a normal frequency band. Fig. 2.5(c) shows the basic waveform of the α wave.

The β wave is a wavelength that appears dominant in the center of the brain and the frontal lobe, and is a fast wave of irregular waveform with a frequency band of 13~30 Hz and an amplitude of 2~20 μV. It is caused by mental activities such as arithmetic, learning, and language transfer or by physical movement that directly move the body. Besides, it is a brain wave that dominate all conscious activities which use human senses. In addition, the β-wave is not occurred only in the awakening state,

but the β wave can also be occurred in situations such as tense or excited state. Fig. 2.5(d) shows the basic waveform of the β wave.

The γ wave is a brain wave with a frequency band of 30 Hz or more and is faster than the β wave. That is found in the entire brain and is a brain wave that harmonizes and unify the processing signals of each brain. It is mainly manifested in intense sports events or complex activities that solve math problem which requires advanced computation, and it is also manifested in extreme anxiety, excitement, and stress. Fig. 2.5(e) shows the basic waveform of the γ wave.

The electrode sensor attachment method used for recording scalp EEG as follows the International 10-20 system [91]. This anatomically draws an imaginary line based on the center of the scalp with the nasion of the forehead bone and the nasal bone, the inion of the occipital region, and the upper part of both earlobes. When the distance from each point to the center of the scalp is assumed to 50%, it is a method of holding the electrode at the ratio of 20%, 20%, and 10%. Each electrode location is named according to the positions from front to back and side to side of the head hemisphere. The frontal lobe is named F, the parietal lobe is P, the calvaria is C, the temporal lobe is T, the occipital lobe is named O, and the electrode is arranged as the left brain side is odd numbered and the right brain side is even numbered. Fig. 2.6 shows the EEG electrode attachment location according to the International 10-20 system.

(a) Basic waveform of δ wave

(b) Basic waveform of Ө wave

(c) Basic waveform of α wave

(d) Basic waveform of β wave

(e) Basic waveform of ɤ wave

Fig. 2.5 Classification for basic waveforms of brain waves
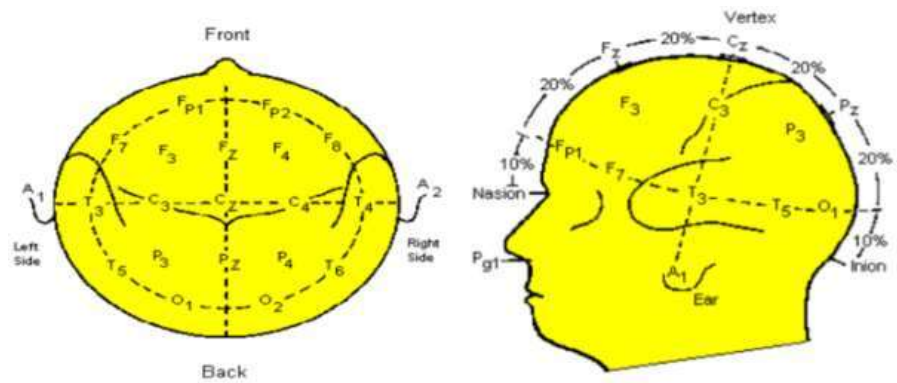
Fig. 2.6 International 10-20 system

3. PPG (Photoplethysmography)

When the blood is discharged from the heart, blood pressure rises at the origin of the aorta and expands the blood vessels. PPG (photoplethysmograph) is to measure and analysis the pulsation during delivery to the peripheral blood vessels due to the increase of blood pressure and exceeding the inertia of the blood vessels in the aorta at a finite rate as time passes continuously. Figs. 2.7 and 2.8 show the basic waveform of the PPG and the measurement and analysis process of PPG, respectively [92].

The type of pulse wave is divided into a blood flow pulse wave that waveform the flow of blood released from the heartbeat at a certain artery area, a pressure pulse wave that waveform the pressure of the blood vessels which delivered the released blood along the arterial wall, and a diameter pulse wave that waveform the diameter of a blood vessel at a certain part with a changes of heartbeat.
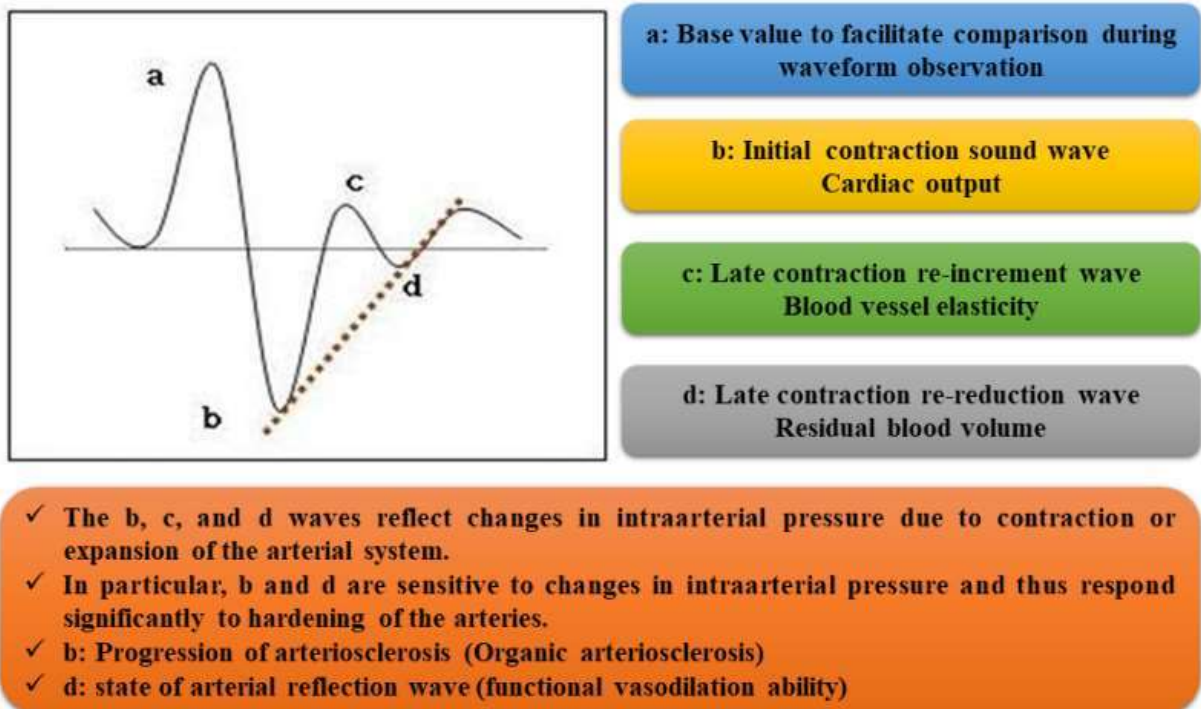
Fig. 2.7 The basic rhythm of the PPG
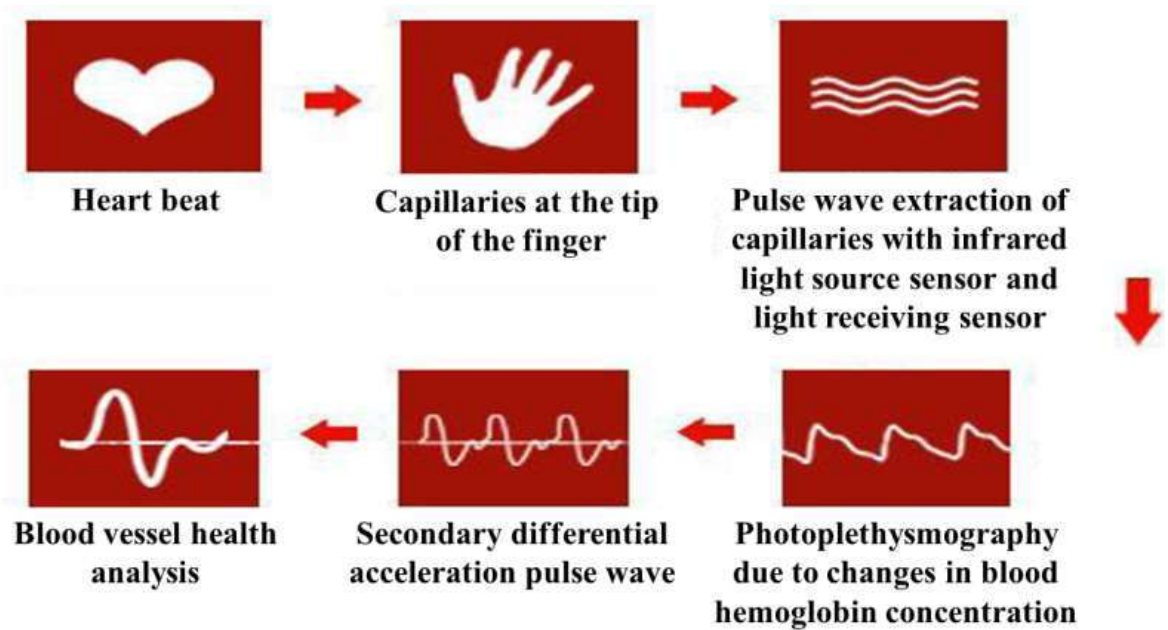
Fig. 2.8 PPG measurement and analysis process

In this experiment, a pulse wave was measured using a diameter (volume) pulse wave. A representative measurement method for measuring a diameter pulse wave is the PPG (Photoplethysmographypulse) method. This method is the same as irradiating the infrared rays to the peripheral blood vessels at the fingertips, but it is divided into a reflection method for detecting the reflected light and a transmission method for detecting transmitted light. In this study, pulse waves were measured by a pulse wave measuring device which was applied the transmitted method. In the transmission method, unlike the reflection method, the light-receiving sensor is located on the opposite side with the finger as the center, so that the light irradiated from the light-emitting unit passes through the finger to detect the amount of light transmitted from the light-receiving unit. Since the hemoglobin component of the blood has the property of absorbing light, the reflected signal which compared to the transmittance in the capillaries is converted and analyzed when light is irradiated. At this time, the absorption rate of light represents the maximum value of the heart rate systolic blood pressure and the minimum value of the diastolic blood pressure. Fig. 2.9 shows the measurement principle of PPG device used in this experiment [92].

The basic nerve that controls the cardiovascular system is the autonomic nervous system. The autonomic nervous system is divided into the parasympathetic nerve and the sympathetic nerve. The parasympathetic nerve appears in a stabilized state, and the sympathetic nerve appears in a state of excitement and tension. According to the balance of these two nerves, the waveform of the pulse wave changes, and the standard deviation and mean deviation of the pulse can be calculated in order to evaluate the body homeostasis index and stress hyperactivity. The measured pulse wave is used to determine the emotional state of the subject by investigating the state of the sympathetic nerve and the parasympathetic nerve in various fields such as clinical medicine, biopsychology, and emotional engineering.
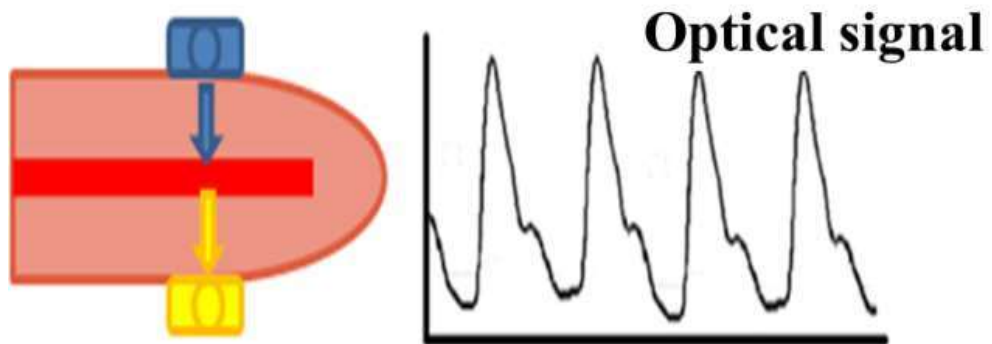
Fig. 2.9 PPG measurement method (Transparent mode)

4. Skin temperature

As shown in Fig. 2.10, the activity of enzymes which is involved in the metabolism of the body, varies greatly depending on the temperature of the environment, thus maintaining the optimum temperature range is important for maintaining life activities. The human body maintains the body temperature of 36.5°C regardless of the external temperature, and the control mechanism of body temperature operates when it is out of the normal body temperature. The purpose of controlling the body temperature of the human body is to maintain the central body temperature (core temperature). Central body temperature refers to the temperature of the central nervous system and the internal structures which are in the abdominal cavity and thoracic cavity. The central body temperature is adjusted to about 37°C under normal condition. In the hypothalamus, there is a body temperature control center that includes both a heat loss and a heat generation center, and information about the central body temperature is transmitted from the central thermoreceptor to the body temperature control center. Under the control of the hepatocerebral hypothalamus, the body temperature is controlled by adjusting the amount of heat dissipation through the surface of the body and the amount of heat generation in the body by the negative feedback action. The basis of body temperature control is to adjust the amount of blood near the skin, and when low-temperature stimulation is received, the blood flow rate to the skin is reduced to suppress heat dissipation. Conversely, when high-temperature stimulation is received, it increases blood flow rate to promote the heat dissipation. The temperature of the external environment is maintained within a narrow range of the thermoneutral zone (25°C~30°C), and changes of blood flow to the skin are sufficient to maintain body temperature. The regulation of body temperature is controlled by the action of the sympathetic nerve. In other words, when sympathetic nerve activity decreases, simple relaxation of blood vessels occurs, blood flow rate to the skin increases, therefore more heat is transferred to the external environment. When the outside temperature goes out of the thermoneutral

zone, other body temperature control organs operate to maintain body temperature [93].
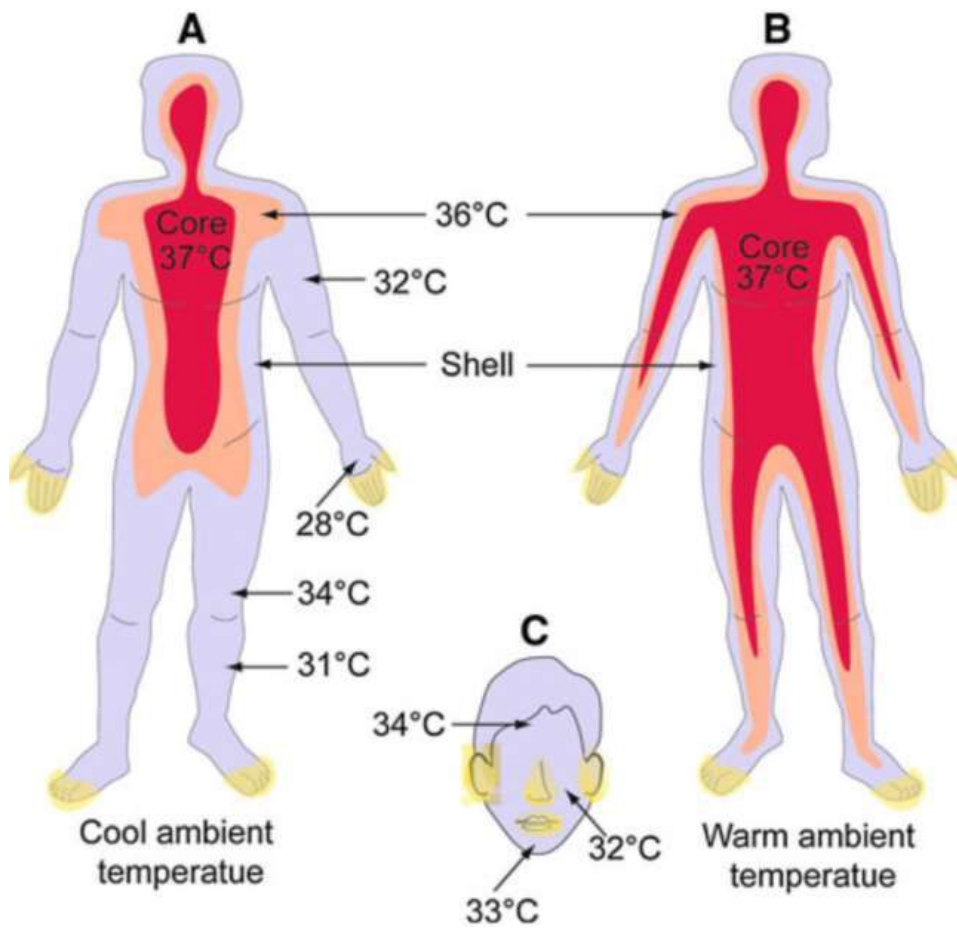
Fig. 2.10 Temperature change of body under cold and hot environment

III. Automotive indoor thermal environment modeling and analytical method

A. Automotive indoor thermal environment modeling

In this study, in order to analyze the thermal environment of automotive indoor in summer and winter condition, the construction of a vehicle indoor was modeled using CATIA V5 R18, which is widely used as a commercial software, and thermal flow analysis was performed using the ANSYS Fluent. Fig. 3.1 shows the modeling of thermal environment of the automobile indoor used in this study. Fig. 3.2 shows the shape of the indoor of automotive using a water thermal seat (cold and hot water seats). The size of the automotive indoor environment excluding the HVAC duct is 1.561 m×2.644 m×1.561 m, which is about 6.44 m^3. In the modeling of thermal environment of automobile indoor, the vent at the upper part of the driver's seat is directed toward the driver's head so that the driver is more affected by the wind blowing from the HVAC duct.
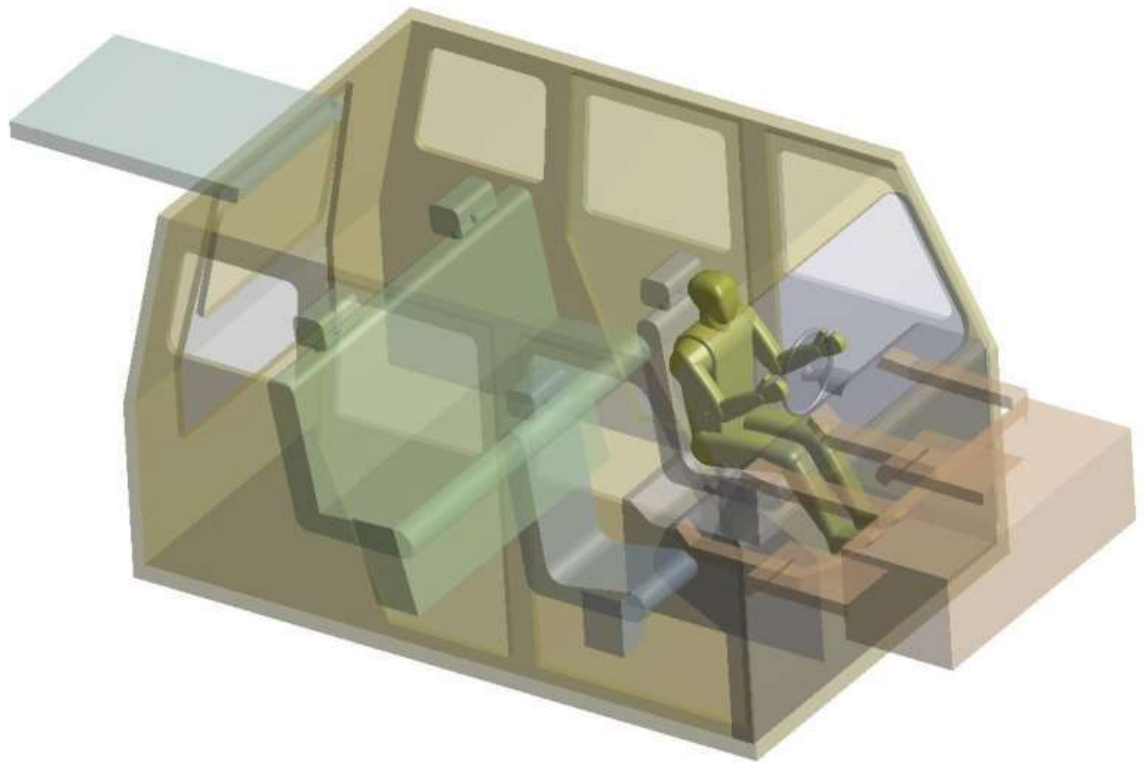
Fig. 3.1 3D modeling of automotive indoor environment
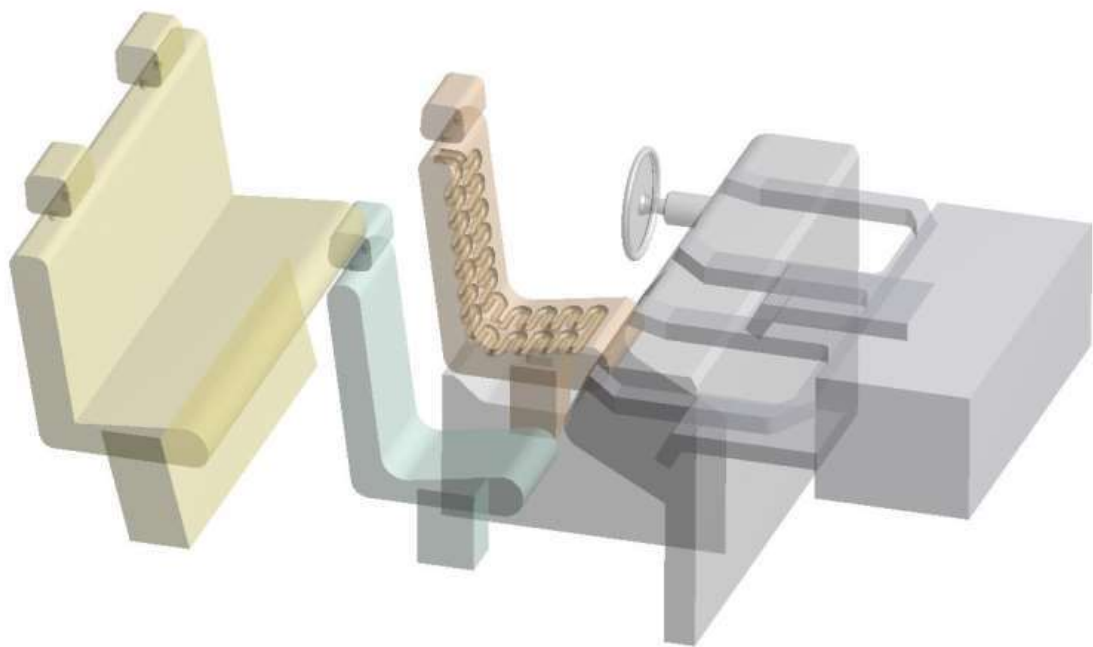
Fig. 3.2 Schematic diagram of automobile inside using the water thermal seat

B. Governing equations

In this study, the three-dimensional Reynolds average Navier-Stokes governing equation was used for the analysis of the automotive indoor thermal environment in summer and winter conditions. The continuity equation used in this study is shown in Eq. (3-1).

$$\frac{d\rho}{dt} + \nabla \cdot (\rho \vec{v}) = 0 \tag{3-1}$$

The momentum equation is expressed as Eq. (3-2).

$$\frac{\partial}{\partial t}(\rho \vec{v}) + \nabla \cdot (\rho \vec{v}\vec{v}) = -\nabla p + \nabla \cdot (\bar{\tau}) + \rho \vec{g} \tag{3-2}$$

where, ρ is density, v is velocity, p is static pressure, $\vec{g}$ is gravitational body force, $\bar{\tau}$ is stress tensor, which can be expressed as Eq. (3-3).

$$\bar{\tau} = \mu \left[(\nabla \vec{v} + \nabla \vec{v}^T) - \frac{2}{3} \nabla \cdot \vec{v} I \right] \tag{3-3}$$

where, μ is the viscosity coefficient and I is the unit tensor. The energy equation is expressed by Eq. (3-4).

$$\frac{\partial}{\partial t}(\rho E) + \nabla \cdot (\vec{v}(\rho E + p)) = \nabla \cdot \left(k_{eff} \nabla T - \sum_j h_j \vec{J_j} + (\overline{\tau_{eff}} \cdot \vec{v}) \right) + S_h \tag{3-4}$$

where k_{eff} is the thermal conductivity, $\vec{J_j}$ is the diffusion flux of jth chemical species, S_h is the source term of the chemical reaction, E is the total energy per

unit mass, and T is the temperature. Total energy per unit mass can be expressed as Eq. (3-5).

$$E = h - \frac{p}{\rho} + \frac{v^2}{2} \tag{3-5}$$

Here, in the case of incompressible flow, enthalpy is $h = \sum_j Y_j h_j + \frac{p}{\rho}$, and Y_j is the mass fraction of jth chemical species, $h_j = \int_{T_{ref}}^{T} c_{p,j} dT.$

In this study, the Realizable $k-\varepsilon$ turbulence model is applied, which is the turbulence model proposed by Shih et al. [94]. The Realizable $k-\varepsilon$ turbulence model is applied a new eddy viscosity formula and a new model equation for dissipation based on the dynamic equation of the mean-square vorticity fluctuation. The meaning of 'Realizable' means satisfying a certain mathematical limitation on the mean stress consistent with the physical behavior of turbulent flow. The k and ε of the Realizable $k-\varepsilon$ turbulence model are shown in Eqs. (3-6) and (3-7).

$$\frac{\partial}{\partial t}(\rho k) + \frac{\partial}{\partial x_i}(\rho k u_j) = \frac{\partial}{\partial x_i}\left[\left(\mu + \frac{\mu_t}{\sigma_k}\right)\frac{\partial k}{\partial x_i}\right] + G_k + G_b - \rho\varepsilon - Y_M + S_k \tag{3-6}$$

$$\frac{\partial}{\partial t}(\rho\varepsilon) + \frac{\partial}{\partial x_i}(\rho\varepsilon u_j) = \frac{\partial}{\partial x_i}\left[\left(\mu + \frac{\mu_t}{\sigma_\varepsilon}\right)\frac{\partial}{\partial x_i}\right] + \rho C_1 S_\varepsilon - \rho C_2 \frac{\varepsilon^2}{k + \sqrt{\nu\varepsilon}} + C_{1\varepsilon}\frac{\varepsilon}{k}C_{3\varepsilon}G_b + S_\varepsilon \tag{3-7}$$

where,

$$C_1 = \max\left[0.43, \frac{\eta}{\eta + 5}\right], \quad \eta = S\frac{k}{\varepsilon} \tag{3-8}$$

G_k is the generation of turbulent kinetic energy due to the mean velocity gradients, G_b is the generation of turbulent kinetic energy due to buoyancy, and Y_M represents the contribution of the fluctuating dilatation in compressible turbulence to the overall dissipation rate. $C_{1\varepsilon}$ and C_2 are constant. σ_k and σ_ε are the turbulent Prandtl numbers. S_k and S_ε are user-defined source terms.

G_k is defined by Eq. (3-9) from the exact equation for the transport of k.

$$G_k = -\overline{\rho u_i u_j} \frac{\partial u_j}{\partial x_i} \tag{3-9}$$

To evaluate G_k in a manner consistent with the Boussinesq hypothesis, it is expressed as Eq. (3-10).

$$G_k = \mu_t S^2 \tag{3-10}$$

where S is the modulus of the mean rate-of-strain tensor, defined as Eq. (3-11). S_{ij} is given by Eq. (3-12).

$$S = \sqrt{2 S_{ij} S_{ij}} \tag{3-11}$$

$$S_{ij} = \frac{1}{2}\left(\frac{\partial u_i}{\partial xj} + \frac{\partial u_j}{\partial x_i} \right) \tag{3-12}$$

G_b is the term for generation of k due to buoyancy, and corresponds to the case where a gravity field and a temperature gradient exist at the same time, and contributes significantly to the generation of ε. G_b is expressed as the following Eq. (3-13).

$$G_b = \beta g_i \frac{\mu_t}{\mathrm{Pr}_t} \frac{\partial T}{\partial x_i} \tag{3-13}$$

Pr_t is the turbulent Prandtl number for energy and g_i is the component of the gravitational vector in the ith direction. μ_t which is the vortex or turbulent viscosity is a combination of k and ε. μ_t is expressed as the following Eq. (3-14).

$$\mu_t = \rho C_\mu \frac{k^2}{\varepsilon} \tag{3-14}$$

In Eq. (3-14), C_μ is a constant.

Y_M is the dilation dissipation term, and can be included in the k equation. This term is proposed by Sarkar et al. [95] and is shown in Eq. (3-15).

$$Y_M = 2\rho \varepsilon M_t^2 \tag{3-15}$$

where, M_t is the turbulent Mach number, and it is defined as Eq. (3-16).

$$M_t = \sqrt{\frac{k}{a^2}} \tag{3-16}$$

In this analysis, the S2S radiation model was used in ANSYS Fluent to apply the solar radiation. The S2S radiation assumes the surfaces to be gray and diffuse. Emissivity and absorptivity of a gray surface are independent of the wavelength. Also, by Kirchoff's law, the emissivity equals the absorptivity ($\varepsilon = \alpha$). For a diffuse surface, the reflectivity is independent of the outgoing(or incoming) directions. The

gray-diffuse model is what is used in ANSYS Fluent. Also, as stated earlier, the exchange of radiative energy between surface is virtually unaffected by the medium that separates them. Thus, according to the gray-body model, when a certain amount of radiant energy (E) is incident on a surface, a fraction (ρE) is reflected, a fraction (αE) is absorbed, and a fraction (τE) is transmitted. Since for most applications the surfaces in question are opaque to thermal radiation (in the infrared spectrum), the surfaces can be considered opaque.

In this study, in order to understand the effect of radiation on thermal comfort, the S2S radiation model was used to calculate the radiation exchange of the enclosure computational areas with gray-diffuse surfaces. This model uses a view factor that includes information such as size, distance, and direction of the two surfaces to calculate energy exchange between the two surfaces. The S2S model ignores absorption, emission, and scattering of radiation, and only analyzes surface-to-surface radiation [96].

The energy flux leaving a surface is composed of directly emitted and reflected energy. The reflected energy flux is dependent on the incident energy flux from the surroundings, which can be expressed in terms of the energy flux leaving all other surfaces as shown in Eq. (3-17).

$$q_{out,k} = \varepsilon_k \alpha T_k^4 + \rho_k q_{in,k} \qquad\qquad (3\text{-}17)$$

where $q_{out,k}$ is the energy flux leaving the surface, ε_k is the emissivity, σ is the Stefan-Boltzmann constant, and $q_{in,k}$ is the energy flux incident on the surface from the surroundings. The incident energy flux $q_{in,k}$ can be expressed as Eq. (3-18).

$$A_k q_{in,k} = \sum_{j=1}^{N} A_j q_{out,k} F_{jk} \qquad\qquad (3\text{-}18)$$

where, A_k is the area of surface k and F_{jk} is the view factor between surface k and j. For N surfaces, it can be expressed as shown in Eq. (3-19) using the view factor reciprocity relationship.

$$A_j F_{jk} = A_k F_{kj} \text{ for } j = 1, 2, 3, \dots N \tag{3-19}$$

Accordingly, the incident energy flux $q_{in,k}$ and the emitted energy flux $q_{out,k}$ can be expressed as Eqs. (3-20) and (3-21), respectively.

$$q_{in,k} = \sum_{j=1}^{N} F_{kj} q_{out,j} \tag{3-20}$$

$$q_{out,k} = \varepsilon_k \sigma T_k^4 + \rho k \sum_{j=1}^{N} F_{kj} q_{out,j} \tag{3-21}$$

which can be re-written as Eq. (3-22).

$$J_k = E_k + \rho_k \sum_{j=1}^{N} F_{kj} J_j \tag{3-22}$$

where, J_k represents the energy that is given off(or radiosity) of surface k, and E_k represents the emissive power of surface k. This represents N equation, which can be recast into matrix form as Eq. (3-23).

$$KJ = E \tag{3-23}$$

where K is an $N \times N$ matrix, J is the radiosity vector, and E is the emissive power vector.

Eq. (3-23) is referred to as the radiosity matrix equation. The view factor between two finite surfaces i and j is given by Eq. (3-24).

$$F_{ij} = \frac{1}{A_i} \int_{A_j} \frac{\cos\theta_i \cos\theta_j}{\pi r^2} \delta_{ij} dA_i dA_j \tag{3-24}$$

where δ_{ij} is determined by the visibility of dA_i to dA_j. For example, $\delta_{ij} = 1$ if dA_i is reached to dA_j, otherwise then $\delta_{ij} = 0$.

C. Analytical method and conditions

To analyze the thermal environment of automotive indoor in summer and winter condition, the operating mode of HVAC system in automobile was applied to both top and bottom. The outdoor temperature in summer was set to 35°C, and the operating air volume of the HVAC system was set to 480 CMH, which is a test condition for cooling performance. The outside temperature in winter was set to 15°C, and the operating air volume of the HVAC system considered 350 CMH, which is a heating performance test condition. Table 3.1 shows the simulation conditions of this study. In this study, the solar ray tracing model was applied to consider the effect of solar radiation in the thermal environment of automotive indoor, and the S2S(Surface to surface) model was used to consider the effect of thermal comfort on the radiation model. Based on the latitude, longitude, and time zone of Gwangju Metropolitan City, Korea; the solar radiation was set as Day : 21, Month : 6, Time of Day : 13 hour in summer, and Day : 21, Month : 12, Time of Day : 13 hour in winter. The boundary condition for the thermal environment of automobile indoor are shown in Fig. 3.3, and it is composed of HVAC duct, dashboard, driver's seat, passenger seat, rear seat, vehicle body, and glass window. In addition, the shape of the air outlet was added for convergence of the analysis. In HVAC duct, there are four vents on the upper side that are two on the left and right side, and two foot vents are located on the lower side that are one on the left and one on the right side. The heat flux for the driver was considered a value of 90 W/m^2 based on ASHRAE Standard 55-2017 [74]. The thermophysical properties of each component and human body in the automotive indoor were applied based on the Adhikari et al. [97], and these are shown in Table 3.2.
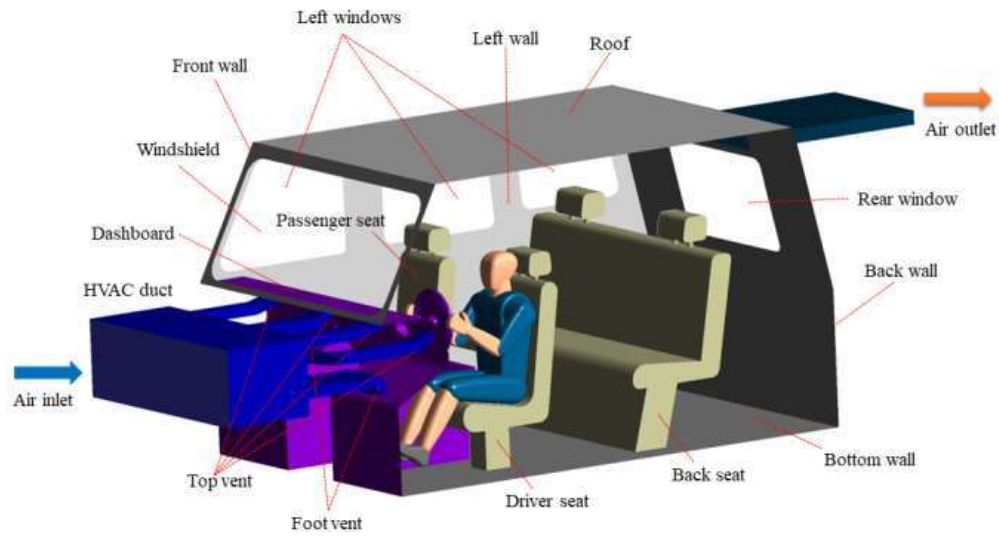
Fig. 3.3 Schematic diagram for boundary conditions

Table 3.1 Simulation conditions of automobile thermal environment in summer and winter

Item	Unit	Summer	Winter
Ambient temperature	˚C	35	15
Air inlet temperature	˚C	12.5	40
Air flow rate	CMH	480	350
Vent side	-	Top & Foot	Top & Foot

Table 3.2 Properties of car interior compartments and human body

Item	Material	Density [kg/m^3]	Specific heat [J/kg·K]	Thermal conductivity [W/m·K]
Windshield, rear glass, side glass	Glass	2529.58	754.0	1.17
Car wall, dashboard	ABS plastic	996.35	1480.6	2.70
Seat	Polyurethan foam	70.00	1685.6	0.05
Clothing	Cotton	1297.01	1480.1	0.04
Driver	Skin	1000	3770.0	0.21

IV. Experimental setup and method

A. Experimental setup and subject conditions

1. Experimental setup

a. Experimental room condition

The experiment of this study was conducted in a constant temperature and humidity room with a size of 8.5×4.5×3.5 (W×D×H, m^3) in the Chosun university, Gwangju, Korea. The single duct air conditioner was installed outside the constant temperature and humidity room, and the internal temperature and humidity were controlled using a duct. For the accuracy experiment, the ceiling, wall, and floor were well insulated to increase airtightness.

In the case of the simulation room where the experiment conducted, it was installed in the constant temperature and humidity room. Insulation material of 1.0×1.8×1.5 (W×D×H, m^3) was attached to the room except for the rear of the room so that the airflow discharged from the HVAC vent was not affected by the airflow discharged from the constant temperature and humidity chamber. In addition, the HVAC of the vehicle with a displacement of 2000 cc was installed in the front of simulation room and airflow was supplied to the simulation room so that the subject could feel the airflow discharged from the vent similarly to the actual vehicle. Fig. 4.1 shows the schematic diagram of the experimental room used in the experiment, and the detailed specifications are shown in Table 4.1.
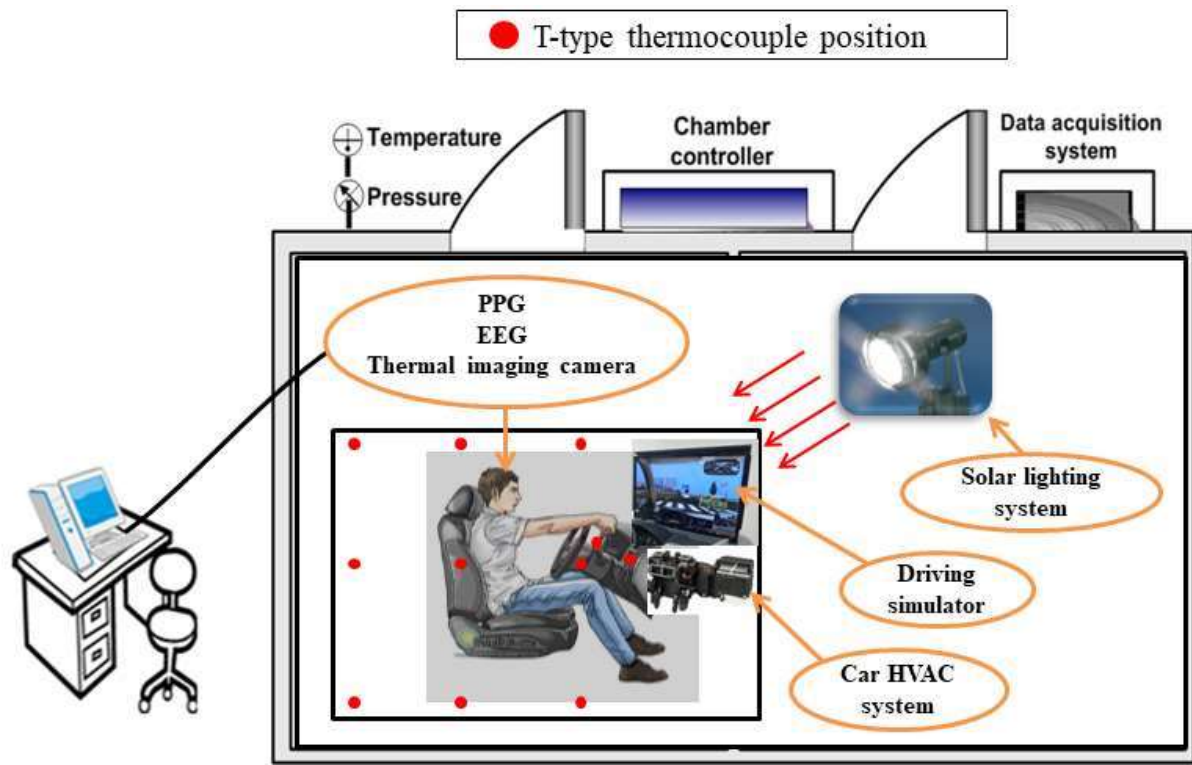
Fig. 4.1 Schematic of experimental room

Table 4.1 Specification of the artificial climate room

Item	Specification
Temperature	-20～60℃
Humidity	5～95% RH
Air flow rate	400 CMM
Accuracy	± 1.5%

b. Solar lighting device

In this study, the artificial solar lighting of the XC-500E model (Technox Inc.) was used to supply solar radiation that affects the driver's thermal comfort when driving in summer and winter conditions. Since the solar lighting system of XC-500E uses artificial solar lighting device (SOLAX) which is very closest to natural sunlight, it can be applied indoor without any restriction even in inclement weather such as rainy weather or evening hours. Fig. 4.2 shows a photograph of the solar lighting device, and Table 4.2 shows the specifications of the solar lighting device.

Fig. 4.2 Photograph of solar lighting device

Table 4.2 Specification of solar lighting device

Item	Specification
Model	XC-500E
Filter	Transparency
Lamp capacity	500 W
Center luminous intensity	26000 cd
Luminescence wavelength band	350～2500 nm

c. Driving simulator and simulation software

In this study, an experiment was conducted using a driving simulator and simulation software to make the similar environment to the actual driving for the subject. The driving simulator used G27 racing wheel (Logitech), and this device is composed of a steering wheel, a gearbox, and a pedal module. And it realized a feeling of operation similar to the actual driving environment by setting the steering wheel angle and force feedback. Fig 4.3 shows a photograph of the driving simulator.

The subject performed a driving simulation by using City car driving 1.5 which driving simulation software. This software is widely used not only in this study but also in other driving simulation studies because the actual urban driving situation and traffic regulations are included in the software. In this experiment, in order to reproduce an environment similar to Korean traffic regulation, the driver's seat was located on the left side, and the experiment was conducted that the traffic regulation was set as the standard rule. Fig. 4.4 shows the operation screen of the driving simulation software.

Fig. 4.3 Driving simulator device

Fig. 4.4 Simulation screen of driving software

d. Cooling and heating seats

In this experiment, the basic seat, ventilation seat, and cold water seat were used for various seats experiments during driving in summer condition. In addition, the basic, heating, and hot water seat were used for various seats experiment during driving in winter condition. Fig. 4.5 shows the temperature variations for various seats in summer and winter condition. In the summer driving environment, the ventilation seat works to circulate the surrounding air, and the cold water seat circulates cold water of 4°C in the seat by using a constant temperature bath. Fig. 4.5(a) shows the temperature variation of the basic, ventilation, and cold water seats at 35°C in the summer condition.

In the winter driving environment, the heating seat heats the seat using an electric heating wire, and the hot water seat warms the seat by circulating hot water of 40°C by using a constant temperature bath. Fig. 4.5(b) shows the temperature variations of the basic, heating, and hot water seats at 15°C in the winter condition.

<Basic seat>   <Ventilation seat>   <Cold water seat>
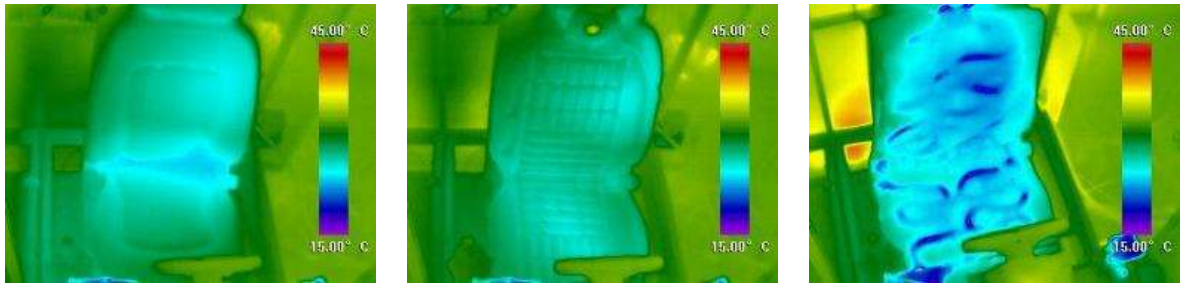
(a) Various seat types in summer
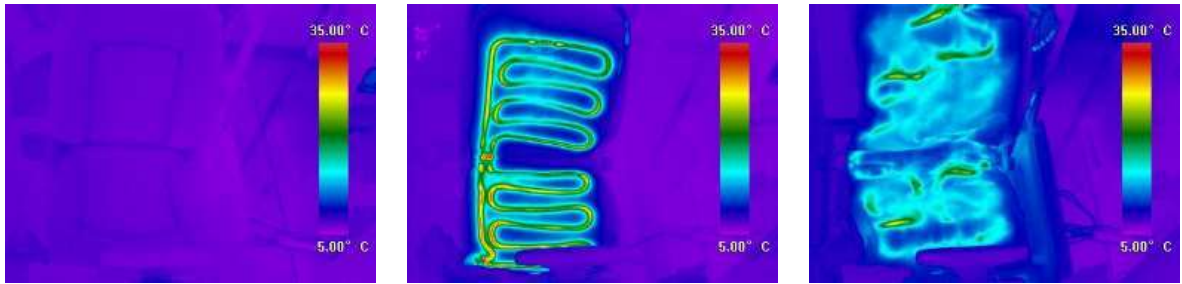
(b) Various seat types in winter

Fig. 4.5 Temperature changes of various seats used in the driving environment of summer and winter condition

e. Infrared lamp

In this study, a local heating experiment of the human body was conducted to investigate the effect on the driver's thermal comfort when the infrared lamp was irradiated on each part of the body in the winter driving environment. The infrared lamp for wall-mounting was used for local heating of the human body. The size of the infrared lamp is 900×830×235 (W×H×D, mm^3). Fig. 4.6 shows the photograph of the infrared lamp used in the experiment, and the specifications of the infrared lamp is shown in Table 4.3.

Fig. 4.6 Photograph of infrared lamp

Table 4.3 Specification of infrared lamp

Item	Specification
Rated voltage	AC 220 V, 60Hz
Power consumption	250 W
Stabilizer	Automatic timer, 2 fuse
Size	900×830×235 (W×H×D, mm^3)
Weight	5.2 kg(±5%)

2. Measurement devices

a. PPG measurement device

A pulse wave measuring device used uBioMacpa (Biosensecreative Inc.) which was measured irradiating and absorbing infrared rays into the peripheral blood vessel of the fingertip through the blood flow ejected from the heart. The measuring device instructed that the subject is not to permit to apply force or excessive movement to the finger before wearing it. Then, the experiment was carried out by wearing the measuring equipment on the index finger of the right hand. Fig. 4.7 shows the wearing photograph of the PPG device, and the specifications are shown in Table 4.4.

Fig. 4.7 Experimental device to measure PPG

Table 4.4 Specification of PPG measurement device

Item	Specification
Measuring range	40～200 BPM
Measurement error	±2%
Band pass filter	0.15～4 Hz

b. EEG measurement device

QEEG-64FX model of Laxtha Inc. was used to measure the subject's brain wave (EEG), and was connected as EEG-cap as shown Fig. 4.8. A2 was used as the reference electrode, and EEG was measured in a monopolar manner at 16 parts and the EEG was measured by selecting HPF, LPF, and notch filter according to the signal to be measured target. After the subject wears the EEG-cap, the electrode-skin impedance of EEG was precisely measured by injecting the EEG conductive paste into the scalp with a syringe in a total of 16 parts. Besides, EEG was measured within a stable range. Fig. 4.9 shows the detailed location for the measurement parts of EEG according to the International 10-20 system, and Fig. 4.10 shows a photograph of the EEG sensor attached to the actual subject in this experiment.

As shown in Table 4.5, the measurement parts of EEG are divided to the prefrontal lobe (Fp1, Fp2), left frontal lobe (F3, F7), right frontal lobe (F4, F8), parietal lobe (C3, C4, P3, P4), and left parietal lobe (P4), Right parietal lobe (P8), left temporal lobe (T7), right temporal lobe (T8), occipital lobe (O1, O2). The detailed specifications of EEG measurement device are presented in Table 4.6.

Fig. 4.8 Electroencephalogram measuring equipment
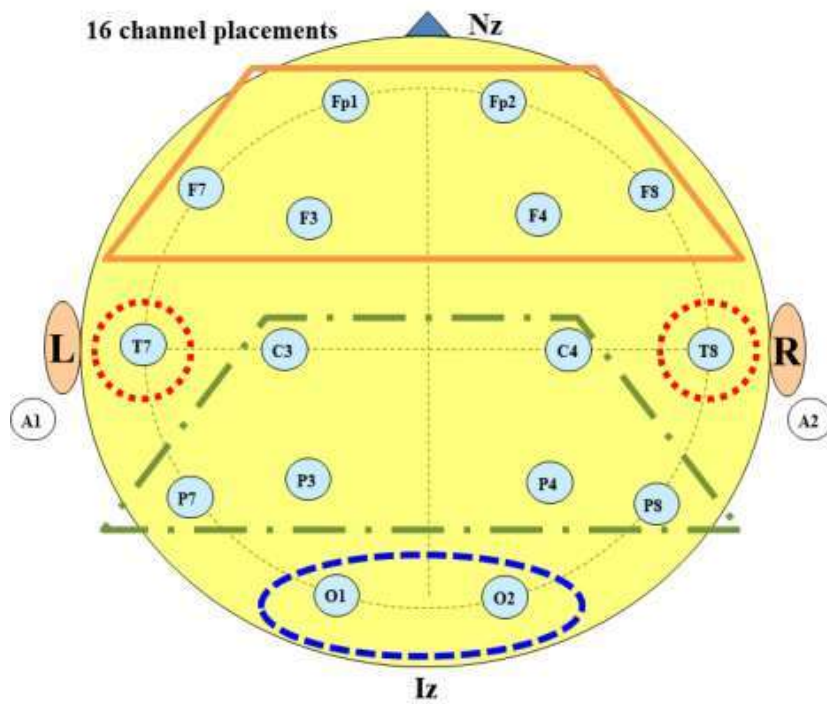
Fig. 4.9 Electrode locations for EEG test

Fig. 4.10 Photograph of subject with attaching of EEG sensor

Table 4.5 Electrode position and lobe at 16 channel system

Electrode position	Lobe
F1, F2	Prefrontal lobe
F3, F7	Left frontal lobe
F4, F8	Right frontal lobe
C3, C4, P3, P4	Parietal lobe
P4, P8	Left, Right parietal lobe
T7, T8	Left, Right temporal love
O1, O2	Occipital lobe

Table 4.6 Specification of EEG measurement device

Item	Specification
Sampling rate	256 Hz
Resolution	12 bit
Band pass filter	0.5～60 Hz
Notch filter	50～60 Hz

c. Thermal imaging camera

To measure the surface temperature of the subject, a thermal imaging camera (Cox company) was used. Fig. 4.11 shows a photograph of the thermal imaging camera. The thermal imaging camera measures the temperature in a non-contact method, and it is one of the most commonly used to measure surface temperature because there is less interference when measuring EEG and PPG than using a T-type thermocouple. Table 4.7 shows the specifications of the thermal imaging camera to measure the surface temperature in this experiment.

Fig. 4.11 Thermal imaging camera for temperature measurement

Table 4.7 Specification of thermal imaging camera device

Item	Specification
Resolution	384×288 pixel
sensor type	LWIR
Thermal resolution	<40mK @f/1.0, 30Hz, 300K
Infrared wavelength band	8～14 μm
Ambient temperature	-10℃～60℃
Temperature measuring range	-20℃～120℃

d. Thermocouple

The T-type thermocouple was used to measure the inlet and outlet temperatures in the cold and hot water seats. Fig. 4.12 shows a photograph of the T-type thermocouple. In addition, the T-type thermocouple of wire form was attached to the upper, middle, and lower parts to measure the vent discharge temperature and the vehicle simulator temperature. Fig. 4.13 shows a photograph of the T-type thermocouple of wire form. The thermocouple used in the experiment was calibrated using ice water and boiling water. The temperature range of the T-type thermocouple is -200℃～300℃, and the Ansi special limits of error is ±0.75%. Table 4.8 shows the detailed specifications of the T-type thermocouple. The temperature range of wire form T-type thermocouple is -270℃～400℃, and the Ansi special limits of error is ±0.75%. Table 4.9 shows the detailed specifications of wire form T-type thermocouple.

Fig. 4.12 Photograph of T-type thermocouple

Fig. 4.13 Photograph for the wire form of T-type thermocouple

Table 4.8 Specification of T-type thermocouple

Item	Specification
Type	T-type
Range	-200°C～300°C
Special limits of error	±0.5°C or ±0.4%
Standard limits of error	±1.0°C or ±0.75%

Table 4.9 Specification for the wire form of T-type thermocouple

Item	Specification
Type	Wire form of T-type
Range	-270°C～400°C
Special limits of error	±0.5°C or ±0.4%
Standard limits of error	±1.0°C or ±0.75%

e. Solar radiation meter

The solar radiation of solar lighting device was measured using a solar radiation transmitter (CR110). The measurement range of the solar radiation meter is 0～1500 W/m^2 and the accuracy is 5%. Fig. 4.14 and Table 4.10 show the photograph and the detailed specifications of the solar radiation meter.

Fig. 4.14 Photograph of solar radiation meter

Table 4.10 Specification of solar radiation meter

Item	Specification
Type	CR110
Storage environment temperature	From -10℃～70℃
Range	0～1500 W/m^2
Accuracy	±5%

f. Mass flow meter

In order to measure the mass flow rate of water in the water thermal seat, a mass flow meter (RHEONIKI Inc.) which is a precise mass flow measurement device was used. The mass flow meter was installed on the inlet side of the water thermal seat. The mass flow meter used in this study is shown in Fig. 4.15, and the detailed specifications of the mass flow meter is shown in Table 4.11.

Fig. 4.15 Photograph of mass flow meter

Table 4.11 Specification of mass flow meter

Item	Specification
Max allowable pressure	250 bar
Max allowable temperature	120℃
Nominal measurement range	10 kg/min

g. Data acquisition device

The data of air at the vent outlet, the inlet and outlet of the water thermal seat, the T-type thermocouple was installed inside the car simulator, the solar radiation meter, and the mass flow meter were collected using a data logger. MX 100 of Yokogawa company was used as a data collection device. The data collected by the data collection device is transmitted to a PC, and the collected data can be monitored through the MX100 standard program provided by Yokogawa company. Fig. 4.16 and Table 4.12 show the photograph and the specifications of the data collection device.

Fig. 4.16 Photograph of data acquisition system

Table 4.12 Specification of data acquisition system

Item		Specification
Model		MX 100 (Yokogawa Inc.)
Measurement interval		100 ms (shortest)
Supplying Voltage		100～220 VAC
Accurancy	Thermocouple	±0.05% of rdg.
	DC voltage	±0.05% of rdg.

3. Subject conditions

Firstly, 20 males and 20 females undergraduate and graduate students with driving experience of 2 years or more were selected as a subject, and then finally selecting 10 male and female subjects through the psychological and health status questionnaire. The subjects don't have a history of neuropsychiatric diseases such as attention deficit disorder, epilepsy, and alcoholism, and the ECG and other test results were all normal.

The selected subjects explained the experimental process in detail through pre-training for each subject 2 days before the experiment so that subjects could improve their understanding of the experiment. In addition, in order to improve the accuracy of the experiment results, the day before the experiment was instructed to take enough sleep for 8 hours. And 6 hours before the experiment, the intake of alcohol, cigarettes, caffeine, and other drugs that could affect human cognitive function was restricted. When any subjects were difficult to proceed the experiment through the pre-test on the day, the experiment canceled and then performed the experiment later. Table 4.13 shows the average age and physical condition of the subjects.

Table 4.13 Anthropometry data of the subjects

Item	Specification	
Gender	Male	Female
Number of subjects	10	10
Age	27.6 ± 2.17	25 ± 7.78
Weight	72.5 ± 5.6 kg	59 ± 7.78 kg
Height	1.74 ± 0.05 m	163.3 ± 3.29 m
Body area	1.57 ± 0.07 m^2	1.63 ± 0.12 m^2

The body surface area was calculated using the equation of DuBois et al. [98], and was shown in Eq. (4-1).

$$A_d = 0.202 \, m^{0.425} \, l^{0.725}$$ (4-1)

The condition of the amount of clothing in this experiment was applied the same experimental clothing in both the cooling and heating experiment based on the wearing of shirts and suit pants, which are the clothes of general office workers in spring and autumn. The amount of clothing was used Eq. (4-2) proposed by McCullough et al. [99].

$$I_{cl} = 0.835 \sum_i I_{clo,i} + 0.161$$ (4-2)

Table 4.14 shows the amount of clothing worn by the subject in summer and winter condition. The amounts of clothing for men and women in the summer were 0.4 clo and 0.41 clo, and the amounts of clothing for men and women in winter were 0.55 clo and 0.56 clo. The metabolism was assumed to be 1.8 met because the subject performed a driving simulation in a comfortable state and a simple questionnaire response was carried out.

Table 4.14 Calculation of the amount of clothing results

Garment Description	Summer		Winter	
	Male ($I_{clo,i}$)	Female ($I_{clo,i}$)	Male ($I_{clo,i}$)	Female ($I_{clo,i}$)
Dress shirt	0.19 clo	0.19 clo	0.25 clo	0.25 clo
Under wear	0.04 clo	0.05 clo	0.04 clo	0.05 clo
Socks	0.02 clo	0.02 clo	0.02 clo	0.02 clo
Straight trousers(thin)	0.15 clo	0.15 clo	0.24 clo	0.24 clo
Amount of clothing(Total)	0.4 clo	0.41 clo	0.55 clo	0.56 clo

B. Experimental method and conditions

1. Driver's thermal comfort experimental method and conditions

The subjects entered the experimental space after stabilizing their bodies in the preparing room for 10 min at a temperature of 25°C, with the EEG and PPG measuring devices attached, and then the basic waveform of the EEG, PPG and the surface temperature of the subject were measured for 5 min. After entering the experimental space, the subjects sat in the driver's seat and initiated the driving simulation. The driving environment was carried out the old city map of free driving mode which software's own function. This map consists of 1 highway, 1 driveway, 3 city areas, 3 driving function training ground, and 1 country road. It consists of a smooth course without a section that gives a strong momentary cognitive load like a tunnel. In addition, the speed limit and traffic regulations were set similarly to those of Korea, and the driving conditions were set to "serenity" and "daytime". The test subjects were instructed to follow the traffic rules the same way as in an actual driving situation in order to investigate the variations in their physiological signals with changes in cabin and vent exit temperatures. In addition, they were instructed to drive without limiting the driving course.

The surrounding environment during driving was set the vehicle and the person at the minimum ratio compared to the entire map in order to observe the change of the biological signal to the temperature during the simulation driving. The simulation was set up so that traffic violations were not enforced, and there was no threat to driving during the simulation. In addition, in order to improve the driving motivation of the driver, the mission to move from the current position to a randomly selected position during driving was continuously performed. Fig 4.17 shows the old city driving map and section used in the driving simulation.
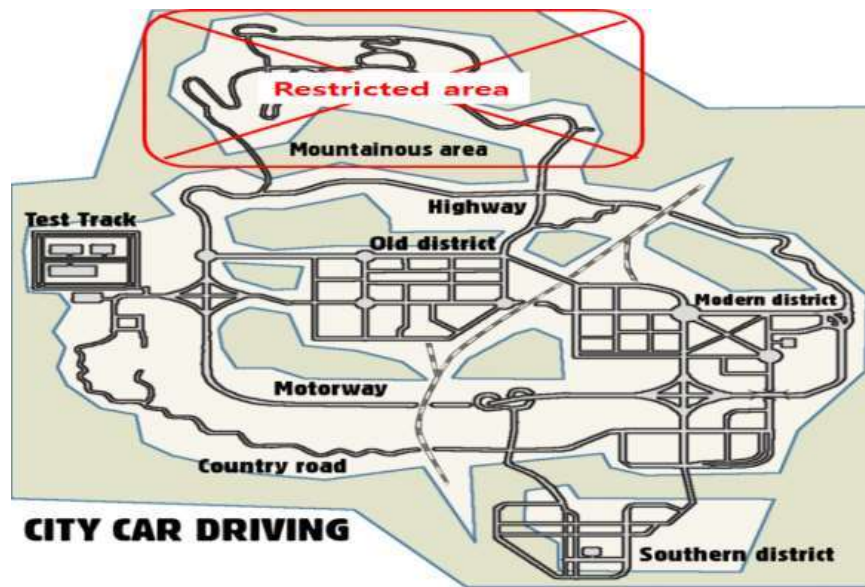
Fig. 4.17 View of the Old city map

In order to simulate the climatic condition in the summer, the experimental condition of the indoor space for cooling experiment was initially set to 35°C which an unpleasant condition. In addition, the HVAC was not operated at first. To similarly consider the influence of the sun provided to the driver in the vehicle, the solar light was installed at an radiation angle of 60° from the front left to the subject's body. The solar radiation on the subject's surface was measured in the grid unit of 3 cm and was calculated based on the numerical integration method using the average value of proximity. Based on this method, the summer solar radiation condition was calculated and it was calculated that the maximum solar radiation was 1,251 W/m^2 and the average solar radiation was 516 W/m^2. Under this environment, the subject entered the simulation room, completed individual adjustment, started driving with measurement of EEG, PPG, and temperature while driving for 4 minutes. After the checking of measurement was completed, the vehicle was instructed to stop on the shoulder, and the subject wrote the subjective thermal comfort questionnaire. Since the initially suggested condition is too hot and unpleasant to the driver, the experiment was conducted only for 4 minutes considering the condition of the subject, and then the experiment was performed for 4 minutes by blowing cold air from the

vent discharge at the temperature of 12.5°C under the same condition. In this condition, the measurement of bio-signals was completed and the cabin temperature was decreased by a step of 2.5°C and the vent discharge temperature was increased by a step of 2°C with conducting of questionnaire survey simultaneously. And then, the driving was performed for 15 minutes. The first 10 minutes are the step of adapting to driving and ambient temperature, and the subject's EEG, PPG, and surface temperature changes were measured during the last 5 minutes. By repeating this process, the measurement of bio-signals and questionnaire were performed five times until the cabin temperature and the vent discharge temperature were finally equal to 22.5°C. In the case of the heating experiment, the indoor space was initially set to the indoor temperature of 15°C with the maximum solar radiation of 575 W/m^2 and average solar radiation of 242 W/m^2. Thereafter, the HVAC was operated with the vent discharge air temperature of 40°C under the same conditions and the experiment was performed for 4 minutes. In contrast to the cooling experiment, the experimental temperature increased at the indoor temperature of 2.5°C and decreased the vent discharge temperature of 2.5°C. The measurement of the EEG and PPG and questionnaire survey were carried out a total of 5 times until the cabin temperature and vent discharge temperature reached 27.5°C at the same time.

In both the cooling and heating experiment, the airflow speed discharged from the vent was operated at 4th-stage based on the HVAC system of a 2000 cc passenger vehicle. The vent of air discharge was opened both at the top and bottom during cooling and heating similar to the control method of general commercial vehicles. Fig. 4.18 shows the overall time schedule of this experiment, and Fig 4.19 shows the actual experiment photos in summer and winter. Besides, Table 4.15 shows the temperature setting condition for each experiment, and Table 4.16 shows the subjective questionnaire for thermal sensation vote, comfort sensation vote, and concentration level vote which was proposed in ASHRAE Standard 55-2017 [74].
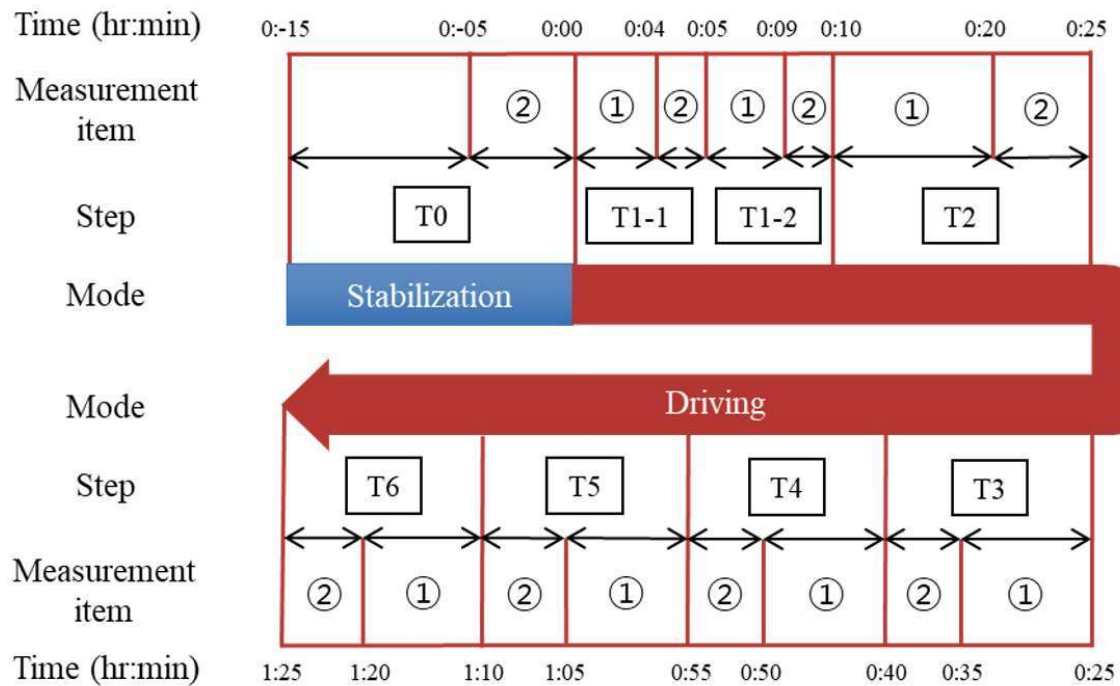
Fig. 4.18 Experimental procedure and measurement items on the driver's thermal comfort in summer and winter conditions
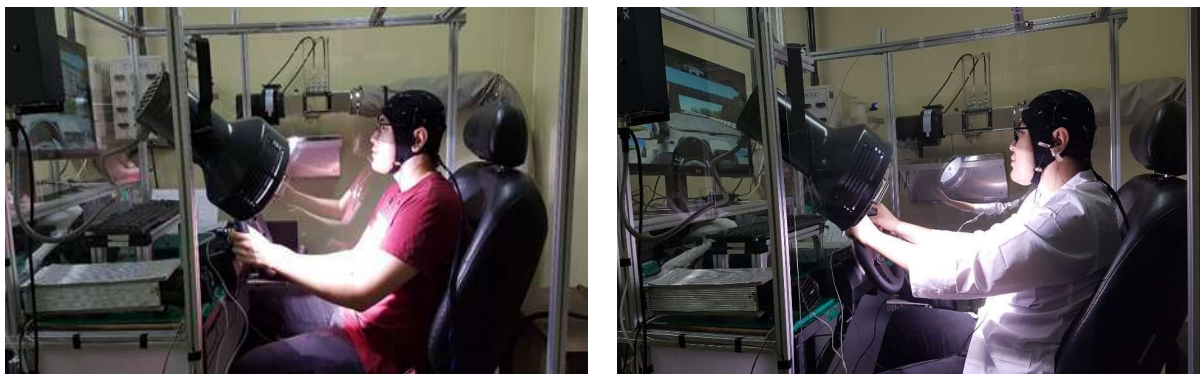
Fig. 4.19 Photograph of physiological signal measurement for driver in cooling and heating conditions

Table 4.15 Setting temperature for cooling and heating mode

Condition	Wind direction	Step number	Vent out temperature[*] (℃)	Cabin temperature[*] (℃)
Cooling	Body & Foot	T0	-	25
		T1-1	-	35
		T1-2	12.5	35
		T2	14.5	32.5
		T3	16.5	30
		T4	18.5	27.5
		T5	20.5	25
		T6	22.5	22.5
Heating	Body & Foot	T0	-	25
		T1-1	-	15
		T1-2	40	15
		T2	37.5	17.5
		T3	35	20
		T4	32.5	22.5
		T5	30	25
		T6	27.5	27.5

* : The average temperature deviation of the entire condition is ±0.01

Table 4.16 Subjective questionnaires (TSV, CSV, CLV)

TSV (Thermal Sensation Vote)

Value	Contents
-3	Very cold
-2	Cold
-1	Slightly cold
0	Neutral
1	Warm
2	Slightly hot
3	Very hot

CSV (Comfort Sensation Vote)

Value	Contents
-3	Very uncomfortable
-2	Uncomfortable
-1	Slightly uncomfortable
0	Neutral
1	Slightly comfortable
2	Comfortable
3	Very comfortable

CLV (Concentration Level Vote)

Value	Contents
-3	Very dis-concentration
-2	Dis-concentration
-1	Slightly dis-concentration
0	Neutral
1	Slightly concentration
2	Concentration
3	Very concentration

2. Driver's thermal comfort experimental method and conditions using various seats

To conduct the experiment on the thermal comfort of the driver with applying the various seats, the cooling experiment was conducted simulation room where the maximum solar radiation of 1,251 W/m^2 and average solar radiation of 516 W/m^2, and the automobile indoor temperature 35°C which were unpleasant in summer condition. For the test of basic seat condition, the subject entered the simulation room and began driving after completing individual adjustments and measured the EEG, PPG, and surface temperature for about 5 minutes after 10 minutes while driving for a total of 15 minutes. After the measurement of bio-signals was finished, the vehicle was instructed to stop on the shoulder, and the subject wrote the thermal comfort questionnaire. After then, the subject was rested in the simulation room at the temperature of 25°C for 15 minutes. After the rest, the HVAC operated with a vent discharge temperature of 12.5°C under the cabin temperature of 35°C, and then the measurement of the EEG, PPG, and surface temperature and questionnaire survey were performed under the same conditions. Continuously, the ventilation seat was mounted and the experiment was performed under the same temperature and time conditions. After completion of the experiment on the ventilation seat, the subject was rest in the simulation room for 15 minutes. And then, the experiment for the cold water seat with a temperature of 4°C was performed in the same manner. After the experiment on the subject's thermal comfort for each seat was completed, a 15-minute break was taken in a simulation room at the temperature of 25°C, so that the previous experimental conditions did not affect the results of each experiment.

The heating experiment was conducted at the simulation room with the maximum solar radiation of 575 W/m^2, average solar radiation of 242 W/m^2, and the automobile indoor temperature of 15°C. For the test of basic seat condition, the subject entered the simulation room and began driving after completing individual adjustments. When the subject was driven by allocating the same time as the cooling test, the

measurement of EEG, PPG, and surface temperature and questionnaire survey were performed. After 15-minute rest, the experiment was performed under the condition with the vent discharge air temperature of 40°C by the operating of HVAC system. After 15-minute rest, the heating seat experiment was performed under the same temperature and time conditions. The temperature of the hot water seat was set to 40°C, and the experiment was conducted in the same manner. Fig. 4.20 shows the overall schedule of the experiment on the driver's thermal comfort using various seats. In both the cooling and heating experiment, the discharged airflow speed from the vent was set to 4th-stage based on the automatic air conditioner system of a 2000 cc passenger vehicle. In addition, The vent of air discharge was opened both at the top and bottom during cooling and heating similar to the control method of general commercial vehicles.
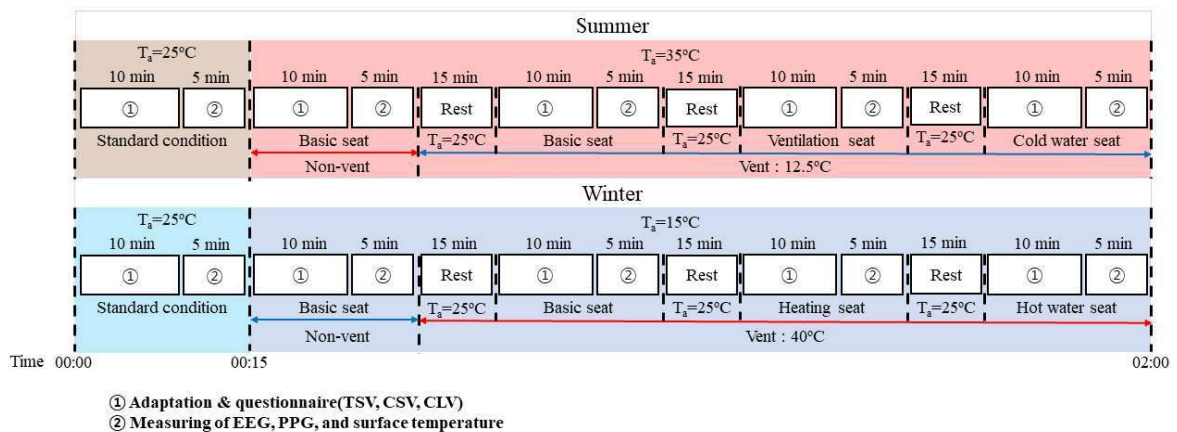
Fig. 4.20 Experimental timetable and measurement items on the driver's thermal comfort applying various seats

3. Driver's thermal comfort experimental methodology using local heating in winter condition

In this study, the indoor temperature of the constant temperature and humidity chamber was set at 15°C as the same to the winter experimental condition. Firstly, the HVAC system was not operated for the thermal comfort test of the driver with applying local heating in winter condition. Subjects were allowed to drive for 15 minutes after they entered the test room. The first 10 minutes were the acclimation time. The driver's EEG, PPG, and surface temperature were measured for 5 minutes, and after completion of the measurement, a questionnaire on TSV, CSV, and CLV was conducted. Thereafter, under the same temperature condition, an infrared lamp of 300 W/m^2 was used to irradiate the chest, hands, thighs, and feet. Under irradiation condition, the driver's bio-signal measurements and questionnaires were carried out by the same manner. After the experiment on the subject's thermal comfort for each part was completed, a 15-minute break was taken in a simulation room at the temperature of 25°C to reduce the effect of the previous experimental condition. In this study, the local heating experiment without using the HVAC system was completed, the subjects took a rest for 30 minutes. The HVAC system was used to perform a local heating experiment in winter condition under the same environment and method. Fig 4.21 shows the overall schedule of the experiment on the driver's thermal comfort with local heating.
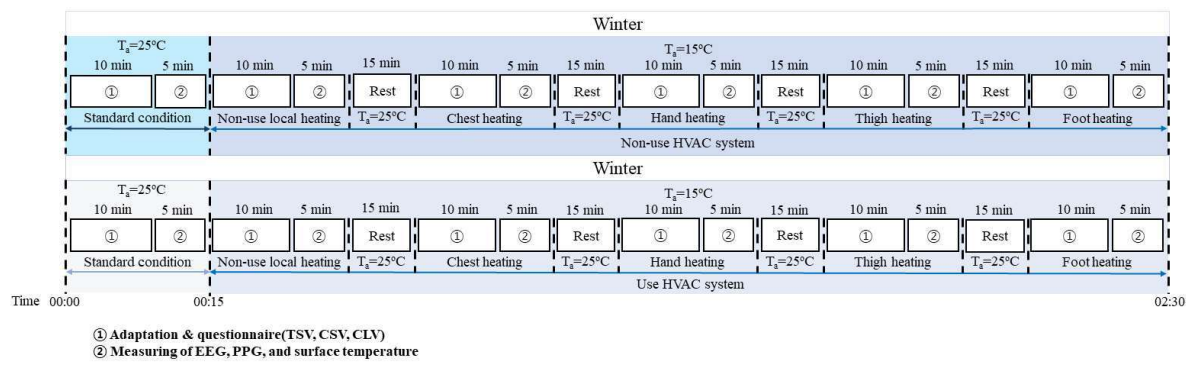
Fig. 4.21 Experimental timetable and measurement items on the driver's thermal comfort applying local heating test

C. Analysis method of experimental results

1. EEG analysis method

To analyze the EEG test results, a Telescan provided by Laxtha Inc. was used. Each EEG data is passed at 4-50 Hz using a band-pass filter, and δ waves that exhibited low frequency waveform is removed in order to minimize noise. Power spectrum analysis was performed by classifying into the frequency band of each EEG through Fast Fourier Transform (FFT).

The analysis of EEG for each measurement location was performed focusing on the components of the relative θ, α, and β waves. In the case of mental activity, β wave appears predominantly in the frontal lobe; however, θ and α waves tend to be suppressed. Based on aforementioned theory, the relative power of each waveform was calculated and the temperature effect was examined. Relative power of this study is shown in Eq. (4-3).

$$Relative\ \ power = \frac{X_{power}}{\theta_{power} + \alpha_{power} + \beta_{power} + \gamma_{power}} \tag{4-3}$$

By calculating the mutual ratio of the α wave representing the sense of stability and the β wave representing the arousal level, as the temperature changes, the activity of the β wave in the prefrontal lobe was monitored to determine the driving concentration of the subject with change of temperature, which is shown in Eq. (4-4).

$$Ratio\ of\ Alpha\ \text{and}\ Beta = \frac{\beta}{\alpha} \tag{4-4}$$

The β wave of the frontal lobe is generally categorized into a low-β wave (13∼ 19.99 Hz) and a high-β wave (20∼29.99 Hz). Low-β waves are divided into the

SMR wave (12~14.99 Hz) which are indicators of attention level, and the Mid-β waves (15~19.99 Hz) which indicate arousal in the stable state. When analyzing the EEG power spectrum, low-β waves are generated during the active mental activities such as learning, memorization, and calculation. The high-β waves are generated in a state of tension or stress.

Since the driving simulation have no dangerous sections on the road and there are few vehicles and pedestrians around, the attention concentration of the subject was analyzed by using the activity of θ wave. The ratio of the sum of the SMR wave and the mid-β wave, which used to analyze the learning concentration and arousal level in the existing EEG researches, which is shown in Eq. (4-5). In addition, using theory for emotional evaluation of Heller [100], it was analyzed as being focused and aroused in a pleasant state from a psychological and physiological perspective when the β-wave of the left frontal lobe is more activated than that of the right-frontal lobe.

$$Concentration \ \ Index = \frac{SMR + Mid\beta}{\theta} \qquad (4\text{-}5)$$

In the case of the occipital lobe analysis, the α wave which mainly appears during meditation is suppressed when opening eyes and maintaining concentration. The θ and α waves tend to increase simultaneously when they are felt drowsiness or boredom. Accordingly, the increase and decrease tendency of the relative θ and α waves was analyzed using Eq. (4-3). In order to analyze whether α wave tends to inhibit β wave with time, the drowsy state of the subject is detected using Eq. (4-4). Table 4.17 shows the pattern of changes in EEG according to situation in the body of this study.

Table 4.17 Pattern of the measured parameters in the central nervous system

Condition	Lobe	Parameter	Patten
Alert, Arousal, Excited	Frontal	β	↑
Concentration index	Frontal	$\dfrac{SMR + Mid\beta}{\theta}$	↑
Increased mental workload	Frontal, Occipital	$\dfrac{\beta}{\alpha}$	↑
Pleasant	Frontal	β	↑
Sleepiness	Occipital	α, θ	↑
Sleepiness, Boredom	Frontal, Occipital	θ	↑

2. PPG analysis method

In order to analyze the PPG test results, the uBioMacpa Vital software by Biosense Creative was used. Since the PPG test was measured and analyzed by irradiating infrared rays into the peripheral blood vessels of the fingers through the ejected blood from the heart, the analysis was performed with same method as the conventional electrocardiogram analysis.

In this experiment, to analyze the PPG change of the subject according to the temperature change while driving in a comfortable state, the stress index and LF/HF which representing the ratio of the sympathetic nervous system and the parasympathetic nervous system were analyzed. In addition, the SDNN (Standard deviation of N-N interval) which represents anti-stress index and homeostasis and the RMSSD (Root Mean square of the successive differences) which evaluates the ability to regulate the heart parasympathetic nerve were also analyzed. These two indices show a decrease in arousal or tense state.

3. Questionnaire analysis method

In this study, the thermal sensation (TSV), comfortable sensation (CSV), and concentration level (CLV) were investigated according to the temperature change. The thermal sensation questionnaire of -3 means very cold, 0 is neutral, and 3 indicates very hot. It was answered by subject on the thermal sensation how they felt under given condition. In the comfortable sensation questionnaire, -3 means very uncomfortable, 0 is neutral, and 3 indicates very comfortable. Besides, in the concentration level questionnaire, -3 means very dis-concentration, 0 is neutral, and 3 indicates very concentration, which are answered on the concentration level how subject felt. Based on these indicators, this study was to investigate the interrelationship between the thermal, comfort, and concentration survey results which felt by the subject and presented the relationship between PPG and EEG.

V. Simulation results and discussions

A. Validation of the simulation results of the automotive thermal environment

1. Validation methodology

An experiment was conducted to verify the simulation results of the thermal environment for the automobile indoor in summer and winter condition. Fig. 5.1 presents the location of thermocouple in the driver's seat. Thermocouples in the driver's seat were installed on both thighs, hips, and back in contact with the subject with 10 cm intervals. In addition, thermocouples were attached to the forehead, both wrists, and ankles of subjects to confirm the effect of the operation of the HVAC system during driving. First, the subject drives a car in summer condition when the air conditioner is not operated for the initial 10 minutes, and then the air conditioner is operated to measure the temperature for 30 minutes. The test in winter condition was also performed by the same method with the summer test.
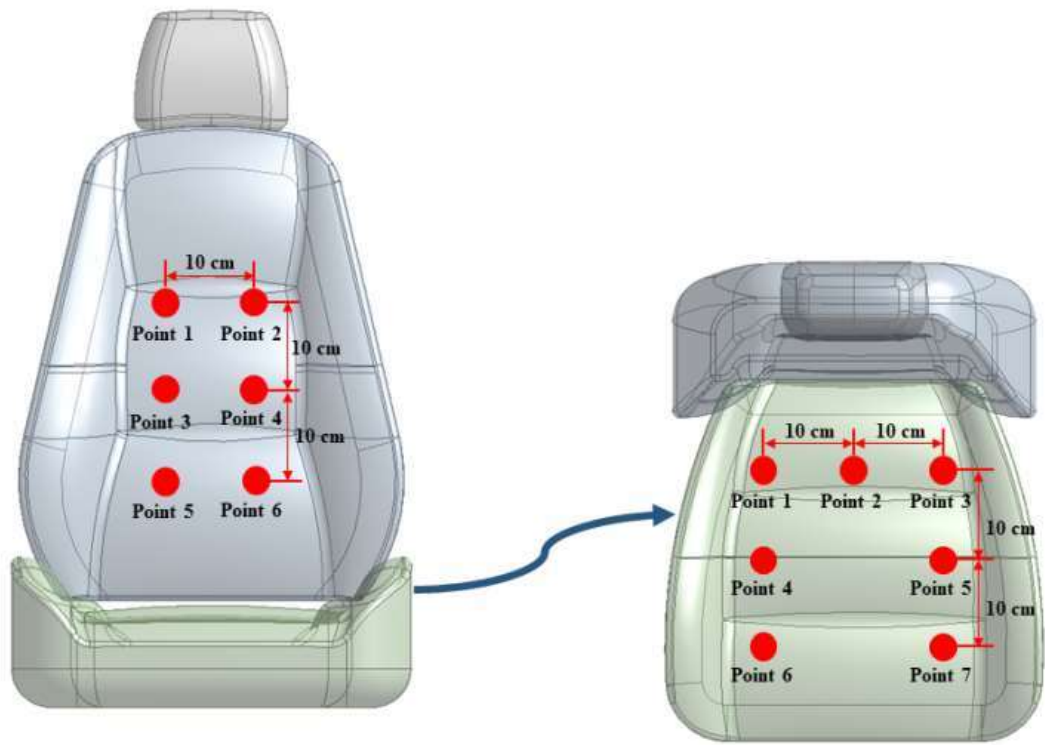
Fig. 5.1 Thermocouple attachment location on the car seat

2. Validation results

Fig. 5.2 shows the comparison of the simulation and experiment results for the thermal environment of automotive indoor in summer condition. Fig. 5.2(a) exhibits the temperature change of the subject's forehead, ankle, and wrist, which did not contact with the driver's seat when the air conditioner was operated for 30 minutes in the summer driving environment. As 5 minutes have passed, the temperature of the driver's forehead, ankle, and wrist in the simulation was 31.1°C, 32.3°C, and 34.0°C, respectively, and the temperature of the driver's forehead, ankle, and wrist in the experiment was 34.8°C, 33.3°C, and 35.3°C, respectively. As 15 minutes have passed, the temperature of the driver's forehead, ankle, and wrist in the simulation was 28.3°C, 30.3°C, and 32.4°C, respectively, and the temperature of the driver's forehead, ankle, and wrist in the experiment was 31.9°C, 32.7°C, and 34.1°C, respectively. In addition, as 30 minutes have passed, the temperature of the driver's forehead, ankle, and wrist in the simulation was 26.4°C, 28.8°C, and 31.1°C, respectively, and the temperature of the driver's forehead, ankle, and wrist in the experiment was 29.1°C, 31.8°C, and 30.9°C, respectively. As a result, temperatures at the forehead, ankle, and wrist in simulation results were lower than those in experiment results. This is because the human body tends to maintain a temperature of 36.5°C, which can't be considered in the simulation. However, it was confirmed that the temperature of the driver's forehead, ankle, and wrist similarly decreased when the air conditioner was operated in summer driving condition.

Fig. 5.2(b) shows the temperature change of the subject's hips, back, and thighs in contact with the driver's seat when the air conditioner is operated for 30 minutes in a summer driving environment. As 5 minutes have passed, the temperature of the driver's hips, back, and thighs in the simulation was 37.2°C, 37.8°C, and 37.3°C, respectively. The temperature of the driver's hips, back, and thighs in the experiment was 35.0°C, 35.4°C, and 35.4°C, respectively. As 30 minutes have passed, the temperature of the driver's hips, back, and thighs in the simulation was 39.7°C,

39.2°C, and 39.4°C, respectively, and the temperature of the driver's hips, back, and thighs in the experiment was 36.4°C, 36.0°C, and 37.3°C, respectively. The temperature of the hips, back, and thighs that are in contact with the driver's seat in simulation results showed higher than those in experimental results. In the simulation, the temperature was high due to non-air flow in there that was in contact with the seat under the hot summer condition. Actually, the subject has some movement while driving, thus air flow in there occurs. However, it was confirmed that the temperature of some parts in contact with the driver's seat shows similar trends that is the increasing tendency of the simulation and experimental results.
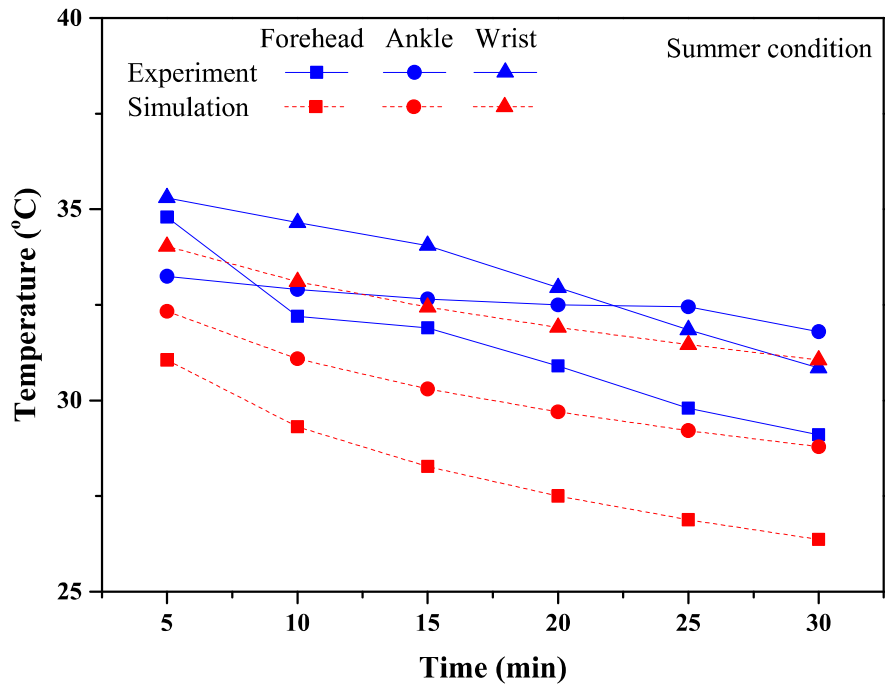
(a) Non-contact region-forehead, ankle, wrist

(b) Contact region-hip, back, thigh

Fig. 5.2 Temperature comparison of the simulation and experiment results for the thermal environment of the automobile indoor in summer condition
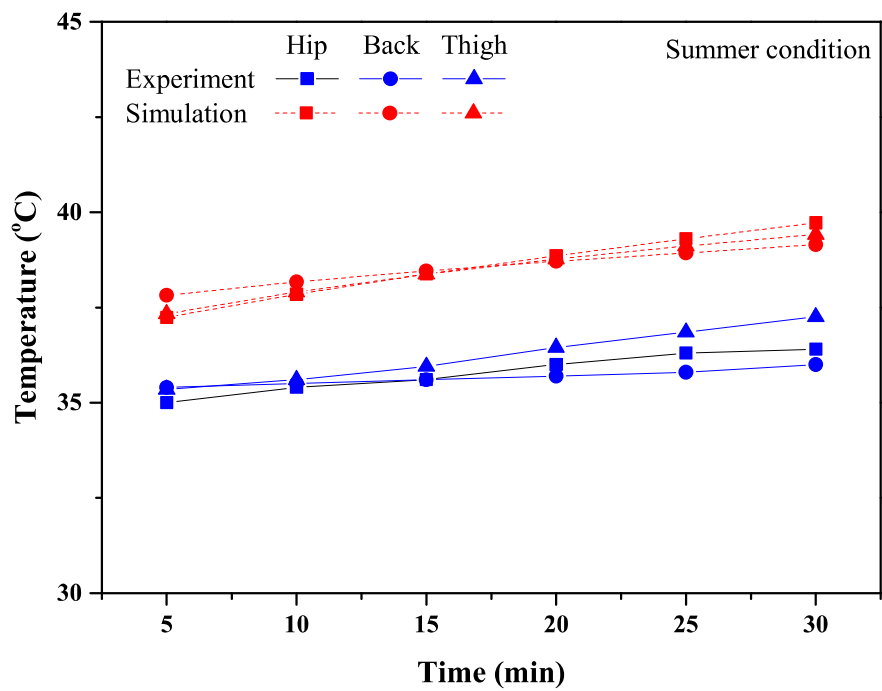
Fig. 5.3 shows the temperature comparison of the simulation and experiment results for the thermal environment of automotive indoor in winter condition. Fig. 5.3(a) shows the temperature change of the subject's forehead, ankle, and wrist which had no contact with the driver's seat when the heater was operated for 30 minutes in the winter driving environment. As 5 minutes have passed, the temperature of the driver's forehead, ankle, and wrist in the simulation was 27.4°C, 27.3°C, and 25.0°C, respectively, and the temperature of the driver's forehead, ankle, and wrist in the experiment was 28.3°C, 22.4°C, and 26.8°C, respectively. As 30 minutes have passed, the temperature of the driver's forehead, ankle, and wrist in the simulation was 30.5°C, 30.1°C, and 26.4°C, respectively, and the temperature of the driver's forehead, ankle, and wrist in the experiment was 29.0°C, 24.1°C, and 29.0°C, respectively. It was confirmed that the simulation and experimental results showed similar trends which is the decreasing tendency of the temperature on the driver's forehead, ankle, and wrist when the heater was operated in winter driving condition.

Fig. 5.3(b) shows the temperature change of the subject's hips, back, and thighs in contact with the driver's seat when the heater is operated for 30 minutes in a winter driving environment. As 5 minutes have passed, the temperature of the driver's hips, back, and thighs in the simulation was 24.9°C, 26.0°C, and 24.8°C, respectively, and the temperature of the driver's hips, back, and thighs in the experiment was 31.7°C, 31.8°C, and 32.8°C, respectively. As 30 minutes have passed, the temperature of the driver's hips, back, and thighs in the simulation was 27.6°C, 27.9°C, and 26.6°C, respectively, and the temperature of the driver's hips, back, and thighs in the experiment was 33.3°C, 33.7°C, and 34.3°C, respectively. The temperature of the hips, back, and thighs that were in contact with the driver's seat in the simulation results were lower than those in experimental results. This is because the human body performs the homeostasis maintenance action to maintain the body temperature constantly, but the temperature decreases under the cold environment in the simulation. However, it was confirmed that the temperature of some parts in contact

with the driver's seat coincided with the increasing tendency both the simulation and experimental results.

The simulation results on the thermal environment of the automotive indoor in summer and winter conditions were compared and analyzed through an experiment. As comparison results between simulation and experimental results, the temperature variation at each parts of the driver showed similar trends and was almost similar, the validity of the simulation results was verified.

(a) Non-contact region-forehead, ankle, wrist
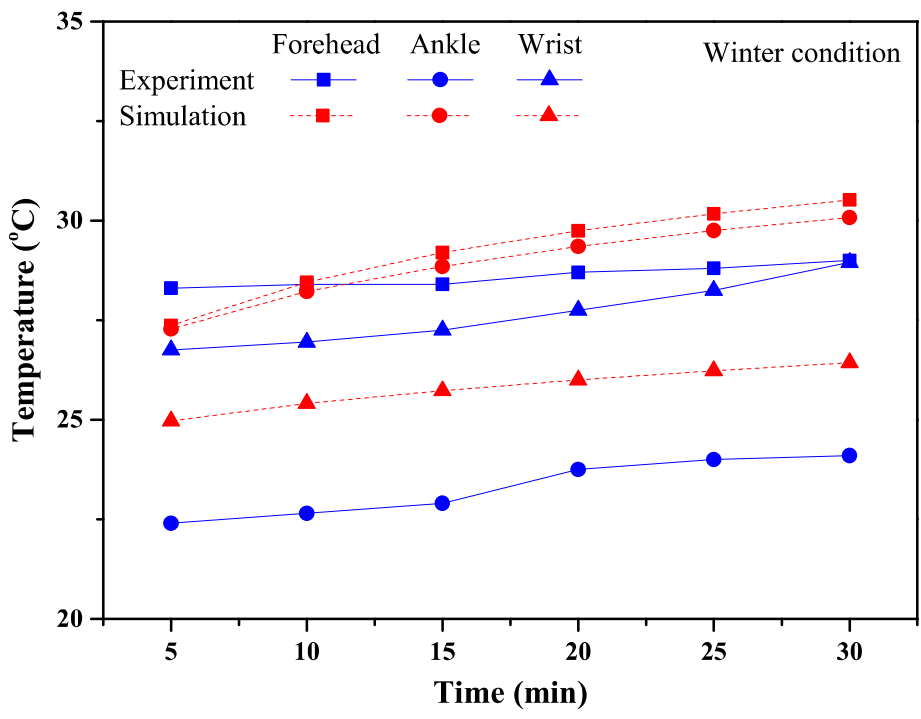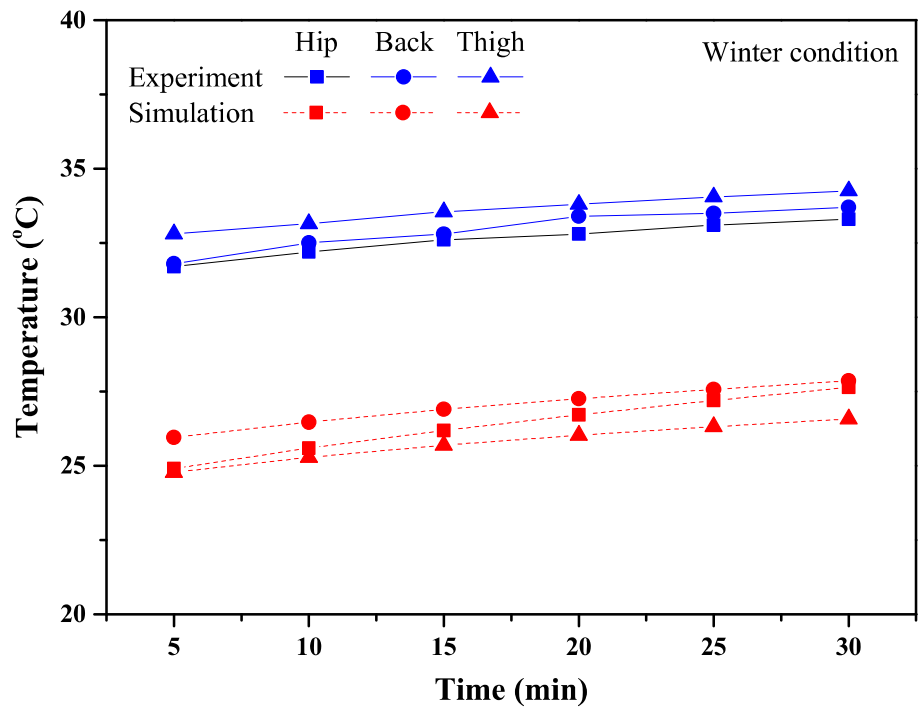

(b) Contact region-hip, back, thigh

Fig. 5.3 Temperature comparison between simulation and experiment results for the thermal environment of the automobile indoor in winter condition

In addition, the result of this study on flow analysis was compared with the result of Li et al. [101] which measured the flow of thermal convection around a manikin sitting in the simplified vehicle cabin by PIV (particle image velocity). The distribution of air velocity of a human in a vehicle cabin from Li et al. [101] and flow distribution in the simulation of this study are shown in Fig. 5.4. As the PIV measurement results of Li et al. [101], it is confirmed that there is no thermal convection in the hips, back, and thighs which are in contact with the seat, and there is air flow in the head and chest. In the results of this simulation, as the HVAC system is operated, the air flow is fast toward the head and feet, and there is no air flow in the hips, back, and thighs which are in contact with the driver's seat. The non-air flow in the hips, back and thighs of this study shows similar tendency with experimental results of Li et al. [101].
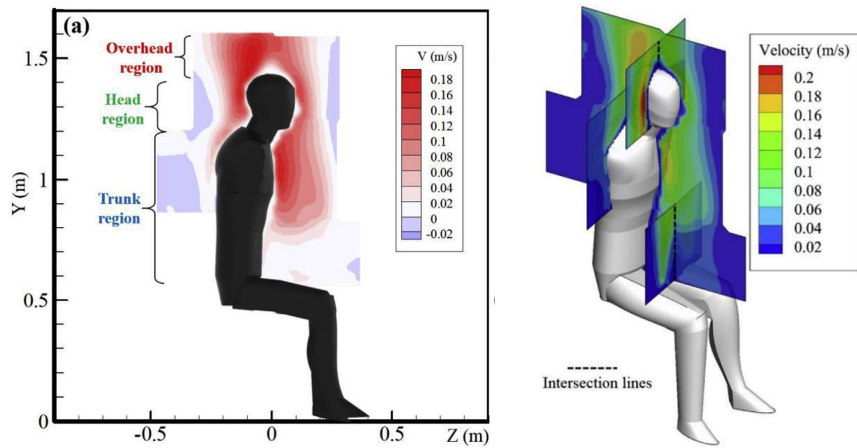
(a) Distribution of air velocity of human in vehicle cabin (Li et al. [101])

(b) Simulation velocity streamline (this study)

Fig. 5.4 Comparison of the flow distribution in simulation between this study and previous research

B. Simulation results of the automotive thermal environment

1. Simulation results of the automotive thermal environment in summer

Fig. 5.5 shows the simulation results of temperature distribution in automobile cabin with the basic seat during cooling. The initial temperatures of the automotive indoor and vent were set to 35°C and 12.5°C, respectively. When 5 minutes have passed after cooling, the temperature at the torso, back, arms, thighs, and hips of the human body was 34.6°C, 37.8°C, 34.0°C, 35.1°C, and 36.8°C, respectively. At the beginning of the air conditioner operation, the temperatures of the human body were overall higher because the indoor heat caused by solar radiation had a greater effect than the cold air from the vent of the air conditioner. The temperature at the head, hands, and feet of the human body was 31.1°C, 29.8°C, and 28.9°C, respectively, and which were relatively low compared to other parts. This is because the top vent is directed toward the face, and the bottom vent is toward the foot, thus the cold air from the vent reduces the temperature at those parts. When 20 minutes have passed after cooling, the temperature at the torso, back, arms, thighs, head, hands, feet, and hips of the human body is 33.3°C, 38.7°C, 32.0°C, 34.1°C, 27.5°C, 25.8°C, 24.7°C, and 37.2°C, respectively. In addition, when the cooling time of 30 minutes has passed, the temperature at the torso, back, arms, thighs, head, hands, feet, and hips of the human body is 32.8°C, 39.2°C, 31.9°C, 33.7°C, 26.4°C, 24.4 °C, 23.4°C, and 37.4°C, respectively. Therefore, the temperature of body decreases overall at this time.

Fig. 5.6 shows the change of the surface temperature of the human body according to time when cooling is operated in the automobile during summer condition with the basic seat. As 5 minutes of the initial cooling have passed, the temperature of torso part is generally 35°C∼38°C. When 10 minutes of cooling have passed, the temperature begins to increase gradually in the back, hips, and thighs of the human body that are in contact with the driver's seat. When 20 minutes of cooling time

have passed, the temperature of the back and thighs which are the part in contact with the driver's seat increases by 36℃～38℃. In addition, when 30 minutes of cooling time have passed, the temperature of the torso, arms, legs, and hands decreases due to the cold air of the air conditioner. In the simulation result, the temperature of the back and hips increases, while the temperature of the thighs tended to decrease. This is due to the cold air effect because the thighs do not in contact with the driver's seat. However, the temperature of the thighs in contact with the driver's seat is gradually increased from 37.3℃ to 39.4℃ with time. Consequently, it is confirmed that the influence of cold air in the air conditioner is relatively not significant in the back, thighs, and hips which are in contact with the driver's seat.
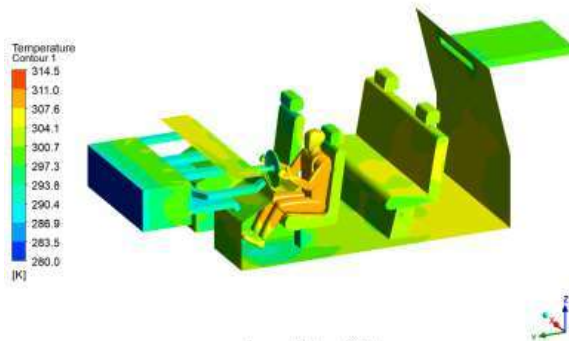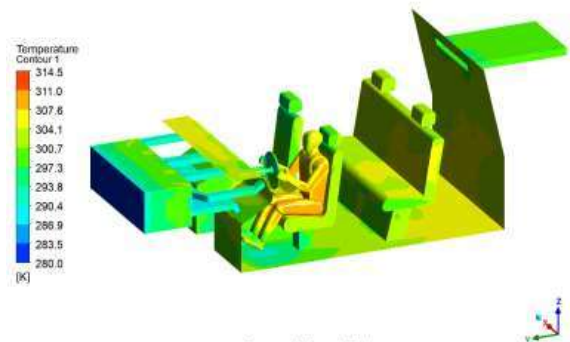
(a) 5 min

(b) 10 min
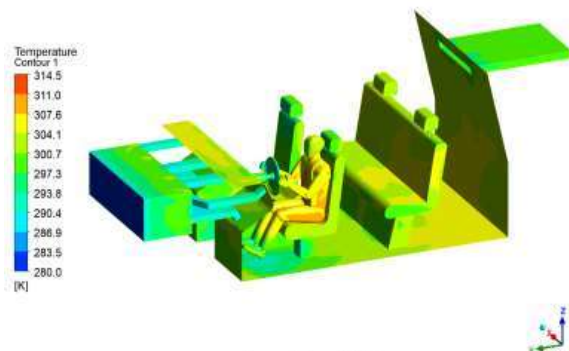
(c) 15 min
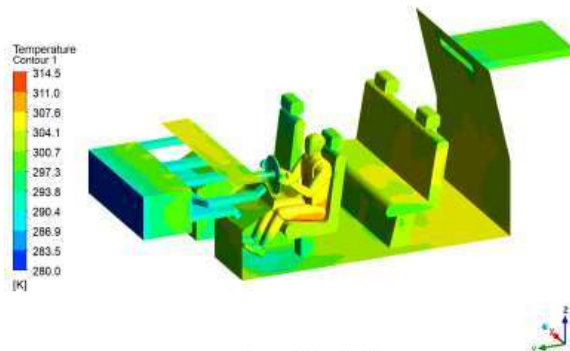
(d) 20 min

(e) 25 min
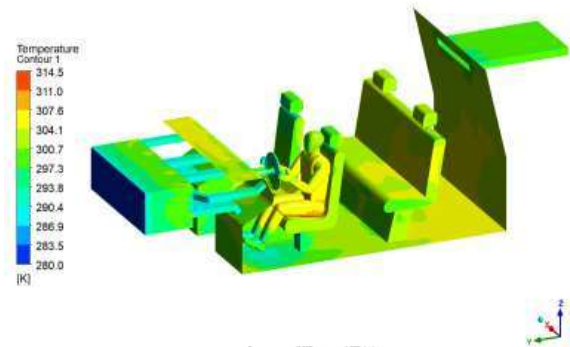
(f) 30 min

Fig. 5.5 Simulation result of temperature distribution in automobile cabin with the basic seat during cooling

(a) 5 min

(b) 10 min

(c) 15 min

(d) 20 min

(e) 25 min

(e) 30 min

Fig. 5.6 Simulation result of surface temperature of human in automobile indoor
with the basic seat during cooling

As the results of the simulation for the basic seat, it is confirmed that some parts of the human body in contact with the seat do not affect by the air conditioner, and the temperature increases. Therefore, a function capable of decreasing the temperature in a vehicle seat is required, and the ventilation seat is generally used in a current automobile to solve this problem. However, the ventilation seat only blows the surrounding air to the body, so it doesn't get a great cooling effect in a short time. Therefore, in this study, a cold water seat is designed to effectively cool the human body in contact with the driver by inserting a cold water pipe into the driver's seat, and the simulation results with time are shown in Fig. 5.7. When 5 minutes of the cooling time have passed, the temperature at the torso, back, arms, thighs, and hips of the human body is 33.6°C, 35.0°C, 32.2°C, 34.0°C, and 35.3°C, respectively. The temperature at the head, hands, feet of the driver is 30.4°C, 28.3°C, and 26.5°C, respectively. The temperature at the torso, arms, head, hands, and feet of the driver is similar to that using the basic seat, but the temperature of thighs and hips in contact with the cold water seat is slightly lower than that using the basic seat. The effect of the cold water seat to reduce the temperature of body in contact with the seat was confirmed. After 20 minutes of cooling, the temperature at the torso, back, arms, thighs, head, hands, feet, and hips of the human body is 30.4°C, 33.6°C, 29.4°C, 31.4°C, 26.7°C, 24.8°C, 22.1°C, and 33.8°C, respectively. Besides, after 30 minutes of cooling, the temperature at the torso, back, arms, thighs, head, hands, feet, and hips of the human body is 29.5°C, 33.0°C, 28.4°C, 30.5°C, 25.6°C, 23.6°C, 20.9°C, and 33.1°C, respectively. In the result of simulation, the temperature of the back which is the contact part of the cold water seat decreases significantly, and the temperature at the torso is also 3.31°C lower than that using the basic seat.

Fig. 5.8 shows the variation in the surface temperature of the human body with time when the cold water seat and the cooling are applied in the automobile during summer condition. After 5 minutes of the HVAC cooling, the average temperature of the human body is 31.5°C, which is about 1.7°C lower than that using the basic seat. When 10 minutes of cooling have passed, the temperature at the back, hips, and

thighs of the human body which is the part in contact with the cold water seat tends to gradually decrease unlike those using the basic seat. After 5 minutes of cooling in HVAC, the temperature of the back and thighs that are in contact with the cold water seat is 31°C~34°C. In addition, after 30 minutes of cooling are operated by HVAC, the temperature at the torso, arms, legs, and hands is averagely about 2.24°C lower when using the cold water seat than when using the basic seat. This is because the use of the cold water seat reduces the temperature of the back, thighs, and hips which are the contact parts of the seat, thus it has the effect on reducing the overall temperature of the human body. The use of a cold water seat with operating the air conditioner in a car during the hot summer condition can reduce the driver's body temperature by about 2.8°C compared to the basic seat. Accordingly, it is confirmed that the use of the cold water seat is provided more thermal comfort effectively to the driver.
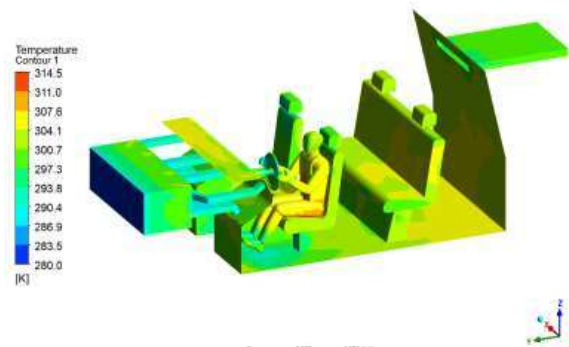
(a) 5 min

(b) 10 min

(c) 15 min

(d) 20 min

(e) 25 min

(f) 30 min
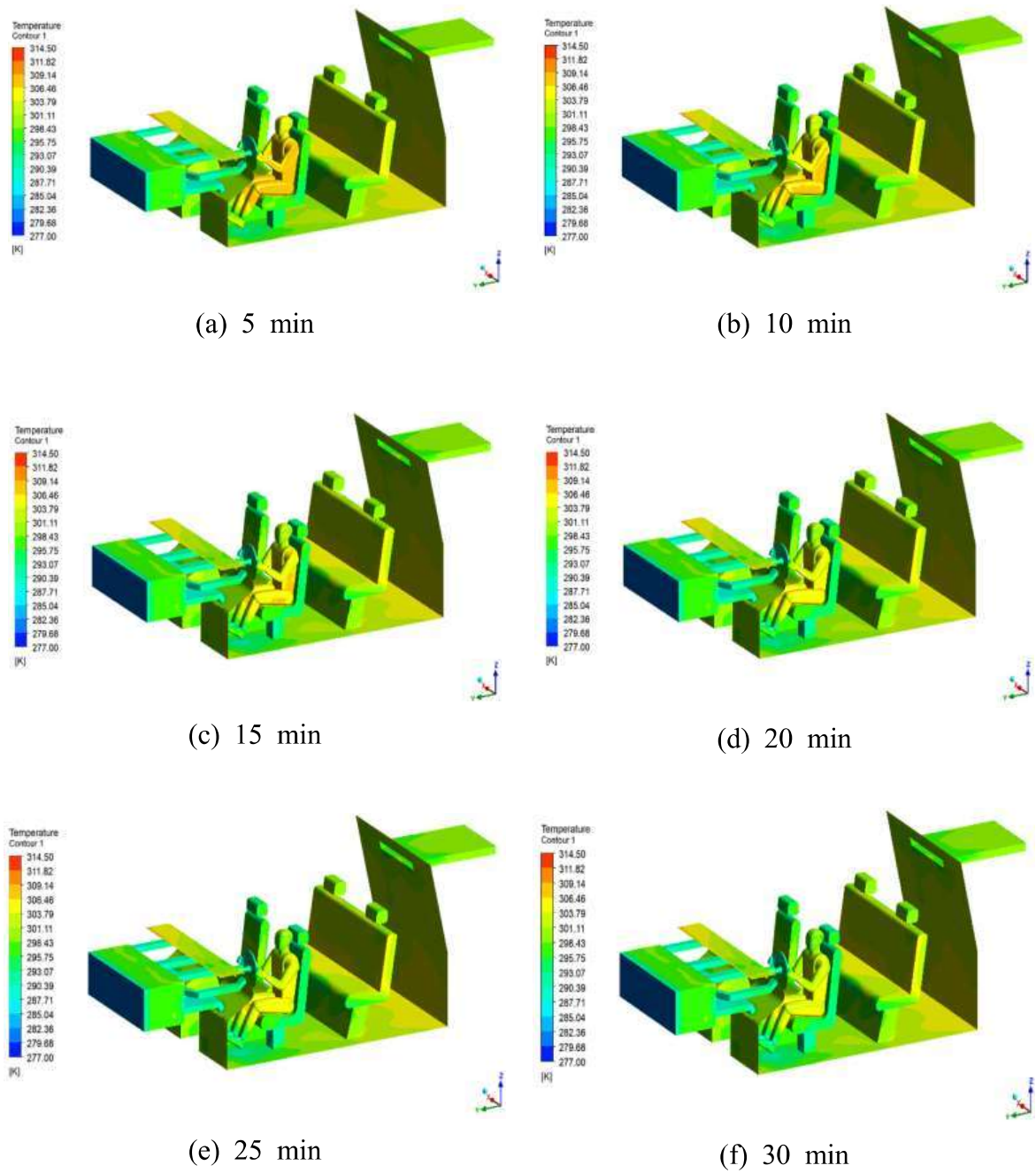
Fig. 5.7 Simulation result of temperature distribution in automobile with the cold
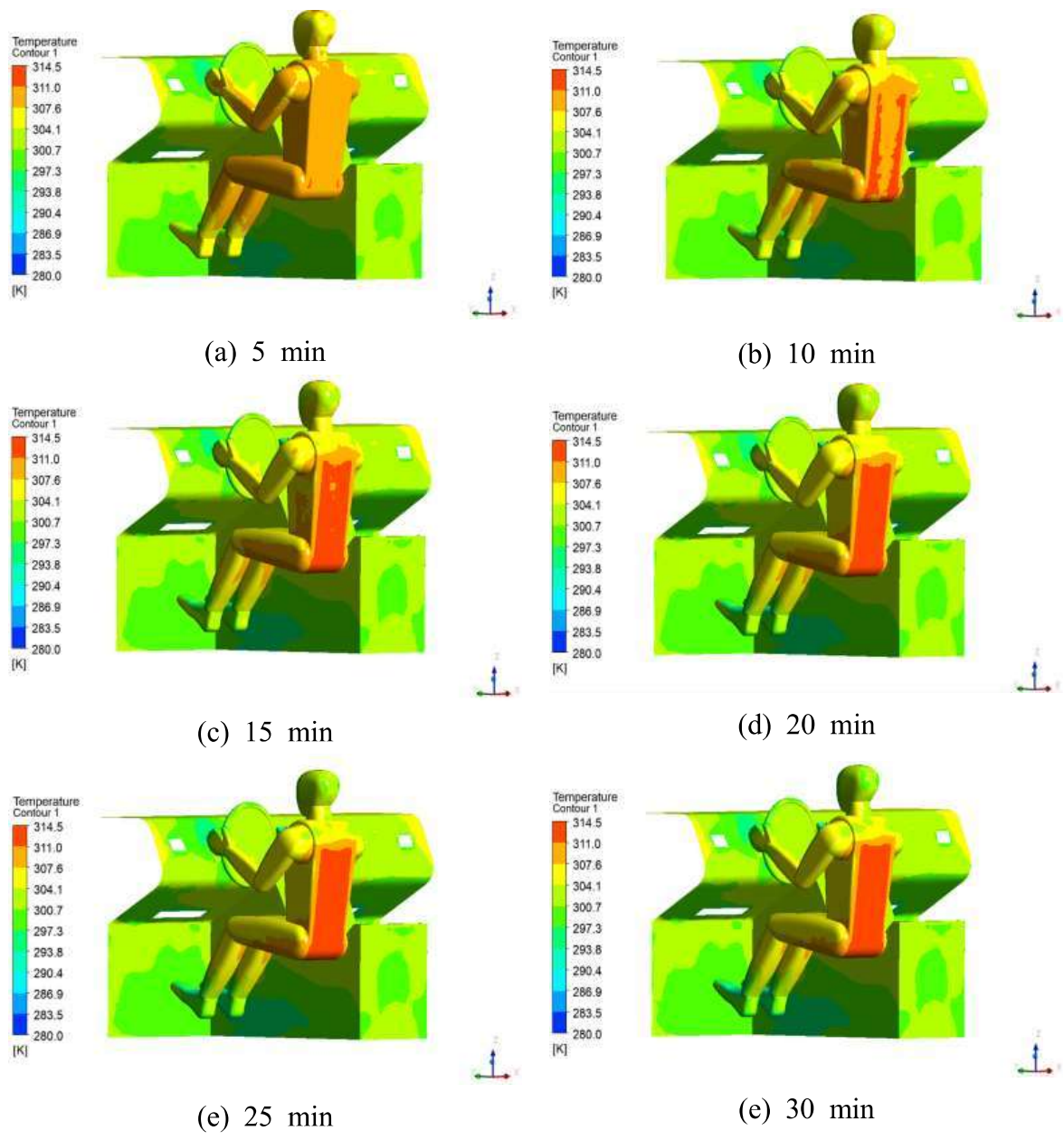water seat during cooling

(a) 5 min

(b) 10 min

(c) 15 min

(d) 20 min

(e) 25 min

(f) 30 min
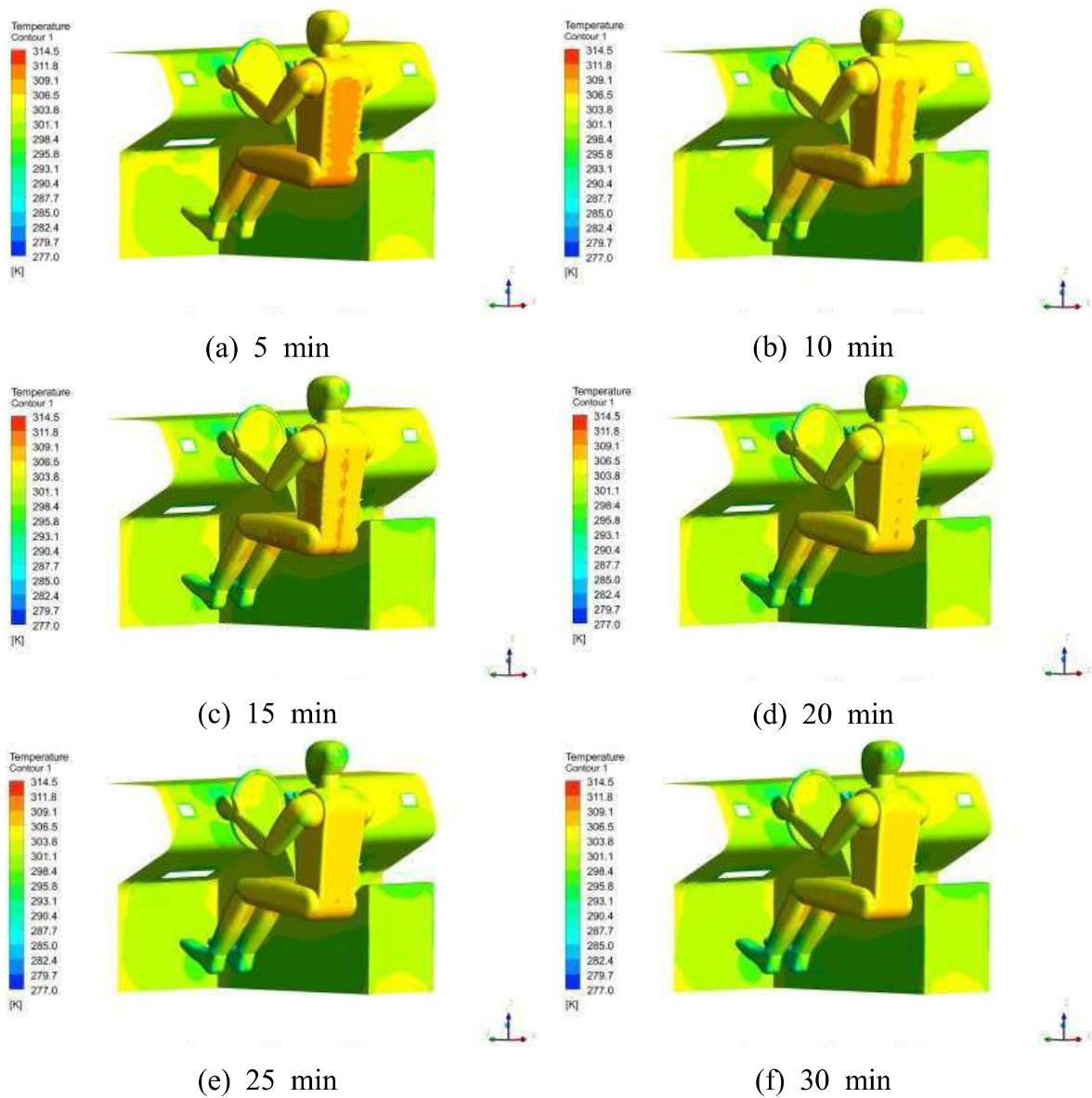
Fig. 5.8 Simulation result of surface temperature of human in automobile with the cold water seat during cooling

2. Simulation results of the automotive thermal environment in winter

Fig. 5.9 shows the simulation results of the thermal environment on the driver according to the operation of the heating in the basic seat of a vehicle during winter condition. The initial temperatures of the automotive indoor and vent are set to 15°C and 40°C, respectively. After 5 minutes of the HVAC heating, the temperature at the torso, back, arms, thighs, and hips of the human body is 24.8°C, 26.0°C, 25.1°C, 24.7°C, and 25.3°C, respectively. At the beginning of the heating operation, the temperature of the human body is lower than that in the summer because the cold air in the indoor has a greater effect on the body temperature than the warm air caused by the heater. Under this condition, the temperature at the head, hands, and feet of the human body is 27.4°C, 29.3°C, and 30.1°C, respectively, and these are relatively high compared to the other parts. This is because the top vent is directed toward the face and the bottom vent is toward the foot, resulting in heating these parts. After 20 minutes of heating in HVAC, the temperature at the torso, back, arms, thighs, head, hands, feet, and hips of the human body is 25.4°C, 27.3°C, 26.2°C, 25.3°C, 29.8°C, 32.8°C, 33.9°C, and 26.3°C, respectively. In addition, when 30 minutes of heating have passed, the temperature at the torso, back, arms, thighs, head, hands, feet, and hips of the human body is 25.6°C, 27.9°C, 26.7°C, 25.5°C, 30.5°C, 33.9°C, 35.1°C, and 26.8°C, respectively. Accordingly, the temperature of these parts shows increase more than before.

Fig. 5.10 shows the variation of the surface temperature of the human body with time when heating in the automobile is operated in winter condition. As 5 minutes of the initial heating is operated, the temperature of human body is averagely 26.3°C. The temperature increased in all parts of the human body according to time. When 30 minutes of heating have passed, the temperature of the head, hands, and feet increases by 3.15°C, 4.98°C, and 4.65°C, respectively, so it shows the highest temperatures. This is because the head, hands, and feet are close to the hot vent and

are affected by the temperature directly. The operation of the heater in winter does not have a greater effect on the driver than when the air conditioner is operated in summer because the airflow volume of the heating in winter is less than that of cooling of the air conditioner in summer. Accordingly, it is confirmed that the operation of the heater of HVAC in the cold winter delivers warmth to the driver effectively, but its effect is not significant compared to the cooling.

(a) 5 min

(b) 10 min

(c) 15 min

(d) 20 min

(e) 25 min

(f) 30 min

Fig. 5.9 Simulation result of temperature distribution for automobile using the basic
seat during heating

(a) 5 min

(b) 10 min

(c) 15 min

(d) 20 min

(e) 25 min

(f) 30 min

Fig. 5.10 Simulation result of surface temperature of human in automobile with the basic seat during heating

As the results of the simulation during heating by using the basic seat of the vehicle, the temperature change at the parts of human body which do not affected by the heater is small. Besides, it is confirmed that the temperature change of the hips and thighs that are in contact with the driver's seat also shows small change. Accordingly, a function to increase the temperature in a vehicle seat is required, thus, the heating seat using heat wires is generally used in a current automobile. However, the heating seat generates electromagnetic wave that is harmful to the human body, and the passengers are directly affected this harmful effect. Therefore, in this study, a hot water seat is designed to effectively warm the human body in contact with the driver by inserting a hot water pipe into the driver's seat. The simulation results of the automobile indoor using the hot water seat are shown in Fig. 5.11. When 5 minutes heating is operated, the temperature at the torso, back, arms, thighs, and hips of the human body is 25.0°C, 25.0°C, 25.6°C, 25.1°C, and 24.5°C, and the temperature at the head, hands, feet of the driver is 30.6°C, 29.9°C, and 33.9°C, respectively. The human body temperature of the driver using the hot water seat shows overall higher than that of the basic seat. When 20 minutes of HVAC heating have passed, the temperature at the torso, back, arms, thighs, head, hands, feet, and hips of the human body is 26.0°C, 28.1°C, 27.4°C, 26.7°C, 34.0°C, 32.8°C, 38.2°C, and 27.5°C, respectively. In addition, after 30 minutes of HVAC heating, the temperature at the torso, back, arms, thighs, head, hands, feet, and hips of the human body is 26.4°C, 29.5°C, 28.1°C, 27.4°C, 35.0°C, 33.7°C, 39.3°C, and 28.9°C, respectively. It can be confirmed that the human body temperature in contact with the hot water seat increases according to the increase of heating time.

Fig. 5.12 shows the variation of the surface temperature of the human body with the time when the hot water seat is used during heating in winter condition. As 5 minutes of heating have passed, the average temperature of the human body is about 0.94°C higher than that using the basic seat. After 10 minutes of heating have passed, the temperature at the back and hips of the human body which is in contact with the hot water seat increases by 26.2°C and 25.6°C. respectively, while the

increasing rate of temperature for thighs is relatively low by 25.7°C. This is because the temperature for the inside parts of the thigh increases, but there are parts exposed to the surrounding air, thus the increasing rate of the average temperature is relatively small. When 20 minutes of heating are operated, the temperature of the back, hips, and thighs that are in contact with the hot water seat increases by 28.1°C, 27.5°C, and 26.7°C, respectively. In addition, after 30 minutes of HVAC heating, the temperature of the torso, hands, and legs using hot water seat is averagely about 1.97°C higher than that using the basic seat. This is because the use of the hot water seat increases the temperature of the back, thighs, and hips which are the contact parts of the seat, therefore it has great the effect on the increase of the overall temperature in the human body. It is confirmed that the use of a hot water seat during heating in a car in cold winter can provide more effective thermal comfort to the driver than that using the basic seat.

(a) 5 min

(b) 10 min
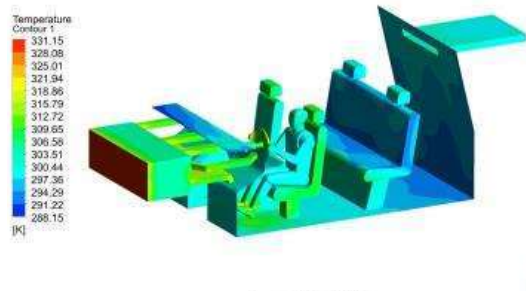
(c) 15 min
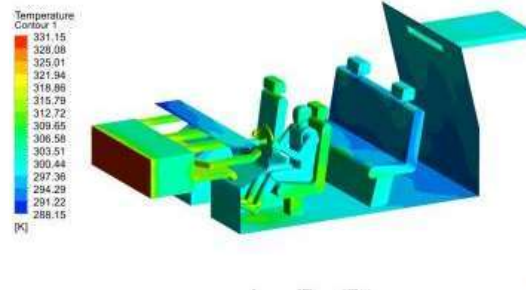
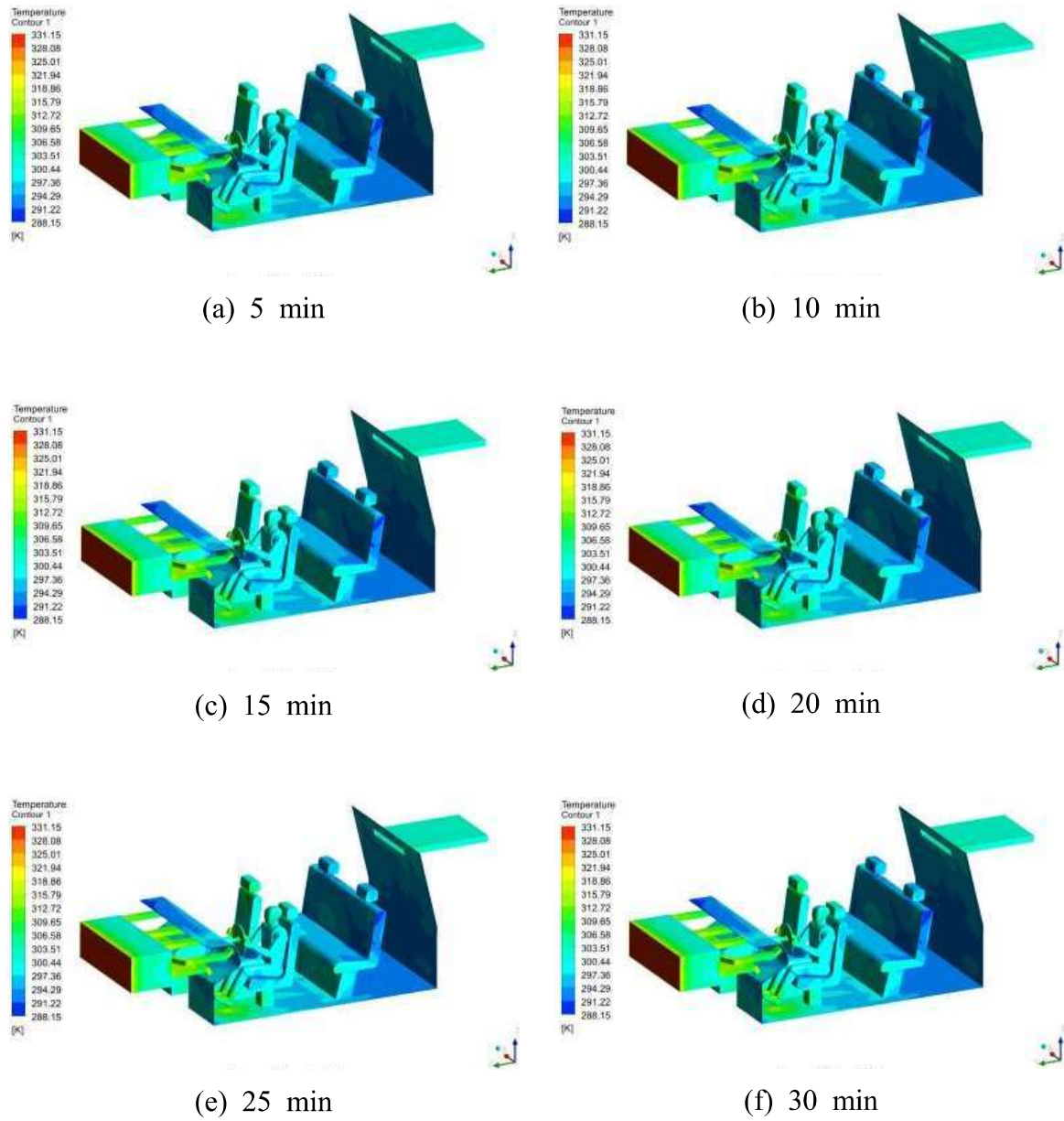(d) 20 min
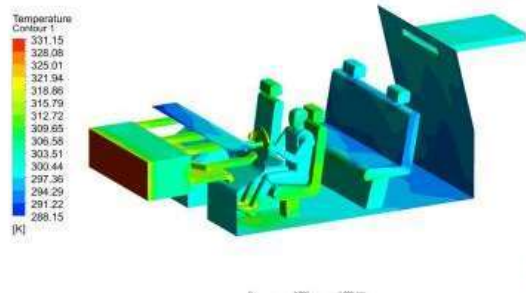
(e) 25 min
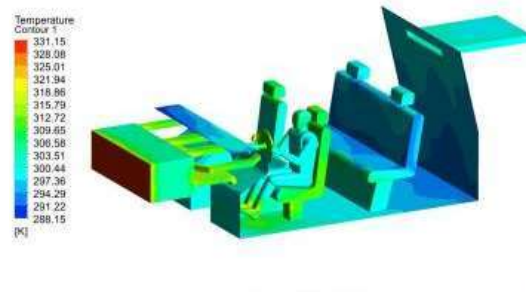
(f) 30 min
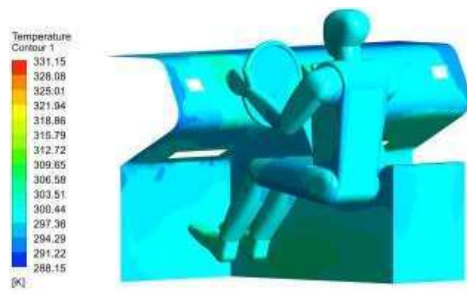
Fig. 5.11 Simulation result of temperature distribution for automobile with the hot water seat during heating

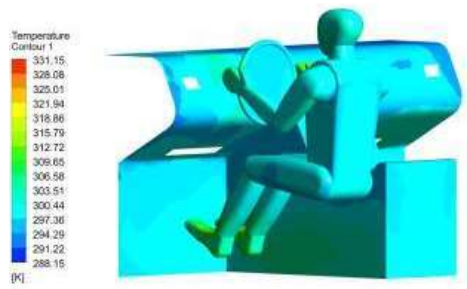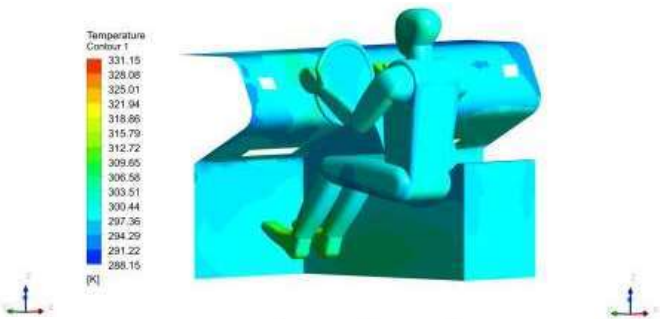(a) 5 min   (b) 10 min

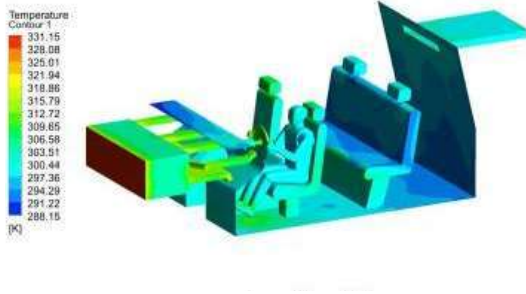(c) 15 min   (d) 20 min

(e) 25 min   (f) 30 min

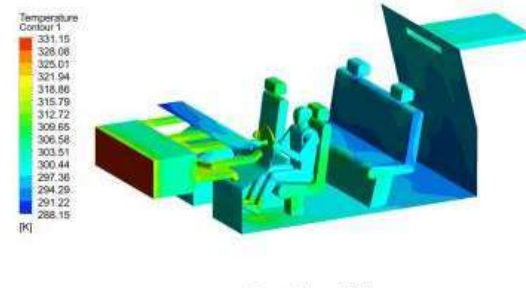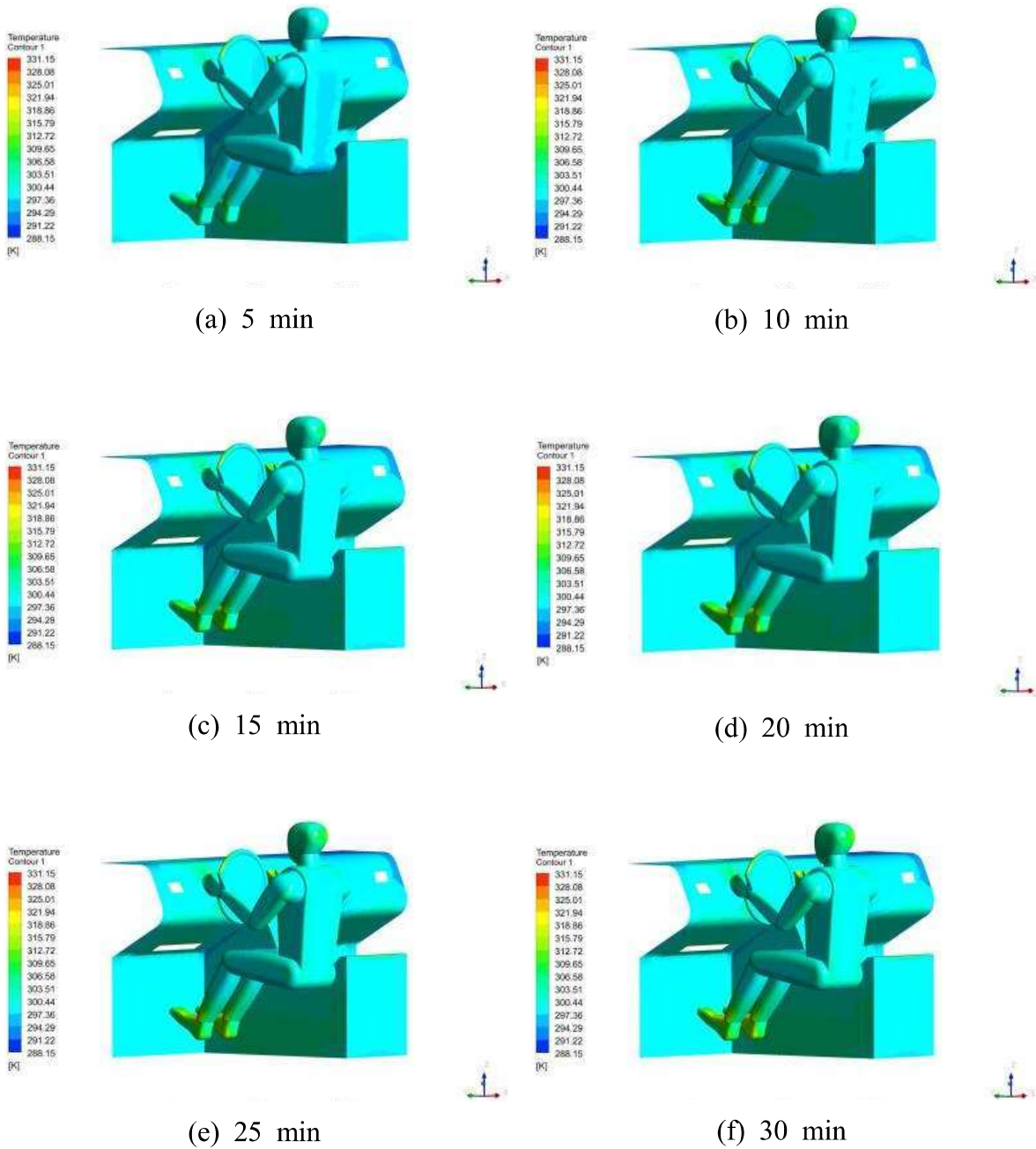Fig. 5.12 Simulation result of surface temperature of human in automobile with the hot water seat during heating

C. Thermal comfort analysis on simulation results of automotive thermal environment

1. Analysis results on thermal comfort of the automotive thermal environment in summer

Fig. 5.13 shows the surface temperature of the human body of the driver when the basic seat and cold water seat are used in the summer automotive indoor condition by the simulation. Fig. 5.13(a) presents the surface temperature of each body part of the driver when the basic seat is used under the automotive indoor in summer. When the basic seat is used during cooling in summer, the surface temperature at the back and hips of driver is relatively high, and it shows a tendency to increase gradually with the passage of time. However, the surface temperature of all bodies except the back and hips tends to decrease gradually as time passed. In particular, the surface temperature of the hands, feet and head shows the large reduction due to the direct influence of the cold air from air conditioner in HVAC. This is because the cooling operation of the air conditioner lowers the surface temperature of the driver and it provide a pleasant environment to the subject during driving in summer. However, it is confirmed that the cold air from air conditioner does not affect to the temperature of the back and hips in contact with the driver's seat.

Fig. 5.13(b) shows the surface temperature of each body part of the driver when the cold water seat is used under the automotive indoor in summer. When the cold water seat is used during cooling in summer, it is confirmed that the surface temperature at all the body of the driver is lower than that using the basic seat. In particular, it is confirmed that the surface temperature of the back and hips in contact with the cold water seat is 6.15°C and 4.28°C, respectively, which are lower than those using the basic seat when 30 minutes passes. Thus, the surface temperature of all human body parts also decreases by 2.96°C on average compared to that using the

basic seat. The use of the cold water seat reduces the surface temperature at back and hips of the driver seat which is in contact with driver's seat, therefore it is confirmed that it provides the comfortable environment to the driver.
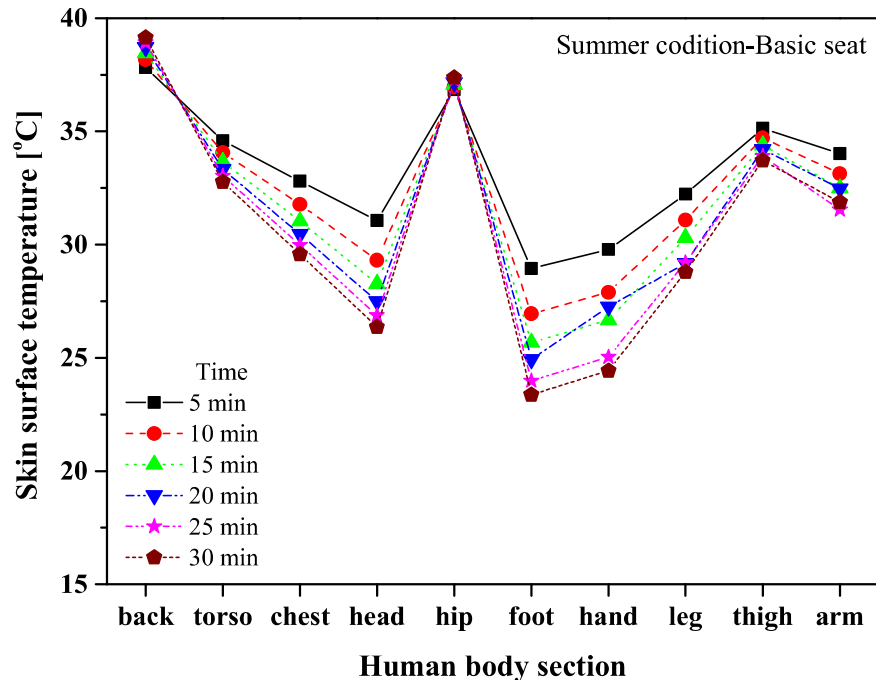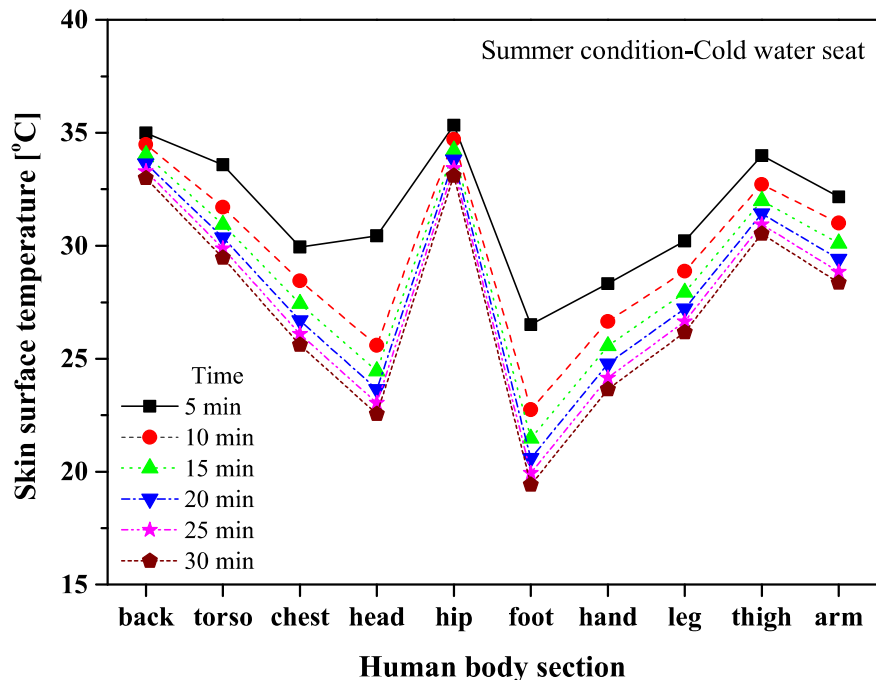
(a) Basic seat

(b) Cold water seat

Fig. 5.13 Surface temperature variation for each part of the body according to the seat type in summer condition

Fig. 5.14 shows the PMV and PPD according to the use of the basic seat and cold water seat in the summer automotive indoor condition from the simulation result. When the basic seat is used during cooling in summer, PMV is 2.14 at 5 minutes, which is a hot environment, and PPD is 82.7%. When 20 minutes of cooling have passed, PMV slightly decreases to 1.96, and the PPD is calculated by 75.2%. After 30 minutes of cooling, PMV and PPD are 1.91 and 72.7%, respectively. It is confirmed that the indoor environment of the car is still in a hot environment. On the other hand, when the cold water seat is used after 5 minutes of cooling in summer, PMV is 1.82 and PPD is 68.3%, respectively. It is confirmed that the PPD is 14.4% lower than that using the basic seat, which can significantly reduce the degree of initial dissatisfaction under the thermal environment in automobile. As the cooling time of 20 minutes has passed, PMV is 1.55 and PPD is 53.9%, respectively. This indicates that the thermal environment in the car is slightly hot to the driver. After 30 minutes of cooling, PMV and PPD are 1.47 and 49.3%, respectively, and PPD is 23.4% lower than that using the basic seat. Accordingly, it is confirmed that the use of the cold water seat during cooling condition can be effectively reduced the driver's dissatisfaction for thermal environment of a vehicle in summer. As the results of simulation, it is confirmed that the use of the cold water seat in the driver's seat can significantly reduce PMV and PPD, and it is confirmed that it can provides a pleasant environment thermally to the driver.
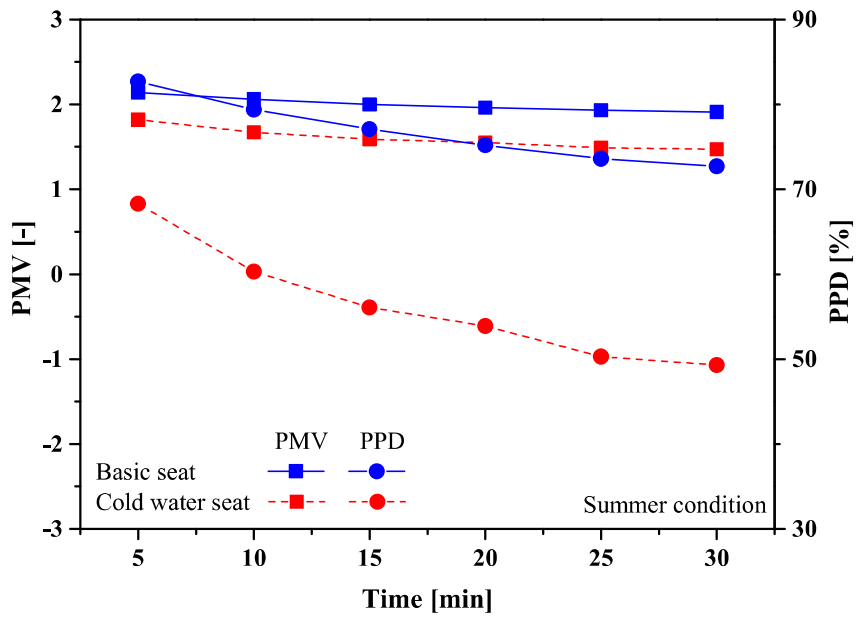
Fig. 5.14 Comparison of PMV and PPD according to use of basic seat and cold water seat in summer condition

2. Analysis results on thermal comfort of the automotive thermal environment in winter

Fig. 5.15 shows the surface temperature of the driver's body according to the use of the basic seat and hot water seat in the automotive indoor for heating by using the simulation method. Fig. 5.15(a) shows the surface temperature of each part of the driver's body when the basic seat is used under the automotive indoor in winter. When the basic seat is used during heating in winter, the surface temperature at the back and hips of the driver is slightly increased. This is because the back and thighs are in contact with the driver's seat, so there is relatively small heat loss. After 30 minutes of heating in winter, the surface temperature of the head, hands, and feet is 30.5°C, 33.9°C, and 35.1°C, respectively, these show the highest surface temperatures. This is because the warm air from the vent of HVAC is discharged toward directly to the head and feet, and the hands.

Fig. 5.15(b) shows the surface temperature of each body part of the driver when the hot water seat is used under the automotive indoor in winter using simulation result. When the hot water seat is used during heating in winter, it is confirmed that the average temperature at all the body surfaces of the driver is 1.55°C higher than that using the basic seat with the increase of time. In particular, it is confirmed that the surface temperature of the back and hips in contact with the hot water seat is 1.60°C and 2.06°C, respectively, and these are higher than those using the basic seat after 30 minutes heating in winter. Moreover, the surface temperature of all human body parts also increases by 1.97°C on average compared to that using the basic seat. The use of the hot water seat increases the surface temperature at back and hips which are in contact with driver's seat, thus it is confirmed that the use of hot water seat can provide the comfortable thermal environment to the driver.
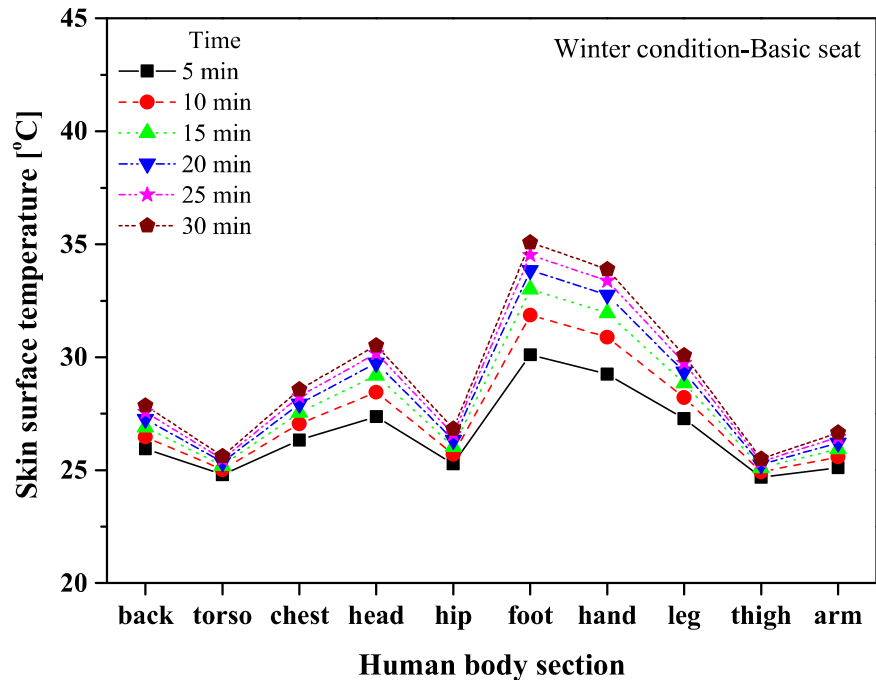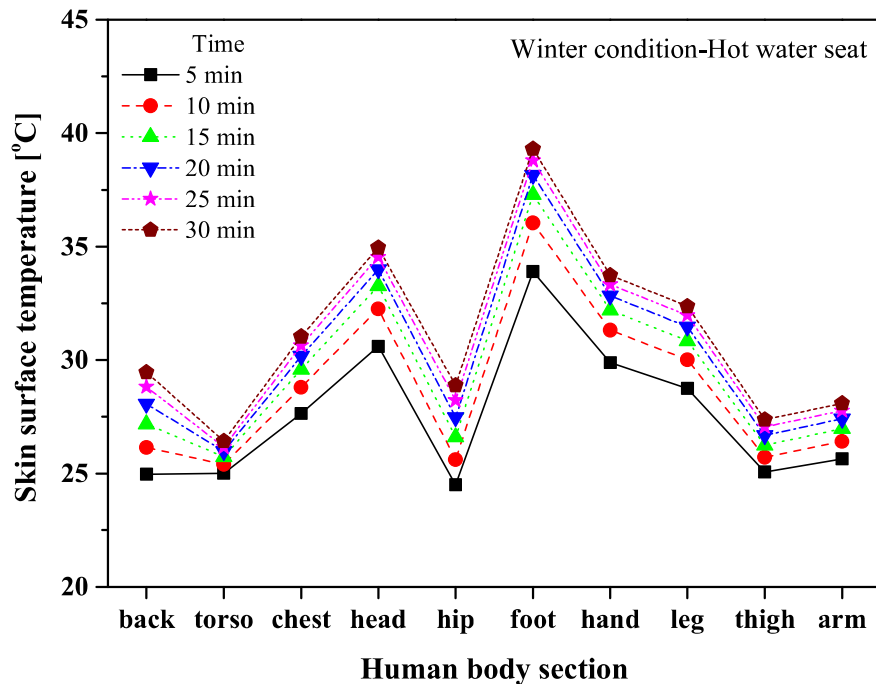
(a) Basic seat

(b) Hot water seat

Fig. 5.15 Surface temperature variation for each part of the body according to the
seat type in winter condition

Fig. 5.16 shows the PMV and PPD according to the use of the basic seat and hot water seat in automotive indoor conditions for simulation of winter using the simulation. When the basic seat is used during heating in winter, PMV is -0.69 and PPD is 14.9% after 5 minutes of heating. When 20 minutes have passed after heating, PMV slightly decreases to -0.56 and the PPD is calculated by 11.6%. In addition, when the heating time of 30 minutes has passed, PMV and PPD are -0.49 and 10.1%, respectively. In general, if the PPD is between -10% and 10%, it can be evaluated as a comfortable environment. However, in this study, after 30 minutes of heating, it was confirmed that the PPD of the indoor environment in the vehicle is just 10.1%, thus it indicates that there is still a slight discomfort condition. When the hot water seat is used after 5 minutes heating in winter, PMV and PPD are -0.22 and 6.0%, respectively. It is confirmed that the PPD is 8.90% lower than that using the basic seat. This means the use of hot water seat can significantly reduce the degree of initial dissatisfaction under the thermal environment of automobiles in winter. Besides, PPD shows less than 10%, therefore it means the thermal environment of the vehicle is to be pleasant state. After 20 minutes of heating, PMV and PPD are -0.07 and 5.10%, respectively. In addition, when the heating time of 30 minutes has passed, PMV and PPD are 0.02 and 5.0%, respectively. The thermally comfort zone is defined by ASHRAE and it has the range from -0.5 to 0.5 for PMV and less than 10% for PPD. The use of hot water seat in the driver's seat during winter satisfies thermally comfort zone in both PMV and PPD, thus it is confirmed that the use of hot water seat can provide a thermally pleasant environment to the driver.
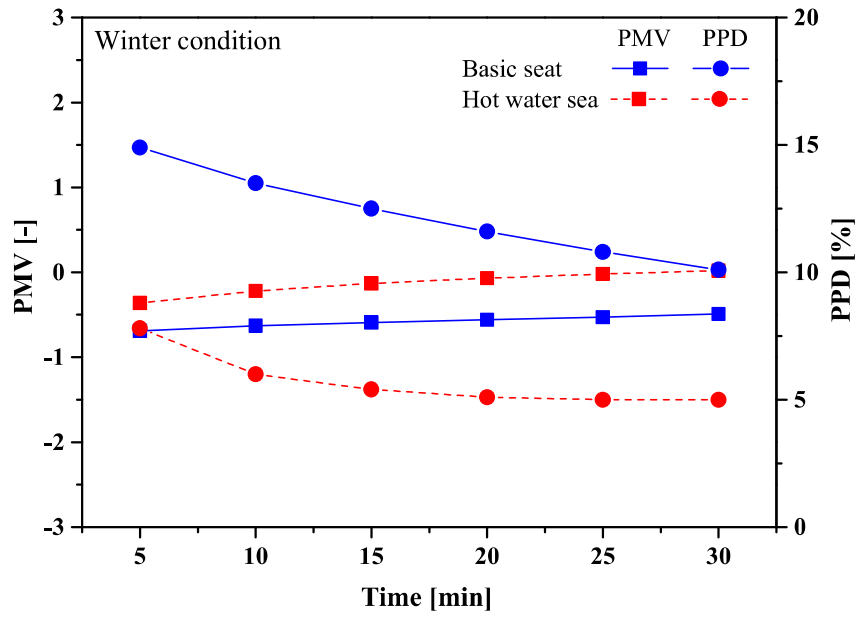
Fig. 5.16 Comparison of PMV and PPD according to use of basic seat and hot water seat in winter condition

VI. Experimental results and discussions

A. Experimental results and discussions on the driver's thermal comfort according to the condition changes of the automotive indoor

1. Experimental results on driver's thermal comfort according to the change of automotive indoor conditions in summer

a. Mean surface temperature measurement results

Fig. 6.1 shows the variation of surface temperature of the driver according to the cabin and vent discharge air temperature under maximum and average solar radiations of 1251 and 516 W/m^2, respectively. A thermal-imaging camera was used to measure the surface temperature of the subject based on rainbow-based color coding. Red indicates a higher temperature, and purple represents a lower temperature. As shown in Fig. 6.1(b), when the cooling mode is not operated at a cabin temperature of 35°C, the surface temperature of the subject shows a sky color, which represents relatively a higher temperature. In particular, the surface temperature on the abdomen of the subject is highest because the solar light directly heats that part, and red in a wide area around the abdomen appears. Fig. 6.1(c) shows the surface temperature of the subject when HVAC with a vent discharge air temperature of 12.5°C was operated at the same cabin temperature of 35°C. The surrounding colors of the subject are mainly sky-blue and blue, which means a decrease of the surrounding temperature of the subject. In addition, the color of the air near the vent is purple, which represents a low temperature. The abdomen where the radiation is concentrated and its surroundings appear yellow and green compared with that when the cooling vent is not operated. The surface temperature of the subject rapidly decreases when

the cooling of HVAC is operated. As the temperature of the cabin decreases, the ambient temperature and the surface temperature of the subject decreases, and they are mostly blue when the cabin and vent discharge air temperatures are 30.5°C and 16.5°C, respectively, as shown in Fig. 6.1(e). The yellow area decreases and the green area increases in the abdomen and body of the subject. Then, the ambient temperature and the surface temperature of the subject decrease continuously until the cabin and vent discharge air temperature of 22.5°C. When the cabin and vent discharge air temperatures are 22.5°C, the surrounding air is purple, indicating the lowest temperature. The largest decrease in surface temperature is observed in the abdomen. This is because the cooling effect is the most effective in the abdomen due to the cold air blowing from the vent outlet directly contacts the surface of the subject, and the surface temperature is the highest because of solar illumination.

Fig. 6.2 shows the variation of the average surface temperature on the left hand, right hand, forehead, and abdomen of the subjects by using the thermal-imaging camera during cooling in a car. At the common room temperature of 25°C, the average surface temperatures on the left hand, right hand, forehead, and abdomen of the subject were 28.6°C, 28.9°C, 31.5°C, and 30.1°C, respectively. When the cabin temperature was 35°C without the vent cooling operation, the average surface temperatures on the left hand, right hand, forehead, and abdomen increased significantly to 37.9°C, 36.6°C, 36.5°C, and 47.4°C, respectively. In addition, the temperature on the abdomen was the highest compared with other surface areas because the solar light irradiated intensely on the abdomen under a cabin temperature of 35°C; however, the surface temperatures of the subjects, except for on the abdomen, were similar. When the vent discharge air temperature was 12.5°C under a cabin air temperature of 35°C, the average surface temperatures on the left hand, right hand, forehead, and abdomen of the subjects were 37.0°C, 34.5°C, 34.5°C, and 41.6°C, respectively. Using vent cooling decreased the surface temperature on the forehead and abdomen of the subject during driving by 3.0°C and 11.5°C, respectively. The surface temperature on the forehead and abdomen of the subject can

be reduced noticeably because of the low discharge air temperature of 12.5°C, despite a high cabin temperature of 35°C. Thereafter, the surface temperature of the subjects gradually decreases as the cabin temperature decreases; however, the decrement of surface temperatures is not significant. The average surface temperatures on the left hand, right hand, forehead, and abdomen of the subject were decreased to 31.9°C, 28.0°C, 29.2°C, and 36.0°C, respectively, in the cabin and at a vent discharge air temperature of 22.5°C. In particular, the temperatures on the abdomen and left hand are significantly reduced because the cooling effect on the abdomen and left hand is relatively high. These parts have higher temperatures because they are directly exposed by irradiating solar light and directly contacted by cold vent discharge air, simultaneously.

(a) Standard condition(25°C)   (b) Cabin 35°C/Non-Vent   (c) Cabin 35°C/Vent 12.5°C

(d) Cabin 32.5°C/Vent 14.5°C   (e) Cabin 30°C/Vent 16.5°C   (f) Cabin 27.5°C/Vent 18.5°C

(g) Cabin 25°C/Vent 20.5°C   (h) Cabin 22.5°C/Vent 22.5°C
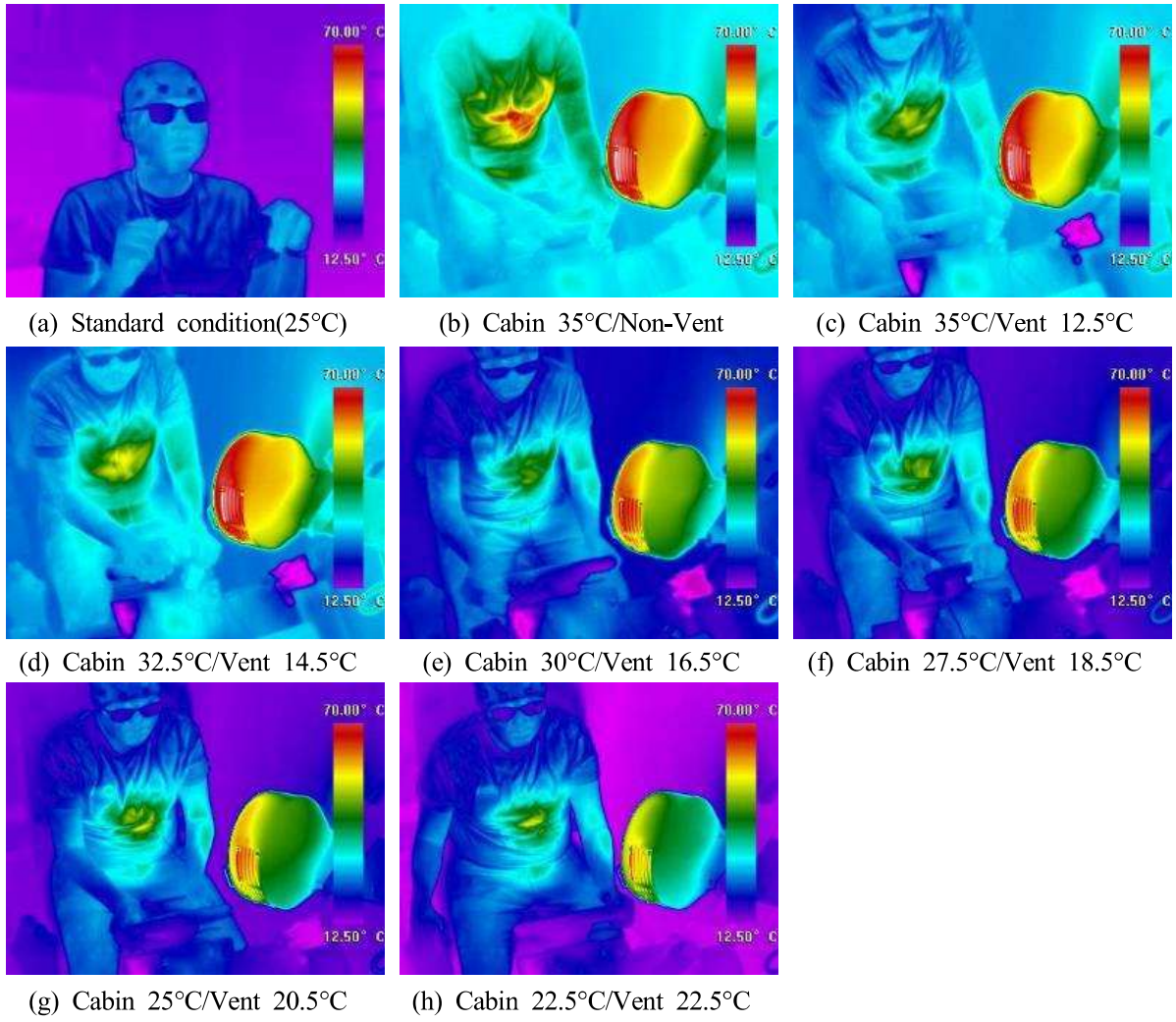
Fig. 6.1 Photograph of driver's thermal imaging during cooling in summer condition
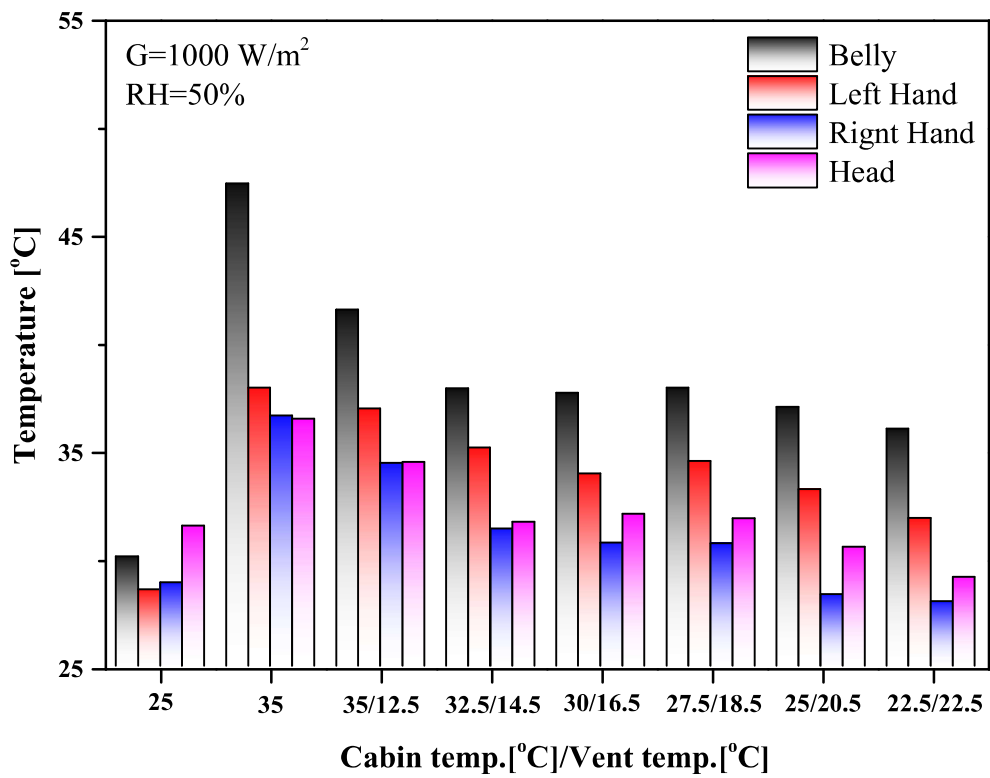
Fig. 6.2 Variation of driver's mean surface temperature during cooling in summer condition

b. Subjective questionnaire survey results(TSV, CSV, CLV)

Fig. 6.3 shows the results of questionnaires of the average TSV, CSV, and CLV of subjects according to the cabin and vent discharge air temperature under solar radiation. The TSV was 2.89 at a cabin temperature of 35°C without vent cooling, which showed that subjects felt very hot. The TSV was significantly reduced to 1.33 when the HVAC with a vent discharge temperature of 12.5°C was operated at a cabin temperature of 35°C. In the results, the thermal sensation of the subjects decreased from very hot to warm. At the cabin and vent discharge air temperatures were 30°C and 16.5°C, the TSV was 0, and it was confirmed that the subjects were in a thermally neutral state. Next, the TSV value gradually decreased as the cabin and vent discharge air temperatures were changed to 22.5°C, and the subjects at the cabin and vent discharge air temperatures of 22.5°C were in a cold state because the TSV was -2.11. In the results of the CSV questionnaire, the CSV at a cabin temperature of 35°C without vent cooling operation was -2.33, which was the lowest. This value indicated that the subjects felt great discomfort because of the high cabin temperature. When the cooling was operated with a vent discharge temperature of 12.5°C under a cabin temperature of 35°C, the CSV increased rapidly to -0.44, and the comfort sensation of subjects was similar to the neutral state. The subjects felt suddenly comfortable compared with the previous condition because the discharge air from the vent with a low temperature of 12.5°C could quickly provide a comfortable environment to the driver, even though it was a hot cabin environment (35°C). Then, the CSV increased until the cabin and vent discharge air temperatures of 25°C and 20.5°C, respectively. The CSV at cabin and vent discharge air temperatures of 25°C and 20.5°C was 1.33, which was the highest; thus, the survey result found that subjects felt the most comfortable in these conditions. Next, the CSV decreased to 0.67 at a cabin and vent discharge air temperatures of 22.5°C. The cabin and vent discharge air temperatures of 22.5°C are relatively cold because of the direct contact of the low temperature air to the body of the driver. According to the results of the CLV questionnaire of the subjects during cooling in the indoor environment of the

car, the CLV was -1.78 at a cabin temperature of 35°C without the vent cooling operation, so it was the lowest. During vent cooling with a low discharge air temperature of 12.5°C, the CLV rapidly increased to -0.33. This is because of the operation of vent cooling with a low temperature of 12.5°C despite a hot cabin temperature of 35°C. The vent cooling provided a thermally pleasant environment to the driver and greatly improved concentration during driving. As the cabin temperature decreased, the CLV tended to increase, and the CLV increased to 1.33 at cabin and vent discharge air temperatures of 25°C and 20.5°C, respectively. However, when the cabin and vent discharge air temperatures were 22.5°C, the CLV decreased to 0.56, which indicates the subjects felt cold and unpleasant, and the concentration of the drivers decreased owing to long-term driving. The CLV showed a similar result to that of the CSV. In the overall results of the subjective questionnaires (TSV, CSV, and CLV), the subjects were comfortable and had a high level of concentration in the temperature ranges of the cabin and vent discharge air temperatures of 30°C and 16.5°C to those of 25°C and 20.5°C, respectively.
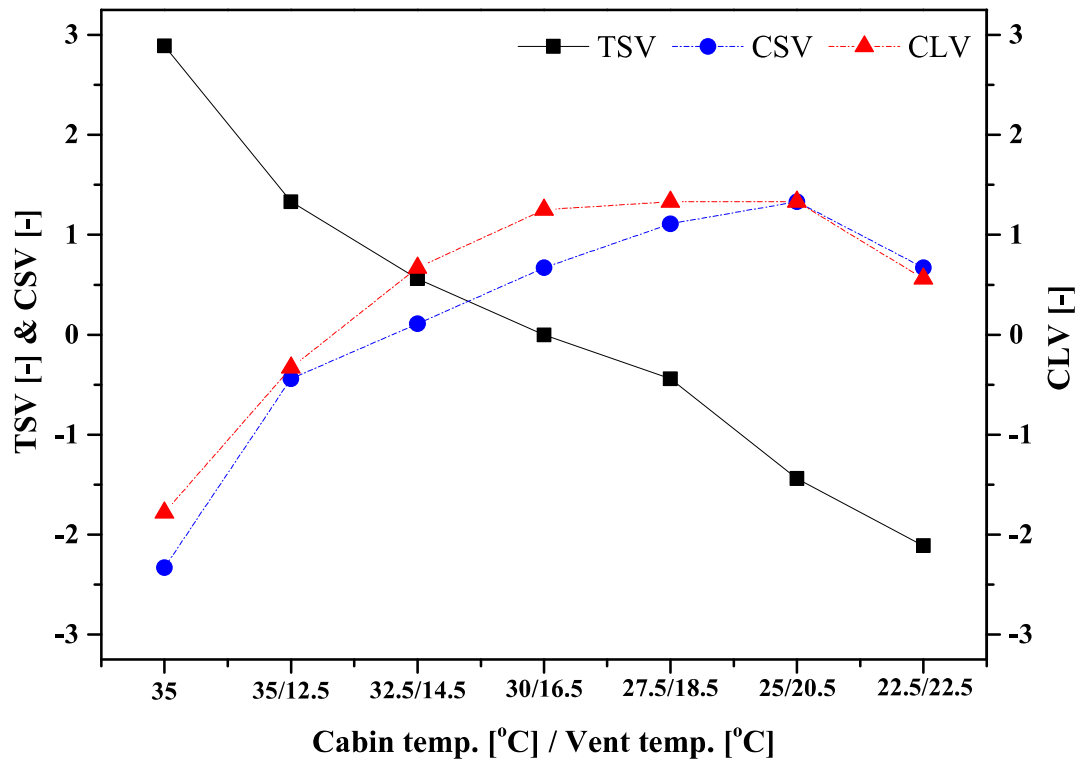
Fig. 6.3 Variations of TSV, CSV, and CLV questionnaires during cooling in summer condition

c. PPG measurement results

Fig. 6.4 shows the variation of the pulse wave of the driver according to the cabin and vent discharge air temperatures in the cooling mode under solar radiation. Fig. 6.4(a) shows the variations of the stress index, TP, and LF/HF. At room temperature (25°C), which was the preparation condition before the experiment, the stress index, TP, and LF/HF showed general values, because it was the common indoor temperature. Unlike the results of questionnaires, the stress index, TP, and LF/HF did not change significantly when the cabin and vent discharge air temperatures were 35°C and 12.5°C, respectively. This is due to short time after the subject started to drive, and the response for feeling by the body was not immediately linked to the pulse wave. Thus, the pulse wave of subjects did not change immediately according to the operating condition. After the body adapted for a certain period at high temperature, the stress index increased rapidly at the cabin and vent discharge air temperatures of 32.5°C and 14.5°C, respectively. Accordingly, TP tended to decrease slightly. This indicates that the ability of the driver to regulate the external environment change and to cope with stress deteriorate during a long time under high temperatures, which also results in an increase of the stress index of the driver. At the cabin and vent discharge air temperatures of 30°C and 16.5°C, the TP increased and stress index decreased; therefore, it can be judged that the subjects were relatively stable and comfortable when driving under these conditions. However, the stress index rapidly increased again at cabin and vent discharge air temperatures of 25°C and 20.5°C. The discomfort of the driver was caused by the direct contact with a low air temperature and the fatigue from a long driving time. The result of the PPG analysis confirmed that there was time gap between the emotional feeling and the PPG reaction during driving.

Fig. 6.4(b) shows the variations of the SDNN and RMSSD in the pulse wave of the subjects during driving. The SDNN and RMSSD at a cabin temperature of 35°C without vent cooling were higher than those at the indoor temperature of 25°C, which was the preparation condition. This is because the subject suddenly entered a hot

environment and the body temperature of the subject increased rapidly. This phenomenon occurred at the stage of human body adaptation in a hot environment. Afterward, the SDNN and RMSSD tended to decrease continuously until the cabin and vent discharge air temperatures of 32.5°C and 14.5°C, respectively, which means that the driver felt uncomfortable under these temperature conditions. SDNN and RMSSD at the cabin and vent discharge air temperatures of 30°C and 16.5°C increased slightly, which is similar to the variation of the stress index. This is due to the body of the driver adapted to the thermal environment, which provided a relatively comfortable environment to the driver. In the results of the PPG analysis under a cooling condition with solar radiation in the summer, the stress index of the driver decreased at cabin and vent discharge air temperatures of 30°C and 16.5°C, as well as 27.5°C and 18.5°C, respectively, while the TP, SDNN, and RMSSD increased simultaneously. Therefore, these two temperature conditions can provide a relatively comfortable driving environment for the driver. Shin et al. [65] conducted an experiment on the variation of bio-signals of drivers according to the cabin temperature inside the car without solar load, and they reported that the cabin and vent discharge air temperatures were set to 27.5°C and 18.5°C, respectively, to improve driver comfort and concentration in the cooling mode. The cabin and vent discharge air temperatures suggested as comfortable temperature conditions in the previous study, which were slightly different from the result of this study. In this study, it is recommended that the cabin and vent discharge air temperatures be set to 30°C and 16.5°C, respectively. The solar radiation effect on the driver causes the driver to feel warmth; thus, the driver feels chill and more comfortable when a vent with a discharged air temperature of 16.5°C is working, even though the cabin temperature is slightly higher than that without solar radiation.
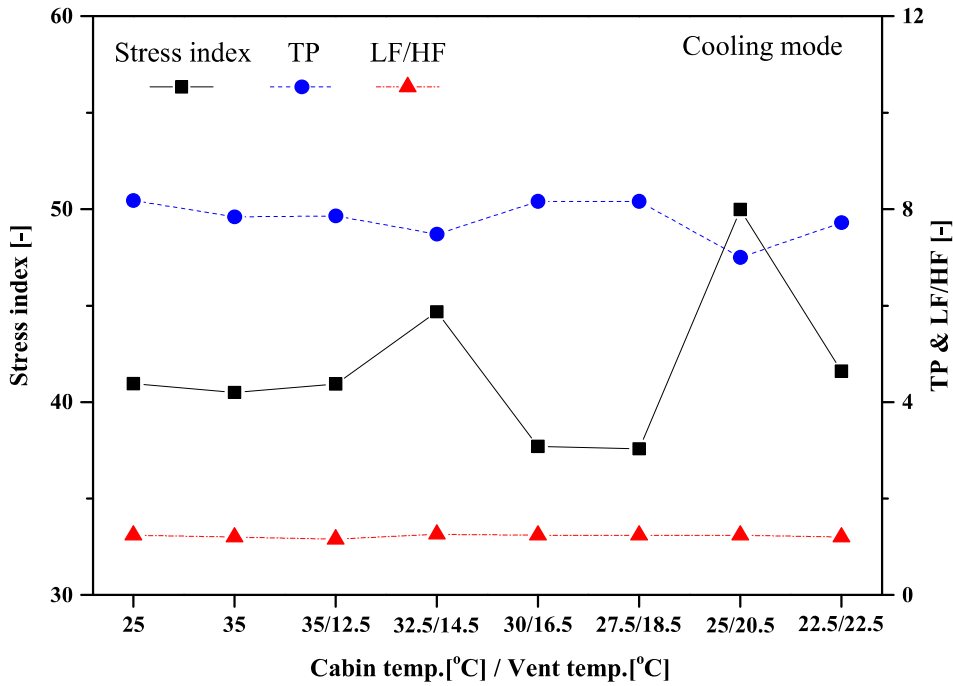
(a) Stress index, TP, and LF/HF
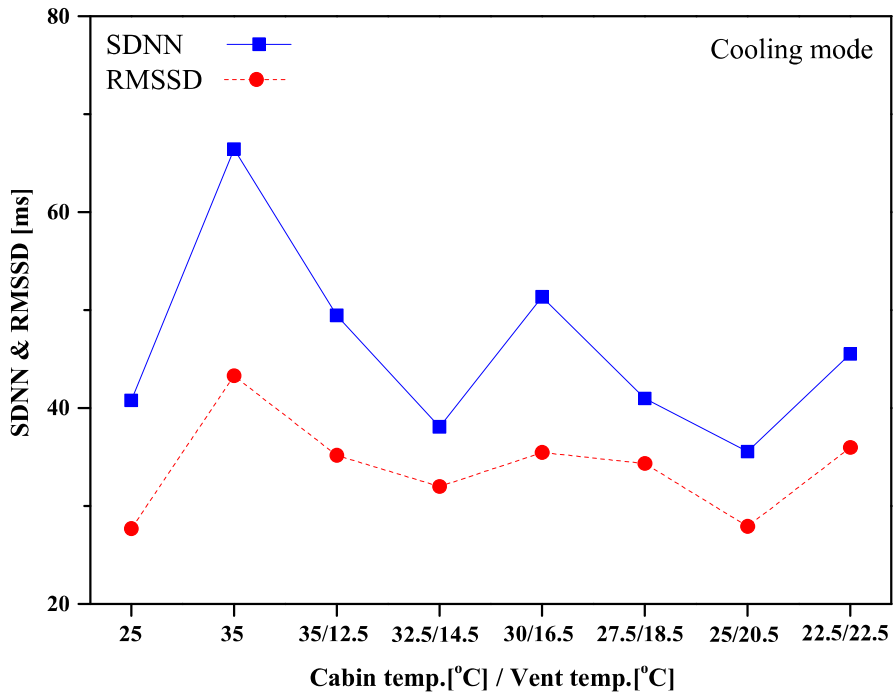
(b) SDNN and RMSSD

Fig. 6.4 Variations of driver's PPG during cooling in summer condition; (a) Stress index, TP and LF/HF, (b) SDNN and RMSSD

d. EEG measurement results

Fig. 6.5 shows the brain mapping using EEG analysis of the subject according to the cabin and vent discharge air temperatures in summer condition under an average solar radiation of 516 W/m^2. In the EEG analysis, the brain mapping was expressed by rainbow color. Red color indicates high EEG activity and purple color indicates low EEG activity. The relative θ wave at the indoor temperature of 25°C showed yellow-green color and red colors, thus the activity of relative θ wave increased. The relative SMR and β waves showed relatively low with purple and sky blue colors, which indicated low activity. When the cooling mode was not operated at a cabin temperature of 35°C, the activity of relative SMR wave decreased by showing purple and blue colors, and the activity of relative high β wave increased by showing yellow-green and red colors. The relative SMR wave is an indicator concentration on driving and the relative high β wave is an indicator of unpleasant condition such as excitement and anxiety. It was confirmed that the subjects were the low concentration on driving and an unpleasant state when the cooling mode was not operated at a cabin temperature of 35°C. When the cooling was operated with a vent discharge temperature of 12.5°C under a cabin temperature of 35°C, the activity of relative θ wave was increased by showing expanded yellow-green and blue colors, however the activity of relative high β wave was decreased by showing more yellow-green color distribution; hence, the subjects were a pleasant state due to the blowing cold air from the vent in a hot environment of 35°C. At the cabin and vent temperatures of 30°C and 16.5°C, the activities of relative SMR and β waves increased by showing yellow-green and sky blue colors, and the activity of relative high β wave decreased by showing sky blue and blue colors. Thus, it was confirmed that the subjects were relatively high concentrated on driving and in comfortable state under this condition. At a cabin and vent discharge air temperatures of 22.5°C, the activities of relative θ and high β waves increased by showing yellow-green and sky blue colors because of the long driving time and drowsiness.
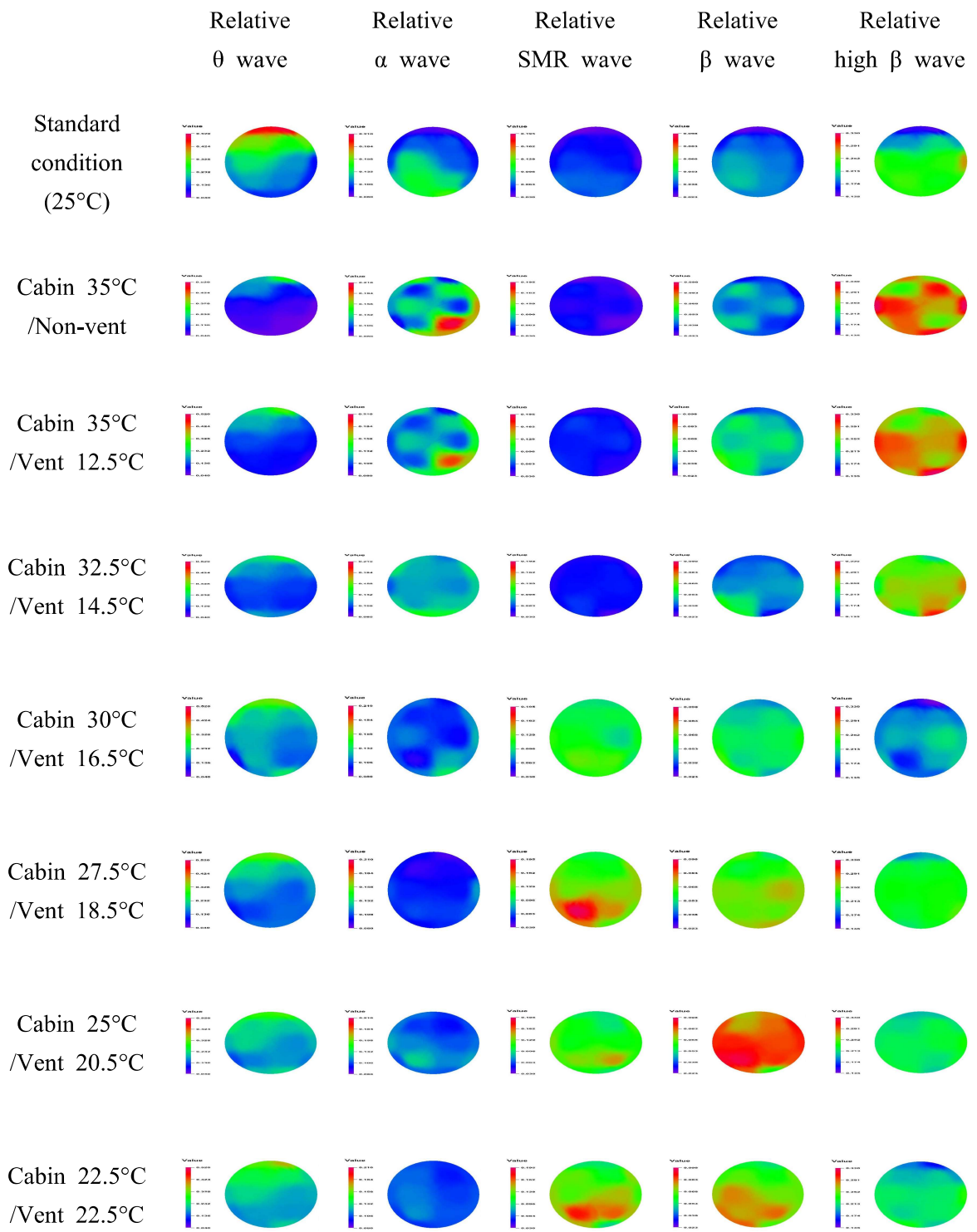
Fig. 6.5 Brain mapping of relative θ, α, SMR, β and high β waves with the cabin and vent discharge air temperatures under summer condition

Fig. 6.6 shows the concentration index (CI) and relative β/α of the driver in the prefrontal lobe of the subject according to the cabin and vent discharge air temperatures with an average solar radiation of 516 W/m^2. At the indoor temperature of 25°C, the concentration was the lowest, and the relative β/α was also low because the subject was in a comfortable state and doing nothing. The concentration showed a tendency to increase when the driver started to drive at a cabin temperature of 35°C without vent cooling, and the relative β/α also increased. Concentration increased at first because of the focus on driving of the subject. The reason for the increase in the relative β/α is that the subject was nervous because of discomfort caused by the high-temperature environment without vent cooling. Both the concentration and relative β/α of subjects were relatively low at cabin and vent discharge air temperatures of 32.5°C and 14.5°C, respectively, because the driver felt comfortable. However, the concentration on driving was reduced owing to slight drowsiness. When the cabin and vent discharge air temperatures were 30°C and 16.5°C, concentration was the highest, and the relative β/α showed an increasing trend. When the cabin and vent discharge air temperatures were 25°C and 20.5°C, concentration tended to decrease, and the relative β/α was the highest. This is considered to be a condition that requires some rest of the driver because the concentration of the subject during driving was reduced owing to a long driving time and the high stress during driving.

Fig. 6.7 displays the relative β/α of the driver in the occipital lobe according to the cabin and vent discharge air temperatures with the maximum and average solar radiation of 1251 and 516 W/m^2, respectively. The relative β/α wave was low at the 25°C preparation condition, and it slightly increased at a cabin temperature of 35°C without vent cooling. Under this condition, the relative β/α wave increased slightly, but it was not a meaningful change because the increase of the relative β/α wave was not significant. Thereafter, the relative β/α wave increased continuously until the cabin and vent discharge air temperatures were 27.5°C and 18.5°C, respectively, This means the subject was focusing on driving. Therefore, the relative α wave that appeared under a relaxed state, such as relaxation of tension, decreased, and the

relative β wave increased. At the cabin and vent discharge air temperatures were 25°C and 20.5°C, the relative β/α wave decreased because the concentration of the subject was slightly reduced due to the a little drowsiness and the increase of fatigue from a long time driving.
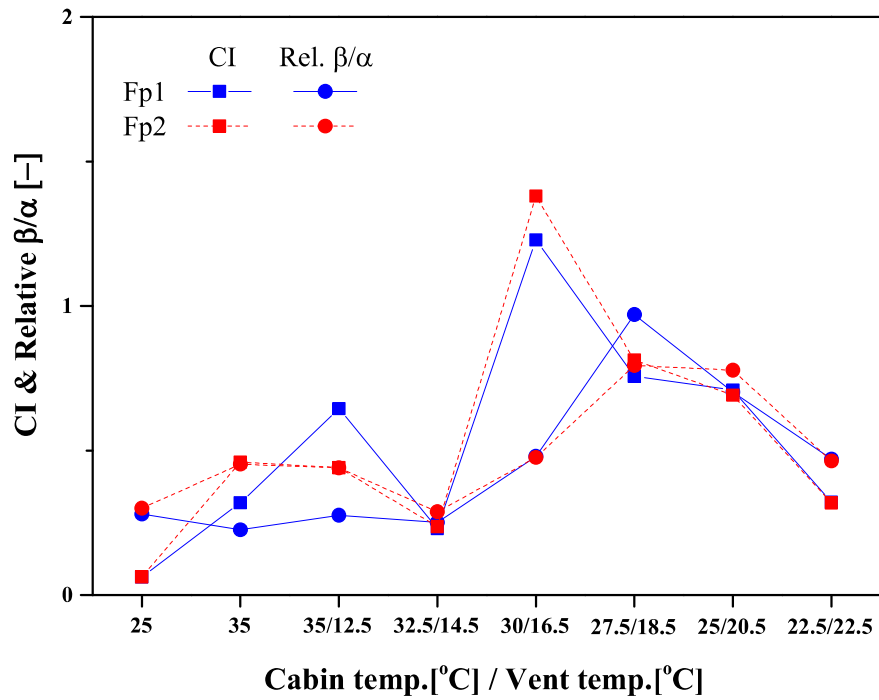
Fig. 6.6 Variations of CI and relative β/α at the prefrontal lobe during cooling under summer condition
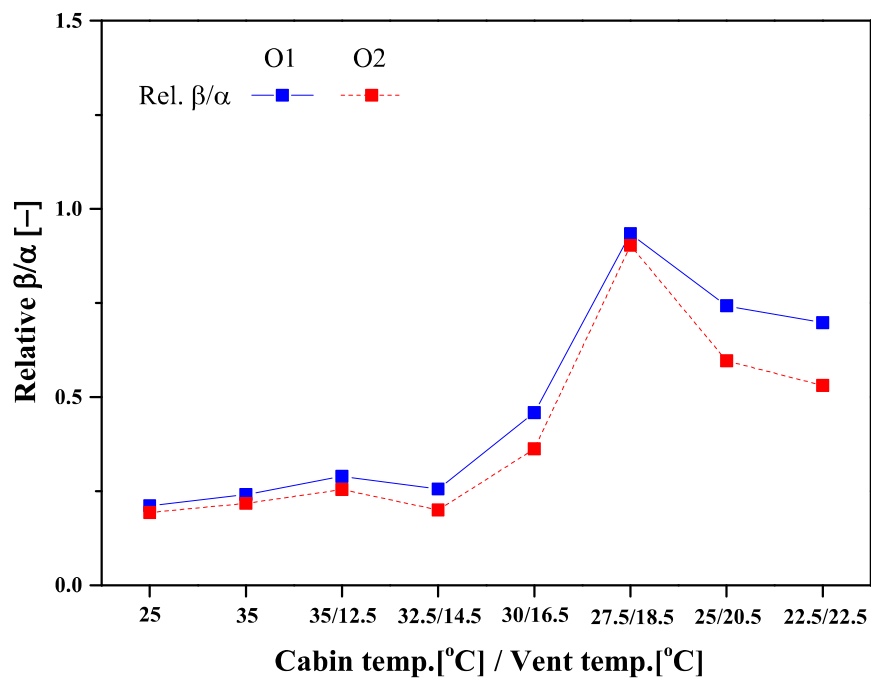
Fig. 6.7 Variations of relative β/α at the occipital lobe during cooling under summer condition

2. Experimental results on driver's thermal comfort according to the change of automotive indoor conditions in winter

a. Mean surface temperature measurement results

Fig. 6.8 shows the variation of surface temperature of the driver according to the cabin and vent discharge air temperatures under the maximum and average solar radiations of 575 and 242 W/m^2, respectively. Fig. 6.8(a) shows the surface temperature of the driver under the standard temperature condition of 25°C. The color of the surface of the subject's forehead, left hand, right hand, and abdomen was overall green. As shown in Fig. 6.8(b), when the heating mode was not operated at a cabin temperature of 15°C, the surface temperature on the forehead, left hand, and right hand of the subjects showed a sky blue color. However, the sky blue color showed at the abdominal surface where the sunlight is irradiated, and the color of the surface around the abdomen in the parts, that is not affected by solar light, was blue. This indicates relatively low temperature. Fig. 6.8(c) shows the surface temperature of the subject when HVAC with a vent discharge air temperature of 40°C was operated at the same cabin temperature of 15°C. The vent showed a relatively high temperature due to its light green color. The surface color of the subject's forehead, left hand, and right hand was a mixture of sky blue and light green, so the temperature slightly increased. In particular, the color at the surface of the abdomen irradiated with the solar light was light green, and the color of the surface around the abdomen was sky blue, which confirming that the temperature increased relatively significantly. As the temperature of the cabin increases, the surface temperature around the subject was blue to sky blue when the cabin and vent discharge air temperatures are 25°C and 30°C, respectively, as shown in Fig. 6.8(g). The color of the surface at the subject's forehead, left hand, and right hand was light green, but the temperature change was not significant. The temperature indication color of the abdomen mixed with yellow and orange, thus it means the temperature increased. In addition, the

surface color around the abdomen showed the increase range of green, which confirming an increase of temperature. When the temperatures of the cabin and vent were 27.5°C, the color of the surface at the subject's forehead and left hand changed from green to dark green, and the color of the surface around the abdomen increased in the range of yellow. The largest increase in surface temperature is observed in the abdomen. This is because the heating effect was the most effective in the abdomen that the warm air blowing from the vent outlet directly contacts the surface of the subject, and the surface temperature is the highest due to the solar light.

Fig. 6.9 shows the variation of the average surface temperature on the left hand, right hand, forehead, and abdomen of the subjects by using the thermal-imaging camera during heating in a car. At the common room temperature of 25°C, the average surface temperatures on the left hand, right hand, forehead, and abdomen of the subjects were 34.8°C, 34.8°C, 34.1°C, and 31.7°C, respectively. When the cabin temperature was 15°C without the vent heating operation, the average surface temperatures on the left hand, right hand, forehead decreased to 25.2°C, 25.6°C, 27.1°C, respectively, and the temperature of abdomen increased slightly to 32.7°C. This is because the temperature of the subject's left hand, right hand, and forehead decreased due to the cabin temperature of 15°C which is the cold condition. However, the temperature of the abdominal surface was irradiated with solar light, thus it shows high temperature. When the vent discharge air temperature was 40°C under a cabin air temperature of 15°C, the average surface temperatures on the left hand, right hand, forehead, and abdomen of the subjects were 25.7°C, 25.9°C, 27.8°C, and 36.6°C, respectively. The effect of the high temperature of 40°C discharged from the vent at a low cabin temperature of 15°C could be lowered by 3.9°C in the abdomen of the driver. However, the surface temperature of the subject increased by 0.5°C on average and had no significant effect. It can be confirmed that the driver is initially in a cold environment when the heating operated in a car during winter. Thereafter, the surface temperature of the subjects gradually increased as the cabin temperature increased. However, the increment of surface temperature is not

significant. The average surface temperatures on the left hand, right hand, forehead, and abdomen of the subject increased to 30.3°C, 29.3°C, 31.7°C, and 42.6°C, respectively, at the cabin and vent discharge air temperatures of 27.5°C. In particular, the temperatures on the abdomen and left hand are significantly increased because the heating effect on the abdomen and left hand is relatively high. These parts have higher temperature because they are directly exposed by irradiating solar light and directly contacted by warm vent discharge air simultaneously.

(a) Standard condition(25°C) (b) Cabin 15°C/Non-Vent (c) Cabin 15°C/Vent 40°C

(d) Cabin 17.5°C/Vent 37.5°C (e) Cabin 20°C/Vent 35°C (f) Cabin 22.5°C/Vent 32.5°C

(g) Cabin 25°C/Vent 30°C (h) Cabin 27.5°C/Vent 27.5°C
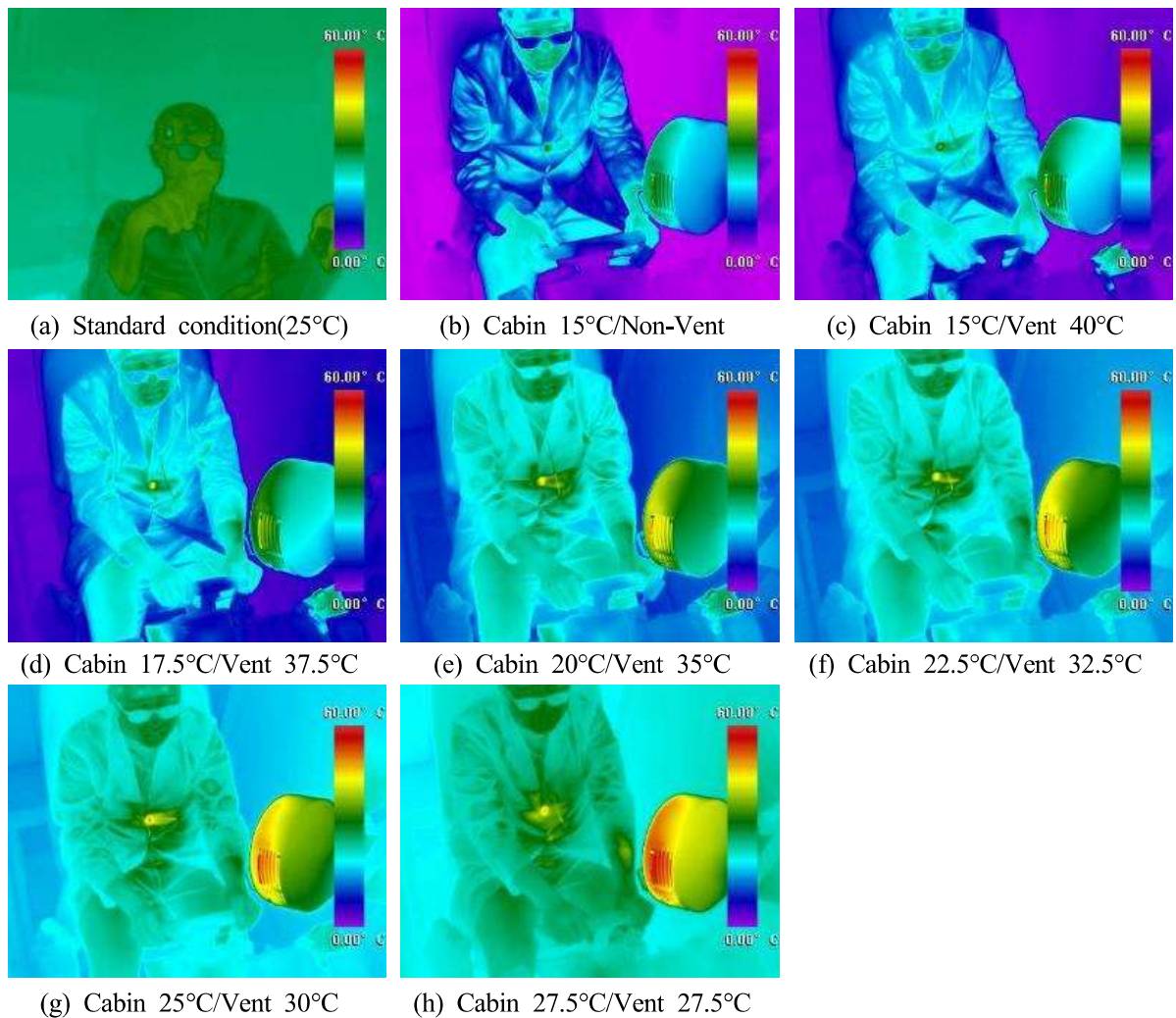
Fig. 6.8 Photography of driver's thermal imaging during heating in winter condition
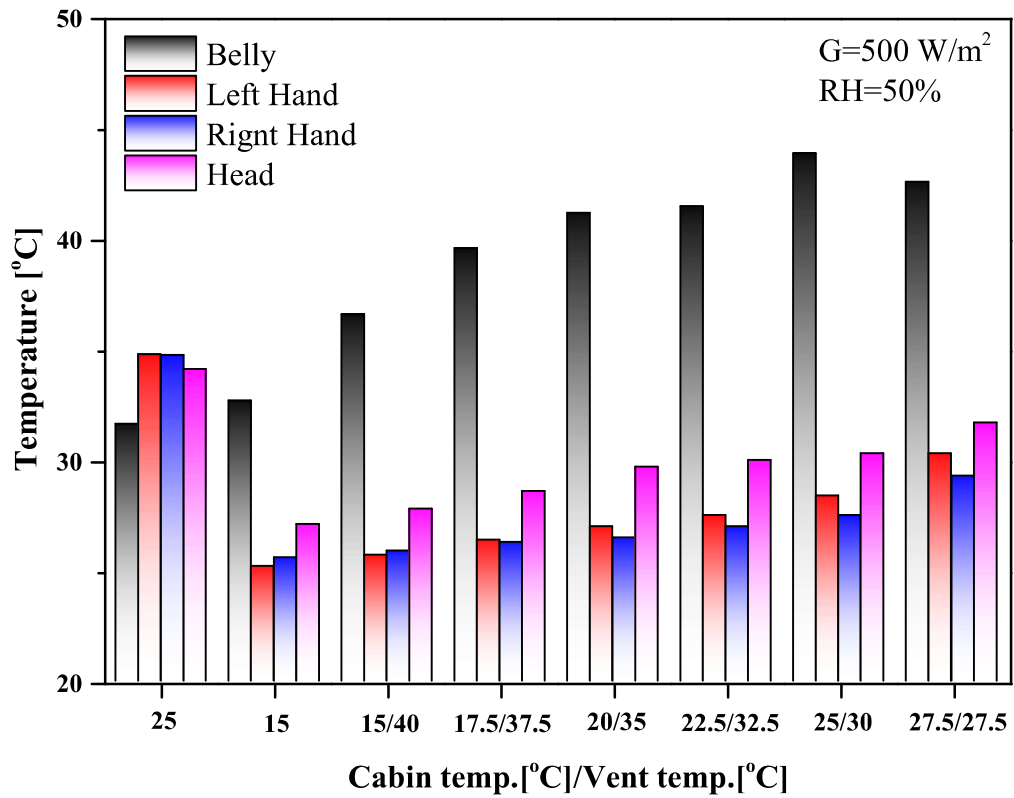
Fig. 6.9 Variation of driver's mean surface temperature during heating under winter condition

b. Subjective questionnaire survey results(TSV, CSV, CLV)

Fig. 6.10 shows the results of questionnaires of the average TSV, CSV, and CLV of subjects according to the cabin and vent discharge air temperature in a vehicle during winter condition under solar radiation. The TSV was -2.63 at a cabin temperature of 15°C without vent cooling, which showed that subjects felt very cold. The TSV was significantly increased to -0.75 when the HVAC with a vent discharge temperature of 40°C was operated at a cabin temperature of 15°C. That means that the thermal sensation of the subjects increased from very cold to slightly cold. At the cabin and vent discharge air temperatures of 17.5°C and 37.5°C, the TSV was -0.25, and it was confirmed that the subjects were in a thermally neutral state. And then, the TSV gradually decreased as the cabin and vent discharge air temperature were changed to 27.5°C, and the subjects at the cabin and vent discharge air temperatures of 27.5°C were in a slightly hot state because the TSV was 1.63.

In the results of the CSV questionnaire, the CSV at a cabin temperature of 15°C without vent cooling operation was -1.38, which was the lowest. This value indicates that the subjects felt great discomfort because of the low cabin temperature. When the heating was operated with a vent discharge temperature of 40°C under a cabin temperature of 15°C, the CSV increased rapidly to 0.13, and the comfort sensation of subjects was the slightly cold state. The subjects felt suddenly comfortable compared with the previous condition because the discharge air from the vent with a high temperature of 40°C could quickly provide a comfortable environment to the driver, even though it was a cold cabin environment (15°C). Then, the CSV increased until the cabin and vent discharge air temperatures reached 20°C and 35°C, respectively. The CSV at cabin and vent discharge air temperatures of 20°C and 35°C was 1.5, which was the highest, thus, the survey result confirmed that subjects felt the most comfortable in these conditions. The CSV decreased to -0.25 at a cabin and vent discharge air temperatures of 27.5°C. This is because the subjects felt slightly hot when the temperatures of the cabin and vent were 27.5°C in the TSV results.

According to the results of the CLV questionnaire of the subjects during heating in the indoor environment of the car, the CLV was the lowest. It was 0 at a cabin temperature of 15°C without the vent heating operation. During vent heating with a high discharge air temperature of 40°C, the CLV rapidly increased to 0.63. This is because of the operation of vent heating with a high temperature of 40°C in spite of a cold cabin temperature of 15°C. The vent heating provided a thermally pleasant environment to the driver and greatly improved concentration during driving. As the cabin temperature increased, the CLV tended to increase, and the CLV increased to 1.25 at cabin and vent discharge air temperatures of 20°C and 35°C, respectively. However, when the cabin and vent discharge air temperatures were 27.5°C, the CLV decreased to 0.25, which means the subjects felt slightly hot and unpleasant, and the concentration of the drivers decreased owing to long-term driving. The CLV showed a similar result to that of the CSV. In the overall results of the subjective questionnaires (TSV, CSV, and CLV), the subjects were comfortable and had a high level of concentration in the temperature ranges of the cabin and vent discharge air temperatures of 17.5°C and 37.5°C to those of 20°C and 35°C, respectively.
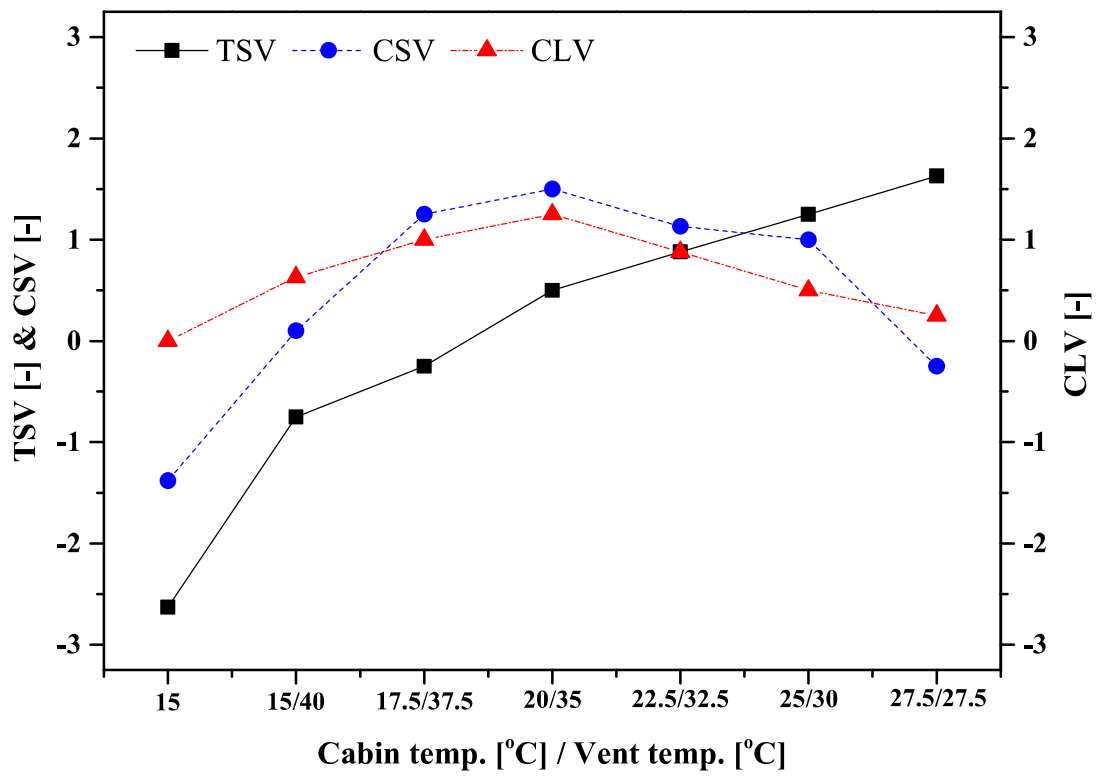
Fig. 6.10 Results of TSV, CSV, and CLV questionnaires during heating in winter condition

c. PPG measurement results

Fig. 6.11 shows the variation of the pulse wave of the driver according to the cabin and vent discharge air temperature in the heating mode under solar radiation. Fig. 6.11(a) shows the variations of the stress index, TP, and LF/HF. Stress index was 35.77 at room temperature of 25°C. At the cabin temperature of 15°C without the operation of vent heating, the stress index increased to 39.66. However, there was no significant change in TP and LF/HF. At the cabin and vent discharge air temperatures of 17.5°C and 37.5°C, respectively, stress index decreased to 35.76 and LF/HF and TP were 1.26 and 8.21. Generally, TP represents immunity, ability to regulate the external environment and ability to cope with stress. Accordingly, it means that the stress coping ability is better as increasing TP. Stress index increased to 39.7 at the cabin and vent discharge air temperatures of 20°C and 35°C, respectively, and TP decreased to 7.73, and LF/HF showed the increasing tendency to 1.27. This is because the concentration for driving was highest in the CLV results, and the sympathetic nerve became active with the slight tension and excitement due to the subject's concentration on driving. Afterwards, the stress index tended to decrease until the cabin and vent discharge air temperatures of 25°C and 30°C, respectively. Accordingly, the TP tended to slightly increase. At the cabin and vent discharge air temperatures of 27.5°C, stress index increased to 36.5 and TP decreased to 7.54. This is because the discomfort of the driver was caused by slightly hot temperature and the fatigue from a long driving time increased.

Fig. 6.11(b) shows the variations of the SDNN and RMSSD in the pulse wave of the subjects during driving. At the indoor temperature of 25°C which was the comfortable condition, SDNN and RMSSD of subjects were 40.5 ms and 30.1 ms, respectively. When the cabin temperature of 15°C without vent heating, the SDNN and RMSSD of subjects decreased to 32.8 ms and 26.1 ms, respectively. This is because the subjects entered a cold environment and felt uncomfortable, and the parasympathetic nerve activity decreased. When the heating was operated with a vent discharge temperature of 40°C under a cabin temperature of 15°C, SDNN and

RMSSD increased. SDNN and RMSSD were the highest 47.3 ms and 38.6 ms at the cabin and vent discharge air temperatures of 17.5°C and 37.5°C, respectively. This is because the parasympathetic nerve was activated by providing a relatively comfortable environment to the driver in these conditions. Afterward, the SDNN and RMSSD tended to decrease until the cabin and vent discharge air temperatures of 22.5°C and 32.5°C, respectively. The SDNN and RMSSD showed the decreasing tendency at the cabin and vent temperatures of 27.5°C, respectively. This is because the activity of the parasympathetic nerve was suppressed as the subject felt a slightly hot at this temperature and provided a relatively unpleasant environment. When the PPG analysis results obtained in this study were comprehensively analyzed, it was confirmed that the subject had the thermal comfort suitable for driving in winter at the cabin and vent temperatures of 17.5°C and 37.5°C.
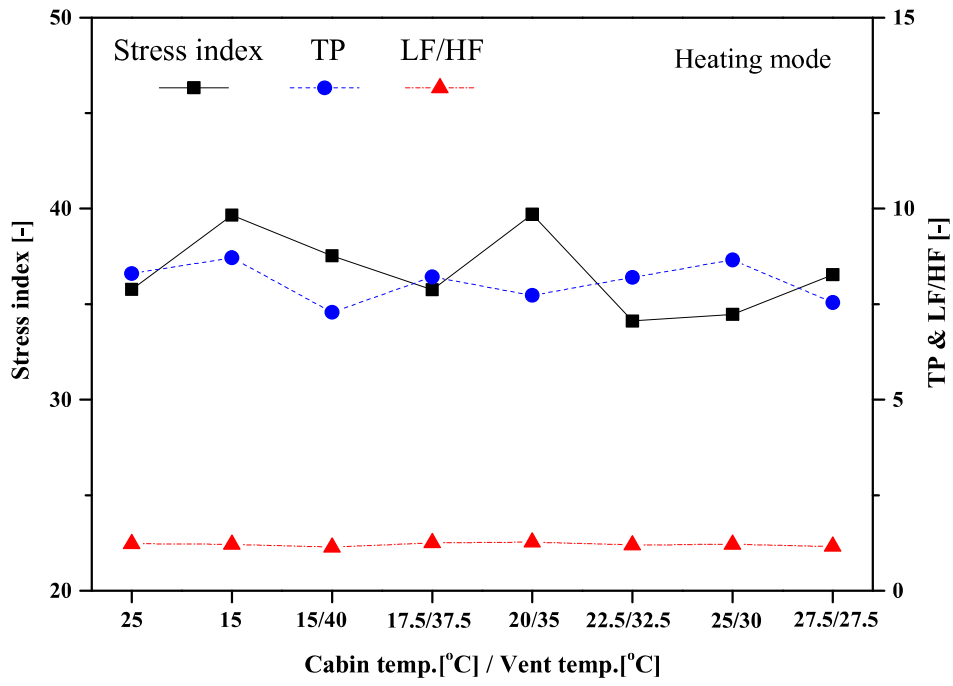
(a) Stress index, TP, and LF/HF
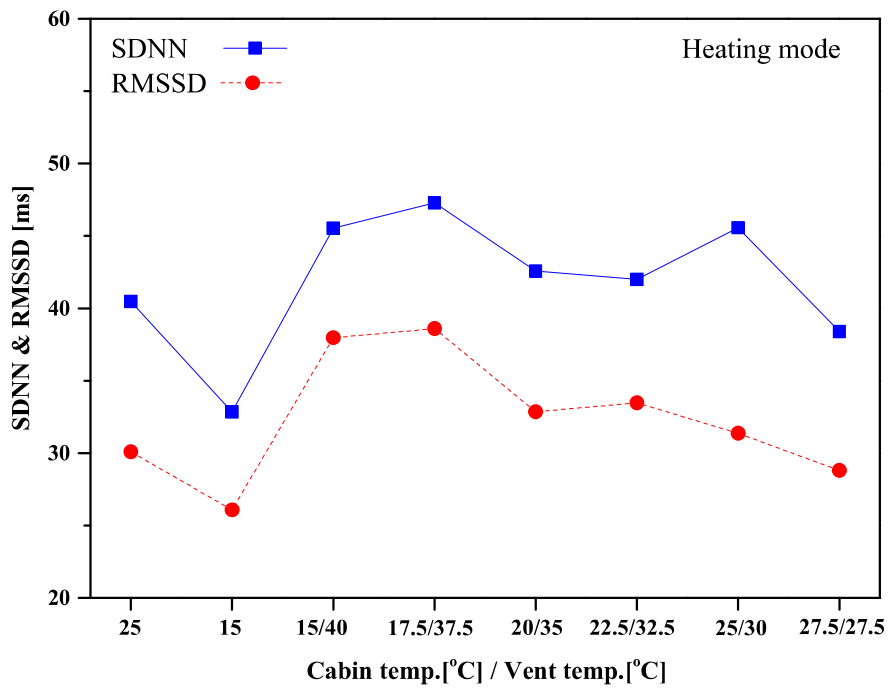
(b) SDNN and RMSSD

Fig. 6.11 Variations of driver's PPG during heating in winter condition; (a) Stress index, TP and LF/HF, (b) SDNN and RMSSD

d. EEG measurement results

Fig. 6.12 shows the brain mapping using EEG analysis of the subject according to the cabin and vent discharge air temperatures in winter condition under the maximum and average solar radiations of 575 and 242 W/m^2, respectively. The relative θ wave at the indoor temperature of 25°C showed yellow-green color, blue and red colors, thus the activity of relative θ wave appeared high. The relative SMR and β waves showed relatively low with purple and blue colors, which indicating low activity. When the heating mode was not operated at a cabin temperature of 15°C, the activity of relative SMR wave increased by showing yellow-green and orange colors, and the activity of relative β wave also increased by showing sky blue and blue colors. This is because the subjects started to driving under this condition, thus the concentration on driving increased. In addition, the activity of relative high β wave increased by showing orange and red colors because the subjects were in an unpleasant state under the cold environment. When the heating was operated with a vent discharge air temperature of 40°C under a cabin temperature of 15°C, the activity of relative β wave increased by showing yellow-green and red colors. Besides, the activity of relative high β wave decreased by showing yellow-green. It means that subjects were in a relatively pleasant state due to the blowing warm air from the vent at a cold cabin of 15°C. Accordingly, concentration level of subjects on driving were improved. At the cabin and vent temperatures of 20°C-25°C and 35°C-30°C, the activity of relative SMR wave was relatively high by showing orange and yellow-green colors. At the cabin and vent temperatures of 27.5°C, the activities of relative θ and α waves increased by showing yellow-green and sky blue colors, and the activity of relative SMR and β waves decreased by showing yellow-green and blue colors. It can be indicated that the fatigue of the driver increased due to the long driving time and drowsiness, thus the concentration level during driving was reduced.
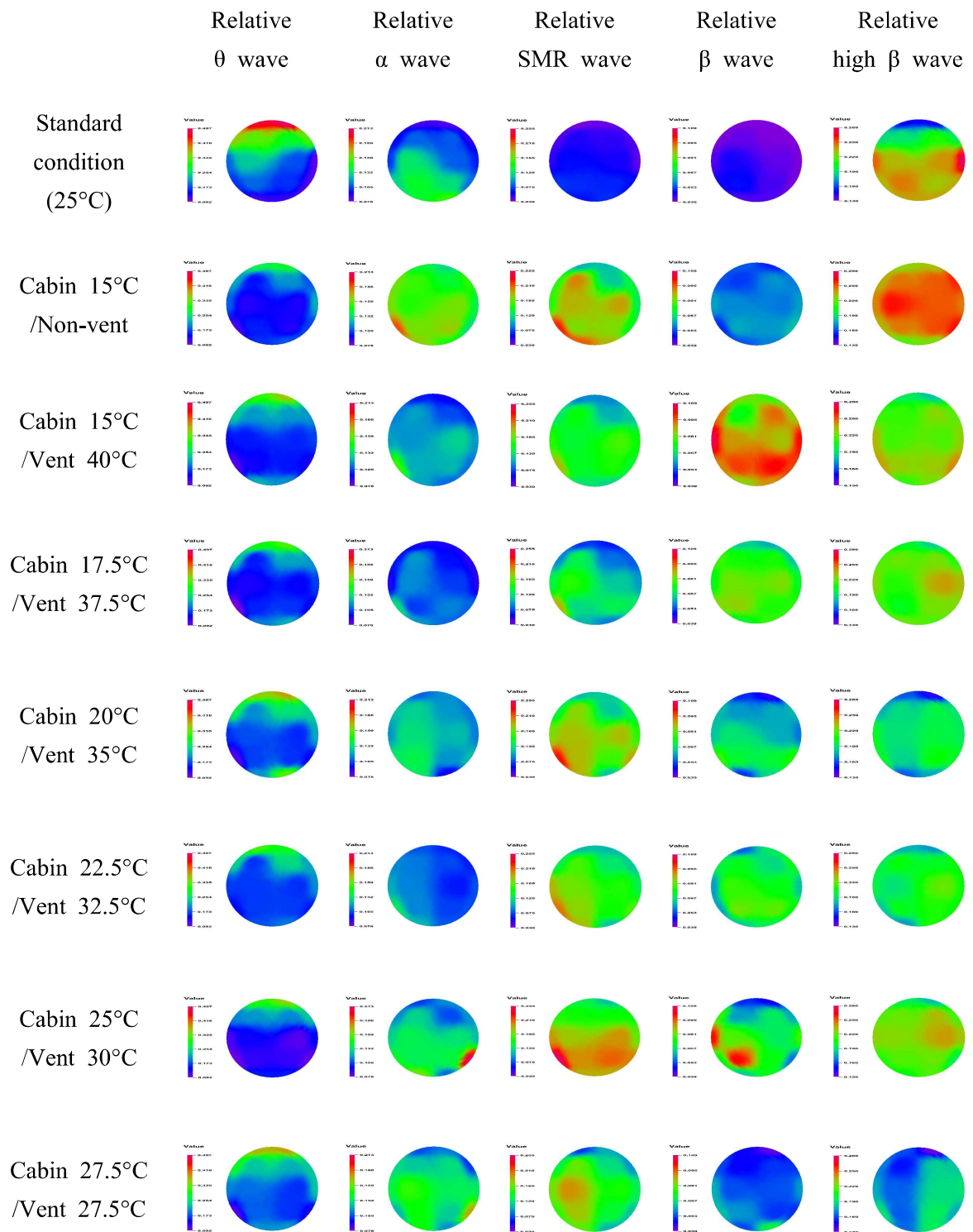
Fig. 6.12 Brain mapping of relative θ, α, SMR, β and high β waves with the cabin and vent discharge air temperatures under winter condition

Fig. 6.13 shows CI index and relative β/α of subjects at the prefrontal lobe. At the indoor temperature of 25°C, the CI index was the lowest, and the relative β/α was also low because the subject was in a comfortable state and doing nothing. The CI index showed a tendency to increase when the driver started to drive at a cabin temperature of 15°C without vent heating, and the relative β/α also increased. The CI index increased at first because of the focus on driving of the subject. When the heating was operated with a vent discharge temperature of 40°C under a cabin temperature of 15°C, both the CI index and relative β/α of subjects were rapidly increased. Accordingly, the operation of vent heating with a high temperature of 40°C was improved the concentration of driver in a cold cabin temperature of 15°C. The CI index and relative β/α of subjects were relatively decreased at cabin and vent temperatures of 17.5°C and 37.5°C, respectively. This is because the driver is in a thermally comfortable state. When the cabin and vent temperatures were 20°C and 35°C, the CI index and Relative β/α tended to decrease, after that the CI index did not show any significant change until a cabin and vent discharge air temperature of 27.5°C.

Fig. 6.14 illustrates the relative α and β waves of the driver in the occipital lobe according to the cabin and vent discharge air temperature with a maximum and average solar radiations of 575 and 242 W/m^2, respectively. The relative α wave was high at the 25°C preparation condition. When a cabin temperature of 15°C without vent cooling, the relative α wave was similar to that of the 25°C which is room temperature. Under this condition, the relative β wave tended to decreased. When the heating was operated with a vent discharge temperature of 40°C under a cabin temperature of 15°C, the relative α wave decreased and the relative β wave increased. This is because the driver was concentrated on driving, so the relative β wave increased. However, the relative α wave which indicates the opposite trend decreased. The asymmetry of relative α wave increased until the cabin and vent temperatures of 20°C and 35°C to the cabin and vent temperature of 27.5°C. This increase of asymmetry indicates mind and body are mentally and emotionally unstable, and this is

due to the discomfort caused by long driving. As the results of the EEG analysis of the subjects, it was confirmed that the temperature conditions for the pleasant environment and good concentration to the driver in winter were from the cabin and vent temperatures of 15°C and 40°C to the cabin and vent temperatures of 20°C and 35°C.

When comprehensively analyzing the results of the subjective questionnaire survey, PPG analysis, and EEG analysis in heating condition, it was confirmed to provide a comfortable and highly concentrated thermal environment for the driver at the cabin and vent temperatures of 17.5°C and 37.5°C and the cabin and vent temperatures of 20°C and 35°C.
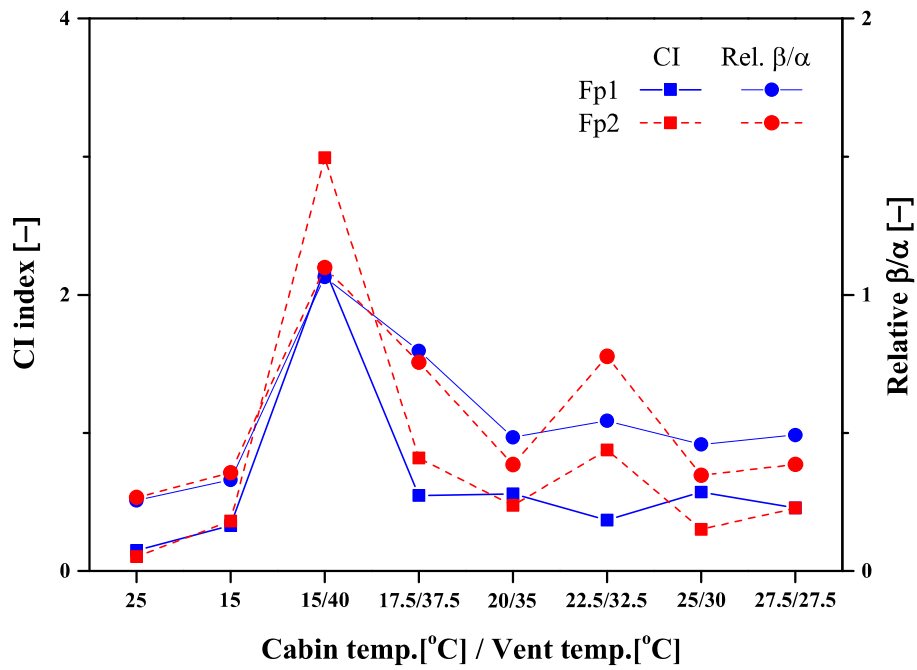
Fig. 6.13 Variations of CI and relative β/α at the prefrontal lobe during heating under winter condition
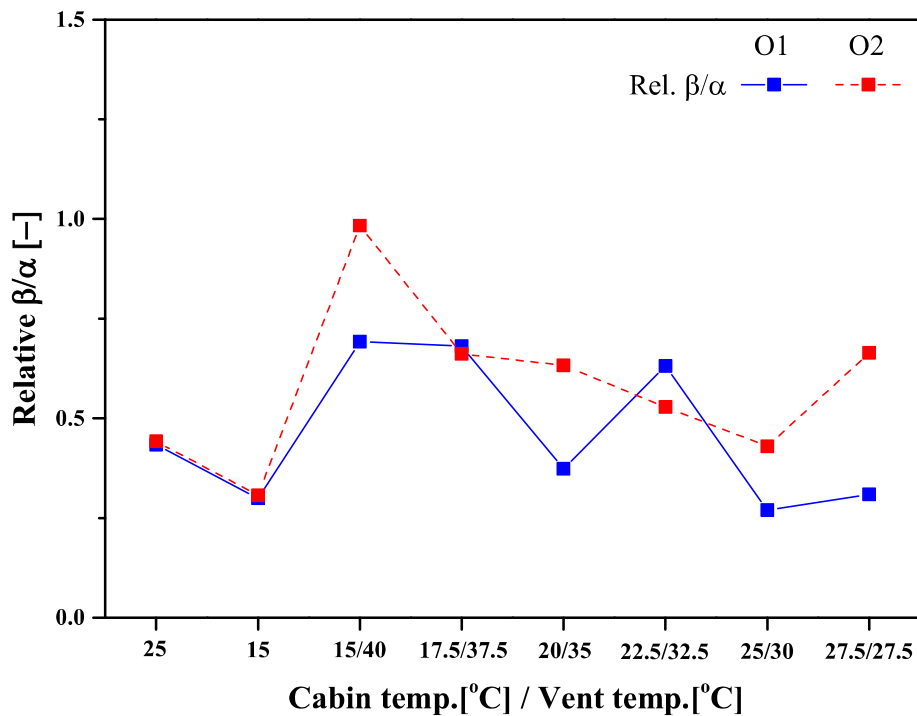
Fig. 6.14 Variations of relative β/α at the occipital lobe during heating under winter condition

B. Experimental results and discussion on driver's thermal comfort according to various seats in automotive indoor conditions

1. Experimental results on the driver's thermal comfort in summer

a. Mean surface temperature measurement results

Fig. 6.15 shows the variation of surface temperature of the driver according to the use of the various seats during cooling in summer under solar radiations. Fig. 6.15(a) shows the measurement of the surface temperature of the subject at 25°C which is the preparatory condition, and the surface colors of the left hand, right hand, and forehead were the light blue. However, the abdominal surface color was blue, which means the temperature was relatively low. This is because the temperature of the clothing was measured and the influence of the outside air condition was relatively significant. As shown in Fig. 6.15(b), when the cooling mode was not operated at a cabin temperature of 35°C, the surface at left hand, right hand, and forehead of the subject showed a sky-blue color. However, the surface temperature on the abdomen of the subject was red color and the surrounding surface color of the abdomen was yellow and green, thus it's temperature was relatively high. This is because the solar light was irradiated directly on the abdomen side. Fig. 6.15(c) shows the surface temperature of the subject when the basic seat used at the cabin and vent temperatures of 35°C and 12.5°C. The surface at left hand, right hand, and forehead of the subject showed a sky-blue color, thus it could be check that the temperature was slightly decreased. Besides, it was confirmed that the abdominal and surrounding surface colors were yellow and green, respectively, and were relatively significantly reduced. This is because the operation of the vent with a cold air of 12.5°C caused

the significant decrease of the temperature in the abdomen where the surface temperature was the highest by solar light. As shown in Fig. 6.15(d), when a ventilation seat was used at the cabin and vent temperatures of 35°C and 12.5°C, the surface color of the subject's left hand, right hand, forehead, and abdomen did not show a significant change compared to that using basic seat. This is because the ventilation seat blows the surrounding wind without changing the temperature and affects only the back and thighs. Fig. 6.15(e) shows the surface temperature of the subject when the cold water seat was used at the cabin and vent temperatures of 35°C and 12.5°C, respectively. The surface color of the subject's left hand, right hand, forehead, and abdomen did not show a significant color change. However, unlike the ventilation seat, the color of the tube in the cold water seat appeared purple, and it confirming that low-temperature water was flowing inside.

Fig. 6.16 shows the average surface temperature of the subjects' left hand, right hand, forehead, and abdomen according to various seats during cooling of a vehicle in summer. At the room temperature of 25°C, the average surface temperatures on the left hand, right hand, forehead, and abdomen of the subject were 33.6°C, 33.3°C, 32.7°C, and 27.7°C, respectively. The abdominal temperature was low because the temperature of the clothing was measured. When the cabin temperature was 35°C without the vent cooling operation, the average surface temperatures on the left hand, right hand, forehead, and abdomen were measured to 36.2°C, 35.2°C, 34.3°C, and 61.2°C, respectively. In particular, the surface temperature of the abdomen was relatively high because the solar light was irradiated to the abdomen in a hot environment (cabin temperature of 35°C). When the basic seat used at the cabin and vent temperatures of 35°C and 12.5°C, the average surface temperatures on the left hand, right hand, and forehead were 35.1°C, 34.9°C, and 33.2°C, respectively. The average surface temperatures on the abdomen and surrounding were 53.8°C and 44.8°C, respectively. It showed the relatively large decrement. This is because the operation of the vent at 12.5°C caused the greatest decrease of the temperature in the abdomen where the surface temperature was the highest by solar light. When a

ventilation seat is used at the cabin and vent temperatures of 35°C and 12.5°C, the average surface temperatures on the left hand, right hand, forehead, and abdomen were measured to 35.0°C, 33.0°C, 32.7°C, and 54.8°C, respectively. This was similar to the experimental results of the basic seat. When a cold water seat of 4°C used at the cabin and vent temperatures of 35°C and 12.5°C, the surface temperatures of the subject's left hand, right hand, forehead, and abdomen were 34.7°C, 31.9°C, 32.4°C and 52.4°C, respectively. It was confirmed that the outlet temperature of the cold water seat was 10°C. This is because the temperature of circulating water in the cold water seat increased through heat exchange in the back and thigh that are in contact with the cold water seat in the hot thermal environment.

(a) Standard condition(25℃)   (b) Cabin 35℃/Non-vent   (c) Cabin 35℃/Vent 12.5℃

(d) Cabin 35℃/Vent 12.5℃   (e) Cabin 35℃/Vent 12.5℃
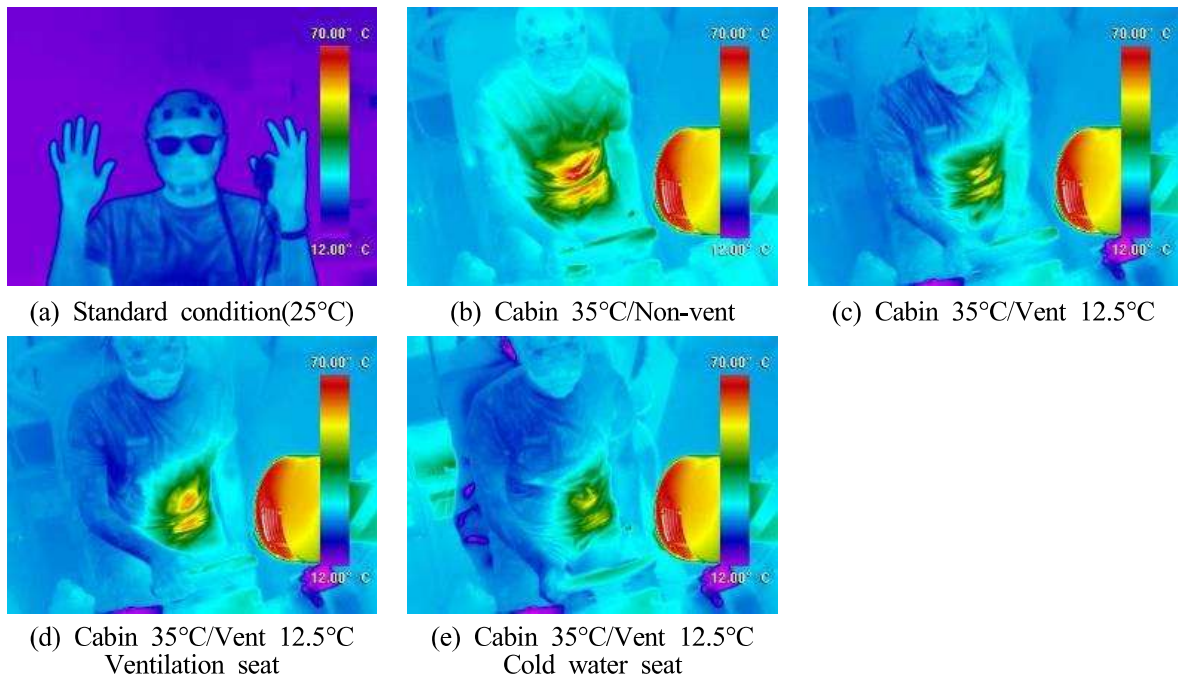Ventilation seat   Cold water seat

Fig. 6.15 Photography of driver's thermal imaging for various seats during cooling in summer condition
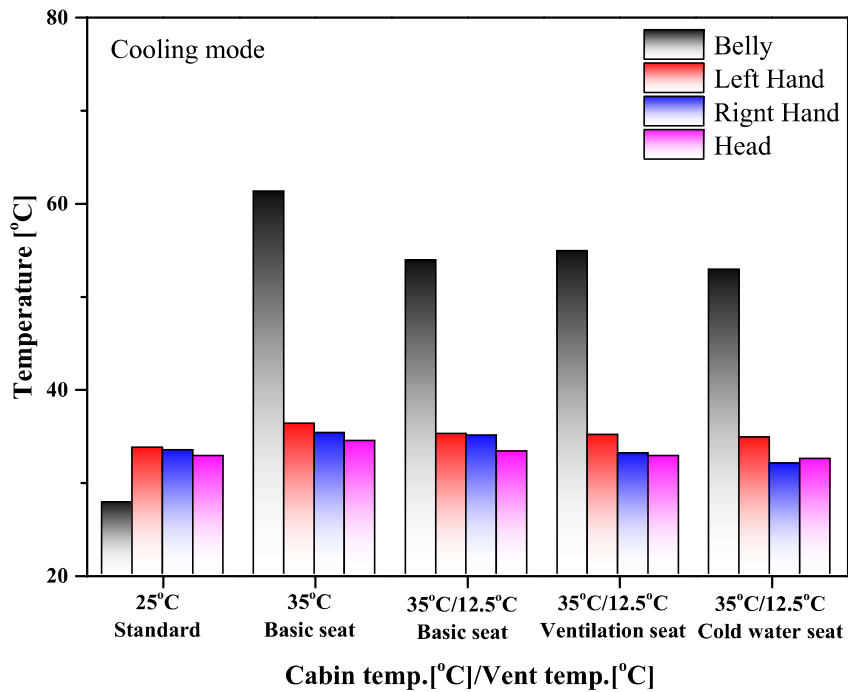
Fig. 6.16 Variation of driver's mean surface temperature for various seats during cooling in summer condition

Fig. 6.17 shows the temperature variation of the hips, back, and thighs which are in contact with the seat according to use the ventilation and cold water seats under summer condition. When 5 minutes have passed using the ventilation seat, the average temperature of the subject's hips, back, and thighs was 32.8°C. As the cold water seat was used for 5 minutes, the average temperature of the subject's hips, back, and thighs was measured by 27.8°C. Accordingly, the average temperature difference of the parts which are in contacted with the seat between the use of the ventilation and cold water seats was 4.91°C. When 30 minutes have passed using the ventilation seat, the average temperature of the subject's hips, back, and thighs increased as 34.4°C. This is because the vent direction is toward the subject's head and legs, so ventilation seat cannot blow cool air (12.5°C) discharged from the vent. As the cold water seat was used for 30 minutes, the average temperature of the subject's hips, back, and thighs was 27.9°C, which was 6.4°C lower than that using the ventilation seat. In particular, the temperature of back using the cold water seat was 25.63°C, which was 8.62°C lower than that using the ventilation seat. Therefore, it was confirmed that the use of cold water seat could significantly reduce the temperature of the hips, back, and thighs which were in contact with the driver's seat at the cabin temperature of 35°C.

In addition, when the ventilation and cold water seats were used, the cooling capacity according to the temperature difference between the outdoor air and parts which were in contact with seat was calculated. When the ventilation and cold water seats were used for 5 minutes, the cooling capacities were 76.2 W and 389.6 W, respectively. When 30 minutes have passed using the ventilation seat, cooling capacity was decreased by 21.3 W because the temperature of the contact parts of body to the seat decreased. When 30 minutes have passed using the cold water seat, cooling capacity was 382.5 W, which was similar to the cooling capacity at 5 minutes. It was confirmed that the cooling capacity using the cold water seat was more higher than that using the ventilation seat, thereby providing a thermally comfortable environment to the driver.
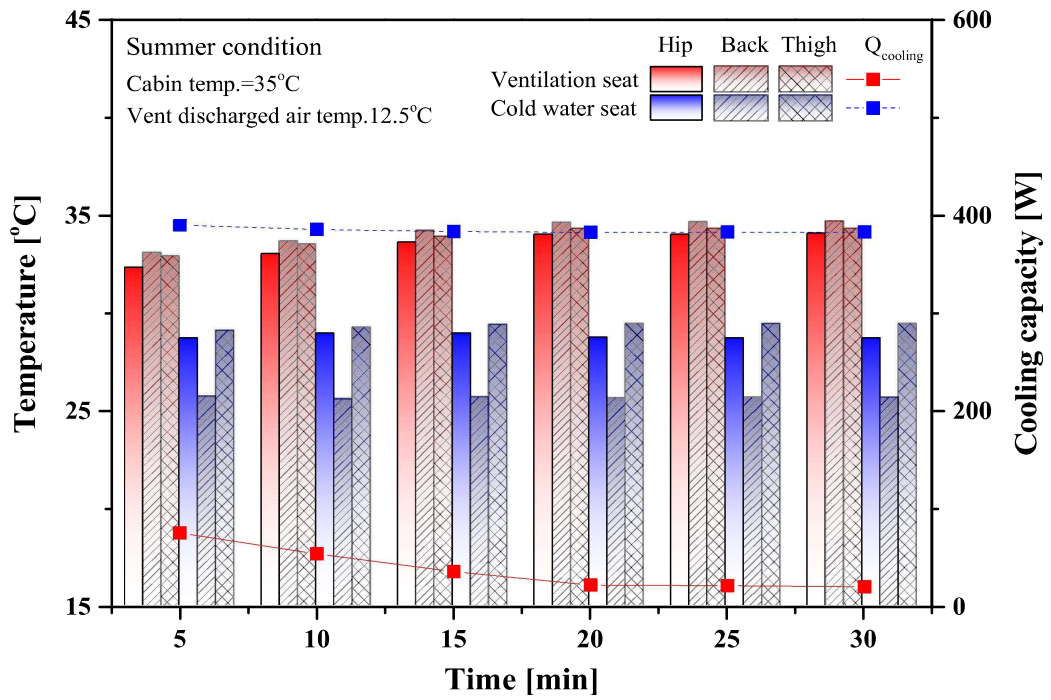
Fig. 6.17 Comparison of the cooling capacity and temperature variation on the subject's hips, back, and thighs according to the use of ventilation and cold water seats in summer condition

b. Subjective questionnaire survey results(TSV, CSV, CLV)

Fig. 6.18 shows the results of questionnaires of the average TSV, CSV, and CLV of the driver according to the use of various seats by cooling of a car in summer under solar radiation. In the results of TSV questionnaires, at the cabin temperature of 35°C in which the vent was not operated, the TSV was 3 and the subjects were very hot. Accordingly, the CSV and CLV were -2.71 and –2.57, respectively, and these were very low. Thus, it indicated that subjects felt unpleasant and difficult to concentrate. When the basic seat used at the cabin and vent temperatures of 35°C and 12.5°C, TSV decreased slightly to 2.71. It was confirmed that the operation of the vent at 12.5°C provided the cool wind to the subject, but at the beginning of driving, the effect was not effective due to the hot thermal environment and the effect of cooling from vent was not immediately reflected. Accordingly, the subject's CSV and CLV were -1.71 and -1.71, respectively, and it was confirmed that the low temperature wind of 12.5°C makes the driver comfortable for given operating conditions. When a ventilation seat was used at the cabin and vent temperatures of 35°C and 12.5°C, TSV of subjects decreased to 2.29, and they felt hot. Therefore, CSV and CLV increased to -1 and -1, respectively, and the subjects answered that they were more comfortable and concentrated driving at this condition. When the cold water seat was used at the same temperature condition, TSV of subjects was 1.14, which indicated that they felt warm. Besides, CSV and CLV showed -0.57 and -0.43, respectively, and subjects answered that they are most comfortable and concentrate on driving well.

In this study, when the subjective questionnaire results (TSV, CSV, CLV) were comprehensively analyzed, it was confirmed that the most comfortable driving environment and the improved concentration could be provided to the driver as the operation of the vent of 12.5°C in the cabin temperature of 35°C, as well as the use of the cold water seat at the temperature of 4°C.
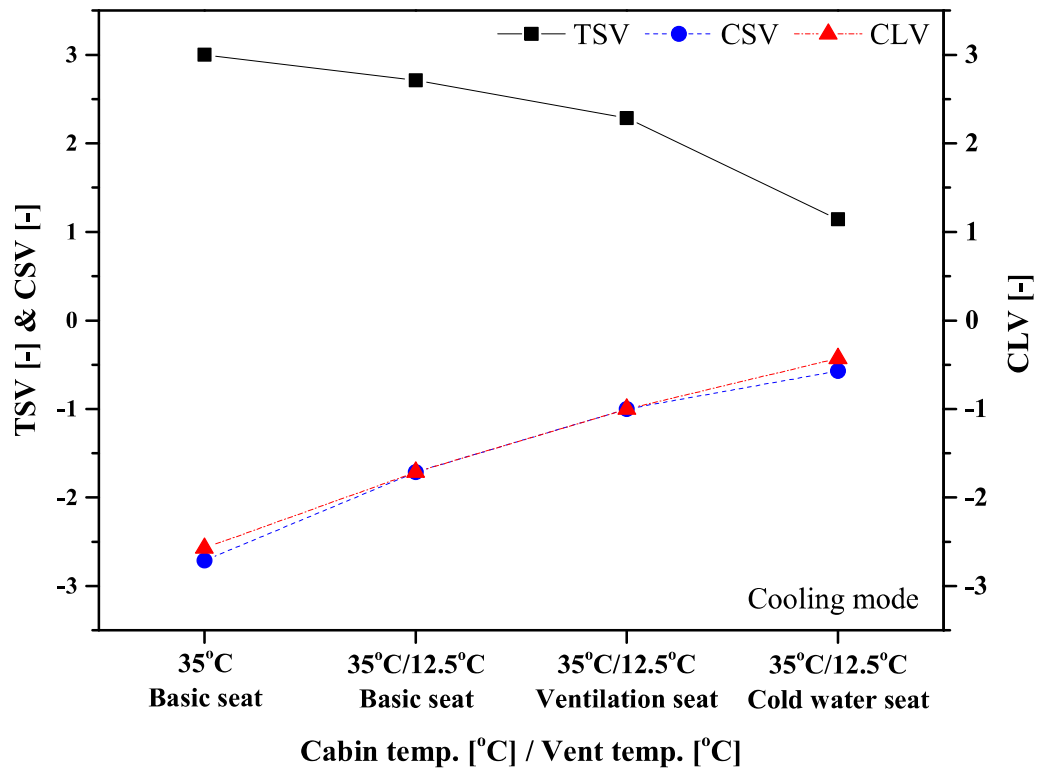
Fig. 6.18 Results of TSV, CSV, and CLV questionnaires for various seats during cooling in summer condition

c. PPG measurement results

Fig. 6.19 shows the variation of the pulse wave of driver according to the use of various seats when cooling of a car in summer under solar radiation. Fig. 6.19(a) shows the variations of the stress index, TP, and LF/HF. The Stress index, TP, and LF/HF of subjects at room temperature of 25°C were 38.7, 8.60, and 1.23, respectively. Thereafter, the subject was performed driving in a cabin temperature of 35°C which is the hot condition, and the subject's stress index increased to 42.3, and TP decreased to 7.90. Under this condition, the stress index increased because the subjects felt uncomfortable, and accordingly, the TP decreased. When the basic seat used at the cabin and vent temperatures of 35°C and 12.5°C, the subject's stress index decreased to 37.3 and TP increased to 8.16. This is because the operation of the vent at 12.5°C in a hot environment (cabin temperature of 35°C) provided a comfortable environment to the subject. On the other hand, when the ventilation seat was used at the cabin and vent temperatures of 35°C and 12.5°C, stress index increased to 42.84 and TP was 8.26. The reason for the increase in the stress index is because the subject felt unpleasant due to the blowing the hot surrounding air in the ventilation seat at the beginning of driving. When the cold water seat was used at the same condition, stress index of subjects decreased to 36.4 and TP increased to 8.76. This is because the cold water seat provided a pleasant environment to the driver in summer condition.

Fig. 6.19(b) shows the variations of SDNN and RMSSD in the pulse wave of the subjects during driving. SDNN and RMSSD were 42.3 ms and 27.8 ms, respectively, at the indoor temperature of 25°C. After that, at the cabin temperature of 35°C without the operation of cooling in the vent, SDNN and RMSSD of subjects decreased to 30.2 ms and 24.0 ms, respectively. This is because the subjects felt unpleasant in a hot environment of 35°C. When the basic seat used at the cabin and vent temperatures of 35°C and 12.5°C, SDNN and RMSSD increased to 33.6 ms and 27.2 ms, respectively, by blowing the cool air to the subject. When a ventilation seat was used at the cabin and vent temperatures of 35°C and 12.5°C, SDNN and

RMSSD of subjects were 34.2 ms and 24.7 ms, respectively. These showed a similar values to the experimental results of the basic seat. When the cold water seat was used at the same temperature condition, SDNN and RMSSD of subjects were 40.7 ms and 26.9 ms, respectively. Accordingly, the use of the cold water seat provided a comfortable environment to the subject, and it could be confirmed from the increment of SDNN and RMSSD.

When the PPG results obtained in this study were comprehensively analyzed, in a hot environment with a cabin temperature of 35°C, the operation of the cooling at the vent with the temperature of 12.5°C provided improved thermal satisfaction on driving of the driver. In addition, it was confirmed that the use of the cold water seat provided a relatively better comfortable thermal environment to the driver.
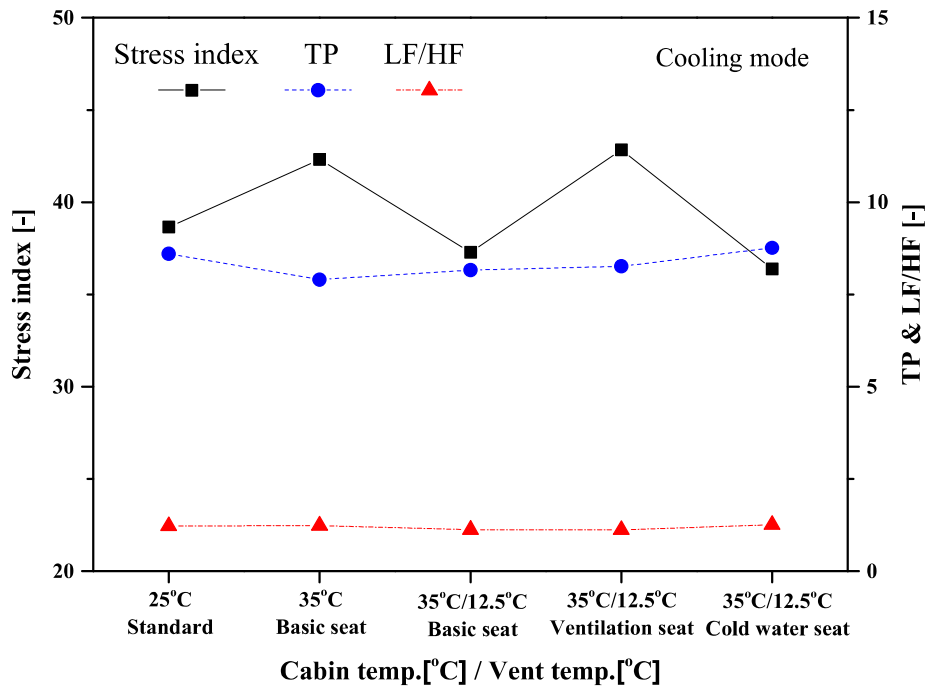
(a) Stress index, TP, and LF/HF
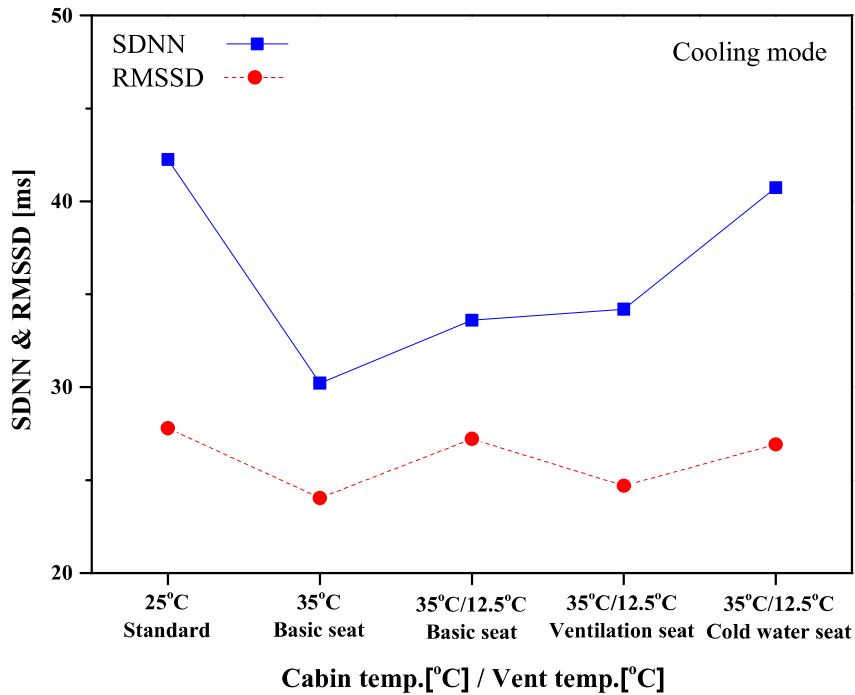
(b) SDNN and RMSSD

Fig. 6.19 Variations of driver's PPG for various seats during cooling in summer condition; (a) Stress index, TP and LF/HF, (b) SDNN and RMSSD

d. EEG measurement results

Fig. 6.20 shows the brain mapping results for the EEG analysis of the subject according to the use of the various seats in summer condition. In the EEG analysis, the brain mapping was expressed by rainbow color. Red indicates high EEG activity and purple indicates low EEG activity. The relative θ and α waves at the indoor temperature of 25°C showed red color, thus the activity of relative θ increased. The activities of relative SMR, β, and high β waves showed relatively low with purple and yellow-green colors. Thus, it was confirmed that the subjects were a comfortable state at the indoor of 25°C. When the cooling mode was not operated at a cabin temperature of 35°C, the activity of relative α decreased by showing yellow-green and red colors, and the activity of relative high β wave increased by showing yellow-green and red colors. Since relative high β wave is an indicator of unpleasant conditions such as excitement and anxiety, it was confirmed that the subjects were an unpleasant state. When the basic seat used at the cabin and vent temperatures of 35°C and 12.5°C, the activity of relative α was decreased by showing expanded yellow-green color distribution and the activity of relative high β wave was increased by showing red color distribution. This means that the subjects were unpleasant. The main cause is that subjects were immediately contacted with the cold air blowing from the vent in a hot environment of 35°C. When the ventilation seat was used at the cabin and vent temperatures of 35°C and 12.5°C, relative high β wave still showed a lot of red color distribution. Therefore, the use of the ventilation seat provided an unpleasant environment to the subjects during driving. When the cold water seat was used at the same cabin and vent temperature condition, relative θ showed red color and relative α wave presented red and yellow-green colors. In addition, relative high β wave showed yellow-green and blue colors. Thus, it was confirmed that the subjects were a comfortable state at this condition.
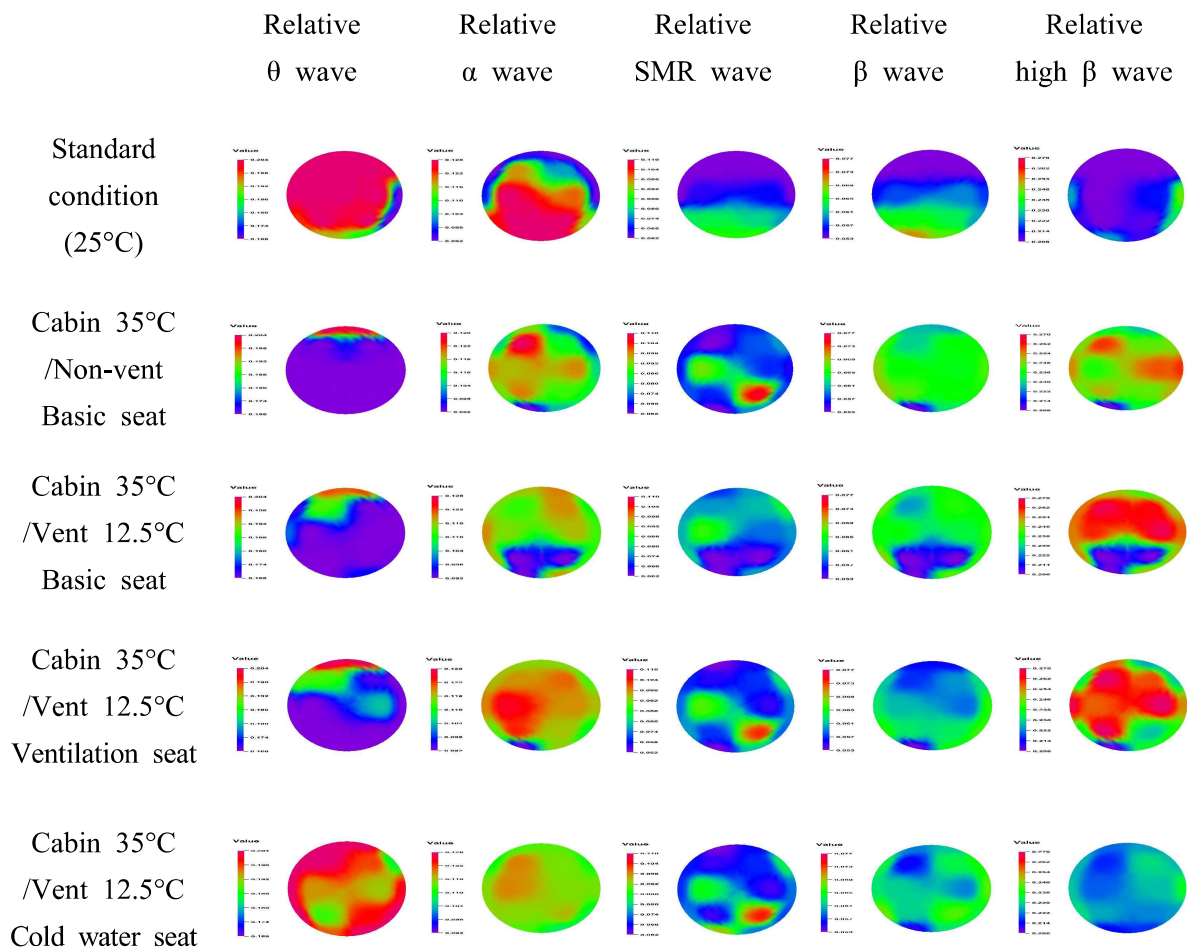
Fig. 6.20 Brain mapping results of relative θ, α, SMR, β and high β waves for various seats during cooling under summer condition

Fig. 6.21 shows the variations of the CI index and relative β/α in the prefrontal lobe of the driver under the summer condition. At the indoor temperature of 25°C, the CI index and relative β/α were the lowest. When the cabin temperature of 35°C without cooling form the vent, the CI index and relative β/α were rapidly increased. This is because the subjects were in a state of the high thermal discomfort by driving in a hot environment. When the basic seat was used with the cooling operation (discharged air temperature of 12.5°C) of HVAC system at the cabin temperature of 35°C, the CI index and relative β/α of subjects tended to slightly increase. This is because the operation of cooling at the air temperature of 12.5°C in the cabin temperature of 35°C improved the concentration of subjects, but then they felt slightly unpleasant due to the blowing sudden cold wind. When cooling operation from the vent with air temperature of 12.5°C and the ventilation seat were used at the cabin temperature of 35°C, the CI index and relative β/α of subjects were decreased. When the cold water seat was used at the same condition, the CI index and relative β/α of subjects were further decreased because the relative β/α was relatively low by the use of the cold water seat and it provided the most comfortable environment to the driver.

Fig. 6.22 shows the EEG analysis results in the occipital lobe of the subject according to the various seats in summer under an average solar radiation. At the indoor temperature of 25°C, the relative α wave was the highest, while the relative α wave tended to rapidly decrease at a cabin temperature of 35°C without cooling of HVAC system. This is because the subjects felt unpleasant in a hot environment under this condition. When the basic seat was used with the cooling operation of HVAC at the cabin temperature of 35°C, the relative α wave decreased slightly and relative β wave increased, thus relative β/α showed the highest. This is because the subjects felt slightly unpleasant due to the concentration of driving and the influence of the cold discharged air from the vent. Which was similar to the results in the prefrontal lobe. At the cabin and vent temperatures of 35°C and 12.5°C, the use of ventilation seat provided a pleasant environment, thus the relative β/α decreased.

When the cold water seat was used at the same condition, it was confirmed that relative β/α was low by providing the relatively most comfortable environment to the driver.
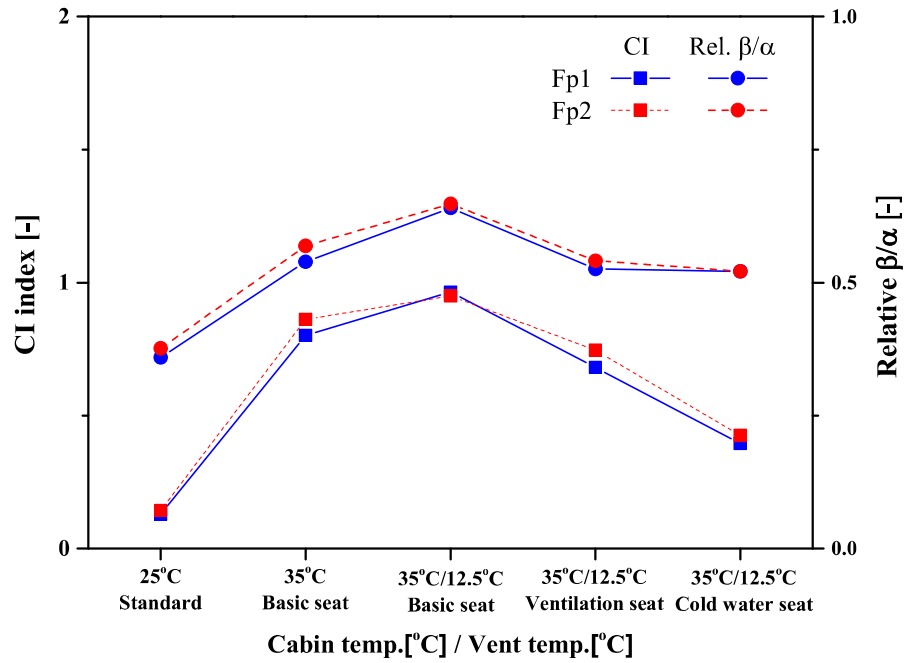
Fig. 6.21 Variations of CI and relative β/α at the prefrontal lobe for various seats during cooling under summer condition
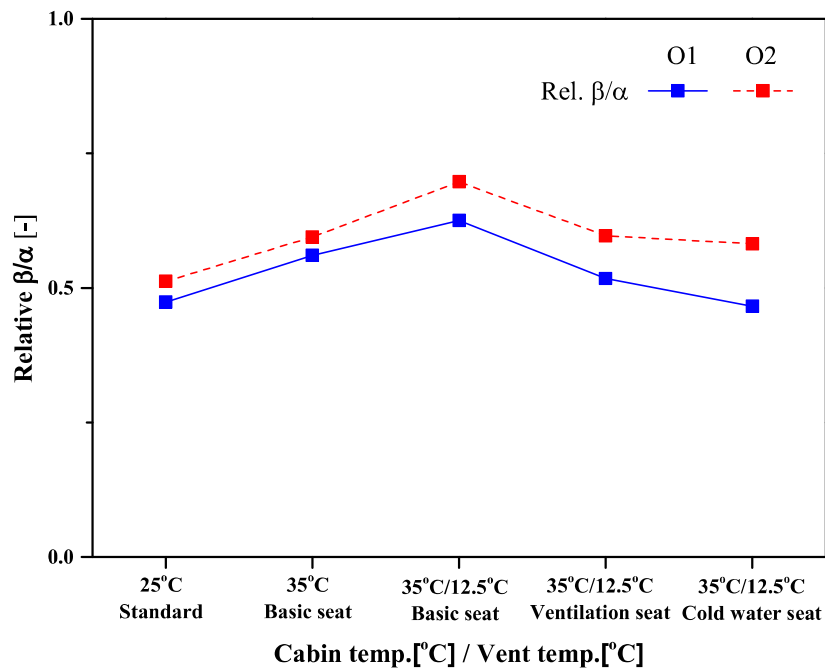
Fig. 6.22 Variations of relative β/α at the occipital lobe for various seats during cooling under summer condition

2. Experimental results on the driver's thermal comfort according to various seats in winter

a. Mean surface temperature measurement results

Fig. 6.23 shows the variation of surface temperature of the driver according to the use of the various seat during heating in winter under solar radiation. Fig. 6.23(a) shows the measurement of the surface temperature of the subject at 25°C which was the preparatory condition, and the surface colors of the left hand, right hand, and forehead were the green. However, the abdominal surface color was the light green, thus the temperature of abdominal surface was relatively low. This is because the temperature of the clothing was measured and the influence of the outside air condition was relatively high. As shown in Fig. 6.23(b), when the heating mode was not operated at a cabin temperature of 15°C, the surface at left hand, right hand, and forehead of the subject shows a light green color. However, the surface temperature on the abdomen of the subject is a yellow color and the surrounding surface color of the abdomen is a green, thus, it's temperature is relatively high. This is because the solar light was irradiated on the abdomen side, and it showed a relatively high temperature due to the influence of solar radiation. Fig. 6.23(c) shows the surface temperature of the subject when the basic seat used at the cabin and vent temperatures of 15°C and 40°C. The surface at left hand, right hand, and forehead of the subject shows a light sky-blue color, the abdominal and surrounding surface colors are green and light green, respectively, thus it was confirmed that the surface temperatures of abdominal and surrounding were reduced. Although the vent discharge temperature was 40°C, the influence on the surface temperature of the driver was reduced by exchanging heat with an cold ambient temperature of 15°C until reaching the subject after discharging from the vent. As shown in Fig. 6.23(d), when a heating seat is used at the cabin and vent temperatures of 15°C and 40°C, the surface color of the subject's left hand, right hand, forehead, and abdomen do not show a

significant change compared to that using a basic seat. This is because the back and thighs where contacted with the heating seat. Fig. 6.23(e) shows the surface temperature of the subject when the hot water seat was used at the cabin and vent temperatures of 15°C and 40C. The surface color of the subject's left hand, right hand, forehead, and abdomen do not show a significant color change. However, the color of the tube in the hot water seat appears dark green. It is confirmed that the color of the tube of the part that exchanges heat with the back, thigh and ambient temperature is sky-blue, which indicating that the temperature is relatively low.

Fig. 6.24 shows the average surface temperature of the subjects' left hand, right hand, forehead, and abdomen according to the use of various seats during heating of a vehicle in winter. At the room temperature of 25°C, the average surface temperatures on the left hand, right hand, and forehead of the subjects were 33.6°C, 33.3°C, and 32.7°C, respectively. The average surface temperature of abdomen was 30.8°C that is relatively low temperature. This is because the temperature of the clothing contacting with cold environment was measured. When the cabin temperature was 15°C without the vent heating operation, the average surface temperatures on the left hand, right hand, forehead, and abdomen were measured to 26.4°C, 25.9°C, 27.4°C, and 36.8°C, respectively. In particular, the surface temperature of the abdomen was relatively high because the solar light was irradiated to the abdomen. When the basic seat used at the cabin and vent temperatures of 15°C and 40°C, the average surface temperatures on the left hand, right hand, and forehead were 25.1°C, 24.8°C, and 26.1°C, respectively. In addition, the average surface temperatures on the abdomen and surrounding were 31.5°C and 27.1°C, respectively. and it showed relatively significant decrement. When a heating seat was used at the cabin and vent temperatures of 15°C and 40°C, the average surface temperatures on the left hand, right hand, forehead, and abdomen were measured to 25.3°C, 25.1°C, 26.0°C, and 30.8°C, respectively. These values was similar to the experimental results of the basic seat. When a hot water seat of 40°C was used at the cabin and vent temperatures of 15°C and 40°C, the surface temperatures of the subject's left hand, right hand,

forehead, and abdomen were 28.4°C, 27.7°C, 27.2°C and 32.7°C, respectively. It was confirmed that the water outlet temperature in the hot water seat of 40°C decreased by heat exchanging at the back and thighs which were in contact with the seat and the cold thermal environment of 15°C.

(a) Standard condition(25°C)   (b) Cabin 15°C/Non-vent   (c) Cabin 15°C/Vent 40°C

(d) Cabin 15°C/Vent 40°C   (e) Cabin 15°C/Vent 40°C
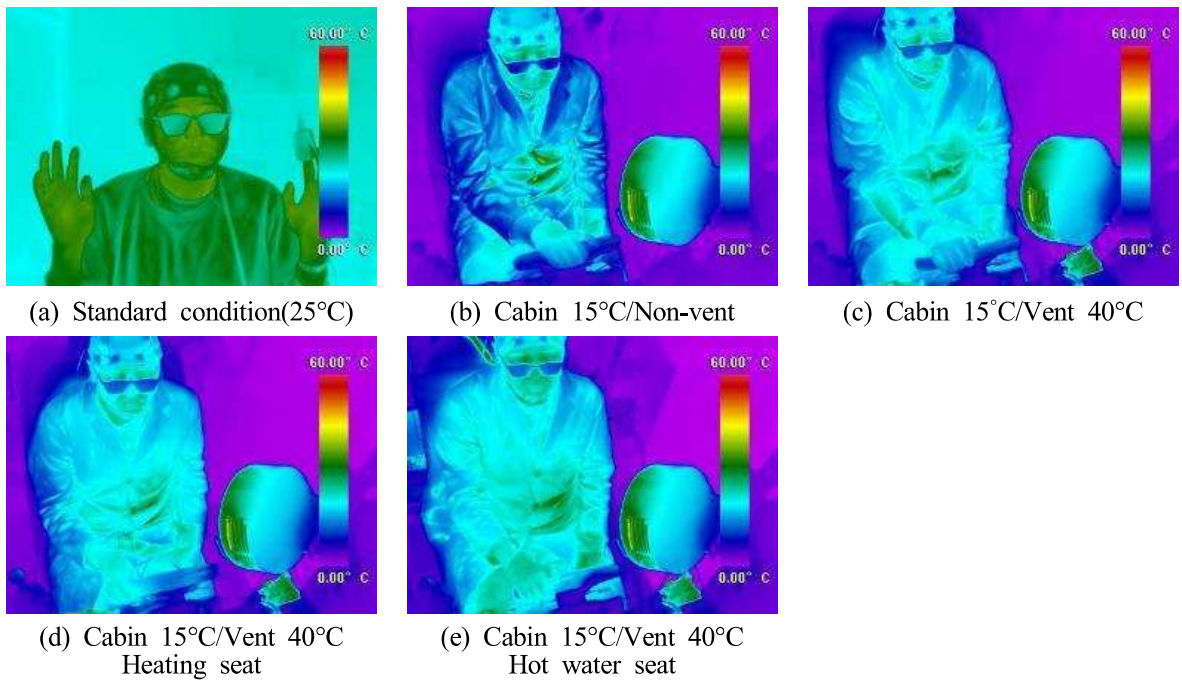Heating seat   Hot water seat

Fig. 6.23 Photography of driver's thermal imaging for various seats during heating in winter condition
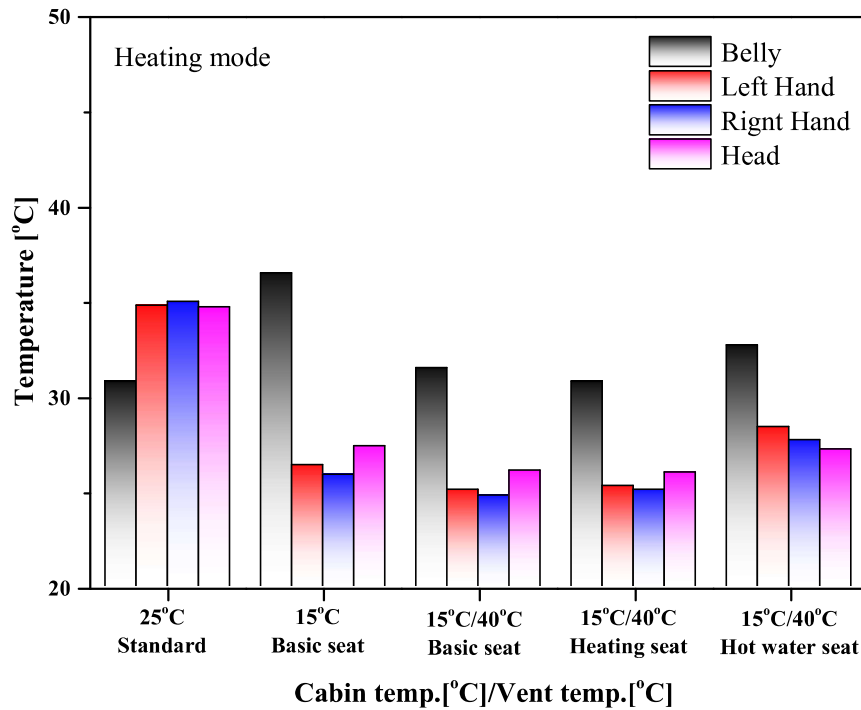
Fig. 6.24 Variation of driver's mean surface temperature for various seats during heating in winter condition

Fig. 6.25 shows the comparison of temperature variation in the hips, back, and thighs which were in contact with the seat according to the use the heating and hot water seats under winter condition. When 5 minutes have passed using the heating seat, the average temperature of the subject's hips, back, and thighs was 37.3°C. In case that the hot water seat was used for 5 minutes, the average temperature of the subject's hips, back, and thighs was measured by 36.2°C. Accordingly, the temperature difference of the contact parts of body with the seat according to the use of the heating and hot water seats was 1.1°C. When 30 minutes have passed using the heating seat, the average temperature of the subject's hips, back, and thighs increased by 41.5°C. When the hot water seat was used for 30 minutes, the average temperature of the subject's hips, back, and thighs was 38.0°C, which was 3.5°C lower than that using the heating seat. The temperature of hips, back, and thighs which were in contact with the seat when using the heating seat was over 40°C. In particular, the temperature of the back was 43.1°C which was the highest. Thus, long-term use of the heating seat in winter can cause discomfort due to high temperature to the body by significantly increasing the temperature of the hips, back, and thighs.

In addition, when the heating and hot water seats were used, the heating capacity according to the temperature difference between the outdoor air and contact parts of body with the seat was calculated. When the heating and hot water seats were used for 5 minutes, the heating capacities were 77.2 W and 69.9 W, respectively. When the heating and hot water seats were used for 30 minutes, the heating capacities were 227.0 W and 170.0 W, respectively. The heating capacity using the heating seat was larger than that using the hot water seat. Moreover, when the heating seat was used, the temperature of contact parts of body with the seat was higher than those when the hot water seat was used.
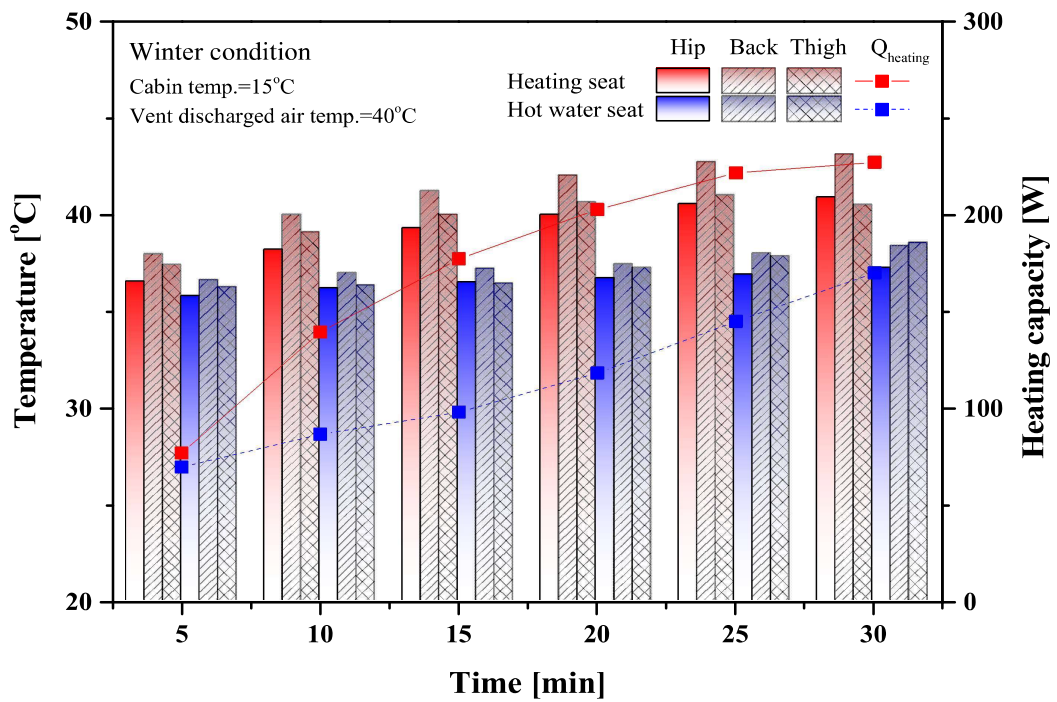
Fig. 6.25 Comparison of heating capacity and temperature variation on the subject's hips, back, and thighs according to the use of heating and hot water seats in winter condition

b. Subjective questionnaire survey results(TSV, CSV, CLV)

Fig. 6.26 shows the results of questionnaires of the average TSV, CSV, and CLV of the driver according to the use of various seats when heating of a car in winter. In the results of TSV questionnaires, at the cabin temperature of 15°C without heating from vent of HVAC, the TSV was -1.57 and it means that the subjects felt cold. Accordingly, the CSV and CLV was -0.71 and 0, respectively, and these were low. Therefore, subjects felt unpleasant and difficult to concentrate. When the basic seat used at the cabin and vent temperatures of 15°C and 40°C, TSV increased to -0.29 and the CSV and CLV also increased to 0.14 and 0.43, respectively. It was confirmed that the high temperature air (40°C) made the driver comfortable during driving. When a heating seat was used at the cabin and vent temperatures of 15°C and 40°C, TSV of subjects increased to 1.29 and the CSV and CLV also increased to 1.57 and 1.86, respectively. Besides, the subjects answered that they were more comfortable and concentrated at these condition. When the hot water seat was used at the same condition, TSV of subjects was 1.57, and which means that they felt warm. Moreover, CSV and CLV was 1.86 and 1.86, respectively, and subjects answered that they were most comfortable and concentrated well on driving.

In this study, when the subjective questionnaire results (TSV, CSV, CLV) were comprehensively analyzed, it was confirmed that the most comfortable driving environment and the improved concentration could be provided to the driver by heating using a hot air (40°C) from vent of HVAC in the cabin temperature of 15°C and the use of the cold water seat at 40°C, simultaneously.

Fig. 6.26 Results of TSV, CSV, and CLV questionnaires for various seats during heating in winter condition

c. PPG measurement results

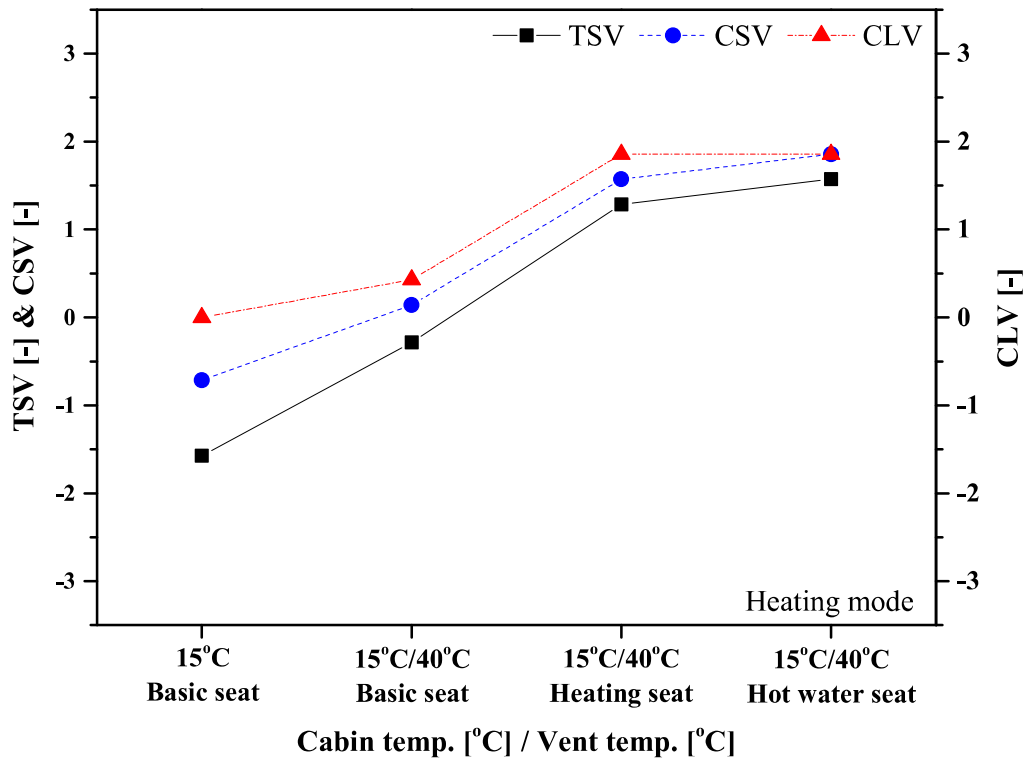Fig. 6.27 shows the variation of the pulse wave of driver according to the use of various seats when heating of a car in winter condition under solar radiation. Fig. 6.27(a) shows the variations of the stress index, TP, and LF/HF. The stress index, TP, and LF/HF of subjects at room temperature of 25°C were 38.4, 8.34, and 1.18, respectively. And then, the subject performed driving in a cabin temperature of 15°C which was the cold condition. The subject's stress index increased to 37.1, while TP increased to 8.52. This is because the subject's pulse was slowed in cold condition and the stress index decreased accordingly. When the basic seat was used at the cabin and vent temperatures of 15°C and 40°C, the subject's stress index decreased to 31.9 and TP increased to 8.55. This is because the operation of the heating at 40°C in a cold environment (cabin temperature of 15°C) provided a comfortable environment to the subject. When the heating seat was used at the cabin and vent temperatures of 15°C and 40°C, stress index increased to 39.0 and TP was 8.25. The reason for the increase in the stress index is because the subject felt unpleasant owing to the high temperature of the heating seat. By this reason, TP was also decreased. When the hot water seat was used at the same condition, stress index of subjects decreased to 33.0 and TP increased to 8.60 because the hot water seat provided a pleasant environment to the driver.

Fig. 6.27(b) shows the variations of SDNN and RMSSD in the pulse wave of the subjects during driving. SDNN and RMSSD were 39.3 ms and 29.1 ms, respectively, at the indoor temperature of 25°C. After that, at the cabin temperature of 15°C without heating of HVAC, SDNN and RMSSD of subjects were 38.2 ms and 32.3 ms, respectively. When the basic seat was used at the cabin and vent temperatures of 15°C and 40°C, SDNN and RMSSD increased to 43.8 ms and 35.1 ms, respectively, by blowing the warm air to the subject. This is because the operation of heating supplied warm air (40°C) using HVAC in a cabin temperature of 15°C and it provided a comfortable environment to the driver. When a heating seat was used at the cabin and vent temperatures of 15°C and 40°C, SDNN and RMSSD of subjects

were slightly decreased to 40.9 and 31.3 ms, respectively, because the high temperature of the heating seat provided an unpleasant environment to the subject. When the hot water seat was used at the same condition, SDNN and RMSSD of subjects was 49.4 ms and 38.1 ms, respectively. Accordingly, the use of the hot water seat could provide a comfortable environment to the subject, therefore they showed the increment of SDNN and RMSSD.

When the PPG results obtained in this study were comprehensively analyzed, it was confirmed that the use of HVAC for heating using warm air (40°C) and hot water seat (supply water temeprature is 40°C) in a cold winter environment (15°C) could provid a relatively comfortable thermal environment to the driver.
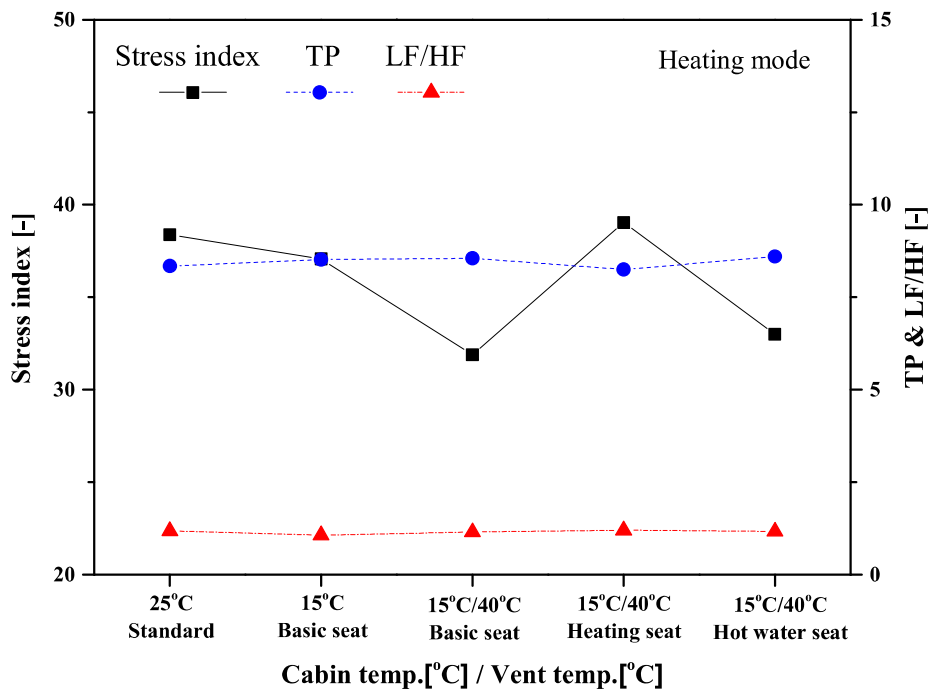
(a) Stress index, TP, and LF/HF
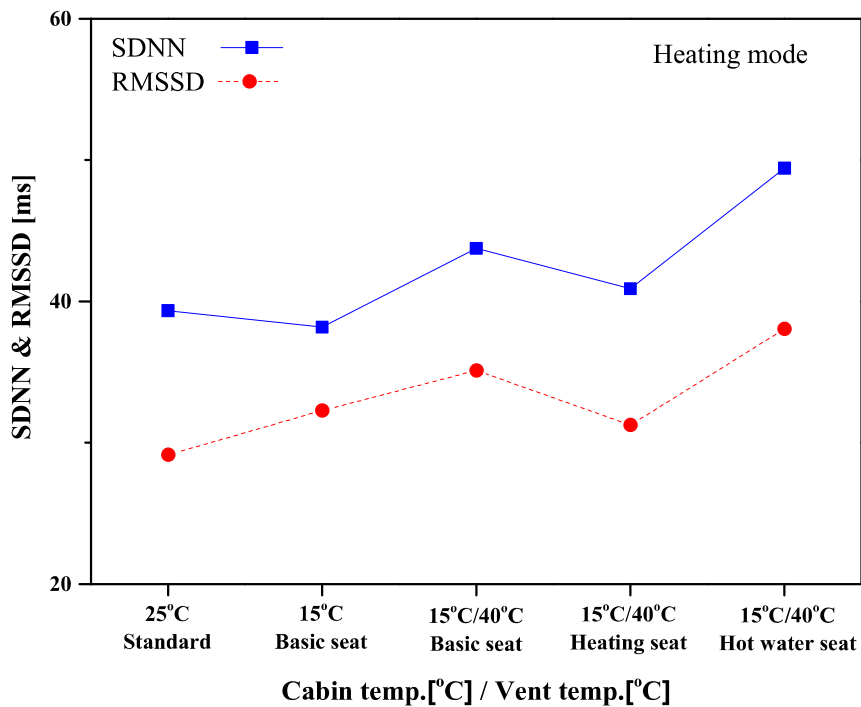
(b) SDNN and RMSSD

Fig. 6.27 Variations of driver's PPG for various seats during heating in winter condition; (a) Stress index, TP and LF/HF, (b) SDNN and RMSSD

d. EEG measurement results

Fig. 6.28 shows the brain mapping results for the EEG analysis of the subject according to the use of the various seats in winter condition. Relative θ wave at room temperature of 25°C showed red color and relative α wave was yellow-green and red colors. Besides, the activities of relative SMR, β, and high β waves were relatively low by showing yellow-green and red colors. Thus, it was confirmed that the subjects were a comfortable state at the indoor of 25°C. At the cabin temperature of 15°C without operation of heating of HVAC, relative α was increased by showing red color distribution. In addition, the activities of relative SMR, β, and high β waves were increased by showing yellow-green and red colors. This is because the subjects started to drive and focused on driving. When the basic seat used at the cabin and vent temperatures of 15°C and 40°C, relative α showed red color and relative high β wave presented yellow-green color. Accordingly, it was confirmed that the subjects were a comfortable state. Moreover, relative β showed orange and light green colors, which confirming that the subject's concentration on driving was relatively high. When the heating seat was used at the cabin and vent temperatures of 15°C and 40°C, the activities of relative θ and α waves showed relatively low with blue and yellow-green colors, and the activity of relative high β wave was high with red and yellow-green color colors. From this, it was confirmed that the use of the heating seat was unpleasant to the subjects. However, when the hot water seat was used at the same cabin and vent temperature of 15°C and 40°C, relative θ and α waves were red and yellow-green colors and relative high β wave was yellow-green color, which confirming that the subjects were a comfortable state for driving.

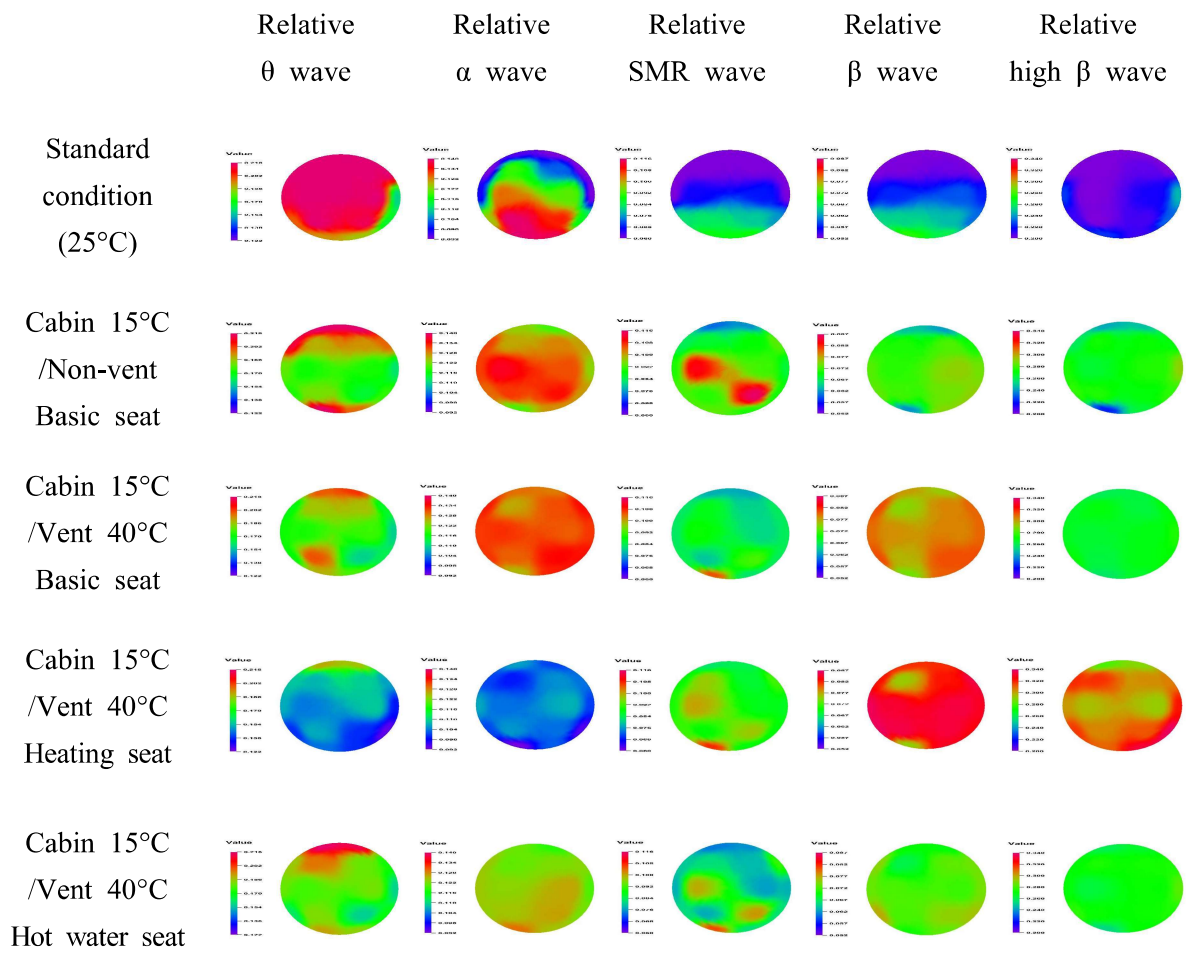|	Relative θ wave	Relative α wave	Relative SMR wave	Relative β wave	Relative high β wave
Standard condition (25°C)					
Cabin 15°C /Non-vent Basic seat					
Cabin 15°C /Vent 40°C Basic seat					
Cabin 15°C /Vent 40°C Heating seat					
Cabin 15°C /Vent 40°C Hot water seat					

Fig. 6.28 Brain mapping results of relative θ, α, SMR, β and high β waves for various seats during heating under winter condition

Fig. 6.29 shows the variations of the CI index and relative β/α in the prefrontal lobe of the driver according to the various seats under the winter condition. At the indoor temperature of 25°C, the CI index and relative β/α were the lowest. When the driving was started at a cabin temperature of 15°C without heating form vent in HVAC, the CI index and relative β/α were rapidly increased. This is because the concentration increased as the subjects started to drive. When the basic seat used with the operation of heating at 40°C in the cabin temperature of 15°C, the CI index and relative β/α of subjects tended to slightly increase because the heating using warm air at 40°C by HVAC in the cabin temperature of 15°C improved the concentration of subjects. When both heating of HVAC with the air temperature of 40°C and the heating seat were used simultaneously at the cabin temperature of 15°C, the CI index and relative β/α of subjects were further increased. Accordingly, the use of the heating seat could improve the concentration on driving of subjects, but subjects felt a little unpleasantness due to the high temperature of heating air. When the hot water seat was used at the same condition, the CI index and relative β/α of subjects tended to decrease because the relative α wave was increased. Therefore, the use of the hot water seat could provide the most comfortable to the driver.

Fig. 6.30 shows the EEG analysis results in the occipital lobe of the subject according to the various seats in winter under the solar radiation. At the indoor temperature of 25°C, the relative α wave was the highest. The relative α wave tended to rapidly decrease at a cabin temperature of 15°C without heating of HVAC because the subjects felt unpleasant in a cold environment. When the basic seat was used with the operation of HVAC with warm air of 40°C in the cabin temperature of 15°C, the relative β/α showed the highest because the warm air of 40°C discharged from the vent improved the concentration on driving of the subject. When the heating seat was used at the cabin and vent temperatures of 15°C and 40°C, the relative β/α of subjects increased. This is because the subjects felt more unpleasant due to the high temperature in the heating seat. When the hot water seat was used at the cabin and vent temperatures of 15°C and 40°C, the relative β/α of subjects was rapidly

decreased because the use of the hot water seat provided a relatively comfortable environment to the subject, resulting that the relative α wave increased.

It was confirmed that the use of a hot water seat using hot water temperature of 40°C at the same condition of cabin and vent could provide the most pleasant environment to the subject on driving in the car in winter condition.
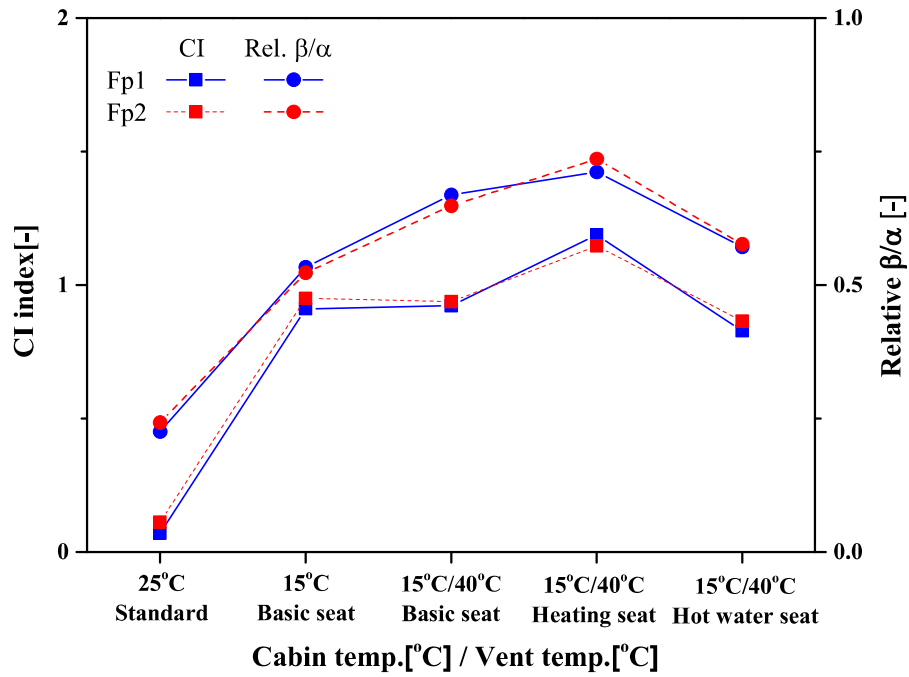
Fig. 6.29 Variations of CI and relative β/α at the prefrontal lobe for various seats during heating under winter condition
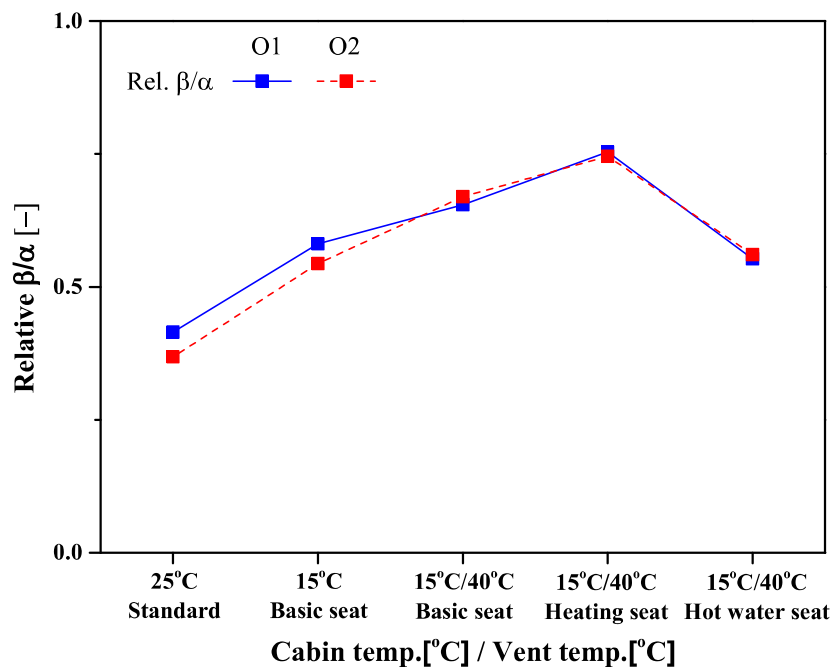

Fig. 6.30 Variations of relative β/α at the occipital lobe for various seats during heating under winter condition

C. Experimental results and discussion on driver's thermal comfort according to the position of local heating in automotive indoor under winter condition

1. Mean surface temperature measurement results

Fig. 6.31 shows the average surface temperature of the subject's forehead, chest, hands, and thighs according to the use of local heating with and without the HVAC system in a vehicle under the winter condition. Fig. 6.31(a) shows the change in the average surface temperature of the subjects according to the use of local heating when the HVAC system is not worked. When the local heating was not used at the cabin temperature of 15°C, the surface temperatures of the forehead, chest, hands, and thighs of the subjects were 27.0°C, 16.5°C, 23.5°C, and 23.7°C, respectively. The surface temperature of chest was the lowest because the surface temperature of the clothes was measured in this case. When the local heating was applied at the chest under the cabin temperature of 15°C, the surface temperatures of the forehead, chest, hands, and thighs were 27.1°C, 32.3°C, 24.2°C, and 22.6°C, respectively. As a result, the chest showed the highest temperature. When the local heating was used at the hands under the same cabin temperature, the surface temperatures of the forehead, chest, hands, and thighs were 27.1°C, 19.6°C, 29.1°C, and 24.7°C, respectively. In addition, in the case of using the local heating at thighs under the cabin temperature of 15°C, the surface temperatures of the forehead, chest, hands, and thighs were 26.8°C, 19.2°C, 23.7°C, and 31.4°C, respectively. In the case of using the local heating at feet under the same cabin temperature, the surface temperatures of the forehead, chest, hands, and thighs were 26.7°C, 17.5°C, 22.7°C, and 24.0°C, respectively. The surface temperature of the forehead was not significantly affected by the use of local heating. The average surface temperature of the subjects was 22.7°C when the local heating was not used. When local heating was used at the chest,

hands, thighs, and feet, the average body temperature was 26.5°C, 25.1°C, 25.3°C, and 22.7°C, respectively. When the HVAC system was not operated, the use of local heating had a great influence on the surface temperature of the area where local heating was applied, but there was no significant effect on other areas in human body.
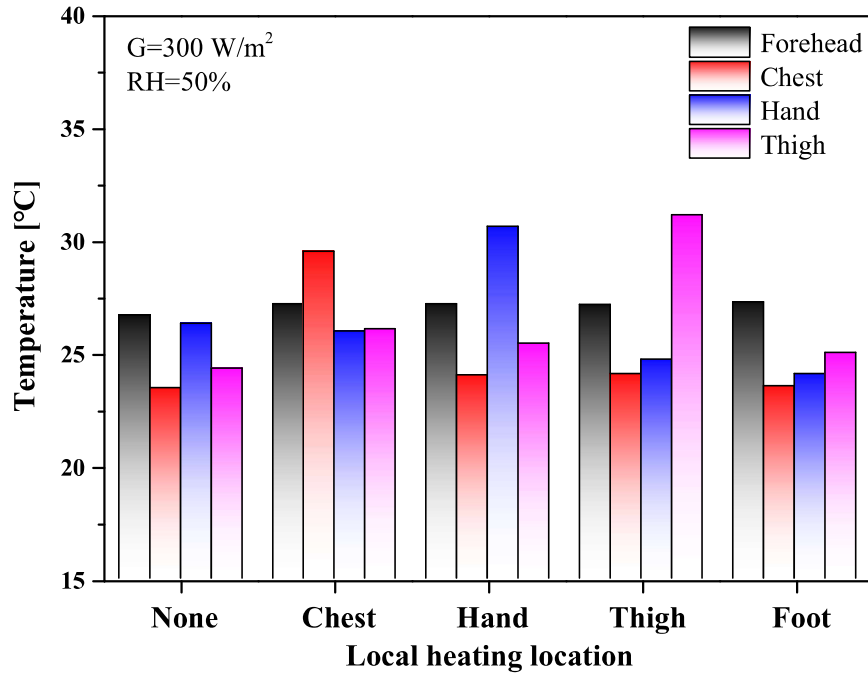
Fig. 6.31(b) shows the variation of average surface temperature of subjects according to the use of local heating when the HVAC system was operated in winther condition. When the local heating was not applied without operation of HVAC system at the cabin temperature of 15°C, the surface temperatures of the forehead, chest, hands, and thighs were 26.7°C, 23.5°C, 26.3°C, and 24.3°C, respectively. When the HVAC system and local heating of the chest was applied at the cabin temperature of 15°C, the surface temperatures of the forehead, chest, hands, and thighs were 27.2°C, 29.5°C, 26.1°C, and 26.0°C, respectively. Besides, when the local heating to the hands was applied while working on the heating of HVAC system at the cabin temperature of 15°C, the surface temperatures of the forehead, chest, hands, and thighs were 27.2°C, 24.1°C, 30.6°C, and 25.4°C, respectively. In addtion, when the HVAC system and local heating to the thighs was applied at the cabin temperature of 15°C, the surface temperatures of the forehead, chest, hands, and thighs were 27.2°C, 24.1°C, 24.7°C, and 31.1°C, respectively. In case that the HVAC system and local heating to the feet were applied under the same cabin temperature, the surface temperatures of the forehead, chest, hands, and thighs were 27.3°C, 23.6°C, 24.1°C, and 25.0°C, respectively. When the local heating was not applied and the HVAC system operated, the average surface temperature of the subjects was 25.2°C. In addition, when local heating was applied to the chest, hands, thighs, and feet under the operation of HVAC system at the cabin temperature of 15°C, the surface temperature of average surface temperatures of the subjects were 27.2°C, 26.8°C, 26.7°C, and 25°C, respectively.

As the comparison results of local heating experiment, the average temperature of the subject's body with operation of heating using HVAC system was 1.72°C higher

than that of the case without operation of heating using HVAC system. Consequently, it was confirmed that the use of both heating of HVAC system and local heating using solar radiation in the car indoor under the cold winter condition can quickly increase the driver's body temperature.
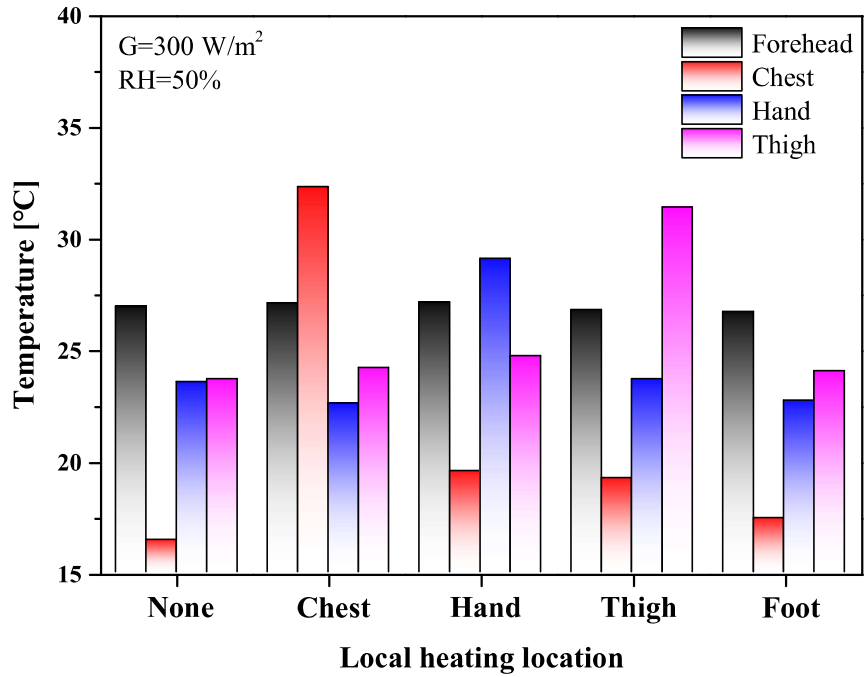
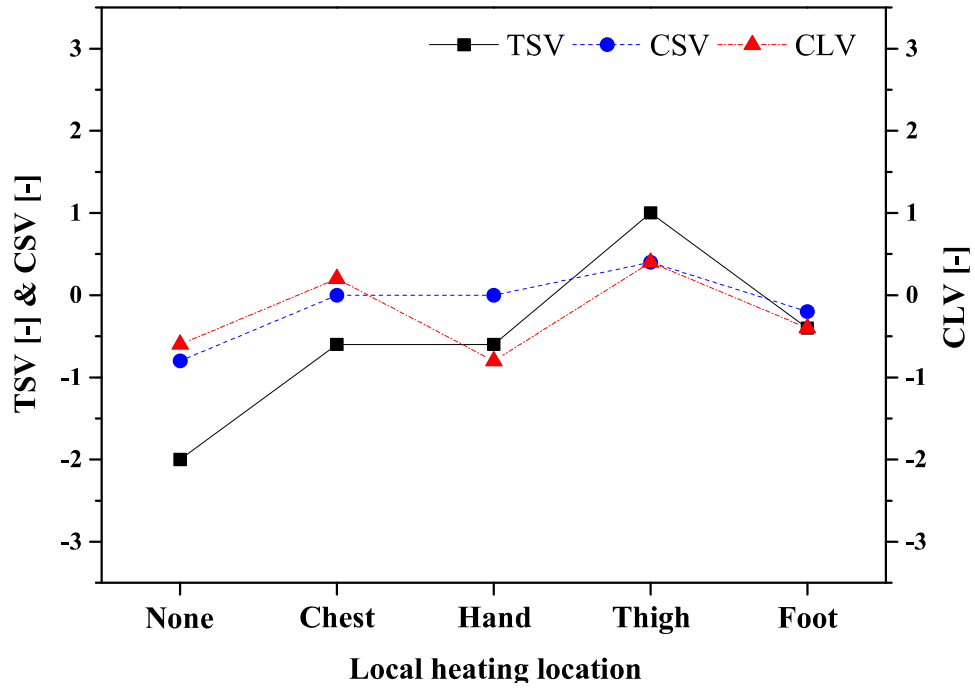(a) non-use HVAC system

(b) use HVAC system

Fig. 6.31 Variation of surface temperature according to the local heating location and the use/non-use of HVAC system

## 2. Subjective questionnaire survey results(TSV, CSV, CLV)

Fig. 6.32 shows the results of the subjective questionnaire survey (TSV, CSV, CLV) according to the use of local heating with and without operation of HVAC system in a vehicle under the winter condition. Fig. 6.32(a) shows the results of the TSV, CSV, and CLV according to the use of local heating when the HVAC system was not operated. When the local heating was not applied at the cabin temperature of 15°C, TSV was –2 and it indicated that subjects felt cold. Under this condition, CSV and CLV were -0.8 and –0.6, respectively, and these were relatively low. When the local heating was applied to the chest at the cabin temperature of 15°C, TSV was -0.6 and CSV and CLV were increased to 0 and 0.2, respectively. In case that local heating was applied to the chest in the cold winter condition, the driver felt comfortable and highly concentrated on driving. When the local heating was applied to the hands under the same cabin temperature, TSV was -0.6 and CSV and CLV were increased to 0 and -0.8, respectively. In the case of using the local heating to the thighs under the cabin temperature of 15°C, TSV was 1, thus CSV and CLV were 0.4 and 0.4, respectively, and those were the highest. When the HVAC system was not operated in the cold winter condition, it was confirmed that the local heating of the thighs was the most comfortable to the driver and could be improved the concentration on driving. When the local heating was applied at the feet under the same cabin temperature, TSV was -0.4 and CSV and CLV were decreased to -0.2 and -0.4, respectively.

Fig. 6.32(b) shows the variations of TSV, CSV, and CLV according to the use of local heating when the HVAC system worked. When the local heating was not applied with the operation of HVAC system at an indoor temperature of 15°C, TSV, CSV, and CLV were 0.2, 1.0, and 1.4, respectively. When the HVAC system and local heating to the chest was applied at the cabin temperature of 15°C, TSV was 1.4. Accordingly, CSV and CLV showed 1.8 and 2.0, respectively, and these were the highest. In case that both HVAC system and local heating to the chest under the

cold winter condition, the driver felt the most comfortable and the highly concentrated on driving. When the local heating to the hands was applied and the heating of HVAC system worked at the cabin temperature of 15°C, TSV, CSV, and CLV showed 0.6, 1.2, and 0.8, respectively. When the both HVAC system and local heating of the thighs were applied at the cabin temperature of 15°C, TSV showed 1.2 and resulting that CSV and CLV were 1.6 and 1.8, respectively, and these were relatively high. When the HVAC system and local heating to the feet were applied at the same cabin temperature of 15°C, TSV, CSV, and CLV were 1.6, 1.2, and 1.2, respectively. The TSV response of the driver using the HVAC system was higher than that without the HVAC system, and resulting that the CSV and CLV were also higher overall. Therefore, it was confirmed that the use of the both HVAC system and local heating to the chest and thighs in the car indoor during the cold winter could provide comfortable environment to the driver and the concentration level on driving was relatively high.

(a) non-use HVAC system
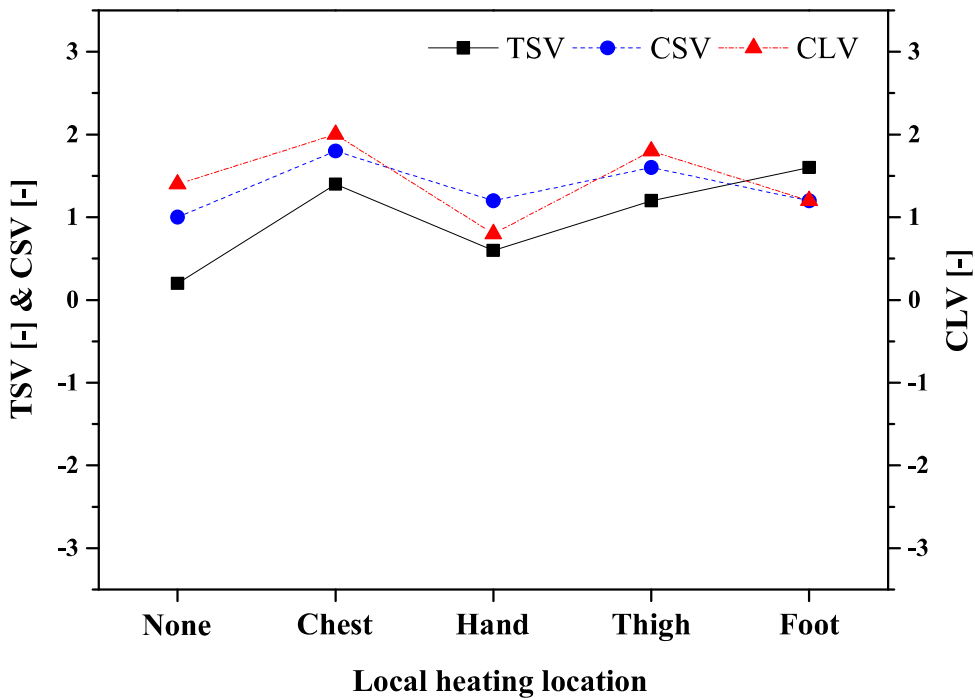
(b) use HVAC system

Fig. 6.32 Results of TSV, CSV, and CLV questionnaires according to the local heating location and the use/non-use of HVAC system
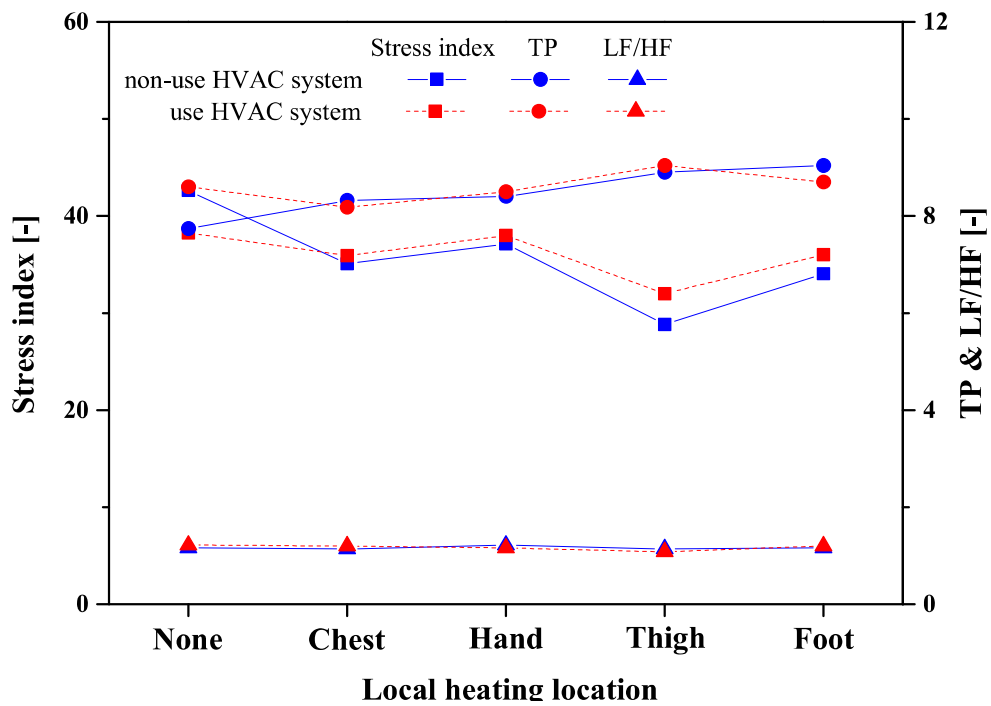
3. PPG measurement results

Fig. 6.33 shows the variation on the pulse wave of subjects according to the use of local heating with and without operation of the HVAC system in a vehicle under the winter condition. Fig. 6.33(a) shows the stress index, TP, and LF/HF according to the use of local heating with and without operation of the HVAC system. When the local heating and HVAC system were not applied at the cabin temperature of 15°C, stress index was 42.6 that is the highest, and TP and LF/HF were 7.74 and 1.16, respectively. It was confirmed that subjects were under a lot of stress in an environment where the local heating and HVAC system were not applied in winter. When the heating of the HVAC system in the same environment was applied, the stress index decreased to 38.3, and TP and LF/HF increased to 8.60 and 1.22, respectively. This is because the working of the HVAC system in winter reduced the subject's stress, thus TP which is the overall control ability of the autonomic nervous system was increased. When the local heating was applied to at the chest without operation of HVAC system at the cabin temperature of 15°C, stress index of subjects was 35.1, and TP and LF/HF were 8.32 and 1.14, respectively. When both of using the HVAC system and local heating at the same cabin temperature, stress index of subjects was 35.9, and TP and LF/HF were measured by 8.18 and 1.20, respectively. It was confirmed that the use or non-use of the HVAC system with the local heating to the chest did not significantly affect the stress index and TP of the subjects. When the local heating was applied to the hands without operation of HVAC system at the same cabin temperature, stress index of subjects was 37.1, and TP and LF/HF were 8.40 and 1.22, respectively. When the heating of HVAC system and local heating were applied at the same cabin temperature, stress index of subjects showed 38.0, and TP and LF/HF were 8.50 and 1.16, respectively. In the case of local heating to the thighs without the HVAC system at the cabin temperature of 15°C, stress index of subjects was 28.2, and TP and LF/HF were 8.90 and 1.14, respectively. Under this condition, stress index of subjects was the lowest, and confirming that the subjects

were in a comfortable state. When the heating of HVAC system and local heating were applied at the same cabin temperature, stress index of subjects was 32.0, and TP and LF/HF showed 9.04 and 1.08, respectively. In this condition, stress index was relatively low, and TP was the highest. Thus, it was confirmed that the use of local heating to the thighs in winter condition could provide a pleasant environment to the driver. In the case of local heating to the feet without operation of HVAC system at the cabin temperature of 15°C, stress index of subjects was 34.0 and TP and LF/HF were 9.04 and 1.16, respectively. At the same cabin temperature, when the heating of HVAC system and local heating were applied at the same time, stress index was 36.0, and TP and LF/HF were 8.70 and 1.20, respectively.

Fig. 6.33(b) shows the variations of SDNN and RMSSD according to the use of local heating with and without operation of HVAC system. When the both local heating and heating of HVAC system were not applied at the cabin temperature of 15°C, SDNN and RMSSD of subjects were 41.9 ms and 36.5 ms, respectively. This is because the environment without application of local heating and HVAC system in winter condition is unpleasant, therefore the physical fatigue of the subjects increased and the stability of the heart was low. When the heating of HVAC system and local heating were applied at the same cabin temperature, SDNN and RMSSD of subjects showed 43.9 ms and 31.9 ms, respectively. When the local heating was applied to the chest without operation of HVAC system at the cabin temperature of 15°C, SDNN and RMSSD of subjects were 49.8 ms and 40.6 ms, respectively. In case that both operation of heating of HVAC system and local heating at the same cabin temperature, SDNN and RMSSD were 44.0 ms and 33.0 ms, respectively. When the local heating was applied without operation of HVAC system at the cabin temperature of 15°C, SDNN and RMSSD were 53.2 ms and 36.7 ms, respectively. At the same cabin temperature, when heating of HVAC system and local heating were applied, SDNN and RMSSD represented 46.5 ms and 34.2 ms, respectively. In the case of the use the local heating to thighs without operation of HVAC system at the cabin temperature of 15°C, SDNN of subjects was 5.1 ms and RMSSD showed the highest

(42.7 ms). When the heating of HVAC system and local heating were applied at the same cabin temperature, SDNN and RMSSD were 54.8 ms and 37.2 ms, respectively, and these were relatively high. Thus, it was confirmed that the use of local heating to the thighs provided a comfortable driving environment by increasing the stability of the heart and decreasing the physical fatigue to the driver. In the case of local heating to the feet without the HVAC system at the cabin temperature of 15°C, SDNN and RMSSD were 56.9 ms and 41.8 ms, respectively. When the heating of HVAC system and local heating were applied at the same cabin temperature, SDNN and RMSSD of subjects were 54.5 ms and 35.7 ms, respectively.

(a) Stress index, TP, and LF/HF
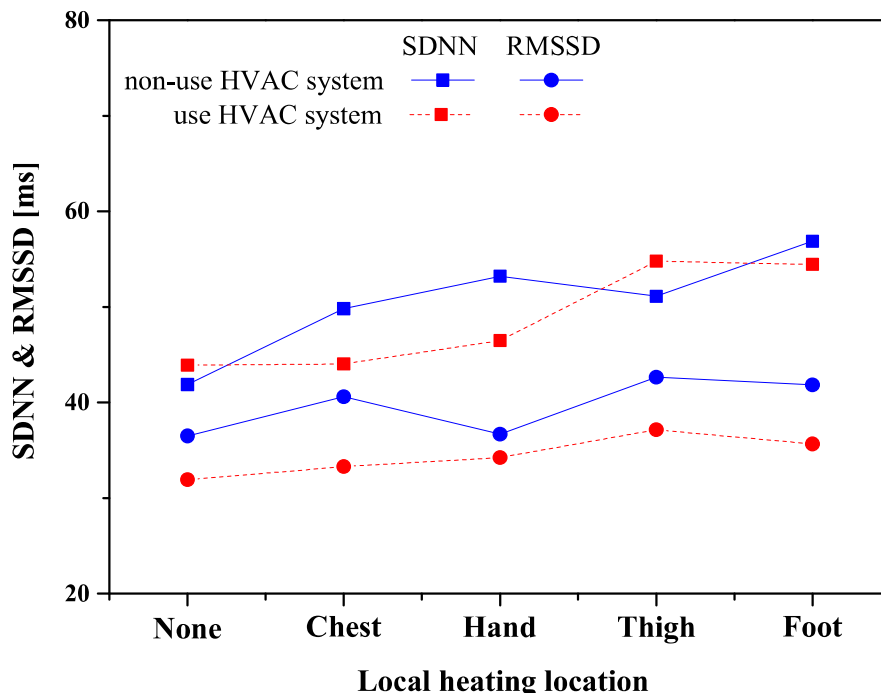
(b) SDNN and RMSSD

Fig. 6.33 Variations of driver's PPG according to the local heating location and the use/non-use of HVAC system
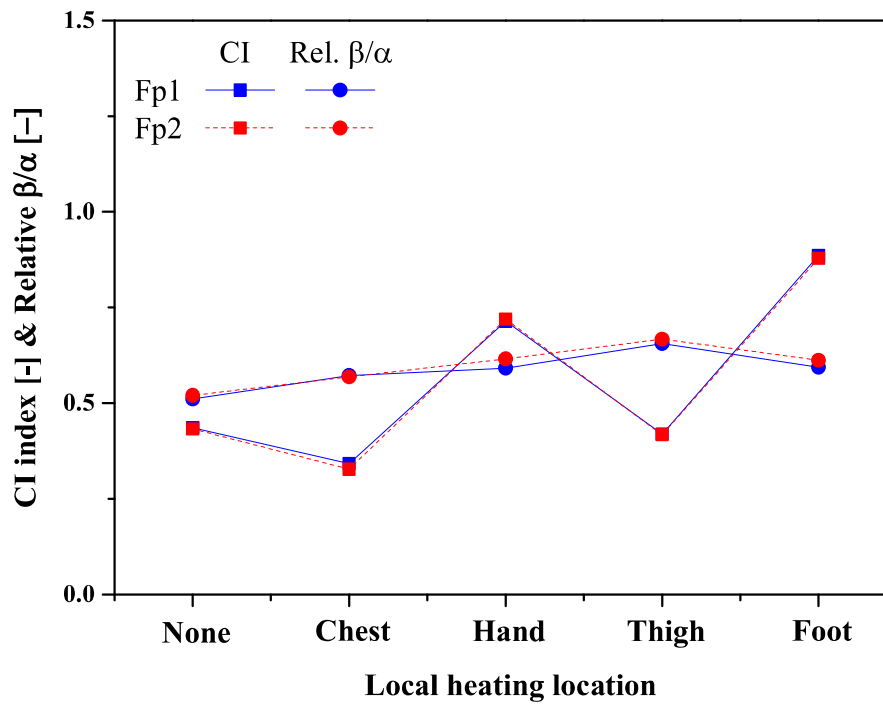
4. EEG measurement results

Fig. 6.34 shows the variation on the brain wave of subjects in the prefrontal lobe according to the use of local heating with and without operation of HVAC system in a vehicle under the winter condition. Fig. 6.34(a) shows the variations of CI index and relative β/α according to the use of local heating without operation of HVAC system. When the both local heating and HVAC system were not used at the cabin temperature of 15°C, the CI index of Fp1 and Fp2 was 0.27 and 0.45, respectively, and the relative β/α of those was 0.60 and 0.50, respectively. There was a slight imbalance in the CI index due to the imbalance of relative θ occurred in the CI index. This imbalance of relative θ is because the subject felt the psychological discomfort in a cold environment. When the local heating was applied to the chest without operation of HVAC system at the cabin temperature of 15°C, the CI index of Fp1 and Fp2 was 0.56 and 0.55, respectively, and the relative β/α of those showed 0.51 and 0.54, respectively. It was confirmed that the CI index of subjects increased when local heating was applied to the chest, thereby improving the subjects' concentration on driving. When the local heating to the hands was applied without operation of HVAC system at the cabin temperature of 15°C, the CI index of Fp1 and Fp2 was the highest 0.86 and 0.87, respectively, and the relative β/α of those also showed the highest 0.67 and 0.68, respectively. In this condition, the concentration level of subjects on driving was the highest, too. In the case of the use the local heating to thighs without operation of HVAC system at the cabin temperature of 15°C, the CI index of Fp1 and Fp2 was 0.50 and 0.49, respectively, and the relative β/α of those was measured to 0.58 and 0.58, respectively. In addition, In the case of local heating to feet without operation of HVAC system at the cabin temperature of 15°C, the CI index of Fp1 and Fp2 showed 0.47 and 0.47, respectively, and the relative β/α of those was 0.57 and 0.56, respectively.

Fig. 6.34(b) shows the variations of CI index and relative β/α according to the use of local heating with the HVAC system. When the local heating was not applied with

operation of heating in HVAC system at the cabin temperature of 15°C, the CI index of Fp1 and Fp2 was 0.44 and 0.43, respectively, and the relative β/α of those showed 0.51 and 0.52, respectively. When the local heating was used to the chest with heating operation of HVAC system at the cabin temperature of 15°C, the CI index of Fp1 and Fp2 was 0.34 and 0.33, respectively, and the relative β/α of those was 0.57 and 0.57, respectively. In case that the local heating was applied to the hands with heating operation of HVAC system at the cabin temperature of 15°C, the CI index of Fp1 and Fp2 was 0.71 and 0.72, respectively, and the relative β/α of those was 0.59 and 0.62, respectively. In this condition, the CI index tended to increase, and it was confirmed that the local heating to the hands improved the driver's concentration level. In the case of the use the local heating to thighs with heating operation of HVAC system at the cabin temperature of 15°C, the CI index of Fp1 and Fp2 was 0.42 and 0.42, respectively, and the relative β/α of those were measured to 0.66 and 0.67, respectively. When both the heating of HVAC system and the local heating to the feet at the cabin temperature of 15°C was applied at the same time, the CI index of Fp1 and Fp2 was 0.89 and 0.88, respectively, and the relative β/α of those was 0.59 and 0.61, respectively.
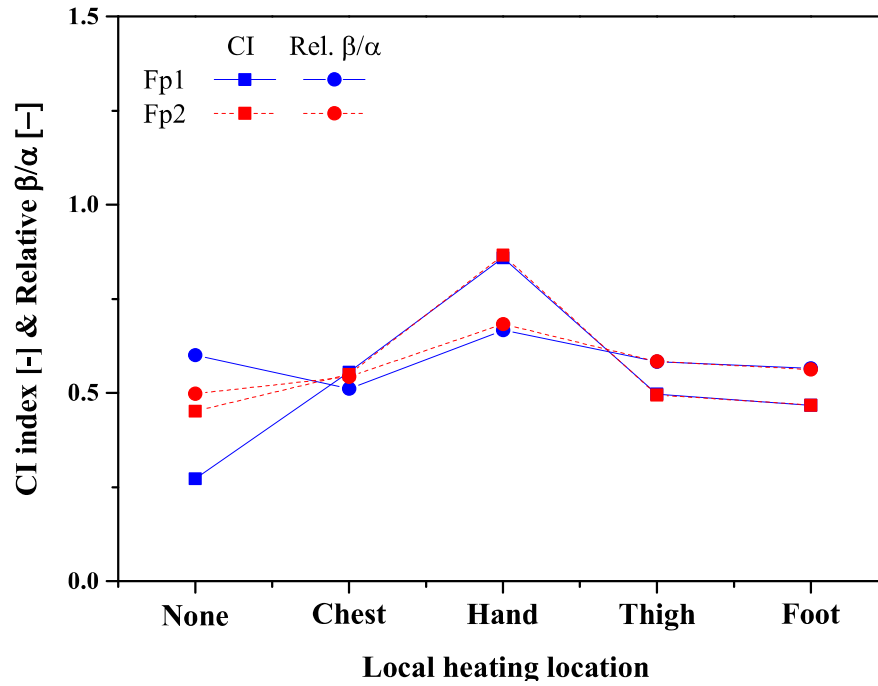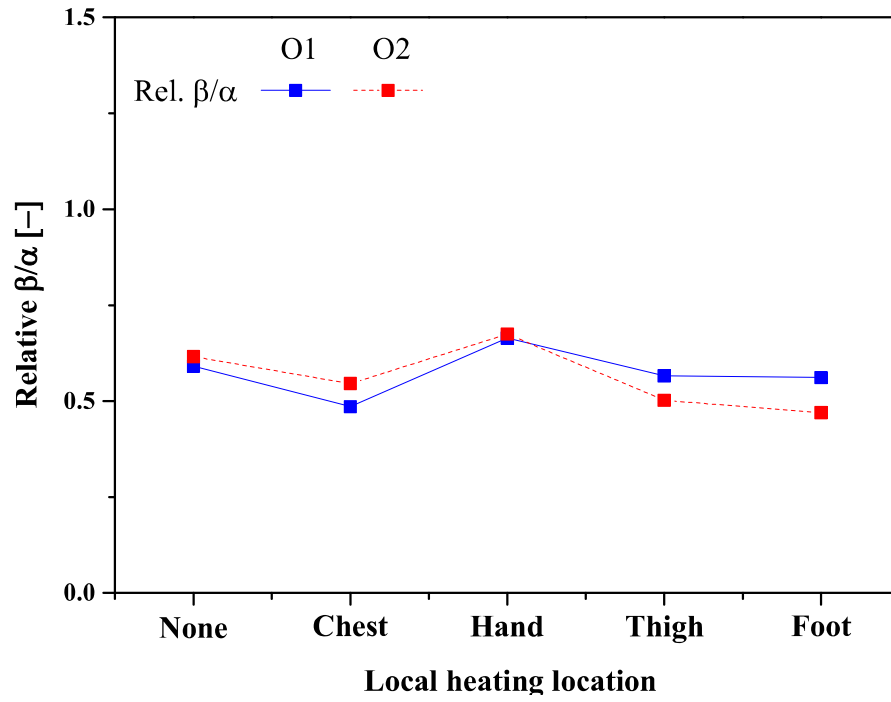
(a) non-use HVAC system

(b) use HVAC system

Fig. 6.34 Variations of CI index and relative β/α at the prefrontal lobe according to the local heating location and the use/non-use of HVAC system

Fig. 6.35 shows the variation on the brain wave of subjects in the occipital lobe according to the use of local heating with and without operation of HVAC system in a vehicle under the winter condition. Fig. 6.35(a) shows the relative β/α in the occipital lobe according to the use of local heating with heating operation of HVAC system. When the both local heating and heating of HVAC system did not used at the cabin temperature of 15°C, the relative β/α of O1 and O2 showed 0.59 and 0.62, respectively. When the local heating was applied to the chest without operation of HVAC system at the cabin temperature of 15°C, the relative β/α of O1 and O2 decreased to 0.49 and 0.55, respectively. The decrease of the relative β/α in the occipital lobe was because the α wave increased, thus subjects were at the comfortable state for driving. It was confirmed that the local heating to the chest was in a more comfortable state than the conditions without operation of heating of HVAC system and local heating. When the local heating to the hands was applied and heating of HVAC system was not used at the cabin temperature of 15°C, the relative β/α of O1 and O2 was 0.66 and 0.67, respectively, and these were highest. This is because the concentration on driving was high as the results of the prefrontal lobe, thus α wave was suppressed. In the case of the use the local heating to thighs without operation of HVAC system at the cabin temperature of 15°C, the relative β/α of O1 and O2 was 0.57 and 0.50, respectively. In the case of local heating to the feet without heating operation of HVAC system at the cabin temperature of 15°C, the relative β/α of O1 and O2 was 0.56 and 0.47, respectively.

Fig. 6.35(b) shows the relative β/α in the occipital lobe according to the use of local heating with heating of HVAC system. When the local heating was not used with heating operation of HVAC system at the cabin temperature of 15°C, the relative β/α of O1 and O2 was 0.51 and 0.56, respectively. When the local heating was used to the chest during heating operation of HVAC system at the cabin temperature of 15°C, the relative β/α of O1 and O2 was 0.54 and 0.58, respectively. When the local heating was applied to the hands without operation of HVAC system at the cabin temperature of 15°C, the relative β/α of O1 and O2 showed 0.57 and

0.57, respectively. In the case of the use the local heating to thighs with heating of HVAC system at the cabin temperature of 15°C, the relative β/α of O1 and O2 was 0.57 and 0.56, respectively. In the case of the use of heating in HVAC system and the local heating to the feet at the cabin temperature of 15°C, the relative β/α of O1 and O2 was 0.57 and 0.58, respectively. When the heating of HVAC system was used in the automotive indoor, the relative β/α in the occipital lobe of the subjects did not show a significant change according to the position of the local heating.

(a) non-use HVAC system
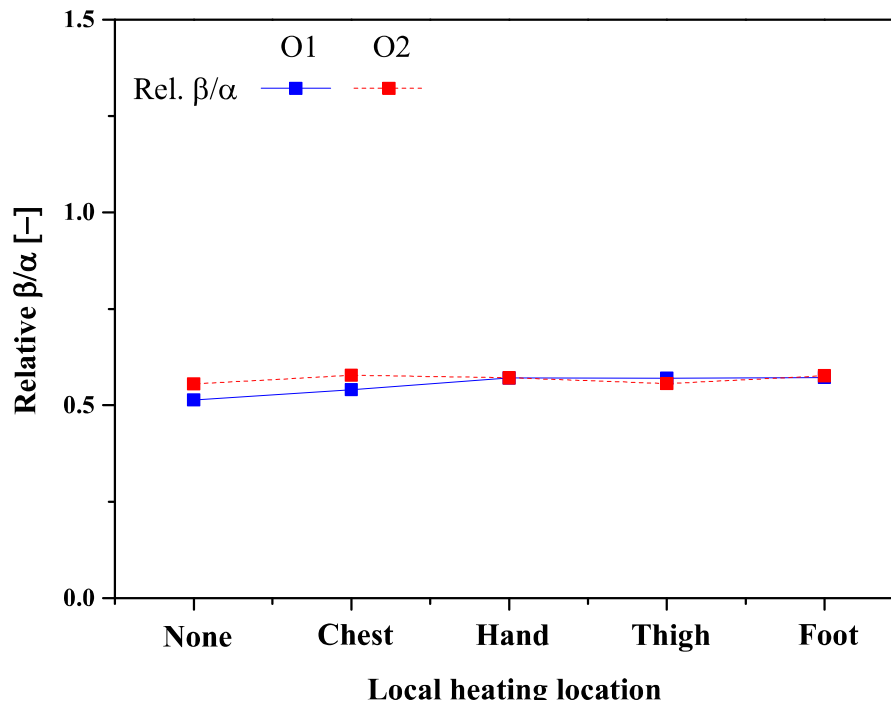
(b) use HVAC system

Fig. 6.35 Variations of relative β/α at the occipital lobe according to the local heating location and the use/non-use of HVAC system

VII. Conclusions

In this study, EEG, PPG, and surface temperature were measured when the subject performed a driving simulation as the automobile cabin temperature and vent discharge temperature in summer and winter were changed from discomfortable conditions to comfortable conditions. Besides, subjective questionnaires (TSV, CSV, CLV) were used to analyze the subject's thermal comfort under the driving environment. In addition, thermal comfort analysis was performed on the initial thermal environment of a vehicle interior in summer and winter. Besides, the subject's bio-signals such as brain waves, pulse waves, and skin temperature were measured according to using various seats under the thermal environment of the vehicle cabin in summer and winter. At the same time, the subject's thermal comfort was analyzed through subjective questionnaires (TSV, CSV, CLV). In addition, thermal comfort was analyzed at the different location of local heating in winter by measuring the subject's bio-signals and performing a subjective questionnaire. Through this, the following conclusions were obtained.

As the simulation results for the thermal comfort of the automobile indoor in summer, the temperature of the body's torso, arms, legs, and hands decreased due to the cold air of the air conditioner. However, the temperature inside the back, hips, and thighs increased due to the contact with the seat. On the other hand, the average surface temperature of the human body using the cold water seat is about 2.96°C lower than that using the basic seat. Accordingly, PPD using the cold water seat is 23.4% lower than that using the basic seat. It was confirmed that the use of the cold water seat could provide more effective thermal comfort to the driver.

As the simulation results for the thermal comfort of the automobile indoor in winter, the temperature of the human body's hands and legs was the highest at 38.0°C and 40.6°C, respectively. However, it did not have a significant effect on the driver compared with the analysis results of vehicle interior thermal comfort in summer because the air flow rate of air conditioner in winter is smaller than that of

summer. The temperature of the part in contact with the hot water seat was increased as time passed, and the average surface temperature of human body using hot water seat was 1.64°C higher than that using the basic seat. When the basic seat is used in winter condition, a slight dissatisfaction on the PPD (10.1%) is presented, and it is 7.8% in the initial 5 minutes when the hot water seat is used, which confirming that a pleasant thermal environment is achieved.

As the average surface temperature measurement result for the thermal comfort of a driver in the automobile indoor during cooling in summer, it was confirmed that the surface temperature of the subject during driving could be reduced by operating the vent of 12.5°C at the cabin temperature of 35°C. As comprehensively analyzing the subjective survey results, PPG analysis results, and EEG analysis results, at cabin/vent temperature of 27.5°C/18.5°C, it was confirmed that a pleasant driving environment could be provided to the driver and concentration on driving could increased.

As the average surface temperature measurement result for the thermal comfort of a driver in the automobile indoor during heating in winter, it was confirmed that the surface temperature of the subject while driving could be increased by operating the vent at 40°C at the cabin temperature of 15°C. As the subjective survey results, PPG analysis results, and EEG analysis results, at cabin/vent temperature of 17.5°C/37.5°C and cabin/vent temperature of 20°C/35°C, it was confirmed that a pleasant driving environment could be provided to the driver and concentration on driving could increase.

As experimental results on the use of various seats based on bio-signals and subjective surveys, the use of the ventilation seat in summer condition provided an unpleasant environment to the driver by blowing the surrounding hot air. While, it was confirmed that the use of the cold water seat was lower the driver's stress index and provided the proper environment with high concentration on driving. In addition, as the results of thermal comfort based on bio-signals and subjective surveys under winter condition, the use of the heating seat provided an unpleasant environment to the driver due to the high temperature of the heating wire. The use of the hot water

seat decreased the concentration on driving, however, it was confirmed that the stress index and relative β/α in the occipital lobe were reduced, which was provided a thermally comfortable environment to the driver.

As the results of local heating position in winter, the temperature of the parts where was applied local heating increased significantly regardless of the use of HVAC, but there was no effect of increasing the temperature in other parts. In the analysis results of PPG and EEG, when a local heating to the thighs was applied, the stress index was the lowest, and SDNN and RMSSD were relatively high when the local heating to the chest and thighs was used. In addition, it was confirmed that the relative β/α in the occipital lobe was low, thus it could provide a comfortable thermal environment to the driver.

Therefore, it was confirmed that thermally comfortable environment can be provided to the driver in the automobile indoor environment by using the cold water seat in the summer. In addition, a hot water seat and local heating to the thighs and chest in winter are also increased thermal comfort to the drive during driving.

VIII. Future work

In this study, the characteristics of the driver's thermal comfort inside an automobile interior in summer and winter conditions have been introduced and summaried. The numerical simulation on thermal comfort of a driver in car interior under summer and winter conditions was performed. Besides, the experiment on the thermal comfort and the driving concentration of the drivers was carried out according to the cabin and vent discharged air temperatures, the use of various seats, and the use of local heating. Based on the result of this study, I will recommend some work as the future work.

First, it is necessary to examine the practical applicability of a water thermal seat (cold and hot water seats) and the local cooling and heating by conducting an experiment on the driver's thermal comfort in a real car on the road, not a driving simulator. Second, it is necessary to conduct an experiment on the driver's thermal comfort in consideration of age, gender, driving experience, etc. based on more subjects, and establish the category of thermal comfort for various condition. Using the developed correlation or algorithm on the thermal comfort, it is necessary to develop a automatic control water thermal seat that controls the temperature based on various biological signals of the driver. Third, research on the energy saving efficiently by applying the water thermal seat to control the temperature based on the bio-signals in the autonomous vehicles and electric vehicles is needed in order to improve the passengers' thermal comfort. In addition, another research to satisfy user's thermal comfort automatically and optimal energy saving by utilizing thermal comfort algorithm in various fields such as building, office, automobile, train, and air plane.

Since this study is an important to directly related to human thermal comfort and energy saving, various future studies related to this study should be carried out continuously as described above. It is expected that energy savings and high thermal comfort can be achieved under various environments in the future.

Reference

［1］ S&T Market Report, 2018, Autonomous Vehicle, Commercializations Promotion Agency for R&D Outcomes, Vol. 65, pp. 1-21.

［2］ Lee, S. M., 2018, Recent Trends and Implications of Autonomous Vehicles, Institute of Information & Communications Technology Planning & Evaluation Weekly Technology Trend, No. 1842, pp. 16-23.

［3］ Mao, Y., Wang, J., Li, J., 2018, Experimental and numerical study of air flow and temperature variations in an electric vehicle cabin during cooling and heating, Applied Thermal Engineering, Vol. 137, No. 06, pp. 356-367.

［4］ Lee H., 2018, Review of recent research on HVAC systems for electric vehicles. Magazine of the SAREK, Vol. 47, No. 12, pp. 12-115.

［5］ HYUNDAI MOTOR GROUP, https://news.hmgjournal.com/TALK/reissue-summer-nottodolist7, HMG JOURNAL, 2017.08.07.

［6］ Korea joongang daily, https://news.joins.com/article/22754265, 2018.06.28.

［7］ Beinews, https://www.beinews.net/news/articleView.html?idxno=8813, 2016.05.25.

［8］ renaultsamsung news letter, https://www.renaultsamsungm.com/new/service/svc_newsletter_201701.jsp, 2020.09.

［9］ brunch, https://brunch.co.kr/@caroute/186, 2018.10.30

［10］ Hong, S. H., Kim, M. E., Kim, M. H., 2006, Thermal Environment Analysis and Thermal Comfort Evaluation of the Automobile Interior, Magazine of the SAREK, Vol. 35, No. 10, pp. 34-45.

［11］ Kim, J, S., Kim, H, K., Jeong, H., Kim, K, H., Im, S, H., Son, W, H., 2005, Human-Computer Interface Based on Bio-Signal, Electronics an Telecommunications Trends, Vol. 20, No. 4, pp. 67-81.

［12］ Healthy house, https://healthyhouse.com/articles/emf/vehicles, 2017.05.16.

［13］ Auto Tribune, http://www.autotribune.co.kr/news/articleView.html?idxno=786, 2016.05.14.

［14］ Yao, Y., Lian, Z., Liu, W., Shen, Q., 2008, Experimental study on physiological responses and thermal comfort under various ambient temperatures, Physiology & Behavior, Vol. 93, Issues 1-2, pp. 310-321.

［15］ Ciuha, U., Mekjavic, I. B., 2016, Regional thermal comfort zone in males and

females, Phsiology & Behavior, Vol. 161, No. 06, pp. 123-129.

[16] Ciuha, U., Tobita, K., McDonnell, A. C., Mekjavic, I. B., 2019, The effect of thermal transience on the perception of thermal comfort, Physiol. Behav., Vol. 210, No. 10, 112623.

[17] Ciuha, U., Mekjavic, I. B., 2017, Thermal comfort zone of the hands, feet and head in males and females, Physiol. Behav., Vol. 179, No. 07, pp. 427-433.

[18] Lai, D., Zhou, X., Chen, Q., 2017, Measurements and predictions of the skin temperature of human subjects on outdoor environment, Physiol. Behav., Vol. 151, No. 09, pp. 476-486.

[19] Zhang, Z., Zhang, Y., Khan, A., 2019, Thermal comfort of people from two types of air-conditioned buildings – Evidences from chamber experiments, Build Environt, Vol 162, No. 9, 106287.

[20] Luo, M., Ke, Z., Ji, W., Wang, Z., Cao, B., Zhou, X., Zhu, Y., 2019, The time scale of thermal comfort adaptation in heated and unheated buildings, Build Environ, Vol. 151, No. 03, pp. 175-186.

[21] Chang, P. F., Arendt-Nielsen, L., Chen, A. C. N., 2005, Comparative cerebral responses to non-painful warm vs. cold stimuli in man: EEG power spectra and coherence, Int J Psychophysiol, Vol. 55, Issue 1, pp. 73-83.

[22] Roelofsen, P., 2002, The impact of office environments on employee performance: The design of the workplace as a strategy for productivity enhancement, J Facil Manag, Vol. 1, Issue 3, pp. 247-264.

[23] Lorsch, H. G., Abdou, O. A., 1994, Impact of the building indoor environment on occupant productivity - part 1: recent studies, measuresand costs, ASHRAE Transactions, Vol. 100, pt. 2, pp. 741-749.

[24] Woods, J. E., 1989, Cost avoidance and productivity in owning and operating buildings, Occup Med., Vol. 4, No. 4, pp. 753-770.

[25] Cui, W., Cao, G., Park, J. H., Ouyang, Q., 2013, Influence of indoor air temperature on human thermal comfort, motivation and performance, Build Environ, Vol. 68, pp. 114-122.

[26] Pepler, R. D., Warner, R. E., 1968, Temperature and learning: An experimental study, Transactions of ASHRAE annual meeting, pp. 211-219.

[27] Seppänen, O., Fisk, W. J., Faulkner, D., 2003, Cost benefit analysis of the night-time ventilative cooling in office building, Healthy Buildings, Vol. 3, pp. 394-399.

[28] Lee, H. J., Chun, C. Y., 2010, The effect of floor surface temperature on occupant's relaxation, Conference of the Architectural Institute of Korea Planning & Design, Vol. 30, Issue 1, pp. 377-378.

[29] Lee, H. J., Choi, Y. R., Chun, C. Y., 2012, Effect of indoor air temperature on the occupants' attention ability based on the electroencephalogram analysis, Journal of the Architectural Institute of Korea Planning & Design, Vol. 28, Issue 3, pp. 217-225.

[30] Kum, J. S., Kim, D. G., Kim, H. C., 2007, A study of physiology signal change by air conditioner temperature change, Jour. Fish. Mar. Sci. Edu, Vol. 19, No. 3, pp. 502-509.

[31] Kum, J. S., Kim, D. G., Choi, K. H., Lee, N. B., Im, J. J., Choi, H. S., Bae, D. S., 2002, Evaluation of thermal comfort on temperature differences between outdoor and indoor thermal conditions in summer, Korean J. Air-Cond. Refrig. Eng., Vol. 14, No. 11, pp. 890-896.

[32] Kim, D. G., Kum, J. S., Park, J. I., 2006, Evaluation of thermal comfort during sleeping in summer – part II : about mean skin temperatures and physiological signals -, Korean J. Air-Cond. Refrig. Eng., Vol. 18, No. 1, pp. 1-6.

[33] Kim, D. J., Kim, H. H., 2004, Comfortableness evaluation method using EEGs of the frontopolar and the parietal lobes, Trans. KIEE, Vol. 53D, No.5, pp. 374-379.

[34] Kang, K. N., Song, S. D., 2013, Study on the evaluation of amenity and physical characteristic of air- conditioning systems applying fluctuation characteristic on natural wind, Journal of the Architectural Institute of Korea Planning & Design, Vol. 29, No. 12, pp. 267-275.

[35] Lan, L., Pan, L., Lian, Z., Lin, H. H. Y., 2014, Experimental study on thermal comfort of sleeping people at different air temperatures, Build Environ, Vol. 73, pp. 24-31.

[36] Liu, Y., Wang, L., Liu, L., Di, Y., 2013, A study of human skin and surface temperatures in stable and unstable thermal environments, J THERM BIOL, Vol. 38, pp. 440-448.

[37] Nguyen, A. T., Singh, M. K., Reiter, S., 2012, An adaptive thermal comfort model for hot humid South-East Asia, Build Environ, Vol. 56, pp. 291-300.

[38] Sarhadi, F., Rad, V, B., 2020, The structural model for thermal comfort based on perceptions individuals in open urban spaces, Build Environ, Vol. 185, No.

107260, pp. 1-14.

[39]   Chan, S. Y., Chau, C. K., 2021, On the study of the effects of microclimate and park and surrounding building configuration on thermal comfort in urban parks, Sustain. Cities Soc., Vol. 64, 102512.

[40]   Tsang, T. W., Mui, K. W., Wong, L. T., 2021, Investigation of thermal comfort in sleeping environment and its association with sleep quality, Build Environ, Vol. 187, 107406.

[41]   Wang, H., Xu, M., Bian, C., 2020, Experimental comparison of local direct heating to improve thermal comfort of workers, Build Environ, Vol. 177, 106884.

[42]   Wang, H., & Liu, L., 2020, Experimental investigation about effect of emotion state on people's thermal comfort. Energy Build., Vol. 211, 109789.

[43]   Rosaria, C., Alessandro, N., Chiara, C., 2020, Comfort seat design: Thermal sensitivity of human back and buttock, Int. J. Ind. Ergon., Vol. 78, 102961.

[44]   Martinho, N. A. G., Silva, M. C. G., Ramos, J. A. E., 2004, Evaluation of thermal comfort in a vehicle cabin, Proceedings of the Institution of Mechanical Engineers, P I MECH ENG D-J AUT, Vol. 218, No. 2, pp. 159-166.

[45]   Cheong, K, H., Teo, Y, H., Koh, J, M., Acharya, U, R., 2020, A simulation-aided approach in improving thermal-visual comfort and power efficiency in buildings, J BUILD ENG, Vol. 27, 100936.

[46]   Chen, Z., Xin, J., Liu, P., 2020, Air quality and thermal comfort analysis of kitchen environment with CFD simulation and experimental calibration, Build Environ, Vol. 172, 106691.

[47]   Alizadeh, M., Sadrameli, S, M., 2018, Numerical modeling and optimization of thermal comfort in building: Central composite design and CFD simulation, Energy Build., Vol. 164, No. 1, pp. 187-202.

[48]   Hodder, S. G., Parsons, K., 2007, The effects of solar radiation on thermal comfort, Int. J Biometeoral, Vol. 51, pp. 233-250.

[49]   Chien, H., Jang, J. Y., Chen, Y. H., Wu, S. C., 2008, 3-D numerical and experimental analysis for airflow within a passenger compartment, Int J Automot Technol., Vol. 9, No. 4, pp. 437-445.

[50]   Lin, C. H., Han, T., Koromilas, C. A., 1992, Effects of HVAC Design Parameters on Passenger Thermal Comfort, SAE920264.

[51]   Kobayashi, Y, T, K., MORI, Y, J., Yoshimura, S, N, C., Tanabe, S, N, C.,

and Oi, H, J, M., 2012, Thermal comfort in car cabin with cooling individual body parts, 10th International Conference on Healthy Buildings, Vol. 2 of 3, pp 1030.

[52] Zhang, H., Lan, D., Xu, G., Li, Y., Chen, W., Tao, W. Q., 2009, Studies of air-flow and temperature fields inside a passenger compartment for improving thermal comfort and saving energy. Part I: Test/numerical model and validation, Appl. Therm. Eng., Vol. 29, Issue 10, pp. 2022–2027.

[53] Zhang, H., Lan, D., Xu, G., Li, Y., Chen, W., Tao, W. Q., 2009, Studies of air-flow and temperature fields inside a passenger compartment for improving thermal comfort and saving energy. Part II: Simulation results and discussion, Appl. Therm. Eng., Vol. 29, Issue 10, pp. 2028–2036.

[54] Barone, G., Buonomano, A., Forzano, C., Palombo, A., 2020, Enhancing trains envelope–heating, ventilation, and air conditioning systems: A new dynamic simulation approach for energy, economic, environmental impact andthermal comfort analyses, Energy, Vol. 204, 117833.

[55] Zhou, x., Lai, D., Chen, Q., 2019, Experimental investigation of thermal comfort in a passenger car under driving conditions, Build Environ, Vol. 149, No. 2, pp. 109-119.

[56] Qi, C., Helian, Y., Liu, J., Zhang, L., 2017, Experiment Study on the Thermal Comfort inside a Car Passenger Compartment, Procedia Eng., Vol. 205, pp. 3607-3614.

[57] Jung, W., Jazizadeh, F., 2019, Comparative assessment of HVAC control strategies using personal thermal comfort and sensitivity models, Build Environ, Vol. 158, No. 6, pp. 104-119.

[58] Kristanto, D., Leephakpreeda, T., 2017, Sensitivity Analysis of Energy Conversion for Effective Energy Consumption, Thermal Comfort, and Air Quality within Car Cabin, Energy Procedia, Vol. 138, pp. 552-557.

[59] Alahmer, A., Abdelhamid, M., Omar, M., 2012, Design for thermal sensation and comfort states in vehicles cabins, Appl. Therm. Eng., Vol. 36, No. 4, pp. 126-140.

[60] Alahmer, A., Omar, M., Mayyas, A. R., Qattawi, A., 2012, Analysis of vehicular cabins' thermal sensation and comfort state, under relative humidity and temperature control, using Berkeley and Fanger models, Build Environ, Vol. 48, No. 02, pp. 146-163.

[61] Alahmer, A., Mayyas, A., Mayyas, A. A., Omar, M. A., Shan, D., 2011,

Vehicular thermal comfort models; a comprehensive review, Appl. Therm. Eng., Vol. 31, Issues 6-7, pp. 995-1002.

[62] Ting, P. H., Hwang, J. R., Doong, J. L., Jeng, M. C., 2008, Driver fatigue and highway driving: A simulator study, Physiol. Behav., Vol. 94, Issue 3, pp. 448-453.

[63] Tsutsumi, H., Hoda, Y., Tanabe, S., Arishiro, A., 2007, Effect of Car Cabin Environment on Driver's Comfort and Fatigue, SAE Transactions, Vol. 116, Section. 6, pp. 335-346.

[64] Shin, Y., Im, G., Yu, G., Cho, H., 2017, Experimental study on the change in driver's physiological signals in automobile HVAC system under Full-load condition, Appl. Therm. Eng., Vol. 112, No. 02, pp. 1213-1222.

[65] Shin, Y., Ham, J., Cho, H., 2019, Investigation on thermal comfort using driver's bio-signals depend on vehicle cabin and vent exit air temperature, J. Mech. Sci. Technol., Vol. 33, Issue 7, pp. 3585-3596.

[66] Ikenishi, T., Kamada, T., Nagia, M., 2013, Analysis of longitudinal driving behaviors during car following situation by the driver's EEG using PARAFAC, 12th IFAC Symposium on Analysis, Design, and Evaluation of Human-Machine Systems, pp. 415-422.

[67] Yang, L., Ma, R., Zhang, H. M., Guan, W., Jiang, S., 2018, Driving behavior recognition using EEG data from a simulated car-following experiment, Accid Anal Prev, Vol. 116, No. 7, pp. 30-40.

[68] Jones, B. W., 2002, Capabilities and limitations of thermal models for use in thermal comfort models, Energy and buildings, Vol. 34, Issue 6, pp. 653-659.

[69] Chakroun C., Al-Fazed S., 1998, Thermal comfort analysis inside a car, Int. J. Energy Res., Vol. 21, Issue 4, pp. 327-340.

[70] Chowdhury, N. F. A., 2015, Ambient temperature effects on driving, Procedia Manuf., Vol. 3, pp. 3123-3127.

[71] Pilcher, J. J., Nadler, E., Busch, C., 2002, Effects of hot and cold temperature exposure on performance: a meta-analytic review, Ergonomics, Vol. 45, No. 10, 682-698.

[72] Zhou, X., Lai, D., Chen, Q., 2020, Thermal sensation model for driver in a passenger car with changing solar radiation, Build Environ, Vol. 183, 107219.

[73] Ravindra, K., Agarwal, N., Mor, S., 2020, Assessment of thermal comfort parameters in various car models and mitigation strategies for extreme heat-health risks in the tropical climate, J ENVIRON MANAGE, Vol. 267,

110655.

[74] ANSI/ASHRAE Standard 55-2017, 2017, Thermal Environmental Conditions for Human Occupancy, ASHRAE (2017) ISSN 1041-2336.

[75] EN15251, 2007. Indoor Environmental Input Parameters for Design and Assessment of Energy Performance of Buildings—Addressing Indoor air Quality, Thermal Environment, Lighting and Acoustics. English version.

[76] Lee, U., Cho, S., 2013, Bio-signal processing sensor IC technology trend, The Magazine of the IEIE, Vol. 40, No. 6, pp. 39-45.

[77] Kim, Y., Choi, M., Kim, J., 2017, Bio-signal Recognition Technology for Driver Status Monitoring, Auto Journal, Vol. 39, No. 12, pp. 21-23.

[78] Runkle, J, D., Cui, C., Fuhrmann, C., Stevens, S., Pinal, J, D., 2019, Evaluation of wearable sensors for physiologic monitoring of individually experienced temperatures in outdoor workers in southeastern U.S., Environ Int, Vol. 129, pp. 229-238.

[79] Lee, W., Lin, K., Seto, E., Migliaccio, G, C., 2017, Wearable sensors for monitoring on-duty and off-duty worker physiological status and activities in construction, Autom. Constr., Vol. 83, pp. 341-353.

[80] Kalaivaani, D, P, T., Krishnamoorthy, D, R., 2020, DESIGN AND IMPLEMENTATION OF LOW POWER BIO SIGNAL SENSORS FOR WIRELESS BODY SENSING NETWORK APPLICATIONS, MICROPROCESS MICROSY, Vol. 79, 103271.

[81] Hashem, M., Kheraif, A, A, A., Fouad, H., 2020, DESIGN AND DEVELOPMENT OF WIRELESS WEARABLE BIO-TOOTH SENSOR FOR MONITORING OF TOOTH FRACTURE AND ITS BIO METABOLIC COMPONENTS, Comput. Commun, Vol. 150, pp. 278-285.

[82] Zhang, X., Chen, C., Zhang, M., Ma, C., Zhang, Y., Wang, H., Guo, Q., Hu, T., Liu, Z., Chang, Y., Hu, K., Yang, X., 2020, Detection and analysis of MEG signals in occipital region with double-channel OPM sensors, J. Neurosci. Methods, Vol. 346, 108948.

[83] Liu, S., Schiavon, S., Das, H, P., Jin, M., Spanos, C, J., 2019, Build Environ, Vol. 162, 106281.

[84] Kartsch, V, J., Benatti, S., Schiavone, P, D., Rossi, D., Benini, L., 2018, A sensor fusion approach for drowsiness detection in wearable ultra-low-power systems, INFORM FUSION, Vol. 43, pp. 66-76.

[85] Sinnapolu, G., Alawneh, S., 2020, Intelligent wearable heart rate sensor

implementation for in-vehicle infotainment and assistance, Internet of Things, Vol. 12, 100277.

[86] Paschalidis, E., Choudhury, C, F., Hess, S., 2019, Combining driving simulator and physiological sensor data in a latent variable model to incorporate the effect of stress in car-following behaviour, Anal. Methods Accid. Res., Vol. 22, 100089.

[87] Simion, M., Socaciu, L., Unguresan, P., 2016, Factors which influence the thermal comfort inside of vehicles, Energy Procedia, Vol. 85, pp. 472-480.

[88] Kim, J., 2007, Air conditioning equipment, munundang, pp. 22-30.

[89] INTERNATIONAL STANDARD ISO 7730, 2005, Ergonomics thermal environment-Analytical determination and interpretation of thermal comfort using calculation of the PMV and PPD indices and local thermal comfort criteria, Third edition.

[90] Laxtha inc, http://www.laxtha.com/.

[91] Trans Cranial Technologies ltd, 2012, 10/20 system positioning manual.

[92] Biosense creative, http://www.ubionet.com/index.html.

[93] Cho, D., 2017, Human body temperature control system, https://blog.naver.com/genetic2002/221098254720.

[94] Shih, T. H., Liou, W. W., Shabbir, A., Yang, Z., Zhu, J., 1995, A New k-ε Eddy-Viscosity Model for High Reynolds Number Turbulent FLows Model Developement and Validation, COMPUT FLUIDS, Vol. 24, No. 3, pp. 227-238.

[95] Sarkar, S., Balakrishnan, L., 1990, Application of a Reynolds-Stress Turbulence Model to the Compressible Shear Layer, ICASE Report 90-18, NASA CR 182002.

[96] ANSYS Inc, 2013, ANSYS Fluent Theory Guide Release 15.0.

[97] Adhikari, VP., Nassar, A., Nagpurwala, QH., 2009, Numerical studies on the effect of cooling vent setting and solar radiation on air flow and temperature distribution in a passenger car, SAE Technical Paper 2009-28-0048.

[98] DuBois, D. and DuBois, E. F., 1916, A formula to estimate approximate surface area, if height and weight are known. Archives of Internal Medicine 17:863-871.

[99] McCullough, E.A. and Jone, B.W., 1984, A comprehensive data base for estimating clothing insulation. IER Technical Report 84-01, Institute for Environmental Research, Kansas State University, Manhattan. ASHRAE

Research Project RP-411, Final Report.

[100]　Heller, W., 1993, Neuro-psychological Mechanisms of Individual Differences in Emotion, Personality, and Arousal, Neuropsychology, Vol. 7, Issue. 4, pp. 476-489.

[101]　Li, J., Cao, X., Liu, J., Mohanarangam, K., Yang, W., 2018, PIV measurement of human thermal convection flow in a simplified vehicle cabin, Build Environ, Vol. 144, pp. 305-315.

국문 초록

자동차 실내환경에서 냉난방시 시트조건에 따른 생체신호 기반 열쾌적성 연구

이름 : 신 윤 찬

학과 : 조선대학교대학원 기계공학과

지도교수 : 조 홍 현

본 연구는 여름철과 겨울철 자동차 실내 온도와 벤트의 토출온도가 불쾌적조건에서 쾌적조건으로 변하는 동안 피험자가 운전 시뮬레이션을 수행할 때 뇌파, 맥파, 표면온도를 측정하였으며, 주관적 설문조사(TSV, CSV, CLV)를 통하여 운전환경에 대한 피험자의 온열쾌적성을 분석하였다. 그리고 여름철과 겨울철 자동차 실내의 초기 열환경에 대한 온열쾌적성 해석을 수행하였다. 또한, 여름철과 겨울철 자동차 실내의 열환경에서 다양한 시트의 사용에 따른 피험자의 생체신호인 뇌파, 맥파, 피부온도를 측정하고 주관적 설문조사(TSV, CSV, CLV)를 통하여 피험자의 온열쾌적성을 분석하였다. 마지막으로, 겨울철 국부난방의 위치에 따른 피험자의 생체신호 측정과 주관적 설문조사를 수행하여 온열쾌적성을 분석하였다. 이를 통하여 다음과 같은 결론을 얻었다.

자동차 실내의 열쾌적성 해석 결과, 여름철 조건에서 기본시트 사용시 시트와 접촉되는 등과 엉덩이의 온도가 높게 나타났다. 냉수시트 사용시 등과 엉덩이의 온도를 크게 감소시켜 이에 따라 PPD도 크게 감소함을 확인하였다. 또한, 겨울철 조건에서 기본시트 사용시 PPD는 10.1%로 약간의 불만족도가 존재하였으며, 온수시트 사용시 초기의 5분에서 PPD는 7.8%를 나타내어 쾌적한 열환경을 달성하였음을 확인하였다.

여름철 냉방시 자동차 실내 운전자 열쾌적성에 대한 평균 표면 온도 측정결과 벤트를 작동시키지 않은 Cabin 온도 35℃에서 12.5℃의 벤트를 작동시킴으로 운전

중인 피험자의 표면온도를 낮출 수 있음을 확인하였다. 주관적 설문조사 결과, PPG 분석 결과, EEG 분석 결과를 종합적으로 분석하였을 때, Cabin 온도 27.5℃/벤트온도 18.5℃에서 운전자에게 열적으로 쾌적한 운전환경을 제공하고 운전에 대한 집중도 높일 수 있는 것으로 확인되었다. 겨울철 난방시 자동차 실내 운전자 열쾌적성에 대한 평균 표면 온도 측정결과 벤트를 작동시키지 않은 Cabin 온도 15℃에서 40℃의 벤트를 작동시킴으로 운전중인 피험자의 표면온도를 높일 수 있음을 확인하였다. 주관적 설문조사 결과, PPG 분석 결과, EEG 분석 결과를 종합적으로 분석하였을 때, Cabin 온도 17.5℃/벤트온도 37.5℃와 Cabin 온도 20℃/벤트온도 35℃에서 운전자에게 쾌적하고 운전에 대한 집중도가 높은 열환경을 제공하는 것으로 확인되었다.

생체신호 및 주관적 설문조사를 기반으로 다양한 시트 사용에 대한 실험 결과를 종합적으로 분석하였을 때, 여름철 통풍시트의 사용은 주위의 더운 공기에 대한 송풍으로 운전자에게 불쾌적한 환경을 제공하였다. 반면에, 냉수시트의 사용시 운전자의 Stress index를 낮추고, 운전에 대한 집중도가 높은 환경을 제공하는 것을 확인하였다. 또한, 겨울철 조건에서 생체신호 및 주관적 설문조사 기반 온열쾌적성 분석 결과 온열시트의 사용은 열선의 높은 온도로 인하여 운전자에게 불쾌적한 환경을 제공하였으며, 온수시트의 사용은 운전에 대한 집중도는 감소하였지만, Stress index와 후두엽에서의 relative β/α를 감소시켜 운전자에게 열적으로 쾌적한 환경을 제공하는 것을 확인하였다.

겨울철 국부난방 위치에 대한 실험 결과, HVAC 사용 유무에 상관없이 국부난방이 적용된 부위의 온도는 크게 상승하였지만, 다른 부위에서의 온도 상승효과는 없었다. PPG와 EEG의 분석 결과에서 HVAC 사용 유무에 상관없이 허벅지에 국부난방을 적용한 경우 Stress index가 가장 낮게 나타났으며, 가슴과 허벅지의 국부난방 적용시 SDNN 및 RMSSD이 상대적으로 높게 나타났다. 또한, 후두엽에서의 Relative β/α를 감소시켜 운전자에게 쾌적한 환경을 제공하는 것을 확인하였다.

따라서, 자동차 실내환경에서 여름철에는 냉수시트를 사용하고 겨울철에는 온수시트의 사용 및 허벅지와 가슴의 국부 난방을 적용함으로써 운전자에게 열적으로 쾌적한 환경을 제공할 수 있음을 확인하였다.

감사의 글

(Acknowledgement)

있었으며, 제 주변 지인분들 모두에게 감사의 말씀 전해 드립니다. 저의 박사학위 논문을 끝까지 포기하기 않고 지도해주신 조홍현 교수님께 다시 한번 감사의 말씀을 전합니다. 이번 논문을 계기로 무슨 일이든지 포기하지 않고 끝까지 할 수 있는 용기를 얻었으며, 앞으로 새로운 분야도 계속 도전할 수 있는 용기를 얻는 계기가 되었습니다

마지막으로, 저를 믿고 응원해주신 사랑하는 가족, 아버지, 어머니, 쌍둥이 형에게 깊은 감사의 마음 전합니다.

2021년 02월
신재생에너지실험실
신 윤 찬 올림